Reliability-Based Design and Planning of Inspection and Monitoring of Offshore Wind Turbines

Reliability-Based Design and Planning of Inspection and Monitoring of Offshore Wind Turbines

Revised Version

PhD Thesis
Defended in public at Aalborg University
17 December 2013

Sergio Márquez-Domínguez

Department of Civil Engineering,
The Faculty of Engineering and Science,
Aalborg University, Aalborg, Denmark

River Publishers
Aalborg

ISBN 978-87-93102-62-0 (e-book)

Published, sold and distributed by:
River Publishers
Niels Jernes Vej 10
9220 Aalborg Ø
Denmark

Tel.: +45369953197
www.riverpublishers.com

Preface

When the wind is blowing fiercely, wind turbines must resist. Wind turbines have to withstand the rough environmental conditions in the most reliable manner and start to produce renewable energy when the wind becomes friendly again. Never give up 'wind turbine' face the winds and be proud of contributing as an energy sources.

Sergio Márquez-Domínguez

Reading this thesis, the reader will get the basic knowledge necessary for successful application of the main theories of structural reliability applied to both onshore and offshore wind turbine substructures considering building materials as steel and concrete. Additionally, the author mentions literature necessary for civil engineers who are unfamiliar with probabilistic methods and stochastic processes. This background is considered as vital theory to understand the development of offshore wind industry. State-of-the-art provides a framework for the theoretical basis of probability and statistics for application in structural reliability-based risk inspections.

The following list of basic literature is recommended to give a background within civil engineering in relation to offshore wind turbine substructures:

1. Probability and statistic for engineers: Benjamin & Cornell (1970), Ang & Tang (1975, 1884 and a new ed. 2007) and Montgomery & Runger (2011).
2. Design and analysis of experiments: Montgomery (2009).
3. Applied statistic and decision theory: Raiffa & Schlaifer (1961).
4. Wind loads: Dyrbye & Hansen (1997), Ghiocel & Lungu (1975) and Kuethe & Chow (1998).
5. Sea loads: Faltinsen (1990). Dean & Dalrymple (1991), Clauss et al. (Vol I-1992 and Vol II-1994) and Newman (1999).
6. Fatigue: Stephens et al. (2001).
7. Stochastic process theory: Newland (1993).
8. Reliability: Thoft-Christensen & Baker (1982), Thoft-Christensen & Murotsu (1986), Madsen et al. (1986), Melchers (1999), Choi et al. (2007), Elishakoff (1999), Sørensen (2011)(*Notes)* and JCSS (2006).
9. Wind turbines design: Burton et al. (2001) and Manwell et al. (2009).
10. Reliability applied to wind turbine design: Tarp-Johansen (2003), Veldkamp (2006) and Frandsen (2007).
11. Risk Based Inspection Planning applied to wind turbines: Straub (2004) and Sørensen (2009).

Acknowledgements

I would like to acknowledge the financial support provided by the Mexican National Council of Science and Technology (Consejo Nacional de Ciencia y Tecnología, CONACYT) under grant CVU: 166987, REG.: 191539 and APPLICATION: 308112. Without this financial support, none of this work would be possible to accomplish. The CONACYT encourages young researchers to develop interesting and fresh ideas in order to build a better country.

Hard life conditions reveal good friends and I was fortunate to discover my friends during this process. So, I would like to thank José G. Rangel Ramirez and David Méndez Morales for their valuable help, good wish and their trust in me.

I wish to acknowledge John Dalsgaard Sørensen for his support, advice and encouragement during my PhD study. Thank you for the opportunity to pursue my PhD degree and for the fruitful knowledge you have taught me during these years.

Strong foundations which have been built by the knowledge acquired from visionary and talented professors such as Miguel Villarreal Espinosa†, Luis Oropeza Lara, Bonifacio Carlos A. Peña Pardo, Neftalí Rodríguez Cuevas and Luis Esteva Maraboto. I would like to thank to all of them as well.

I am glad to have met smart and talented people during my PhD studies. I really appreciate their good wish, constructive criticism, conversations, help and valuable moments.

The best and the strongest brotherly embrace goes to my family for the breath of energy that they gave me every Saturday night and for the happiness that I felt by seeing them together. Thanks to my parents who have established support, education and human values to our family.

To my family with love
Parents: Lucina Domínguez-Lagunes and Celestino Márquez-León
Brothers and sisters: Crescencio, Celia† (our angel), Irma, Silvia, Hugo, Lilia.

Sergio Márquez-Domínguez
From: Zempoala, Veracruz, México.
Aalborg University; Aalborg, Denmark.
October 2013

Summary

Maintaining and developing a sustainable wind industry is the main motivation of this PhD thesis entitled *"Reliability-based design and planning of inspection and monitoring of offshore wind turbines"*. In this thesis, statistical methods and probability theory are important mathematical tools used to estimate the load characteristics which affect the strength of wind turbine substructures. Reliability methods (FORM/SORM) are applied to determine the probability of failure of both onshore and offshore wind turbines. So, technical and economic strategies are presented in order to find an optimum balance between the costs of the substructures and the annual wind energy production as well as to maximize the benefits coming from adequate operational control configurations which will increase the material saving in the substructures. The key goal is to decrease the cost of energy (CoE) considering, at the same time, a suitable life-cycle for the offshore wind turbines, assuring an acceptable risk level.

The probabilistic tools relate to and use the expertise developed in the oil and gas industry. The expertise can be applied to the wind industry in order to optimize the structural design with respect to the fatigue damage. Improvement could be made possible by using design and limit state equations (LSEs) to be applied to steel and reinforced concrete offshore wind turbines (OWT) substructures for both new and existing wind turbines. These design and LSEs can be established by taking into account an intricate load interaction produced by the natural phenomena, i.e. wind and waves. This load interaction has an important influence on the dynamical behaviour as well as on the fatigue damage of the wind turbine structure, influencing its reliability and stability.

In summation, wind, currents and sea loads can be considered as stochastic processes which will produce fatigue damages in the offshore wind turbines substructures. Steel and reinforced concrete components can contain cracks and fractures due to fatigue. This project concentrates on the development of methodologies to be applied for steel and reinforced concrete onshore and offshore wind turbine foundations with the aim of improving the design, decreasing structural costs and increasing benefits.

Recently, wind energy technology has started to adopt risk and reliability based inspection planning (RBI) as a methodology based on Bayesian decision theories together with structural reliability analysis to identify suitable strategies in order to inspect and control the deterioration problems in offshore wind turbines substructures.

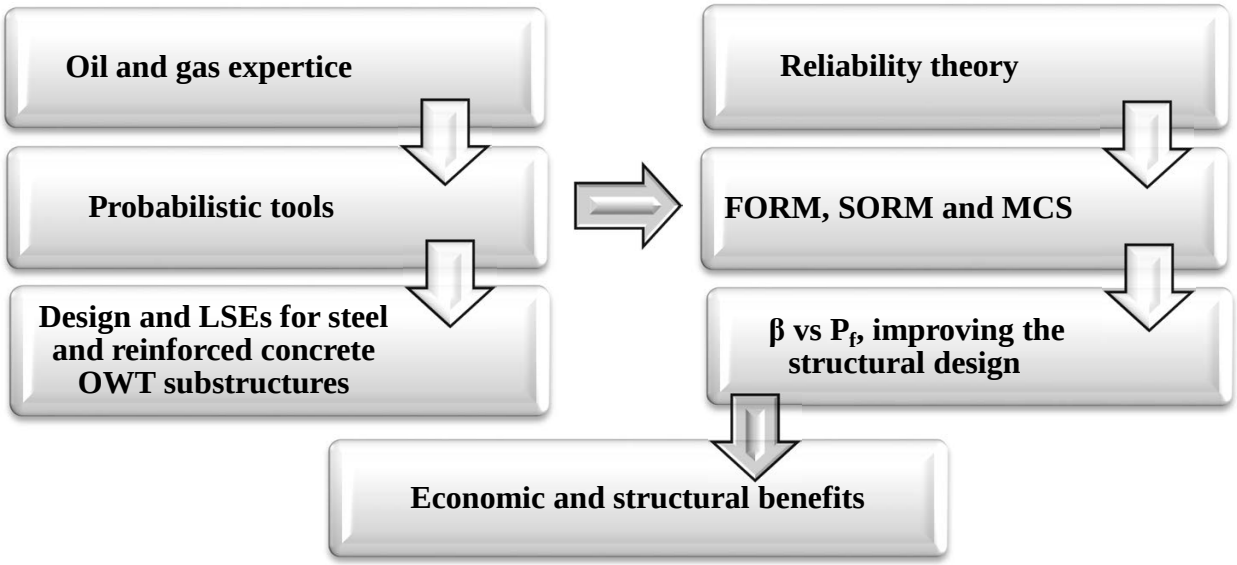

Figure 1. Wind turbine reliability methodology

Summary in Danish

Fastholdelse og udvikling af en bæredygtig vindindustri er den vigtigste motivation for denne ph.d.-afhandling med titlen "Pålidelighedsbaseret design og planlægning af inspektioner og kontrol af havvindmøller". I denne afhandling er statistiske metoder og sandsynlighedsteori vigtige matematiske værktøjer, der anvendes til at estimere og modellere de belastninger, der påvirker styrken af fundamenter til vindmøller. Pålidelighedsmetoder (FORM/SORM) er anvendt til at bestemme sandsynligheden for svigt i både onshore og offshore vindmøller. Tekniske og økonomiske strategier præsenteres til at finde en optimal balance mellem omkostningerne af substrukturerne og den årlige vindenergiproduktion samt at maksimere benefits ved passende konfiguration af kontrolsystemer, som således kan øge materiale besparelser i substrukturerne. Det overordnede mål er at reducere prisen for energien / cost of energy (CoE) og samtidigt inkludere hele livscyklus for havvindmøllerne, samt sikre et acceptabelt sikkerhedsniveau.

De probabilistiske metoder relaterer til og benytter den ekspertise, der er udviklet i olie- og gas industrien. Ekspertisen kan anvendes i vindindustrien til at optimere det strukturelle design med hensyn til udmattelse. Forbedringer kan opnås ved at formulere design og limit state ligninger (LSE) til anvendelse i konstruktionselementer i stål og armeret beton i offshore vindmøllerfundamenter for både nye og eksisterende vindmøller. Disse design og limit state ligninger kan formuleres under hensyntagen til en kompleks belastningsinteraktion fra kontrolsystem og naturlaster, dvs. vind og bølger. Denne belastningsinteraktion har en væsentlig indflydelse på den dynamiske opførsel samt på udmattelse af de bærende konstruktionsdele, og derved påvirker deres sikkerhed og stabilitet.

Til opsummering så kan vind, strøm og bølgebelastninger betragtes som stokastiske processer, der kan resultere i udmattelse i havvindmøllers bærende konstruktionsdele. Stål og armerede betonelementer kan indeholde revner og defekter på grund af udmattelse. I dette projekt koncentreres om udvikling af metoder, der anvendes for stål og armerede beton havvindmølle fundamenter med det formål at forbedre design, reducere strukturelle omkostninger.

Indenfor de seneste år har vindenergi industrien startet på at anvende risiko og pålidelighedsbaseret inspektionsplanlægning (RBI) som en metode, der er baseret på Bayesiansk beslutningsteori sammen med strukturel pålidelighedsanalyse til at identificere optimale strategier til inspektion og kontrol af udmattelsesproblemer i havvindmøllers bærende konstruktioner.

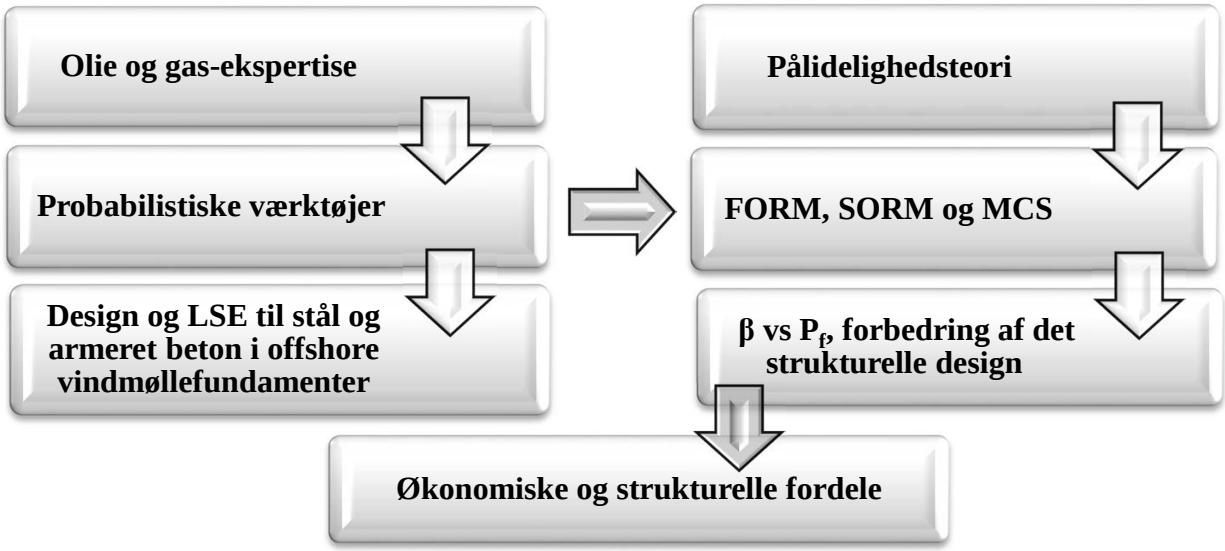

Figur 1. Pålideligheds-baseret metodologi for vindmøller

CONTENTS

LIST OF TABLES

LIST OF FIGURES

NOMENCLATURE

A	Weibull scale factor
a	Crack depth
a_c	Critical crack depth typically the thickness (T)
a_0	Describes the crack depth after (N_I) cycles
a(t)	Crack depth at time 't'
AEP_{net}	Net annual energy production
ALS	Conditional or accidental limit state
AOE	Annual operating expenses
α-vector	Unit vector which is orthogonal with respect to the linearized failure surface
B	Weibull shape factor
$\beta_{CC}(t_0)$	Coefficient defined for the concrete strength at the initial time (t_0) for load application
B_T	Total expected benefits
β / β_O	Cumulative reliability index
$\Delta\beta$	Annual reliability index
β_S	System reliability index
β^P	Parallel reliability index
C	Material parameters
c_d	Smallest detectable crack length
C_E	Cost of the energy in the supplier marked
CoE	Costs of the Energy
C_T	Total costs due to energy losses
c(t)	Crack length at time 't'
C_z	Cost of the steel in the market
DOFs	Degrees of freedom (DOFs)
D_{ac}	Fatigue damage accumulation
Δ	Uncertainty related to Miner's rule for linear damage accumulation
ΔE	Change in loss of energy due to changes in the operational configuration
$\Delta K(a)$	Stress intensity ranges for one- and two-dimensional models
ΔP_f	Annual probability of failure
$\Delta P_{F,MAX}$	Maximum acceptable annual probability of failure
Δs	Stress range
Δs_c	Stress range at the inflection point
$\Delta\sigma^e$	Equivalent stress range
ΔW	Cost model
Δz	Marginal change in saved material area in the substructure
E_1	Event (1)
E_2	Event (2)
ε	Physical uncertainty of the material / Uncertainty of the fatigue life
ξ	Omission sensitivity factor
EU	European Union
e_p	Reliability elasticity coefficient
FAST	Fatigue, Aerodynamics, Structures, and Turbulence simulation code
$f_{cd,fat}$	Design value of the compressive concrete strength reduced for fatigue
f_{ck}	Characteristic compression strength
f_{ck0}	Reference strength equal to 10 MPa
FCR	Fixed charge rate
FDF	Fatigue design factor
FLS	Fatigue limit state
FM	Fracture mechanic approach

FORM	First Order Reliability Method
GW	Gigawatt
GWh	Gigawatt hour
g	Fatigue limit state equation
$g(x)$	Failure function
$\gamma_{C,fat}$	Partial safety factor for concrete in fatigue verification
γ_f	Partial safety factors for fatigue load
γ_m	Partial safety factors for fatigue material strength
h	Failure elements or hot spots
h(t)	Limit state modelling the crack detection
$H_{K,m,\sigma\varepsilon}$	Hessian matrix with second-order derivatives of the log-likelihood function
ICC	Initial capital cost
K	Material parameter / Statistical uncertainty of material testing results
k	Number of bins or intervals with constant amplitude of fatigue loading
k_s	Factor estimated for unknown standard deviation and coefficient of variation
L	Mechanism level
LLC	Land lease cost
LRC	Replacement / Overhaul cost
LSE	Limit State Equation
λ	Expected value of the smallest detectable crack size
M	Safety margin
m	Material parameters determined by laboratory tests
μ	Mean value
MCS	Monte Carlo Simulation
M_L	Linearized limit state equation
MLM	Maximum-Likelihood Method
MPI	Magnetic Particle Inspection
MW	Megawatt
n	Number of mechanisms concatenated / Total number of tests
n_i	Number of loading cycles
n_F	Number of tests where failure occurs
n_R	Number of tests where failure did not occur after n_i stress cycles (run-outs)
N	Material fatigue life in a fracture mechanic model
N*	Number of cycles at the inflection point
N_I	Fatigue initial life estimated by the number of stress cycles to the crack nucleation
N_i	Number of cycles to the failure
N_P	Fatigue propagation life
NREL	National Renewable Energy Laboratory
op	Operational strategy configuration
O&M	Operation and maintenance / Operation and maintenance costs
OWT	Offshore wind turbine
Ω	Sample space
p	Deterministic or statistical parameter
P_f	Cumulative probability of failure
PFI	Probability of False Indication
P_f^{FORM}	Probability of failure in a linear approximation to the failure function
P_f^{MC}	Probability of failure is given by a crude Monte Carlo simulation
POD	Probability of detection curves
P_f^P	Probability of failure for a parallel system
PRADSS	Program for Reliability And Design of Structural Systems

P_f^S	Probability of failure for a series system
P_f^{SORM}	Probability of failure in a second-order approximation to the failure function
P_F^U	Updated failure probability
$\overline{P}_W$	Average wind machine power
Φ_m	m-dimensional standard normal distribution function
R	Resistance or material strength / Ratio of the unit costs
RBI	Risk and reliability based Inspection Planning
R^P_{system}	System reliability function for parallel systems
R^S_{system}	System reliability function for series systems
ρ	Coefficient of correlation
S	Environmental loads
S_C	Structural components
SLS	Serviceability limit state
$S_{c,max}$	Maximum stress level
$S_{c,min}$	Minimum stress level
Sn	Sequences of failure
SORM	Second Order Reliability Method
σ	Standard deviation
$\sigma^2_{M_L}$	Variance of the linearized safety marge
T	Years to be neglected in an operational strategy
T_I	Initial time
T_L	Service life
T_F	Fatigue life
U	Standard normal variables / Mean wind speed
u*	Design point. Point with the greatest failure probability
$U_{cut\text{-}in}$	Initial mean wind speed
$U_{cut\text{-}out}$	Final mean wind speed
ULS	Ultimate Limit State
X	Stochastic variable
x	Represent a realization of a stochastic variable
X_{SCF}	Stochastic variable related to stresses due to fatigue loads
X_W	Stochastic variable related to determination of the external loads
Y	Uncertainty related to geometry function
z	Material design/design parameter (cross sectional area)

Chapter 1
GENERAL FRAMEWORK

1.1 Introduction

A large amount of electricity is produced every day in order to satisfy the increasing demand in communication, transport and the massive industrial production of basic supplies for living. This demanding amount of energy use is depleting the natural sources, such as oil and coal (Hughes & Rudolph, 2011; Zittel & Schindle, 2007). The energy requirements are growing quite fast while the daily burning of oil and gas, which are considered the main contributors to the global warming, obligates both privately owned companies and governments around the world to work together with the aim of developing renewable energy sources and thereby mitigating the environmental impact on traditional sources. Therefore, an extraordinary effort is being done by the European Union (EU) in order to regulate the sustainable energy production in future years. As a result of this meaningful effort, efficient energy policies have been established allowing a significant technological progress in energy matters (European Union, 2009). Due to these policies, the technological progress is clear and promising. The main target of 20% of energy use coming from renewable energy by 2020, which has been adopted by the EU, is not unrealistic to being reached. Thereby, new challenges are being studied in order to set an even better renewable energy future (EWEA, 2011).

Energy being harvested from sun, wind and waves can be considered as an important contribution to solution of both pollution and the energy demand at the same time. Thus, nowadays these green energy options are developed as sustainable energy resources where experts consider wind as the fastest, most achievable and most cost-effective source to produce power. At this moment, it is worth to mentioning that wind is a kind of indirect solar energy from which approx. 1% becomes wind which is caused by the unequal warmth of the earth's surface compared with the ocean mass (Pearce, 2008; Wallace & Hobbs, 2006). This kinetic energy of the wind can be transformed into useful electricity by wind turbines placed both onshore and offshore. Offshore wind turbines are designed larger, taller and more efficient with time, but they are facing rough environments which results in requirements for stronger offshore wind turbine substructures, such as larger steel jackets foundations (Burton, 2001; Manwell, 2009). Deeper waters and harsher environments potentially make the offshore wind energy production larger but also expensive due to the high costs of substructures which must resist higher fatigue loads, coming from wind and wave, corrosion and wear. Therefore, in order to maintain a sustainable industry, technical and economical efforts are done to find the cost optimal between fatigue loads, cost of substructures and energy production. The key goal is to decrease the cost of energy (CoE) considering an optimal and suitable life cycle of each component involved and also the whole system, assuring an acceptable risk level (Toft, 2010). Furthermore, inspection, maintenance and repair activities are vital actions for achieving acceptable and optimal reliability levels. Monitoring and mitigation actions should optimally be planned and optimized within a framework based on Bayesian decision theory which has been developed and applied during the last decades in the oil and gas industry, giving a theoretical background that can be applied also for the wind turbine industry (Rangel-Ramírez, 2010; Nielsen, 2013). In simpler terms, the strong demand for energy, global warming, pollution and a large amount of energy in waves, wind and currents motivate us to use renewable energy sources to produce electricity.

1.2 State-of-the-art

This section gives an overview of the state-of-the-art concerning the literature which is needed to develop a structural reliability background to be applied for both offshore and onshore wind

turbines. Until a few years ago, traditional engineering was based on deterministic methods to design the main civil works which are built according to the expertise of skilled designers in the field. This developed expertise has been captured in codes and standards which are normally written considering a conservative structural reliability level. Recently, engineering has turned to increased use of probabilistic methods to improve the structural designs which can take into account both material and load uncertainties. This probabilistic engineering approach leads to increased use of the materials' maximum strength capacity but at the same time also maintains both acceptable risk and reliability levels according to the work developed. Consequently, the structural designs are done looking for equilibrium between costs and structural safety and also keeping in mind functionality and comfort. An interesting overview about these structural engineering approaches and their development is described by Moan (2008). Concepts of probability and statistics with a clear tendency to develop the engineer's skills with respect to making decisions were described by Benjamin and Cornell (1970) as well as Ang and Tang (1975, Vol. I-reprinted 2007, 1984 (Vol. II)). Based on probability and stochastic methods, structural reliability methods have been developed. Structural reliability is considered attractive and useful to assess the structural safety levels where material and loads uncertainties play an important role. For this reason, a theoretical background of the main probabilistic theories is essential to understand the reliability knowledge (JCSS, 2006). Between 1982 and 1986, Thoft-Christensen, who is considered a pioneer in structural reliability and its applications, did two important contributions to the literature (Thoft-Christensen & Baker, 1982; Thoft-Christensen & Murotsu, 1986). In Madsen et al. (1986), a complete historical background about the development of the theory of structural reliability is presented together with the most important methods applied to structural safety. Melchers (1999) presented the techniques and theories for the analysis and prediction of the structural reliability index. In Sørensen (2011), the knowledge after years of experience working on the reliability field is reflected in lecture notes where risk and decision making are incorporated. Risk and decision theory is normally based on analytical and numerical techniques where probability and statistics contribute to the evaluation of a logic solution of a problem, which is the best decision according to costs, time, risks and even safety considerations (Montgomery & Runger, 2011; Raiffa & Schlaifer, 1961). Design and analysis of experiments can be considered a helpful mathematical tool when series of tests or experiments need to be analysed considering the main variables in the system (Montgomery, 2009).

The First Order Reliability Method and the Second Order Reliability Method (FORM/SORM) as well as simulation techniques such as Monte Carlo Simulation are considered effective structural reliability methods to assess the reliability to be applied for different structures with diverse degrees of complexity, e.g. bridges, oil and gas platforms, buildings, and even ships, see e.g. Ayala-Uraga (2009). Structural reliability analysis can be performed to assess the behaviour of individual components built in combination with different materials. For instance, reinforced concrete slab foundation, designed for onshore wind turbines, are built with steel reinforcement bars and concrete as well as wind turbine blades, where different fibre layers of material composite are used. Therefore, in order to develop the main stochastic models useful for onshore and offshore wind turbines, in this thesis, the main reliability theories are applied to both reinforced concrete slab foundations studied for onshore wind turbines and jacket type substructures built for offshore wind turbine.

Probabilistic methods have also been developed and applied in the wind turbine field. In Tarp-Johansen (2003), fatigue lifetime and reliability evaluation of larger wind turbine components (hub, main shaft, and main frame) have been described and also the uncertainties influencing the lifetime distribution and their quantification have been discussed. Frandsen (2005) presents a fatigue turbulence model within a wind farm, which considers also the influence of wake turbulence intensity. Veldkamp (2006) can be considered the most practical and complete probabilistic approach applied to wind turbine fatigue design. Combining Tarp-Johansen's stochastic model and

the fatigue turbulence model proposed by Frandsen in Sørensen et al. (2007-2008), a probabilistic approach has been developed for wind turbine fatigue design in a wind farm.

Structural reliability applications have been developed for the offshore wind turbine field, considering offshore foundations and support structures, see e.g. Sørensen and Toft (2010) where contributions on uncertainty analysis and reliability methods for wind turbines are presented. Uncertainty involved in the wind turbines design can be modelled by application of the Maximum Likelihood Method and Bayesian approach in cases where test/measurement data are available. Calibration of the partial safety factors in codes and standards for offshore wind turbines can also be based on probabilistic approaches where reliability theory is a fundamental part. Typically, the objective is to minimize the difference between the reliability indices estimated for the offshore wind turbine substructure components and a target reliability level which can be assessed by risk-based methods. Sørensen (2011) describes calibration of safety factors (Fatigue Design Factors) to be used for the fatigue design of steel substructures for offshore wind turbines. Moreover, in statistical decision and risk analysis, generic approaches to risk-based inspection planning for steel structures have been developed by Straub (2004). Sørensen (2009) describes a framework for risk-based life cycle approach for optimal planning of operation and maintenance based on pre-posterior Bayesian decision theory applied to offshore wind turbines where probabilistic indicators can be used to quantify indirect information about the damage of critical components, e.g. gearboxes. In Nielsen and Sørensen (2011), a similar framework was described for operation and maintenance procedures since costs of operation and maintenance are significant contributors to the costs of energy. The study was done for a single wind turbine with a single component where the costs were evaluated for two distinct maintenance strategies. Nielsen and Sørensen (2010) explain that operation and maintenance (O&M) are expensive and show how the risk-based planning of O&M has the potential of reducing these costs based on Bayesian network models used to establish a probabilistic damage model. In order to define reliability acceptance criteria, risk failure levels for different structures are often established in codes and standards which define the reliability target to be reached in the structural design (Straub & Kiureghian, 2011). Generally, every country has its own standards. A general classification of the some of the most common design codes is described in the following:

- Design of fixed offshore steel structures for oil and gas platforms: NORSOK (1998) and ISO 19902 (2007).
- IEC 61400-1 (2007) and IEC 61400-3 (2009) are international standards for land based and offshore wind turbines, respectively.
- Design of offshore wind turbines steel substructures: DNV-OS-J101 (2013); DNV-RP-C203 (2012) and EN 1993-1-9 (2005)
- Guideline for the certification of offshore wind turbines: GL (2005)
- Onshore wind turbines: Eurocodes (EN1992-1-1, 2004 and EN1992-2, 2005), are recommended for fatigue verification to be applied in reinforced concrete buildings and bridges. DNV-OS-J101 (2013) and DNV-OS-C502 (2012) are considered for fatigue verification to design of offshore concrete structures

Stochastic loads such as wind and wave loads together with the influence of the control system will determine the structural physical response of the wind turbines components. This response can be estimated by direct field measurements or by laboratory testing where the full structure behaviour is modelled by a scaled model. Normally, both ways are expensive and, therefore, data is hard to get. For these reasons, wind turbines are modelled by computational models. Some of them are commercially free and others are available in the wind turbine market. The most common computational models (emulators) in the research field are FAST, HAWC2 and GH Bladed (see Jonkman & Buhl, 2005; Larsen, 2009; and Bossanyi, 2009). FAST is based on Jonkman et al. (2009) where a definition of a 5 MW NREL is emulated as reference.

1.3 Objectives

Objective 1: Development of new and reliable strategies with the key aspect to improve the operation and maintenance planning is established as the main objective. These strategies are to be applied to both onshore and offshore wind turbines in order to reduce structural costs, increase the lifetime of the substructure and to develop a skilled design. The design should satisfy minimum criteria to the structural safety and reliability level determined according to the structural risk considerations. The probability of failure is estimated using probabilistic methods, First and Second Order Reliability Methods (FORM/SORM), and a simulation technique, Monte Carlo Simulation (MCS). Bayesian statistical methods can be applied as a basis to develop O&M planning procedures which can be helpful in taking optimal maintenance decisions.

Objective 2: Fatigue damage can affect the lifetime of both onshore and offshore wind turbine foundations. Therefore, fatigue damage is an important issue to be investigated in detail. Structural damage and economic consequences must be considered with respect to structural reliability criteria with the aim of reducing the cost of energy (CoE). An important aspect of this is to establish probabilistic fatigue models which can be applied to reinforced concrete slab foundations as well as jacket type substructures where the stochastic fatigue loads are mainly from wind and wave loads. The stochastic fatigue models should be developed based on a rational treatment of the main uncertainties involved in the complex interaction between stochastic loads (wind and waves) and strength of the materials, i.e. steel and concrete.

1.4 Outline and key methods

The project "*Reliability-based design and planning of inspection and monitoring of offshore wind turbines"* is organized by eight chapters where a brief description of the *key methods* to be implemented is presented as follow:

This chapter (1) describes the *state-of-the-art* needed as the basis for the main reliability approaches applied to both offshore and onshore wind turbines substructures. An overview of the main standards and design codes is also included. In the same manner, useful simulation software is mentioned which can be implemented to emulate the wind turbine behaviour. A general framework of the *reliability update theories* is described in detail based on *Bayesian statistical methods* using available information. Modelling and monitoring techniques are established considering different sources of information identified as important for wind turbines.

In Chapter 2, the main aspects needed for structural reliability assessment are described. This includes the *target reliability level* to be used for fatigue damage assessment of wind turbine substructures where *different failure modes* are considered taking into account various uncertainties. Reliability methods for estimation of the probability of failure are also described incl. FORM/SORM methods and simulation techniques.

Fatigue modelling is considered by Chapter 3 where *fatigue design models* are presented. These fatigue models are developed based on the *S-N approach* and the Miner's rule. S-N curves are defined for welded steel connections and reinforced concrete in order to estimate the probability of failure for individual components. While in Chapter 4, the theoretical framework of *system reliability assessment* is developed, Chapter 5 deals with *operational control strategies* which are established looking for economic targets considering fatigue failure. Chapter 6 provides the reliability assessment background taking into account inspections and fatigue life modelled by a Fracture Mechanic approach. An important contribution of this thesis is developed in Chapter 7 where a statistical analysis for reinforcement steel bars and different concrete strengths is presented. The results of these statistical analyses can be used as basis for probabilistic modelling of fatigue strength and reliability analysis of wind turbine components made in reinforced concrete. Finally, in Chapter 8, conclusions and future work are established.

Chapter 2
RELIABILITY ASSESSMENT

A clear understanding of the main concepts applied for structural reliability analysis is important for the reliability assessment of wind turbine structural components. For this reason, the main objective of this chapter is to define the most important concepts used by the reliability assessment. This chapter is based on Thoft-Christensen and Baker (1982), Sørensen (2011) and Choi et al. (2007).

In Sørensen (2011), the main steps in a reliability assessment are defined as follows:

1. Select a target reliability level.
2. Identify the significant failure modes of the structure.
3. Decompose the failure modes in series systems of parallel systems of single components (only needed if the failure modes consist of more than one component).
4. Formulate failure functions (limit state functions) corresponding to each component in the failure modes.
5. Identify the stochastic variables and the deterministic parameters in the failure functions. Further, specify the distribution types and statistical parameters for the stochastic variables and the dependencies between them.
6. Estimate the reliability of each failure mode.
7. In the design process, change the design if the reliabilities do not meet the target reliabilities. In the reliability analysis, the reliability is compared with the target reliability.
8. Evaluate the reliability result by performing sensitivity analyses.

2.1 Target reliability level

Reliability- and risk-based methods for analysis and assessment of structures can be idealized by four levels according to Madsen et al. (1986) and Sørensen (2011). These levels are considered relevant for assessment of the structural reliability.

• *Level I methods*: Design methods in which the uncertain parameters are modelled by one characteristic value, as for example the partial safety factor defined by code and standards.

• *Level II methods*: Methods in which iterative calculations are involved to estimate an approximation of the failure probability for one structural component and also system components. Uncertain parameters are modelled by the mean values and the standard deviations, and by the correlation coefficients between the stochastic variables which are assumed to be normally distributed. The reliability index method can be considered as an example.

• *Level III methods*: Methods where the exact probability of failure can by estimated for a structure or structural component by modelling the uncertain parameters by joint distribution functions of the all quantities which affect the response of the structure.

• *Level IV methods*: Methods where the costs of failure are taken into account and the *'risk'* is used as a measure of the reliability. In this way, different designs taking uncertainty into account can be compared in decision making based on cost-benefit considerations.

Table 1 provides a description of the reliability methods, which are classified by four levels.

Table 1. Structural reliability levels (Melcher, 1999, p. 62).

Level		Probability distributions	Limit state functions	Uncertainty data	Results
I	Code level methods	Not used	Linear functions (usually)	Arbitrary factors	Partial safety factors
II	Second moment methods	Normal distributions only	Linear, or approximated as linear	May be included by second moment data	'Nominal' failure probability P_{fN}
III	Exact reliability methods	Related to equivalent Normal distributions by variable transformation	Linear, or approximated as linear	May be included as random variables	Failure probability P_f
IV	Decision methods	Any of the above, plus economic data			Minimum cost, or maximum benefit

2.2 Failure modes

Structural reliability from an engineer's point of view can be understood as the ability of a structure to fulfil the structural design requests for a defined time period. Mathematically, structural reliability can be defined as the probability that a structure will not attain the specified design requests for a specified time period which can be considered as the service life of the structure. Design request can be fixed to specific *design limits* which are often denoted *limit state conditions* or *failure modes*. On the other hand, *risk* can be defined as the expected consequences given an (unwanted) event (consequence multiplied by the probability of failure). In structural design, the event can be the structural collapse which may result in fatalities.

The failure modes can be divided as follows:

Ultimate Limit States (ULS) which can be defined by maximum load carrying capacity or maximum material strength capacity. Ultimate limit state conditions are related to the structural collapse of one structural component or the whole structure caused by rupture due to fatigue of the material, corrosion, fracture, buckling, formation of elasto-plastic mechanisms and large deformations.

Fatigue design has been considered since the early 1970s as a specific design criterion or failure mode which is called 'Fatigue Limit State', see Moan (2008). The concept of fatigue limit states has been considered to be important when the oil and gas industry was concerned about the fatigue strength (Moan, 2005). The *Fatigue limit state* (FLS) is related to the structural damage accumulation due to cyclic loads. Fatigue damage can be identified by cracks which can cause mechanisms of failure, material fracture and structural instability and even the structural collapse.

Conditional or accidental limit states (ALS) are defined by accidental loads coming from e.g. extraordinary events as explosions, fire or floods. A ship crash in a wind turbine substructure can be considered as an accidental load. These conditional loads are generally caused by instantaneous actions which can exceed the material strength or can even cause the instability of the structure.

Serviceability limit states (SLS) are related to the normal use of the structures when the structure has excessive deflection, excessive vibration, drainage, leakage, or local damage. The limit can be established when the structure does not satisfy the function for which it was built any more in safe conditions.

In a deterministic structural design, the design limits are formulated in *design equations.* A deterministic design can be improved by a probabilistic design which takes into account the *uncertainties* related to environmental loads and material strength. This probabilistic design can be performed by *Limit State Equations* (LSE).

Engineering based on probability and risk can be developed in order to understand and include the natural randomness of the physical phenomenon such as wind and wave and, therefore, get the necessary knowledge for a possible probabilistic design based on damage prediction. Structural fatigue damage in a wind turbine is considered a kind of deterioration mechanism which affects both the whole wind turbine performance and individual elements. Fatigue damage is a consequence of environmental and operational loads that, step by step, will decrease the optimal behaviour and strength of the structure or structural components during their service life. Environmental loads have cyclic and random characteristics with a high degree of uncertainty. In the reliability assessment, the identification of the uncertainties is a difficult task. A wind turbine can be exposed to phenomenological uncertainties related to its behaviour under extreme loads conditions. Regarding the reliability assessment, fatigue limit state equations are formulated in connection with the establishment of structural safety boundaries, e.g. crack width, deflections and also loads. For instance, in a jacket type wind turbine foundation, fatigue limit state equations can be established by a stochastic model which makes an explicit account of uncertainties connected to loads, strengths and calculation methods. In probabilistic design, the single components are designed to a level of safety, which accounts for an optimal balance between failure consequences, material consumption and the probability of failure. Finally, the correlation between different physical mechanisms is modelled by limit state equations where the stochastic variables are represented by a stochastic model.

In traditional codes, the design is considered deterministic, and the uncertainties are reflected and taken into account by safety factors. An improved design can be done using probabilistic design methods where reliability levels according to the structural failure risk are considered. This also implies potential material cost reductions. Further, if inspections are performed, even lower material costs can be obtained. An optimal balance between costs and inspections should be considered in order to keep a sustainable wind industry. Such reliability- and risk-based approaches have been used for the offshore oil and gas industry, see e.g. Faber et al. (2005) and Moan (2005) and also for offshore wind turbines, see Sørensen (2011).

This thesis is focused on fatigue limit states for wind turbines substructures made of steel and concrete.

2.3 Wind turbine uncertainties

A physical understanding and background will give us a better basis for modelling the uncertainties related to wind turbines. An overview about wind and sea loads effects on the structures in general is presented in Dyrbye & Hansen (1997) and Faltinsen (1990), respectively. In Ghiocel & Lungu (1975), environmental loads are modelled from a probabilistic point of view. Furthermore, a mathematical framework of stochastic theory is described by Newland (1993).

According to Ang & Tang (2007), uncertainties, classified as *epistemic* or *aleatory uncertainties,* are involved in environmental loads or their effects on the structures. Epistemic uncertainties should be accounted for in a probabilistic design. *Epistemic uncertainty* can be improved/decreased reducing the statistical uncertainty by getting more data from laboratory tests, measurements or computational simulations. For instance, *Measurement uncertainties* can be improved by using better field measurement techniques as well as *model uncertainties* can be decreased by developing more accurate models for the loads, strengths and resistances. On the other

hand, *aleatory uncertainty* cannot be reduced by statistical estimation of the randomness or by updating of the data bases. In wind turbine design, aleatory uncertainty is e.g. represented in the extreme environment that a wind turbine must face. Other references as e.g. Melchers (1999) and Moan (2008) mention a detailed classification about uncertainties in reliability assessment. Human intervention plays an important role in the design, fabrication and uses of structures where the *human error* is an important factor which often can be reduced by *quality controls* and by relevant 'quality assurance'. Human errors can be defined as deviation of an event or process from acceptable engineering practice.

A wind turbine limit state condition is exposed to uncertainties which can be modelled by stochastic variables which can be represented by probability functions according to the phenomenon to be studied. In addition random fields and stochastic processes can be relevant to model specific uncertainties in space and time. In Figure 2**,** a general classification is shown of the stochastic uncertainties modelled by stochastic variables often used in the literature. A more detailed explanation is given in Chapter 3.3 (fatigue stochastic model).

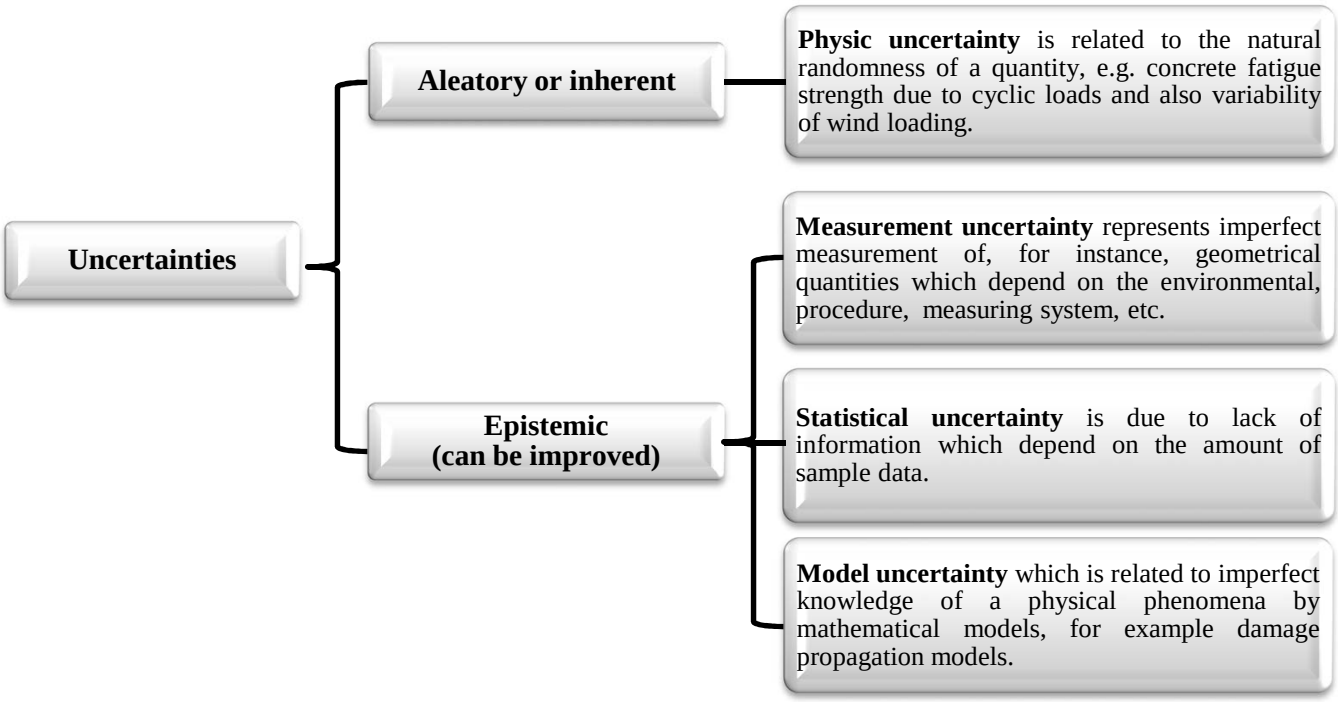

Figure 2. Uncertainty modelling.

2.4 Reliability methods

In structural reliability assessments, the limit state equation or failure function defines the safety margin associated with the resistance, 'R', and the environmental loads, 'S'. The failure function is denoted by $g(x)$, and the probability of failure is defined by P_f

$$g(x) = R(x) - S(x) \tag{1}$$

$$P_f = P[g(x) < 0] \tag{2}$$

In Equation (1), the *failure states of the structure* is defined by $g(x)<0$ (negative values). $g(x) = 0$ and $g(x) > 0$ define the *failure surface* and the *safe states* (positive values), respectively.

If in Equation (1), 'x' represents variables/parameters in the resistance and load models which are represented by stochastic variables 'X'. The safety margin '***M'*** is defined by:

$$\mathrm{M} = \mathrm{g}(\mathrm{X}) = \mathrm{R}(\mathrm{X}) - \mathrm{S}(\mathrm{X}) \tag{3}$$

An important step (step 5 in above list) in a reliability analysis is to decide which quantities should be modelled by stochastic variables and which ones should be represented by deterministic parameters.

In structural reliability, the safety margin typically results from a mechanical analysis of the structure. This safety margin can be established by linear or non-linear functions with correlated or independent stochastic variables 'X' which can be Normal or Non-normal distributed. In order to estimate the reliability of the structures, FORM/SORM and simulations techniques can be applied (Sørensen, 2011):

- **FORM techniques:** In First Order Reliability Methods, the stochastic variables, 'X', are transformed into a standardized, independent normal distributed space called 'u-space'. The failure surface (limit state equation) is approximated by a tangent plane in the design point (u*) which is the point with the largest likelihood of failure. The reliability index (β) is defined as the shortest distance between u* and the origin of the u-space.

- **SORM techniques:** In Second Order Reliability Methods, a second-order approximation to the failure function in the design point (u*) is applied. Therefore, the probability of failure can be estimated based on the quadratic approximation of the failure surface, see Figure 3.

- **Simulation techniques:** Samples of the stochastic variables are generated on basis of the probability functions modelling the uncertainties. In crude Monte Carlo simulation, the relative number of samples corresponding to failure is used to estimate the probability of failure. In simpler terms, if an experiment is performed by a number of tests, the probability of failure is estimated as follows:

$$P_f^{MC} = \frac{\text{No. of failures}}{\text{Total No. of tests}} \tag{4}$$

It is noted that several more advanced simulation techniques can be found in the literature and are in some cases also applied in practical applications. The advanced simulation techniques include e.g. Importance sampling, Directional simulation, Latin hypercube simulation, Subset simulation and Asymptotic Sampling.

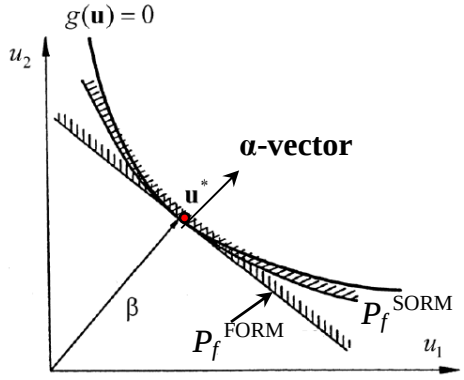

Figure 3. FORM/SORM techniques, graphic representation (Sørensen, 2011).

In this thesis, the reliability assessments have been performed by FORM technique together with Monte Carlo simulation which is used as 'verification' of the accuracy of FORM results.

The reliability index approach is a mathematical optimization problem which is used to find the point on the structural response surface (limit-state approximation) or the shortest distance from the origin to the surface (β) in the standard normal space (Choi et al. 2007). Therefore, different ***safety index approaches*** can be defined in a structural reliability assessment. These approaches will depend on the characteristic of the stochastic variables and in the linearity of the safety margin (Sørensen, 2011).

2.5 Sensitivity measures

A sensitivity analysis can be performed in order to estimate the influence of a set of stochastic variables as well as the statistical parameters involved in a reliability assessment (step 8 above). Three sensitivity measures are often used:

2.5.1 α-vector

In Figure 3, the α-vector is a unit vector which is orthogonal with respect to the linearized failure surface (limit state equation). The α-vector will represent the individual influence of each stochastic variable involved in the linearized limit state equation ($M_L = -\alpha_i^T \cdot u_i = 0$) considering that the variance of 'M_L' is defined by:

$$\sigma_{M_L}^2 = \alpha_1^2 + \alpha_2^2 + \cdots + \alpha_n^2 = 1 \tag{5}$$

For independent stochastic variables, α_i^2 gives the percentage of the total uncertainty associated with u_i. If X_{SCF1}, X_{SCF2} and X_{SCF3} are correlated stochastic variables associated with X_{SCF}, then $\alpha_{SCF1}^2 + \alpha_{SCF2}^2 + \alpha_{SCF3}^2$ gives the percentage of the total uncertainty considered by X_{SCF}.

2.5.2 Reliability elasticity coefficient (e_p)

Each stochastic variable is represented by distribution functions which, at the same time, are influenced by statistical parameters. The influence of the statistical parameters (p) on the reliability index (β) can be measured by reliability elasticity coefficients (e_p) as follows:

$$e_p = \frac{\partial \beta}{\partial p} \cdot \frac{p}{\beta} \tag{6}$$

2.5.3 Omission sensitivity factors (ξ)

The omission sensitivity factor is a measure of the influence on the reliability index (β) if a stochastic variable is considered as a deterministic parameter (fixed).

$$\xi = \frac{1}{\sqrt{1 - \alpha_i^2}} \tag{7}$$

Chapter 3

WIND TURBINE FATIGUE MODELLING

3.1 S-N approach

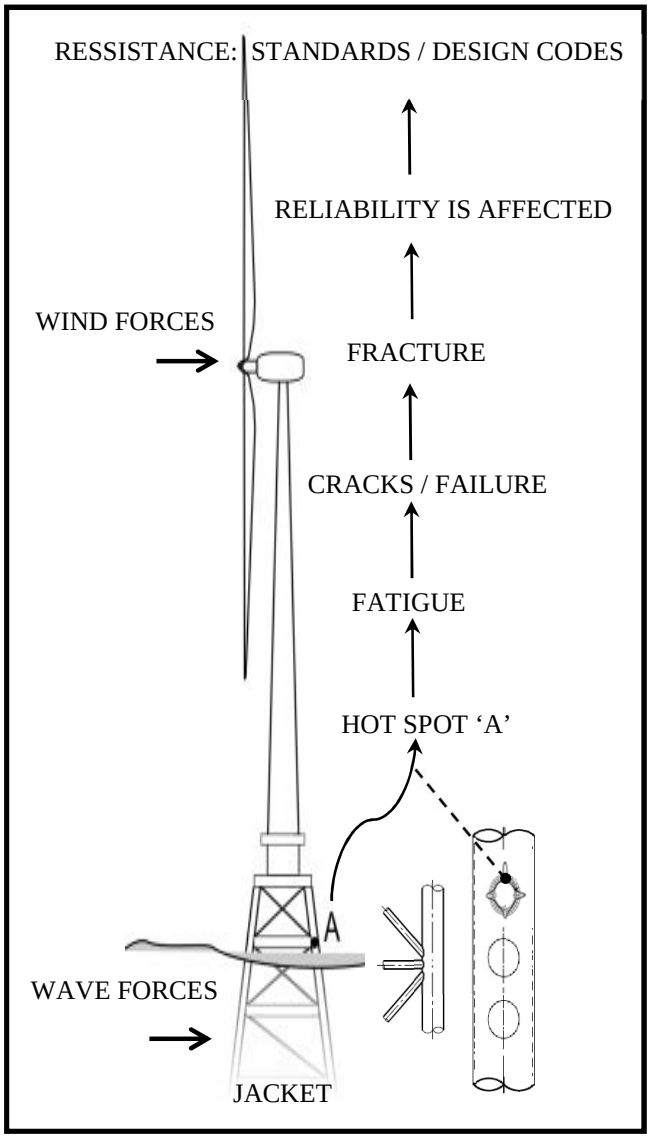

Figure 4. Structural fatigue framework.

The main objective of this thesis is to develop the basis for strategies for onshore and offshore wind turbines in order to reduce the costs of the substructure and also to establish the basis for improving the design basis in existing standards and codes, see Appendix A.2, A.3 and A.4. Structural steel and reinforced concrete are the most popular materials used to build wind turbine substructures. These materials are exposed to dynamic cyclic loads produced by the random interaction between wind, wakes and the wind turbine rotor as well as by the interaction between sea loads and the substructure. These stochastic interactions together with the influence of the wind turbine control system are the main sources of the fatigue load and the resulting fatigue damage. Figure 4 shows a jacket type wind turbine substructure where a high stress concentration (Hot spot 'A') is exposed to external loads. Hot spot 'A' is located in a brace toe of a welded connection.

Development of stochastic models for the fatigue limit state and estimation of the resulting reliability can be considered as a contribution to strategies to maintain and develop sustainable wind energy. This thesis is focused on the establishment of fatigue approaches especially in steel and concrete substructures following the trend and problems of the wind industry. For instance, in Appendix A.5, a probabilistic fatigue model for reinforced concrete structures is considered.

It is noted that special emphasis is on studying the reliability of substructures with respect to the stochastic modelling and (partial) safety factors using representative code based design equations. Therefore a detailed model of the load and structural modelling is not necessary.

The need to assess and estimate the probability of failure of both new and existing reinforced wind turbine concrete components has been the inspiration to develop stochastic models for uncertainties of the fatigue strength of reinforcement and concrete. Reinforced concrete substructures are the most used foundation for onshore wind turbines, and reinforced high-strength concrete could in the future be a cost-efficient alternative to steel for offshore wind turbine substructures, see e.g. Waagaard (2003) and Holmen (1984).

In Chapter 7 a statistical analysis is presented considering test data from laboratory fatigue tests which were performed on specimens of (high-strength) concrete (Lohaus et al. 2012) and steel reinforcement bars (Hansen & Heshe, 2001). This statistical analysis is considered as a major contribution of this thesis and the estimated uncertainties can be used as basis for probabilistic modelling and reliability analysis of wind turbine structures with reinforced concrete components.

Figure 4 shows a framework for structural fatigue assessments related to offshore wind turbine substructures. Stress concentration in a welded detail (Hot spot 'A') is sketched caused by the environmental loads where failure is caused by the initiation and development of cracks through the material thickness (Straub, 2004). Cracks, as physical result of fatigue damage, can cause a 'stepped' decrease of the structural reliability due to structural failure, fracture or even the complete collapse of the structure.

Wilhelm Albert observed the fatigue phenomena for first time in 1829 (Ameen & Szymanski, 2006). In the early 1970s the oil and gas industry was quite concerned with understanding fatigue strength (Moan, 2005). Nowadays, the wind industry is developing models and understanding of the fatigue processes relevant for this industry, see e.g. Stephens (2001) for background on metal fatigue and Ameen & Szymanski (2006) and Thun (2006) for fatigue of concrete structures.

Failure following crack initiation and crack development are considered the fatigue criteria and can be described by S-N and fracture mechanics approaches. The S-N approach was initiated by August Wöhler in 1860. Wöhler developed the idea of a fatigue limit state and proposed the S-N curves. S-N curves are obtained by laboratory tests, and they are often used by design codes together with Palmgren and Miner's hypothesis to describe the fatigue damage accumulation (D_{ac}) in the materials under cyclic loads taking into account that stress amplitude governs the fatigue strength:

$$D_{ac} = \sum_{i}^{k} \frac{n_i}{N_i} \leq \Delta \tag{8}$$

where n_i and N_i are the number of loading cycles and number of cycles to the failure for Δs_i, respectively. k is the number of bins or intervals with constant amplitude of fatigue loading. While in a deterministic design, Δ=1, represents failure, in a probabilistic limit state equation Δ represents the uncertainty related to Miner's rule for linear damage accumulation. Therefore, fatigue limit state equations can be formulated as follows:

$$g = \Delta - D_{ac} \tag{9}$$

A Bi-linear Basquin equation can be applied for fatigue estimation in structural steel.

$$N_i = K_1 \cdot \Delta s_i^{-m_1} \text{ and } N_i = K_2 \cdot \Delta s_i^{-m_2} \tag{10}$$

K_1 and m_1 are material parameters determined by laboratory tests for $N_i \leq N_C$, K_2 and m_2 are material parameters for $N_i > N_C$, N_C corresponds to the number of cycles at the inflection point, and Δs_c is the stress range at the inflection point. Δs_i is the stress range corresponding to the fatigue stress spectrum (Δs_i, n_i) obtained e.g. by rainflow counting method.

Equation (10) can be generalised by including the effect of the mean value of the fatigue loading such that it can be used for modelling the fatigue life of composite materials such as glass fibres for wind turbine blades, see e.g. (Toft, 2010) and also for reinforced concrete. The mean value of the

fatigue stress, represented by the R-value, is important for composite materials. For reinforced concrete components, negative R-values indicate compression and thereby that fatigue of the concrete can be important. Statistical analysis and stochastic modelling of the reinforcement bars and the concrete fatigue strength are described in Chapter 7 as well as in Appendix A.5. The probabilistic modelling is based on the fatigue model for concrete proposed in the new FIB Model Code 2010.

In the simple case where a linear SN-curve is considered (e.g. or welded steel details) uncertainty can be introduced by the following simple model:

$$\log N_i = \log K - m \log \Delta s_i + \qquad (11)$$

where 'ε' represents the uncertainty of the fatigue life. N_i, in Equation (8) can be estimated for plain concrete by linear S-N curves which are established in Eurocode 2 (EN1992-1-1:2004 and EN1992-2:2005) for fatigue verification of onshore concrete structures. Based on DNV-OS-J101 and DNV-OS-C502, fatigue verification can be performed for offshore structures. In appendix A.5, a sensitivity analysis and influence of the different stochastic variables in a stochastic model for fatigue of concrete is performed based on the design model in Eurocode 2. According to Thun (2006), Eurocode fatigue models are based on studies made by Cornelissen (1984, 1986).

3.2 Structural modelling

Turbulent wind, wakes, waves, currents, tides as well as phenomena as icing on the blades, marine growth and scour are natural environmental processes which need to be considered in order to understand their random behaviour and harshness, and their influence of fatigue of wind turbine components. Wind turbines are exposed to these natural phenomena which create high demands of the structures. This demand is represented by cyclic stresses along the time. The cyclic stresses are the key to be applied in the Palmgren and Miner's rule which describes the fatigue damage accumulation and therefore also important to formulate the fatigue limit state equation.

It is possible to estimate the cyclic stresses by various means, e.g. field measurements on prototype wind turbines, laboratory tests and computational simulations. Specialized simulation codes have been developed in order to emulate the structural response under the natural processes explained above. However, measurements, laboratory tests and code simulations must be validated. An example of an aero-elastic simulator capable of simulating extreme and fatigue loads for wind turbines is FAST code (Fatigue, Aerodynamics, Structures, and Turbulence). In a simulation analysis using FAST, wind turbine aerodynamic and structural response to wind-inflow conditions is determined in time domain. FAST considers the aerodynamics of the blades with active control means, considering many operational configurations which can be implemented. It is worth mentioning that a good reference to understand aerodynamics and flow conditions is Kuethe and Chow (1998). Finally, the output of the simulations is time-series of the aerodynamic loads and deflections useful in the fatigue analysis of the structural elements of a wind turbine; see Jonkman and Buhl (2005). Next, the stress distribution can be estimated by counting methods and can e.g. be represented by 'Markov matrices'. For instance, the rainflow counting method where the total number of stress ranges (Δs_i) can be grouped such that the number of stress ranges in each group 'i' is represented by the number of loading cycles 'n_i' per year. Often the fatigue stress ranges are modelled by a Weibull distribution for different combinations of mean wind speeds and turbulence intensities when assessing the fatigue load for the individual fatigue critical details (Hot spots). An Omni-directional distribution of wind speeds could be conservative.

A general overview (Jonkman & Buhl, 2005) on the theoretical background of FAST is described in the following. FAST is based on a combined modal and multi-body dynamics formulation. While the blades and tower have a modal formulation, the support platform, base plate, nacelle, generator, gears, hub, tail are simulated according to a multi-body dynamic formulation. This multi-body formulation makes it difficult to emulate the dynamic response of a multi-body structure as jacket type foundations by the aero-elastic code. Mode shapes are specified as 6^{th} order polynomials. FAST is based on relative degrees of freedom (DOFs) (no constraint equations) where equations of motion are derived and implemented using Kane's Method. Blade and tower beam mode assumptions are based on Bernoulli-Euler beams under bending (no axial or torsional DOFs and no shear deformation), and linear modal representation considers small to moderate deflections characterized by lowest modes. Other assumptions for the support platform pitch, roll, and yaw rotations employ small angle approximations with correction for orthogonality. All other DOFs may exhibit large displacements without loss of accuracy.

In Appendices A.2-A.4, the dynamic behaviour of the generic 5MW NREL OWT model is simulated using FAST (Jonkman et al. 2009). Load cases considered are based on IEC 61400-1 for onshore wind turbines and IEC 61400-3 and DNV-OS-J101 for offshore wind turbines. Substructures such as jacket type are difficult to simulate in conventional aero-elastic simulators due to multi-body dynamic formulation. Therefore, jacket type wind turbine foundations are simulated by a fixed-bottom monopile substructure representing an equivalent jacket OWT substructure in order to obtain representative hot spots stresses time series, see e.g. Gao et al. (2010).

3.3 Fatigue stochastic model

Expertise from the oil and gas industry is used to assess the factors influencing the costs related to design, inspection, repair and failure of OWTs facilities. Design equations and limit state equations, are developed using these principles in order to optimize the design of OWT substructures with respect to fatigue loads. Reliability of the fatigue critical details can be performed using the S-N approach with S-N curves in combination with the Palmgren and Miner's rule as generally recommended in codes and standards. The inherent uncertainty related to the physical uncertainty of the material fatigue strength and external loads need to be considered as well as the model uncertainty related to the Palmgren and Miner's damage accumulation rule. 'Δ' is assumed log-normal distributed, and represents the model uncertainty related to Miner's rule which is formulated based on assumptions as linear damage accumulation and establishes that the order of the stress cycles does not influence the total damage. Those assumptions often are not true and are modelled by a model uncertainty, which is a kind of epistemic uncertainty that can be reduced by experiments made with different load histories; see e.g. Nielsen (2013). 'X_W' is introduced as a log-normal distributed stochastic variable that models the inherent uncertainty related to determination of the external fatigue loads, e.g. wind and wave. 'X_{SCF}' is a stochastic variable that considers the inherent uncertainty related to determination of stress ranges given the fatigue loads. 'X_{SCF}' is assumed to be log-normal distributed. 'LogK' is modelled by a normal distributed according to specific S-N curve. 'K' represents the statistical uncertainty due to a limited number of tests together with the S-N curve fatigue strength. A detailed explanation about the uncertainties involved in the fatigue based damage design has been established by Straub (2004) where the fatigue uncertainties have been divided in fatigue modelling, loading and fatigue resistance. Straub (2004) underlines the uncertainty due to the variability of environmental loads modelling and stress calculations as well as the sources of the uncertainties due to applied S-N curve and its validation.

3.4 Reliability assessment for a structural component

Once the stochastic model has been established, the reliability related to a limit state equation can be obtained by first and second order reliability methods or simulation techniques such as Monte Carlo Simulation; see e.g. Madsen et al. (1986) and Sørensen (2011). Then, the reliability index, β(t), corresponding to the cumulative probability of failure, P_F (t), is defined by:

$$(t) = -\Phi^{-1}(P_F(t)) \tag{12}$$

where (t) is the reliability index at time *t* and Φ( ) is the standardized normal distribution function.

The annual probability of failure is obtained from

$$\Delta P_F(t) = P_F(t) - P_F(t - \Delta t);\ t > 1\,\text{year}\,\text{and}\,\Delta t = 1\,\text{year} \tag{13}$$

Table 2 shows the relationship between the reliability index and the probability of failure.

Table 2. Relationship: vs. P_F (Sørensen, 2011).

P_F	10^{-5}	10^{-4}	10^{-3}	10^{-2}
	4.3	3.7	3.1	2.3

Chapter 4

SYSTEM RELIABILITY ASSESSMENT

A description of reliability assessment theory applied to structural systems is presented by e.g. Thoft-Christensen and Murotsu (1986) as well as Sørensen (2011). In this chapter, some concepts and formulas related to system reliability assessment are introduced. In a *traditional, deterministic design*, structures are designed using partial safety factors and characteristic values to verify that each element and failure mode have sufficient reliability. For structures, where consequences of failure are large, additional robustness requirements often have to be fulfilled partly securing that system effects are accounted for. Such a design mainly based on checking elements and failure modes one by one can be considered un-conservative for large, complex systems.

In a *modern reliability assessment*, the main goal is to determine the probability of failure of the whole structure taking into account factors as correlation between strength of individual elements, statically indeterminateness, and multiple failure modes such as tension, compression, bending, strain softening, buckling, global instability, fatigue failure, etc. The probability of failure of every mode can be estimated by FORM/SORM techniques or Monte Carlo simulation, see Madsen et al. (1986) and Sørensen (2011). Next, system reliability can be estimated modelling the system by series and/or parallel systems of the single elements. The design of the substructures/elements can then be optimized with respect to e.g. fatigue, as explained below. This optimized design can contribute to decrease the cost of the energy (CoE). In the following, some basic concepts of system reliability theory needed in order to assess the system reliability of a wind turbine substructure subject to fatigue loads are described.

4.1 Classical and modern reliability theory by set theory

Set theory is a fundamental mathematical tool in the formulation of probabilistic problems in engineering. Using the terminology of set theory, a *sample space* (Ω) is the set of all possibilities in a probabilistic problem, and a *sample point* is associated by every single possibility. So, *an event* is a subset of the sample space.

A fatigue model is formulated for each single critical detail/element of the substructure; and consequently, the corresponding limit state equation can be used to estimate the reliability index (β) in each single hot spot located in e.g. welded connections.

Union and intersections are important concepts in systems modelling. For instance, the *union* between (E_1) and (E_2) which can describe events associated with *linearized limit state equations* can be applied for fatigue failure events of different hot spots. Generally speaking, the union event can describe different failure modes in one or more offshore wind turbine substructures; see Figure 5.

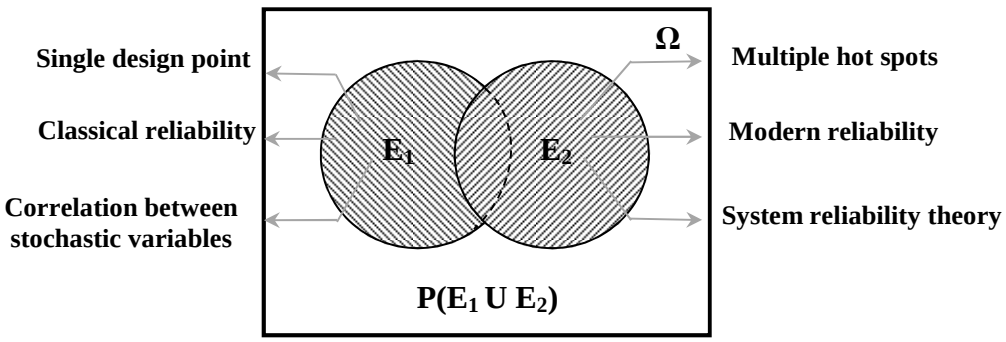

Figure 5. Union between (E_1) and (E_2), linearized system reliability approach, using a linearized limit state equation for failure modes.

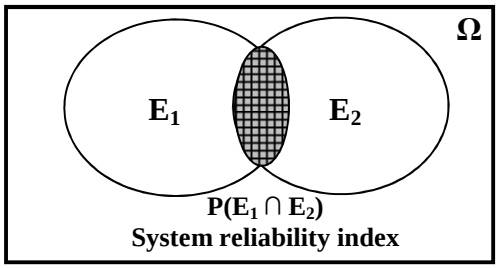

Figure 6. Intersection between (E_1) and (E_2) representing failure in a parallel system model.

A *system reliability index* for a parallel system where failure is represented by intersection of failure events is illustrated in Figure 6.

4.2 FORM fatigue system models

The main difference between statically determinate structures and statically indeterminate or redundant structures is the load redistribution effects. Redundant structures will collapse when simultaneous failures, which are represented by a number of failure elements, occur corresponding to formation of a mechanism (Ghosn et al. 2010). Jacket type offshore wind turbine foundations can be considered as an example of an indeterminate substructure which is built by steel modules where each tubular element or brace is connected to the main frame (jacket legs) by welded tubular joints where hot spot are generally located. For each hot spot, a limit state equation is established, and the correlation/dependency is defined by the interaction between the stochastic variables involved. The limit state equation can be defined by Ultimate Limit State (ULS) conditions, service state conditions or by fatigue progressive damage. This thesis is dealing with fatigue damage propagation in welded details located in steel wind turbines substructures.

A substructure is generally characterised by multiple potential mechanisms which are represented by different failure modes related to different hot spots. For steel substructures of the jacket type, fatigue failure typically does not result in total collapse. Therefore, a system model based on *linearized limit state equations* can be applied as the basis of a series system model with fatigue failure modes as elements; see Figure 9. Appendix A.3 is based on such a *linearized fatigue failure model*. Assessment of the consequence of fatigue failure can be based on non-linear finite element analyses such as a push-over analysis which can model the progressive damage of the substructure due to fatigue failure at different welded joints. Combination of hot spots will define different failure mechanisms, and these mechanisms will be correlated in a *generalized series system model* defined as an arrangement of *parallel systems* or by hot spots joined in a *series system*. A generalized series system with mechanisms joined in a parallel approach considers that non-failed elements can often take over the load from the failed element, and the generalized series system with series approach establishes that the whole structure would collapse when the weakest element or sequence of elements fail, see Figure 8.

A realistic substructure has a high number of mechanisms. For illustration, some of the dominant mechanisms are shown in Figure 7 where a jacket type steel substructure is shown. Hot spots could appear at different welded connections. These hot spots are considered potential failure elements which can be modelled by fatigue limit state equations. A series system can be established by a group of hot spots where the structural collapse can occur when the weakest element fail (Figure 9). A linearized FORM approximation theory can be applied in order to estimate the probability of failure. General system reliability methods can be used to estimate the system probability of failure and the corresponding system reliability index see e.g. Thoft-Christensen and Murotsu (1986) and Sørensen (2011).

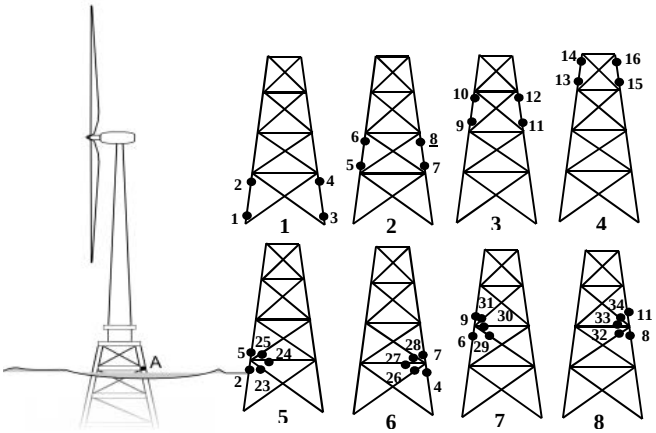

Figure 7. Examples of fundamental mechanisms.

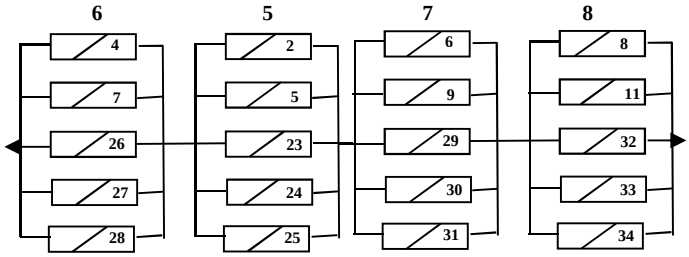

Figure 8. Generalized series system with mechanism joined in a parallel approach.

According to Appendix A.3, the number of sequential mechanisms can have an important influence on the system reliability index (β_S). In consequence, the generalized series system models are analysed considering different failure sequences (Sn) where 'n' is the number of mechanisms concatenated at different mechanism levels (L_1 to L_5) which is established by the number of ductile elements joined in each mechanism, see Figure 9.

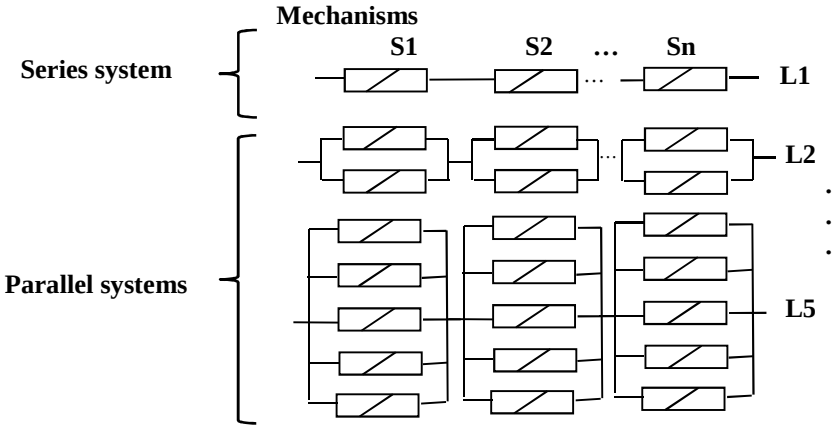

Figure 9. Sequences of failures (Sn) where 'n' represents the number of mechanisms concatenated, and 'L' shows the mechanism level.

In Figure 10, three mechanisms are modelled in a stepped sequence of failure by parallel mechanisms with different mechanism levels. A stepped sequence of failure can often represent the fatigue damage propagation of a jacket type steel substructure where the number of failure elements (hot spots) will vary from mechanism to mechanism.

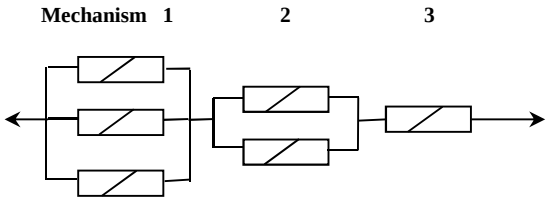

Figure 10. Stepped sequence of failure.

4.3 Examples

Appendix A.3 describes an example based on the assumption of equal failure risk for every welded joint in a jacket type substructure. It means that the equal reliability index (β_O) for each hot spot is considered in the fatigue failure analysis. This assumption can be considered conservative since in a realistic case the substructures will typically have different stress concentrations at different welded connections, see Martindale and Wirsching (1983). Therefore, each welded joint can have different fatigue life, and the risk level could be different even in neighbour connections. Thereby, every hot spot can be considered to have unequal reliability indices (β_O).

A linearized series system methodology is proposed following these steps:

1. Aerodynamic and hydrodynamic wind turbine modelling by specialized software.
2. Identify the highest stressed hot spots or critical welded details and obtain the stress time series.
3. Apply a counting method such as the rainflow counting in order to obtain the fatigue stress range spectra and combine it with the S-N relationship to model the fatigue failure.
4. Estimate the fatigue reliability index (β_O) by FORM/SORM or simulation techniques.
5. Considering the damage propagation in the substructure, establish the mechanisms of failure to be analysed in the ***generalized series system model*** defined by an arrangement of ***parallel systems*** or by hot spots joined in a ***series system.***
6. Represent the ***generalized series system model*** by a system of linearized limit state equations ($_i - {}^T_i U = 0$). The linearized series system model should be based on the correlation/dependency between stochastic variables.
7. Estimate the system reliability using the linearized limit state equations using e.g. the SYSREL program (COMREL & SYSREL: USER MANUAL, 2003).

Different models can be established that consider the influence of the relevant correlation/ dependencies between the stochastic variables for offshore steel wind turbine support.

As an example correlation/dependencies between stochastic variables in S-N approach for six hot spots is considered. The fatigue reliability index (β_O) for the six hot spots is considered to be equal (conservative assumption).

Case 1.

- Δ ‘s fully correlated
- X_W ‘s fully correlated
- X_{SCF} ‘s fully correlated
- Log K ‘s independent

The alpha vectors for the six components become:

$$\alpha^T_1 : (\alpha_{X\Delta}, \alpha_{XW}, \alpha_{XSCF}, \alpha_{XLogK1}, \quad 0, \quad 0, \quad 0, \quad 0, \quad 0)$$
$$\alpha^T_2 : (\alpha_{X\Delta}, \alpha_{XW}, \alpha_{XSCF}, \quad 0 \quad , \alpha_{XLogK2}, 0, \quad 0, \quad 0, \quad 0)$$
$$\alpha^T_3 : (\alpha_{X\Delta}, \alpha_{XW}, \alpha_{XSCF}, \quad 0 \quad , \quad 0, \alpha_{XLogK3}, 0, \quad 0, \quad 0)$$
$$\alpha^T_4 : (\alpha_{X\Delta}, \alpha_{XW}, \alpha_{XSCF}, \quad 0 \quad , \quad 0, \quad 0, \alpha_{XLogK4}, 0, \quad 0)$$
$$\alpha^T_5 : (\alpha_{X\Delta}, \alpha_{XW}, \alpha_{XSCF}, \quad 0 \quad , \quad 0, \quad 0, \quad 0, \alpha_{XLogK5}, 0)$$
$$\alpha^T_6 : (\alpha_{X\Delta}, \alpha_{XW}, \alpha_{XSCF}, \underbrace{\quad 0 \quad , \quad 0, \quad 0, \quad 0, \quad 0, \alpha_{XLogK6}}_{\text{Log K's independency}})$$

The vector 'u' is represented by $u = \begin{Bmatrix} u_{X_\Delta} \\ u_{X_W} \\ u_{X_{SCF}} \\ u_{X_{LogK}} \end{Bmatrix}$

The linearized series system model is represented by $_i - \ ^T_i U = 0$ where each α_i are the alpha vectors at the design points considered. β_{oi} represents the accumulated reliability index for the hot spots considered. Therefore, the linearized safety margins can be written:

$$M_1 = \ _0 - \ X_\Delta \cdot u_{X_\Delta} - \ X_W \cdot u_{X_W} - \ X_{SCF} \cdot u_{X_{SCF}} - \ X_{LogK1} \cdot u_{X_{LogK1}} = 0$$
$$M_2 = \ _0 - \ X_\Delta \cdot u_{X_\Delta} - \ X_W \cdot u_{X_W} - \ X_{SCF} \cdot u_{X_{SCF}} - \ X_{LogK2} \cdot u_{X_{LogK2}} = 0$$
$$M_3 = \ _0 - \ X_\Delta \cdot u_{X_\Delta} - \ X_W \cdot u_{X_W} - \ X_{SCF} \cdot u_{X_{SCF}} - \ X_{LogK3} \cdot u_{X_{LogK3}} = 0$$
$$M_4 = \ _0 - \ X_\Delta \cdot u_{X_\Delta} - \ X_W \cdot u_{X_W} - \ X_{SCF} \cdot u_{X_{SCF}} - \ X_{LogK4} \cdot u_{X_{LogK4}} = 0$$
$$M_5 = \ _0 - \ X_\Delta \cdot u_{X_\Delta} - \ X_W \cdot u_{X_W} - \ X_{SCF} \cdot u_{X_{SCF}} - \ X_{LogK5} \cdot u_{X_{LogK5}} = 0$$
$$M_6 = \ _0 - \ X_\Delta \cdot u_{X_\Delta} - \ X_W \cdot u_{X_W} - \ X_{SCF} \cdot u_{X_{SCF}} - \ X_{LogK6} \cdot u_{X_{LogK6}} = 0$$

Similar model can be established for different combinations of correlation/dependencies between the stochastic variables. For instance:

Case 2:

- Δ 's fully correlated
- X_W 's fully correlated
- X_{SCF} 's independent
- Log K 's independent

$$M_1 = \ _0 - \ X_\Delta \cdot u_{X_\Delta} - \ X_W \cdot u_{X_W} - \ X_{SCF_1} \cdot u_{X_{SCF_1}} - \ X_{LogK1} \cdot u_{X_{LogK1}} = 0$$
$$M_2 = \ _0 - \ X_\Delta \cdot u_{X_\Delta} - \ X_W \cdot u_{X_W} - \ X_{SCF_2} \cdot u_{X_{SCF_2}} - \ X_{LogK2} \cdot u_{X_{LogK2}} = 0$$
$$M_3 = \ _0 - \ X_\Delta \cdot u_{X_\Delta} - \ X_W \cdot u_{X_W} - \ X_{SCF3} \cdot u_{X_{SCF_3}} - \ X_{LogK3} \cdot u_{X_{LogK3}} = 0$$
$$M_4 = \ _0 - \ X_\Delta \cdot u_{X_\Delta} - \ X_W \cdot u_{X_W} - \ X_{SCF4} \cdot u_{X_{SCF_4}} - \ X_{LogK4} \cdot u_{X_{LogK4}} = 0$$
$$M_5 = \ _0 - \ X_\Delta \cdot u_{X_\Delta} - \ X_W \cdot u_{X_W} - \ X_{SCF_5} \cdot u_{X_{SCF_5}} - \ X_{LogK5} \cdot u_{X_{LogK5}} = 0$$
$$M_6 = \ _0 - \ X_\Delta \cdot u_{X_\Delta} - \ X_W \cdot u_{X_W} - \ X_{SCF6} \cdot u_{X_{SCF6}} - \ X_{LogK6} \cdot u_{X_{LogK6}} = 0$$

Case 3:

- Δ ‘s independent
- X_W ‘s fully correlated
- X_{SCF} ‘s fully correlated
- Log K ‘s independent

$$M_1 = {}_0 - X_{\Delta_1} \cdot u_{X_{\Delta_1}} - X_W \cdot u_{X_W} - X_{SCF} \cdot u_{X_{SCF}} - X_{LogK1} \cdot u_{X_{LogK1}} = 0$$
$$M_2 = {}_0 - X_{\Delta_2} \cdot u_{X_{\Delta_2}} - X_W \cdot u_{X_W} - X_{SCF} \cdot u_{X_{SCF}} - X_{LogK2} \cdot u_{X_{LogK2}} = 0$$
$$M_3 = {}_0 - X_{\Delta_3} \cdot u_{X_{\Delta_3}} - X_W \cdot u_{X_W} - X_{SCF} \cdot u_{X_{SCF}} - X_{LogK3} \cdot u_{X_{LogK3}} = 0$$
$$M_4 = {}_0 - X_{\Delta_4} \cdot u_{X_{\Delta_4}} - X_W \cdot u_{X_W} - X_{SCF} \cdot u_{X_{SCF}} - X_{LogK_4} \cdot u_{X_{LogK_4}} = 0$$
$$M_5 = {}_0 - X_{\Delta 5} \cdot u_{X_{\Delta 5}} - X_W \cdot u_{X_W} - X_{SCF} \cdot u_{X_{SCF}} - X_{LogK_5} \cdot u_{X_{LogK_5}} = 0$$
$$M_6 = {}_0 - X_{\Delta_6} \cdot u_{X_{\Delta_6}} - X_W \cdot u_{X_W} - X_{SCF} \cdot u_{X_{SCF}} - X_{LogK_6} \cdot u_{X_{LogK_6}} = 0$$

Case 4:

- Δ ‘s independent
- X_W ‘s independent
- X_{SCF} ‘s independent
- Log K ‘s independent

$$M_1 = {}_0 - X_{\Delta_1} \cdot u_{X_{\Delta_1}} - X_{W_1} \cdot u_{X_{W_1}} - X_{SCF_1} \cdot u_{X_{SCF_1}} - X_{LogK_1} \cdot u_{X_{LogK_1}} = 0$$
$$M_2 = {}_0 - X_{\Delta_2} \cdot u_{X_{\Delta 2}} - X_{W_2} \cdot u_{X_{W_2}} - X_{SCF_2} \cdot u_{X_{SCF_2}} - X_{LogK2} \cdot u_{X_{LogK2}} = 0$$
$$M_3 = {}_0 - X_{\Delta_3} \cdot u_{X_{\Delta_3}} - X_{W_3} \cdot u_{X_{W_3}} - X_{SCF_3} \cdot u_{X_{SCF_3}} - X_{LogK3} \cdot u_{X_{LogK3}} = 0$$
$$M_4 = {}_0 - X_{\Delta_4} \cdot u_{X_{\Delta_4}} - X_{W_4} \cdot u_{X_{W_4}} - X_{SCF_4} \cdot u_{X_{SCF_4}} - X_{LogK4} \cdot u_{X_{LogK4}} = 0$$
$$M_5 = {}_0 - X_{\Delta 5} \cdot u_{X_{\Delta 5}} - X_{W_5} \cdot u_{X_{W_5}} - X_{SCF_5} \cdot u_{X_{SCF_5}} - X_{LogK5} \cdot u_{X_{LogK5}} = 0$$
$$M_6 = {}_0 - X_{\Delta_6} \cdot u_{X_{\Delta_6}} - X_{W_6} \cdot u_{X_{W_6}} - X_{SCF_6} \cdot u_{X_{SCF_6}} - X_{LogK6} \cdot u_{X_{LogK6}} = 0$$

The correlation between the linearized limit state equations is given by ρ_{ij} which is calculated by ${}_{ij} = {}^{-T-}_{i}{}_{j}$. In a series system model (level 1 in Figure 9), a high correlation coefficient implies larger reliability. On the other hand, for a parallel system the independency between elements implies higher system reliability.

Once the linearized system has been established, the next step is to define the failure mechanisms in a sequence of failure in order to calculate the system reliability index (β^s) which is estimated by solving the linearized system equation considering e.g. lower and upper Ditlevsen bounds in SYSREL.

Figure 11 shows a sketch of a sequence of failures with three Level 2 (L2) parallel mechanisms linked with each other. Each parallel mechanism is considered to be a minimal-cut set in the sequence of failure which has six linearized limit state equations or components (hot spots) whit the same reliability index (β_{oi}).

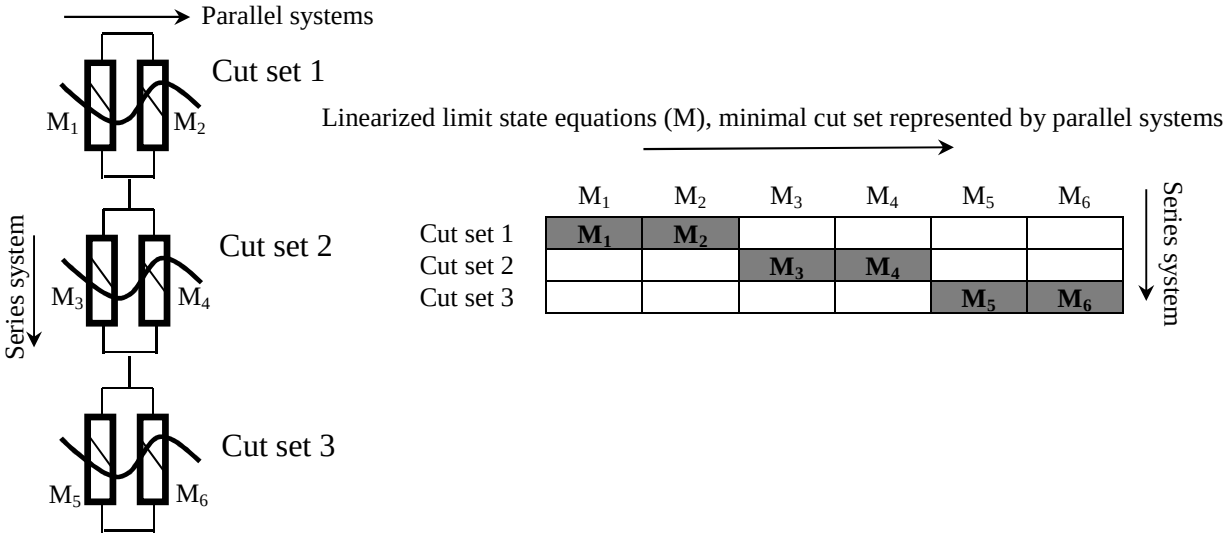

Figure 11. Example of a linearized system model in SYSREL using minimal-cut sets.

Figure 12 taken from Appendix A.3 shows some fatigue failure sequences configured with different mechanism levels.

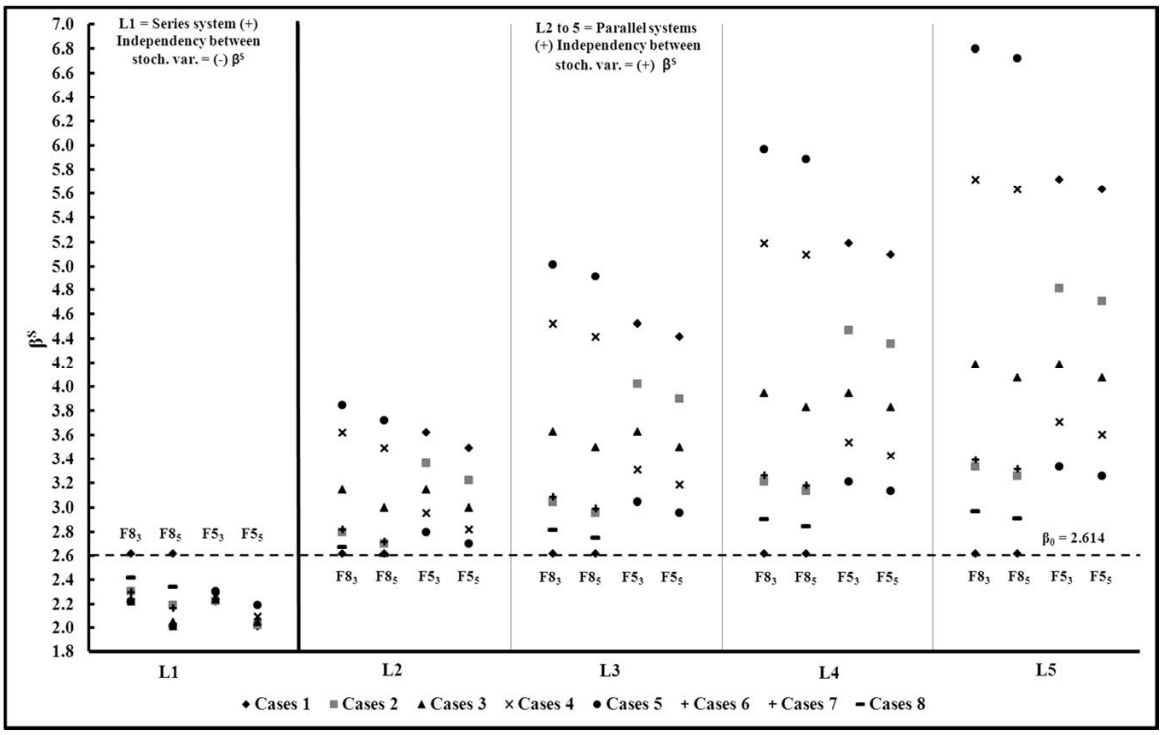

Figure 12. Representative scheme of the general system reliability approach.

The nomenclature used in Figure12 is described in detail in Appendix A.3 on system effects of fatigue failure modes for welded details in jacket type OWT substructures. From the figure 12, it is seen that more independence between stochastic variables implies a decrease in the structural system reliability. On the other hand, taking into account loads redistribution between the structural components, series systems of parallel mechanism show that more independence between stochastic variables can imply an increase in the structural system reliability.

Chapter 5

OPERATIONAL CONTROL STRATEGIES FOR FATIGUE

5.1 Influence of operational aspects

In Directive 2009/28/EC it is stated that every member of the EU should produce 20% of the overall share of electricity production from renewable sources by 2020 with an additional 10% for the transportation sector. As a result, Denmark based on its national action plans will satisfy successfully that request by increasing the wind energy production which is estimated to be around 11,000 GWh by 2020. One-third of the total capacity and about 50% of energy production is expected to be from offshore wind turbines (Schwabe et al. 2011).

Offshore wind turbines are exposed to severe environmental conditions as well as larger uncertainties which are associated with strong wind and large wave loads. Offshore locations can potentially make the offshore wind energy production expensive due to high costs of the substructures, which must resist higher fatigue loads, corrosion and wear caused by the harsh environmental conditions. As mentioned in the introduction, the key goal is to decrease the cost of energy (CoE). Therefore, a detailed treatment of the uncertainties must be done improving the design and optimizing the plans of installation, operation and maintenance of the offshore wind infrastructures. The treatment of the uncertainties must consider that wind turbines are operated with specific and detailed power production configurations, which are inherently linked to fatigue reliability levels in the components to be analysed.

The wind speed changes fast and randomly in time and space, requiring the use of complex control systems integrated in the wind turbine such as active pitch control, yaw control, etc. Control systems determine the potential power output of the offshore wind turbine and can help keep reasonable levels of structural integrity. In Figure 13, operational control systems are sketched as mediators between power production, structural response and external loads. Therefore, in order to determine the impact of the control strategies, a reliability-based approach can be established based on stochastic models for the fatigue failure. The objective is to identify cost-optimal control strategies.

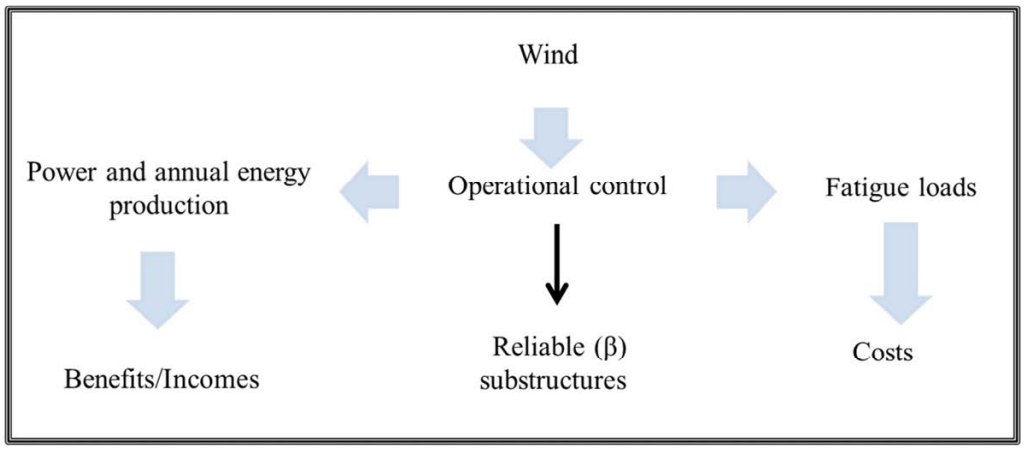

Figure 13. Relationship between operational controls and reliable OWT's substructures.

Figure 14 shows the general components involved in the costs of wind energy where the influence of the operational control is represented by a cost-benefits relationship. This relationship depends on fatigue damage and energy losses. A level IV reliability method needs to be developed where the reliability index is estimated by a fatigue stochastic model and linked with a cost-benefit study.

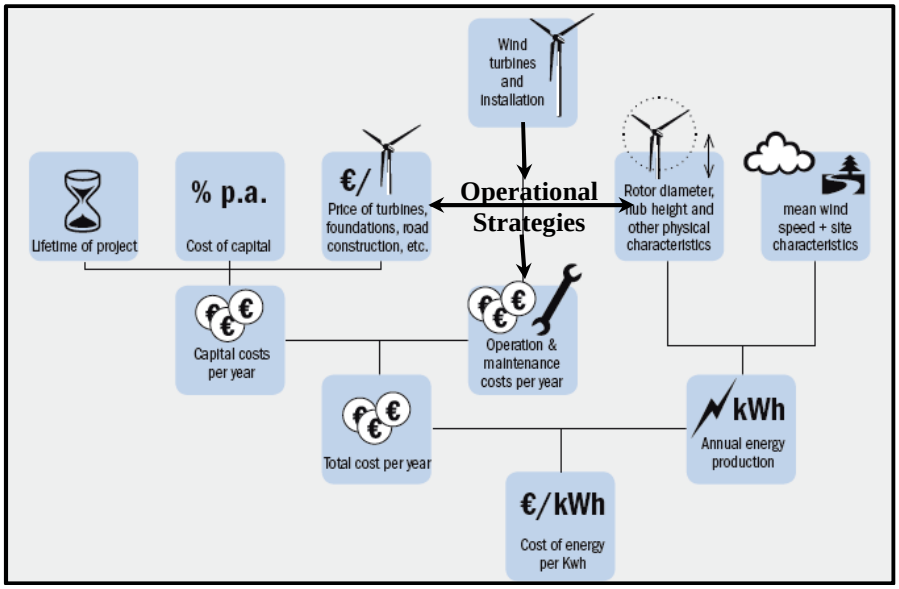

Figure 14. Main components involved in the costs of wind energy (From Schwabe et al. 2011).

Figure 15 shows the direct operational control influence for an offshore wind turbine substructure where operational strategies are related to the structural response, for instance taking into account hot spot 'A' where changes in the control configuration imply a direct influence on the fatigue loads and at the same time influence the production of the annual wind energy. This means that varying production periods, operational wind speed and desired energy production may have a significant effect on the structural reliability, and a positive economic impact could be involved. This problem is considered in Appendix A.4 with the main objective to analyse the cost-benefit impact due to operational strategy changes. In Appendix A.4, the influence of the operational control for a wind turbine is studied with the main objective to optimize the design of the substructures with respect to fatigue loads and, as a consequence, decrease the cost of energy (CoE) for offshore wind turbine substructures. The influence of the operational strategy on the structural reliability is established by limit state equations based on the S-N approach where the fatigue damage propagation is included for a jacket type substructure.

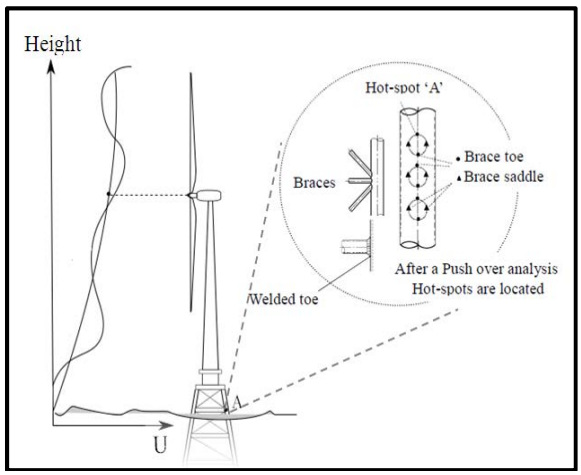

Figure 15. Operational control influence in the fatigue loads at Hot spot 'A'.

Operational conditions are generally characterized by:

- Wind speed at the site
- Wind turbine power curve
- Operational modes
- Wind farm layout
- Wind turbulence intensity
- Extreme loads and recurrence periods
- Wake effects

These conditions are considered in the models described below and in Appendix A.4.

5.2 Cost of Energy (CoE)

In Fingersh et al. (2006), the cost of the energy is defined by:

$$\mathrm{CoE} = \frac{(\mathrm{FCR\ x\ ICC})}{\mathrm{AEP_{net}}} + \mathrm{AOE} \tag{14}$$

where 'CoE' is considered the cost of energy ($/kWh) (constant $), 'FCR' is the fixed charge rate (constant $) (1/yr), 'ICC' represents the initial capital cost ($), 'AEPnet' is equal to the net annual energy production (kWh/yr), 'AOE' is the annual operating expenses which is defined by Equation (15).

$$\mathrm{AOE} = \mathrm{LLC} + \frac{(\mathrm{O\,\&\,M\ +\ LRC})}{\mathrm{AEP_{net}}} \tag{15}$$

where 'LLC' is land lease cost (not relevant for offshore sites), 'O&M' is the O&M costs and LRC represents replacement/overhaul cost.

In Equation (14), the initial capital cost (ICC) is defined by the sum of the *turbine system cost* and the *balance of station cost*. Accordingly, the turbine system costs can be defined by e.g. the main wind turbine component costs such as rotor, drive train, nacelle, operational controls, safety system, condition monitoring and tower. Therefore, the main elements are defined and classified in the following.

- Rotor
  - Blades
  - Hub
  - Pitch mechanisms and bearings
  - Spinner, nose cone

- Drive train, nacelle
  - Low-speed shaft
  - Bearings
  - Gearbox
  - Mechanical brake, high-speed coupling, and associated components
  - Generator

    - Variable-speed electronics
    - Yaw drive and bearing
    - Main frame
    - Electrical connections
    - Hydraulic and cooling systems
    - Nacelle cover

- Control, safety system, and condition monitoring

- Tower

- Balance of station
    - Foundation/support structure
    - Transportation
    - Roads, civil work
    - Assembly and installation
    - Electrical interface/connections
    - Engineering permits

When offshore turbines are evaluated with respect to costs, the following additional components should be considered:

- Marinization (added cost to handle marine environments)
- Port and staging equipment
- Personal access equipment
- Scour protection
- Surety bond (to cover decommissioning)
- Offshore warranty premium

CoE has a clear relationship to the turbine system costs and foundation/support structure costs where operational controls, safety systems and conditional monitoring clearly play an important role. This relationship is already presented in Figures 13, 14 and 15. Thereby, an 'optimal costs-benefits model' needs to be established.

5.3 Economical Model: Costs vs. benefits

In Appendix A.4, a 'simple' cost model is established where the costs of the optimal 'reduced' operational strategy are determined by considering the reduction in the annual energy production if the operation of the wind turbine is reduced during the service life of the offshore wind turbine. Moreover, the benefit is estimated from the reduced initial design cost due to material savings of the substructure. Therefore, the decision problem is formulated as an optimization problem considering the cost-benefit relationship:

$$\begin{aligned} &\max_{p(z,op)} \quad \Delta W(z,op) = B_T(z,op) - C_T(z,op) \\ &\text{s.t. } \Delta P_t(t,z,op) \le \Delta P_F^{max} \quad , \quad t = 1,2,\dots,T_L \end{aligned} \tag{16}$$

The optimization model maximizes the cost-benefit where 'B_T' is the total expected benefits during the service life 'T_L' considering the influence of the operational strategies (op) and material design represented by a design variable (z), e.g. a cross-sectional geometrical parameter of a tubular member. 'C_T' is the total costs due to reduced energy production associated with the operational strategies (op). It is assumed that marginal changes in expected benefits by reduced material consumption (due to reduced fatigue load) can be written as $\Delta B_T(z,op) = C_z \cdot \Delta z$ where 'C_z' represents the cost of steel in the market and 'Δz' is the marginal change in saved material in the substructure. Further, it is assumed that marginally $\Delta C_T(z,op) = C_E \cdot \Delta E$ where 'C_E' is the cost of the energy in the supplier marked and 'ΔE' is the change in reduction of energy produced due to changes in the operational configuration (op). Therefore, the change in total income (ΔW) will depend of the operational strategy (op) and of the ratio of the unit costs $R = \left(\frac{C_E}{C_Z}\right)$.

5.4 Operational strategies

In order to investigate the influence of operational control, the influence of the Weibull 'tails' on the annual energy production is especially considered, see Figure 16.

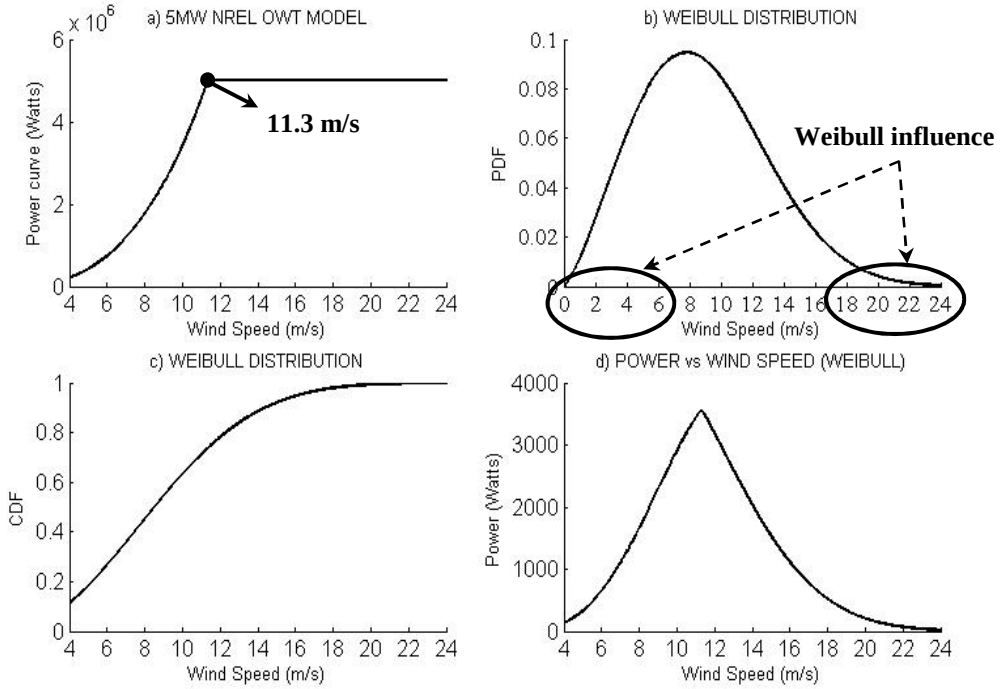

Figure 16. Wind power vs. wind speed considering the influence of the Weibull 'tails'.

The optimal control configuration has the important aim to produce maximum annual wind energy with acceptable quality and at the same time reducing the fatigue loads. The main key to find the optimal operational strategy is to get a balance between the minimum losses of annual energy production and an acceptable reliability level.

Operational control strategies can change during the service life of an OWT substructure. Thereby, the influence of each strategy can be estimated considering the influence of the Weibull 'tails' on the annual energy production, see Figure 17 where two cases are analysed in detail:

Case 1: (22-24)U(1-25)T
Case 2: (4-6)U(1-25)T+(20-22)U(25-25)T+(22-24)U(1-25)T

'U' is the operational mean wind speed in (m/s), and 'T' represents years to be 'eliminated' from production. e.g. '(22-24)U(1-25)T' indicates that the wind turbine is parked for mean wind speeds in the interval [22-24 m/s] from year 1 to year 25. The service life of the wind turbine (T_L) is considered to be 25 years.

In Figure 17, Cases 1 and 2 are graphically represented where the scratched areas represent the operational periods which the wind turbine is in parked conditions.

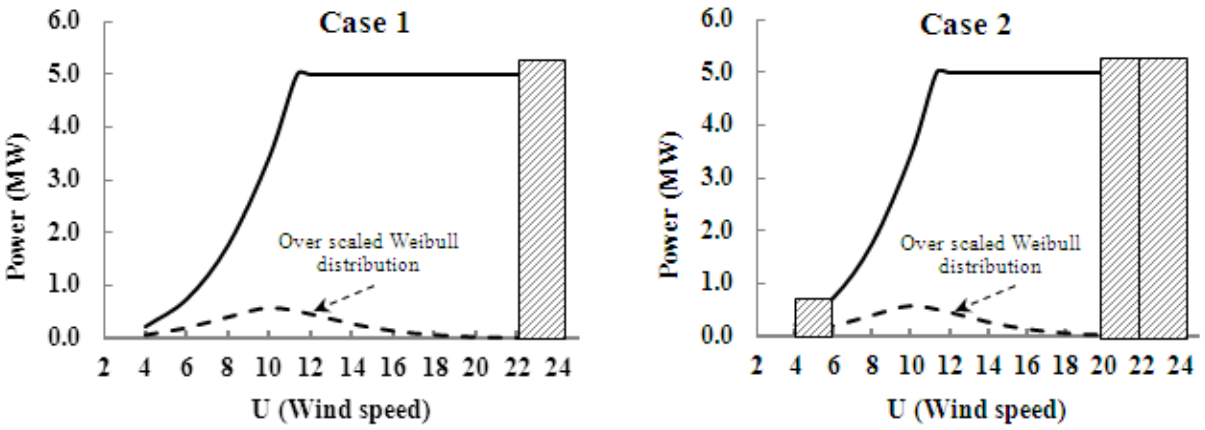

Figure 17. Operational strategies: Cases 1 and 2.

In Tables 3 and 4, the operational control strategies are shown by a matrix representation where the columns represent each year of the operational wind turbine service life and the rows are the operational mean wind speeds.

Table 3. Matrix configuration of Case 1: (22-24)U(1-25)T where the wind turbine is in parked condition.

	Operational control strategy																								
vel /year	1	2	3	4	5	6	7	8	9	10	11	12	13	14	15	16	17	18	19	20	21	22	23	24	25
4 m/s																									
6 m/s																									
8 m/s																									
10 m/s																									
12 m/s																									
14 m/s																									
16 m/s																									
18 m/s																									
20 m/s																									
22 m/s																									
24 m/s																									

Table 4. Matrix configuration of Case 2: (4-6)U(1-25)T+(20-22)U(25-25)T+(22-24)U(1-25)T where the wind turbine is in parked condition.

	Operational control strategy																								
vel /year	1	2	3	4	5	6	7	8	9	10	11	12	13	14	15	16	17	18	19	20	21	22	23	24	25
4 m/s																									
6 m/s																									
8 m/s																									
10 m/s																									
12 m/s																									
14 m/s																									
16 m/s																									
18 m/s																									
20 m/s																									
22 m/s																									
24 m/s																									

Once the operational strategy have been defined, the annual energy production and reduction in energy produced, $\overline{P}_W$, can be estimated for the reference 5MW NREL offshore wind turbine by Equation (17):

$$\overline{P}_W = \sum_{i=1}^{T_L} \sum_{j=1}^{N_B} \left\{ \exp\left[-\left(\frac{U_{j-1}}{A} \right)^B \right] - \exp\left[-\left(\frac{U_j}{A} \right)^B \right] \right\} P_W \left(\frac{U_{j-1} + U_j}{2} \right) \quad (17)$$

For the Weibull distribution, 'A' is the scale factor considered equal to 10 m/s, and 'B' is a shape factor assumed equal to 2.30. 'U' is the mean wind speed in (m/s), and 'T_L' is the service life (in years). N_B represents the bins. $U_{cut\text{-}in}$ and $U_{cut\text{-}out}$, are the cut-in and cut-out mean wind speeds, respectively. Thereby, the annual energy production can be estimated. The reduced energy production ('losses' of energy) can be estimated for each mean wind speed defined by the bins.

Table 5 shows the Annual energy produced by a wind turbine estimated as well as the annual energy 'losses' according to the operational strategy defined in Case 2 and Equation (17).

Table 5. Annual energy and total energy losses for Case 2 after 25 years for 5MW NREL wind turbine.

$U_{cut\text{-}in}$ /$U_{cut\text{-}out}$ (m/s)	**Annual energy production (MWhr)**	**Case 2 Operational strategy**	**Energy losses (MWhr)**
(4-6)	610.96	(610.96)(25years)=	15274.02
(6-8)	1957.13		--
(8-10)	4012.65		--
(10-12)	5779.41		--
(12-14)	4560.31		--
(14-16)	2712.24		--
(16-18)	1379.51		--
(18-20)	600.12		--
(20-22)	223.06	(223.06)(1 years)=	223.06
(22-24)	70.72	(70.72)(25 years)=	1767.93
Total:	21906.11		17,265.01

After a service life of 25 years, the total energy produced is equal to 547,652 MWhr, and the total energy 'loss' is 17,265 MWhr corresponding to 3.15% of the total amount of energy produced by the 5MW offshore wind turbine. Likewise in Figure 18, twenty four operational control strategies are plotted taking into account the energy losses.

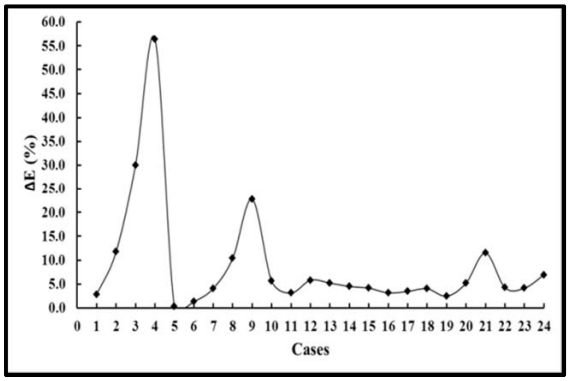

Figure 18. Total energy losses after 25 years for cases defined in Appendix A.4.

5.5 Reliability assessment

In Appendix A.4 is presented a representative stochastic model based on DNV-RP-C203 (2012). Design and limit state equations are established where the operational strategies can be taken into account in both design and reliability assessment with respect to fatigue failure. A wind turbine substructure with service life (T_L) equal to 25 years and fatigue design life (T_F) equal to 75 years is considered, i.e. the fatigue design factor (FDF) is equal to 3 as recommended by various design standards.

Table 6 shows the reliability assessment of Hot spot 'A' (Figure 15) in the form of the annual, the accumulated reliability indices and also the design parameter 'z' considering *'normal operational conditions'* for two different S-N curves, se below:

Table 6. Reliability assessment normal operational conditions (Appendix A.4).

S-N curve	β_o	$\Delta\beta_o$	z
D	2.61	3.25	0.96
F	2.61	3.25	1.21

Design parameter 'z' could represent the normalized cross sectional area. In a reliability assessment, the cross section parameter 'z' can be estimated in design by different operational strategies and the reliability assessment can be performed as follows:

1. Design: Normal operational configuration (i.e. no reduction in operation)
   Reliability assessment: Normal operational configuration (i.e. no reduction in operation)
2. Design: Normal operational configuration
   Reliability assessment: An operational strategy is applied (due to less fatigue load cycles the reliability is increased)
3. Design: An operational strategy is applied
   Reliability assessment: An operational strategy is applied
4. Design: 'z' parameter is modified (by iterations) such that the same reliability level is obtained as in a normal operational configuration (as obtained in point 1). In Appendix A.4, examples are shown how the design parameter thereby can be reduced due to the decrease in fatigue cyclic loads.
   Reliability assessment: An operational strategy is applied

In Appendix A.4, different operational strategies by considering Point 4 (above mentioned) are modelled and applied in a reliability assessment. Applying the 'simple' economic model, Figure 19 shows the ratio of saved steel material vs. increased income considering the operational strategies defined in Appendix A.4 where a steel unit cost in the marked, C_Z=1.0, and the ratio of the unit costs equal to C_E/C_Z = 0.30 are used. It is seen that Cases 5 and 16 can be considered as optimal 'reduced' operational strategies corresponding to an optimum 'equilibrium' between costs and benefits maximizing the CoE. For Case 5, the marginal material change, Δz, is 0.20% while the loss of energy, ΔE, is estimated equal to 0.32%. The positive income, ΔW, becomes 0.10%. Similarly, for Case 16 a positive income, ΔW, is estimated to approximately 0.06% using that marginal changes in Δz and ΔW are equal to 1.0% and 3.15%, respectively. The potential actual increase in income, ΔW, should be considered taking into account the high costs of the substructures and therefore the benefits during in design life may be substantial.

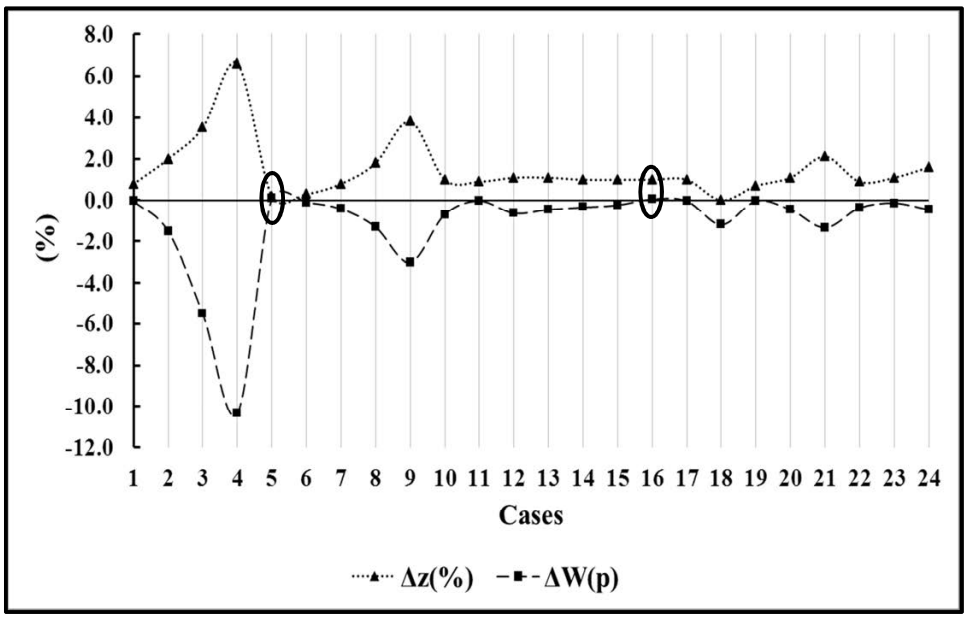

Figure 19. Steel material saved vs. increased incomes produced in the offshore wind turbine substructure considering the operational configuration strategies defined in Appendix A.4. C_z=1.0 and C_E/C_z=0.30.

Chapter 6

RELIABILITY-BASED INSPECTION PLANNING

6.1 Introduction

In the oil and gas industry, risk and reliability based inspection planning (RBI) strategies have been developed in order to optimize the cost of inspection planning and also the design of the substructures with respect to fatigue loads. RBI has also been considered for application in offshore wind turbines considering special aspects such as wind dominated loading, wind farm locations with wake effects, internal dependence of different components (mechanical, electrical and structural) and the effect of the wind turbine control system. A chronological background, which joins the oil and gas expertise together with its applications in offshore wind industry, can be found in e.g. Skjong (1985), Madsen (1987), Thoft-Christensen and Sørensen (1987), Fujita et al. (1989), Madsen and Sørensen (1990), Sørensen and Faber (1991), Moan (1993, 2005 and 2009), Faber et al. (2005), Sørensen et al. (2005), Sørensen et al. (2007), Sørensen (2009), Rangel and Sørensen et al. (2010), Dong et al. (2010) and recently Nielsen (2013). In Straub et al. (2006), RBI is considered a suitable strategy to inspect and control the deterioration damage in offshore substructures looking for economic benefits.

Bayesian decision analysis and structural reliability methods compose the basic principles of the RBI planning which requires a significant computational effort. In Faber et al. (2000), Straub (2004), Faber et al. (2005) and Straub and Faber (2006), the computational efficiency has been solved/improved by the application of a generic approach which makes RBI convenient for applications in offshore structures.

The RBI analysis represents an effective method to deal with structures exposed to deterioration damage where the most suitable maintenance strategy is identified by a ‘decision tool’. The decision analysis will accomplish the task of directing the necessary and sufficient mitigation activities. The decision analysis is based on information previously collected. In simpler terms, RBI analysis is defined as a methodological procedure applied to build up the cheapest inspection plans with all its benefits involved. The main steps of this methodology for steel offshore structures are e.g. described following Rouhan et al. (2004). In short, these steps are described as:

1. Collection of information
2. Risk screening meeting
3. Detailed RBI which addresses inspection plan for each relevant tubular joint and also can be extended to systems taking into account the correlation between hot spots
4. A first scheduling phase
5. The inspection campaign is established for the offshore wind turbine farm, given the results of the first scheduling phase

For existing structures, the reliability can be updated based on e.g. the following information:

- No-failure: Information that the structure has survived up to a given date can be used to update the reliability for the remaining design lifetime.
- Inspections: Information resulting from inspections can be used to update the estimate of the reliability for the remaining design lifetime. Inspection results could be no-detection or detection of cracks with measured/estimated crack lengths. It is important to consider the

reliability of the inspection methods which can be modelled by probability of detection curves (POD curves).
- Information to improve the estimate of the fatigue load, e.g. from condition monitoring systems or load observers.

Sørensen (2011) presents a reliability-based calibration of fatigue factors for offshore wind turbines in a wind farm considering wake effects. Tarp-Johansen et al. (2003) establish a calibration of partial safety factors for extreme loads on wind turbines. In this thesis, the influence of inspection is considered in Appendix A.1 where a reliability-based approach is used to assess the calibration of appropriate fatigue design factors (FDF) required for welded details in offshore wind turbines substructures where a stochastic model has been developed for assessment of the reliability with respect to fatigue failure. Fatigue life is modelled by S-N curves where design and limit state equations are established for the accumulated fatigue damage. A fracture mechanics approach is considered for determining the influence of the inspections on the inherent reliability of the substructure.

6.2 Reliability assessment taking into account inspections

For offshore oil and gas structures, inspections of fatigue critical details are often performed in order to secure a sufficient reliability level. For offshore wind turbines with steel substructures, a similar reliability assessment could be done so as to establish the inspection periods during the service life of the substructure. The reliability assessment can be performed by matching S-N approach with a linear elastic fracture mechanics theory. The S-N approach will define the fatigue damage increment until the first crack appears. A fracture mechanic approach can model the growth of cracks which will depend on the stress time series and stress concentrations in fatigue critical details e.g. obtained by a finite element analysis. The costs of inspections and possible repairs in case of fatigue cracks should be compensated by a cheaper initial cost due to lower fatigue design factors. Appendix A.1 describes the basis for reliability and risk-based inspection planning taking into account their influence on the reliability level.

Inspection planning can be based on the requirement that the annual probability of failure in all years has to satisfy a reliability constraint:

$$\Delta P_F(t) \le \Delta P_{F,MAX}\,,\ 0 \le t \le T_L \tag{18}$$

where $\Delta P_{F,MAX}$ is the maximum acceptable annual probability of failure. A similar requirement can be formulated based on the cumulative probability of failure:

$$P_F(T_L) \le P_{F,MAX} \tag{19}$$

Inspection plans are often based on two assumptions. The first assumption considers no cracks detection. However, if a crack is found, then a new inspection plan has to be made based on the observation and available information. The second assumption establishes that if inspections are made and the probability of fatigue failure exceeds a critical defined value, then inspections are made considering different time intervals. Often this approach results in increasing time intervals between inspections.

The inspection planning procedure described above does not consider the costs of inspections, repairs and failures. Costs are taken into account by a risk-based inspection planning approach where the following additional information is required:

- A decision rule to be used in connection with inspections. The decision rule should specify the action to be taken if a crack is detected. This could be grinding, repair by welding, not repair, replacement, etc.
- Costs of inspections
- Costs of repairs
- Costs of failure
- Discounting

Further, a model is needed for estimating the probability of collapse (total failure) given fatigue failure of the detail considered.

For an existing structure, the reliability can be updated based on the available information. The following type of information can be used: if an inspection has been performed at an initial time (T_I) and no cracks are detected, the probability of failure can be updated. In order to model a no-detection event, a limit state equation based on a fracture mechanics approach will be defined modelling the crack growth. The reliability of the inspection methods can be estimated by a probability of detection (POD) curve.

6.3 Fatigue lives modelled by Fracture Mechanics (FM) approach

The Fracture Mechanics approach, which is considered the 'heart' of the risk based inspection planning (RBI), will model the crack growth determining the structural fatigue failure. Figure 20 shows different cracks growth models that can be used depending on the fatigue critical detail. An FM model is calibrated such that the same reliability level is obtained by using the S-N approach which is based on fatigue tests. Straub (2004) performs a calibration by a least-squares algorithm based on β-space and also Nielsen (2013) describes a calibration process for fatigue progressive damage:

1. The service life (T_L) of the substructure involved will determine the number of time steps to be analysed.
2. The probabilistic model, which contains the stochastic information, is established by an S-N approach which defines the fatigue damage until the first crack appears. In the S-N approach described in Chapter 3, the fatigue life (T_F) of the substructure is modelled by the limit state equation.
3. The reliability index is determined for each time step (service year) by reliability methods such as FORM/SORM and/or simulation techniques such as Monte Carlo Simulation.
4. An FM model is chosen.
5. The FM approach is initialized with parameters according to the FM model.
6. The variables to be optimized are set to initial values.
7. As in step 3, the reliability index as function of time using the FM model is estimated.
8. An optimization algorithm is applied and the optimization parameters in the FM model are determined such that the difference in reliability obtained by the FM and S-N approaches is minimized.

Since initiation or nucleation, propagation and failure represent the phases of cracks due to fatigue damage, the material fatigue life (N) is often represented by Equation (20):

$$N = N_I + N_P \tag{20}$$

where 'N' is the number of stress cycles to failure; N_I represents the fatigue initial life estimated by the number of stress cycles to the crack nucleation. N_I can be considered as a stochastic variable which represents the *uncertainty* due to the crack initiation time. N_P represents the fatigue propagation life, which is considered as the number of stress cycles from crack initiation until the crack goes through the material thickness or until a critical crack size is reached (unstable crack growth).

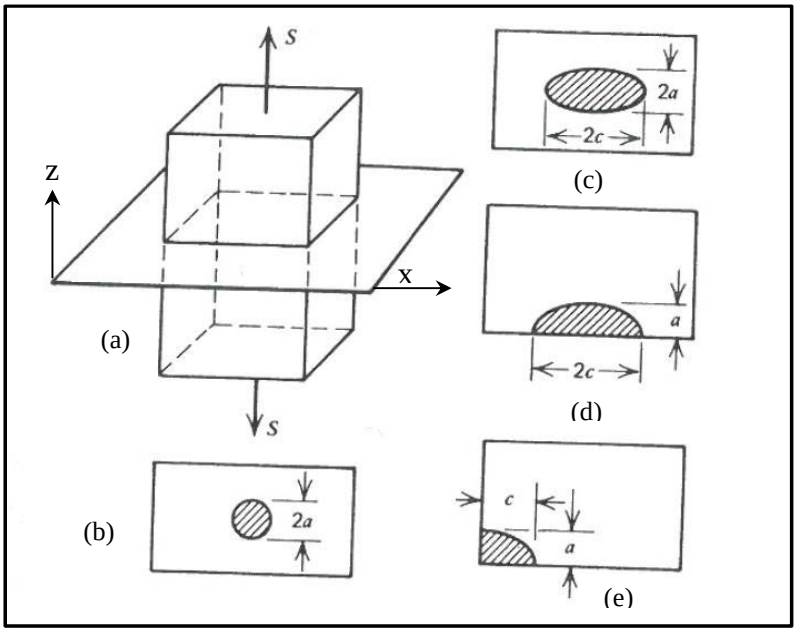

Figure 20. Common circular and elliptical embedded surface cracks, a) Tensile loading (s) and crack plane (x,y), b) Embedded circular crack, c) Embedded elliptical crack, d) Surface semi-elliptical crack and e) Quarter-elliptical corner crack. (Stephens et al. 2001)

The crack propagation phase represented by the crack growth rate can be modelled by the Paris' law where the following one-dimensional crack growth model is used for the crack depth '***a***' as function of number of cycles ***N***. A bi-dimensional crack growth model for steel jacket substructures can also be used, see e.g. Sørensen et al. (2005).

$$\frac{da}{dN} = C \cdot \Delta K(a)^m, \qquad a(0) = a_0 \tag{21}$$

'C' and 'm' are material parameters estimated by laboratory testing; 'a_0' describes the crack depth after (N_I) cycles. The stress intensity ranges is estimated from:

$$\Delta K(a) = Y \Delta_e \sqrt{a} \tag{22}$$

where 'Y' in a probabilistic modelling models the *uncertainty* related to geometry function. Specific models for the stress intensity ranges ΔK(a) for one- and two-dimensional models can be found in BS7910 (2005) for a number of different geometries and loading conditions.

$\Delta\sigma_e$ represents the equivalent stress range determined by Equation (23):

$$\Delta_e = \left(\frac{1}{n} \sum_{i=1}^{n} \Delta_i^m \right)^{1/m} \tag{23}$$

The total number of stress ranges per year, n is given by:

$$n = \sum_{i=1}^{n} n_i \tag{24}$$

The stress ranges Δ are in a probabilistic modelling defined by Equation (25):

$$\Delta = X_W X_{SCF} \cdot Y \cdot \Delta_e \tag{25}$$

X_W and X_{SCF} are stochastic variables which represent the ***model uncertainties*** related to modelling the external fatigue loads and the estimating the stress concentration factors given the fatigue loads, respectively.

A representative ***stochastic model*** presented in Appendix A.1 is shown in Table 7, partially based on BS 7910 (2005).

Table 7. Uncertainty modelling used in the fracture mechanical reliability analysis.

Variable	Dist.	Expected value	Standard deviation
a_0	LN	0.2 mm 0.1 mm (high material control) / 0.5 mm (low material control)	0.132 mm
$\ln C$	N	$\mu_{\ln C}$ (reliability based fit to SN approach)	0.77
m	D	m-value (reliability based fit to SN approach)	
X_{SCF}	LN	1	See Appendix A.1
X_W	LN	1	See Appendix A.1
n	D	Total number of stress ranges per year	
a_C	D	(Thickness)	
Y	LN	1	0.1

D: Deterministic, N: Normal, LN: LogNormal

In Table 7**,** the initial crack length is modelled as a stochastic variable with Log-normal distribution, and the crack initiation time N_I is assumed to be neglected. Alternatively in Lassen (1997), the crack initiation time N_I is modelled with a Weibull distribution with expected value μ_0 and coefficient of variation equal to 0.35.

In reliability-based inspection planning, the parameters μ_{lnC} and 'm' can be fitted (as described above) such that the difference between the reliability as function of time using the S-N approach and the fracture mechanical approach is minimized by a optimization algorithm.

The limit state equation can be written in terms of the number of cycles to failure:

$$g(\mathbf{X}) = N - n\,t \tag{26}$$

where ‘t’ is time in the interval from ‘0’ to the service life T_L.

Equivalently, the limit state equation can be written in terms of crack depth:

$$g(\mathbf{X}) = a_c - a(t) \tag{27}$$

where a(t) is the crack depth at time ‘t’ and ‘a_c’ is the critical crack depth, typically the thickness.

6.4 Probability of Detection (POD) curves

A Probability of Detection (POD) curve is needed for each relevant inspection technique to model the reliability of the inspection technique. If inspections are performed using an Eddy Current technique (below or above water) or a MPI technique (below water), the inspection reliability can be represented by following POD curve:

$$\mathrm{POD(x)} = 1 - \frac{1}{1 + \left(\mathrm{x} / \mathrm{x}_0\right)^{\mathrm{b}}} \tag{28}$$

where e.g. x_0 and b are POD parameters which are indicated in Table 8.

Table 8. POD curve parameters from DNV Report No. 95-2018.

Inspection method	x_0	b
MPI underwater	2.950 mm	0.905
MPI above water, Ground test surface	4.030 mm	1.297
MPI above water, Not ground test surface	8.325 mm	0.785
Eddy current	12.28 mm	1.790

Other POD models such as exponential, lognormal and logistics models can be used, for instance considering visual inspections. A POD curve using an exponential model can be written:

$$POD(x) = 1 - \exp\left(-\frac{x}{\lambda}\right) \tag{29}$$

where λ is the expected value of the smallest detectable crack size. The exponential POD curve is used to model visual inspection. Also the Probability of False Indication (PFI) can be introduces and modelled by probabilistic models.

In Appendix A.1, two inspection methods are applied with POD curves sketched in Figure 21:

- Inspection with Eddy Current, see POD curve, see Table 8.
- Visual inspection with an exponential POD curve with expected value of the smallest detectable cracks lengths equal to 50 mm.

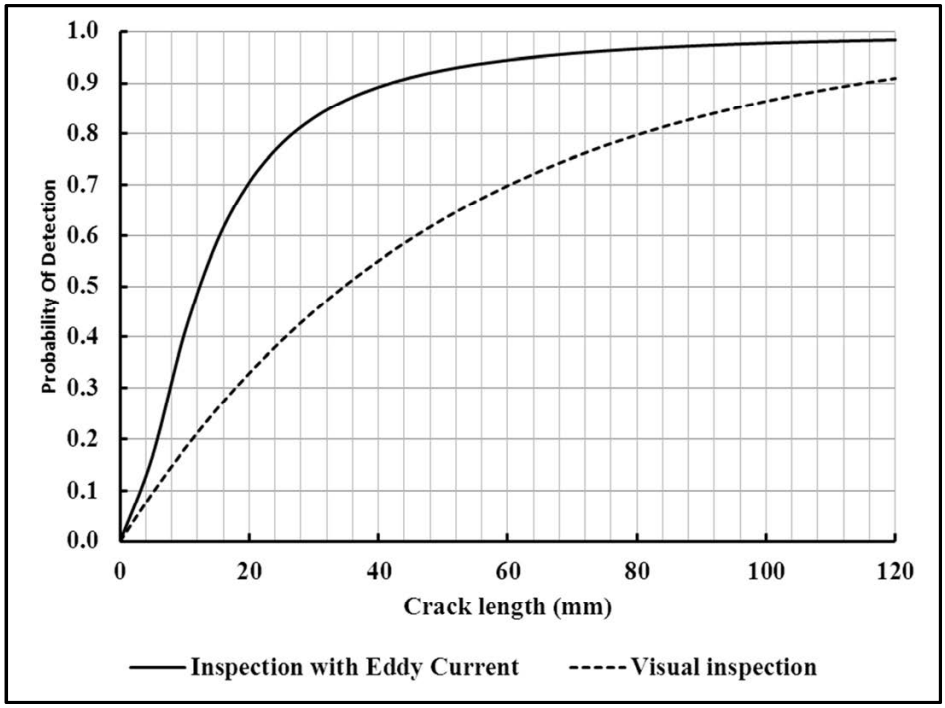

Figure 21. POD curves.

6.5 Updating probability of failure

If an inspection has been performed at time T_I and no cracks are detected, the probability of failure can be updated by:

$$P_F^U\left(t\middle|\text{no - detection at time } T_I\right) = P\left(g(t) \le 0 \middle| h(T_I) > 0\right),\ t > T_I \tag{30}$$

where $h(t)$ is a limit state modelling the crack detection event. If the inspection technique is related to the crack length, $h(t)$ is written as:

$$h(t) = c_d - c(t) \tag{31}$$

where c(t) is the crack length at time t and c_d is smallest detectable crack length. c_d is modelled by a stochastic variable with distribution function equal to the POD curve:

$$F_{c_d}(x) = \text{POD}(x) \tag{32}$$

Similarly, if the inspection technique is related to the crack depth, h(t) is written:

$$h(t) = a_d - a(t) \tag{33}$$

where $a(t)$ is the crack length at time t and a_d is smallest detectable crack length. a_d is modelled by a stochastic variable with distribution function equal to the POD curve:

$$F_{a_d}(x) = \text{POD}(x) \tag{34}$$

If two independent inspections are performed at time T_I and no cracks are detected then the probability of failure can be updated by:

$$P_F^U\left(t\middle|\text{no - detection at time } T_I\right) = P\left(g(t) \le 0 \middle| h_1(T_I) > 0 \cap h_2(T_I) > 0\right),\ t > T_I \tag{35}$$

where $h_1(t) = a_{d_1} - a(T_I)$ and $h_2(t) = a_{d_2} - a(T_I)$ are the limit states modelling the inspections. In the same way other combinations of inspections can be modelled.

6.6. Influence of inspections on reliability assessment

As a safety factor for fatigue design, the Fatigue Design Factor (FDF) value can be used:

$$FDF = \frac{T_F}{T_L} \tag{36}$$

T_L is the design life, and T_F represents the fatigue design life of the substructure. It is worth mentioning that for a linear S-N curve FDF is connected to partial safety factors for fatigue load, γ_f and fatigue strength, γ_m by $FDF = \left(\ _f\ _m\right)^m$.

In Appendix A.1, Tables 9 and 10 show the required FDF values if equidistant inspections are performed considering two types of inspections, inspection with Eddy Current and visual inspection.

The results indicate that significant reductions in required FDF values can be obtained if inspections are performed.

Table 9. Required FDF values for minimum cumulative reliability level. S-N curve: "With cathodic protection". Inspections with the Eddy Current technique.

β/number of inspections	0	1	2	4	10
2.5	3.4	2.7	2.3	1.3	1
3.1	6.1	5.0	4.1	2.8	1

Table 10. Required FDF values for minimum cumulative reliability level. S-N curve: "With cathodic protection". Close visual inspection.

β/number of inspections	0	1	2	4	10
2.5	3.4	3.0	2.7	2.3	1
3.1	6.1	5.3	5.0	3.6	1.3

The results presented in Appendix A.1 show that the basic approach can be used for assessment of the required reliability level as well as for calibration of fatigue design factors estimated for offshore wind turbine substructures.

Chapter 7

STATISTICAL ANALYSIS OF STEEL REINFORCEMENTS AND CONCRETE STRENGTHS

Reliability assessment of both new and existing reinforced concrete structures/components applied in wind turbines is an area in which almost no research has been published. This chapter focuses on probabilistic analysis with respect to fatigue failure of reinforced concrete elements. The analysis is applied in onshore wind turbine foundations and also it could be potentially extended for both onshore and offshore reinforced concrete structures. A probabilistic assessment requires development of stochastic models that account for the uncertainties both in the fatigue strength of the materials and in the external loads due to wind and sea loads. Therefore, a stochastic fatigue model to assess the reliability of reinforced concrete elements is developed in the following. The stochastic modelling considers both the fatigue strength of the steel reinforcement and of the concrete. Fatigue failure of plain concrete is related to the compressive stresses so the steel reinforcement is related to tensile stresses. The stochastic modelling can be considered as a contribution within wind turbine design with the aim of decreasing the costs of energy (CoE). The application of the stochastic models is intended for e.g. the reliability-based calibration of partial safety factors for wind turbine standards. This requires design and limit state equations to be established considering a rational treatment of the uncertainties involved in the complex interaction between two materials, steel reinforcement and concrete, as well as loading from wind and waves.

This chapter describes a statistical analysis of test data from laboratory fatigue tests which have been performed with concrete specimens (Lohaus et al. 2012) and with steel reinforcement bars (Hansen & Heshe, 2001). The statistical analysis is performed using the Maximum-Likelihood Method (MLM). The statistical analysis is based on the number of cycles to failure, and tests with run-outs (no failure) are also taken into account. Further, the effect of statistical uncertainty is evaluated. The statistical model is discussed considering its impact on the fatigue reliability level of reinforced concrete elements.

7.1 Background of test data and statistical analysis

Extensive research has been made with the aim of explaining the behaviour and mechanical response of the materials with respect to fatigue. The mechanical behaviour for use in design codes is typically represented by S-N curves together with Miner's rule. This chapter is, as mentioned above, focused on the reinforced concrete which can be considered as a composite material characterized by the concrete as the matrix and the steel bars as the fibre reinforcement. Therefore, reinforced concrete elements have to be designed to deal with both tensile and compressive stress cycles generated by the external loads.

7.1.1 Test data for fatigue of concrete

During the last 10–20 years, there has been increased focus on the application of structures with high-strength and ultra-high-strength concrete. This has increased the importance of modelling the influence of cyclic stresses on fatigue properties of this type of structures; see Lohaus et al. (2012) where a large number of test data is described and used as basis to the fatigue model established for reinforced concrete included in the formulation of the new FIB Model Code 2010. This section presents a comparative statistical analysis of the new FIB Model Code 2010, CEB-FIB Model Code 90 and Eurocode 2 (EN1992-2:2005) using some of the fatigue test data in Lohaus et al. (2012).

In Lohaus et al. (2012), 272 experimental tests are described. They have been taken from different research works which were performed considering different concrete types under compressive fatigue loads. Figure 22 shows some of these experimental test results with or without fibres as well as with and without heat treatment. Run-out tests are also included, and the minimum stress level was maintained equal to $S_{c,min,i}$=0.05 for each test, see below. In Figure 22 (from Lohaus et al. 2012), the number of cycles to failure is presented as mean values as well as maximum and minimum compressive stress levels are related to the mean values of the static short-term strength. Each mean value was obtained using at least three test specimens.

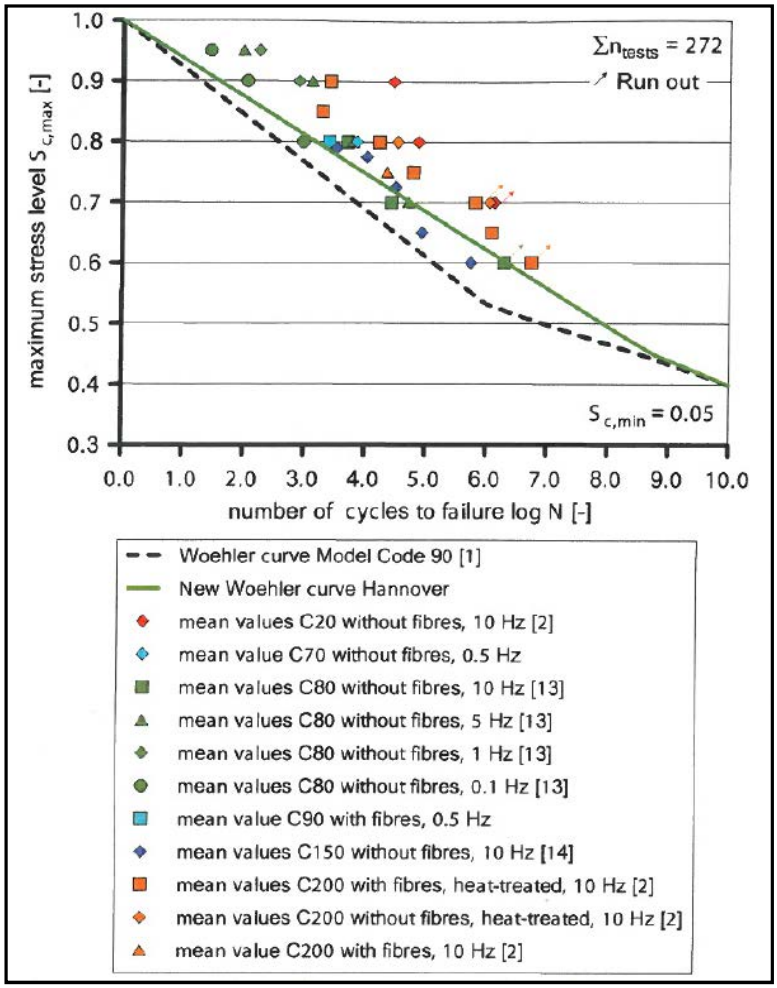

Figure 22. Fatigue tests results of normal-strength, high-strength and ultra-high-strength concrete with or without fibres as well as with and without heat treatment. Run-outs tests are included and the minimum stress level is constant ($S_{c,min,i}$=0.05). From Lohaus et al. 2012. [1] is CEB-FIB Model Code 90, [2] is Wefer (2010), [13] is Grünberg and Oneschkow (2011) and [14] is Anders and Lohaus (2007).

The S-N curve proposed in Eurocode 2 (EN1992-2:2005) for fatigue assessment of concrete bridges establishes that the number of cycles to failure, N_i, can be estimated by:

$$\log N_i = 14\left(\frac{1-S_{c,max,i}}{\sqrt{1-\frac{S_{c,min,i}}{S_{c,max,i}}}}\right) \tag{37}$$

where $S_{c,max,i}$ and $S_{c,min,i}$ are maximum and minimum stress levels, respectively. Design values of $S_{c,max,i}$ and $S_{c,min,i}$ are similarly defined in the design codes FIB Model Code 2010, CEB-FIB Model Code 90 and Eurocode 2 by:

$$S_{c,min,i} = \frac{Sd \cdot \ c,min,i \cdot \ c}{f_{cd,fat}} \quad ; \quad S_{c,max,i} = \frac{Sd \cdot \ c,max,i \cdot \ c}{f_{cd,fat}} \tag{38}$$

γ_{Sd} and η_c are not included in the Eurocode 2 model. Moreover, the stress ratio, R_i, is introduced by:

$$R_i = \frac{S_{c,min,i}}{S_{c,max,i}} \tag{39}$$

$f_{cd,fat}$ is the design value of the compressive concrete strength reduced for fatigue. The new FIB Model Code 2010 can also be applied for high-strength and ultra-high-strength concrete strengths (based on tests up to f_{ck} = 200 MPa by Lohaus et al. 2012), see Equation (40). In Appendix A.5, $f_{cd,fat}$ is determined according to EN 1992-1-1:2004. A similar formulation is defined in the CEB-FIB Model Code 90, see Equation (41). In Lohaus et al. (2012), it is mentioned that the CEB-FIB Model Code 90 applied for characteristic compressive strengths f_{ck} larger than 125 MPa would lead to an underestimation of the fatigue life. The new FIB Model Code 2010 formulation leads with higher number of cycles to failure, especially for high-strength concretes. Therefore, Equation (40) can be useful for practical applications considering the increase in fatigue-relevant loads for high-strength and ultra-high-strength concrete strengths.

$$f_{cd,fat} = 0.85 \cdot \ _{CC}(t_0) \cdot \frac{f_{ck}}{_{c,fat}} \left(1 - \frac{f_{ck}}{40 \cdot f_{ck0}}\right) \tag{40}$$

$$f_{cd,fat} = 0.85 \cdot \ _{CC}(t_0) \cdot \frac{f_{ck}}{_{c,fat}} \left(1 - \frac{f_{ck}}{25 \cdot f_{ck0}}\right) \tag{41}$$

f_{ck} is the characteristic strength of concrete defined as a 5 % quantile and $\gamma_{C,fat}$ is the partial safety factor for concrete in fatigue verification (equal to 1.50 in EN 1992-1-1:2004 in). $\beta_{CC}(t_0)$ is a coefficient defined for the concrete strength at the initial time for load application, t_0. In this chapter, $\beta_{CC}(t_0)$ is taken equal to 1.0 for simplicity. f_{ck0} is a reference strength equal to 10 MPa. γ_{Sd} = 1.0 or 1.1 and η_c are determined according to CEB-FIB Model Code 90.

Figure 23 shows a comparison between the S-N curves defined in CEB-FIB Model Code 90 (section 6.7.4-Fatigue) and in the new FIB Model Code 2010 described by Lohaus et al. (2012) (section 4.2 - design concept) as well as the S-N curve in Eurocode 2 established for bridges. Moreover, Figure 23 shows tests data both for resulting in failure as well as in run-out (Lohaus et al. 2012). The S-N curves are plotted considering a constant $S_{c,min,i}$=0.05. From Figure 23, it is observed that the S-N curve in CEB-FIB Model Code 90 seems to be the most conservative. In section 7.3, a statistical analysis is presented using the test data taken from Lohaus et al. (2012).

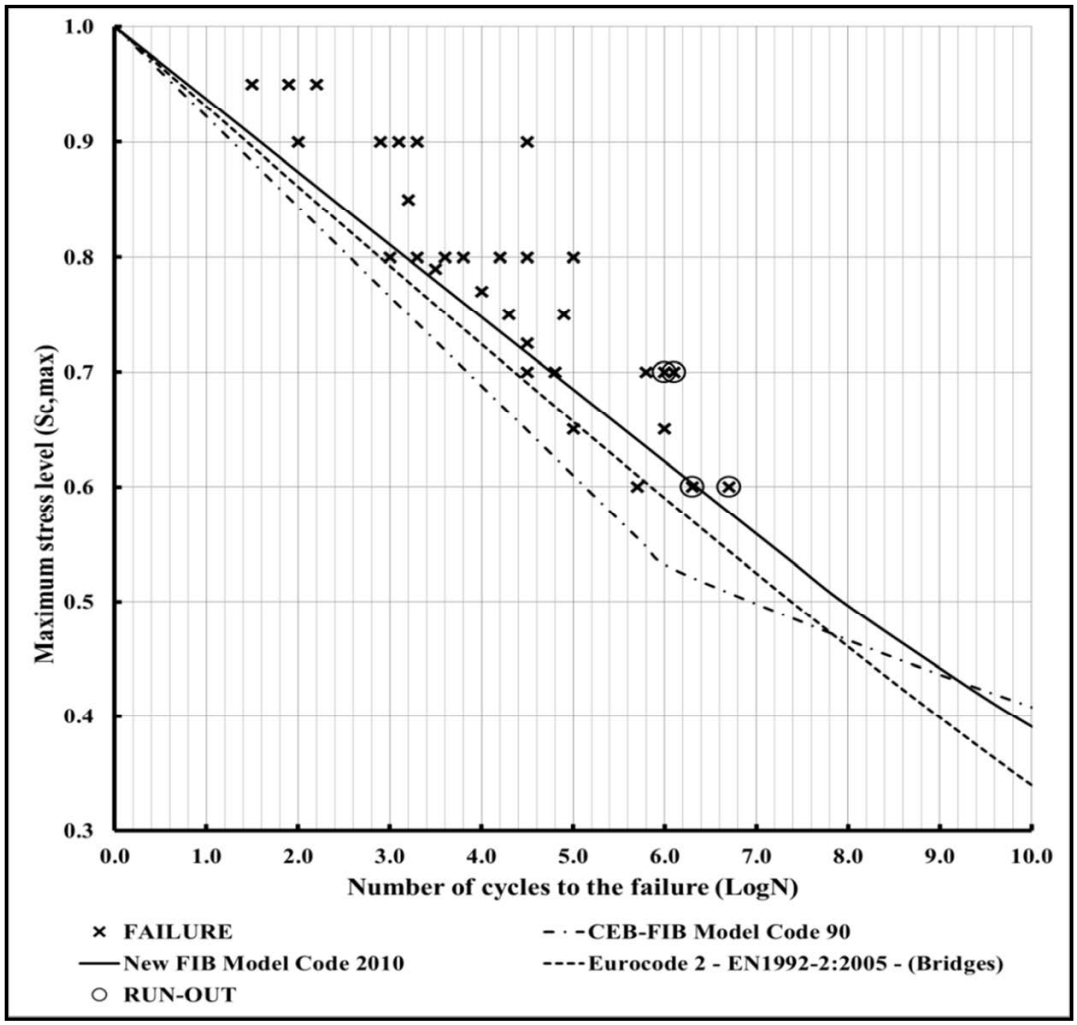

Figure 23. Comparison between different S-N curves: Eurocode 2 defined for bridges, CEB-FIB Model Code 90 and the New FIB Model Code 2010. Also shown are the data from Figure 22 (Lohaus et al. 2012). Run-out tests are included.

7.1.2 Test data of reinforcing steel

In the literature, some fatigue strength test results can be found for steel reinforcement. This section is based on test results from Hansen and Heshe (2001) where two blocks of steel reinforcing bars have been tested in order to estimate the fatigue capacity. The first block, sketched in Figure 24, was made up by 29 steel bars with a diameter equal to 10 mm and length 590 mm, and the second block consisted of 33 steel reinforcing bars with 16 mm of diameter and 600 mm length, see Figure 25. Additionally, 35 reinforced concrete specimens of 500 mm x 300 mm x 100 mm were casted as short beams with two main embedded steel bars with 16 mm in diameter. The concrete specimens were also made with additional steel reinforcing bars with diameter equal to 12 mm and 20 mm. The concrete was designed as an ultra-high-strength fibre reinforced concrete with compressive strength in the range 100-200 MPa. Steel fibres were included to ‘solve’ the problem of brittleness in an ultra-high-strength concrete. Tests results are shown in Figure 26. For more testing details, see Hansen and Heshe (2001).

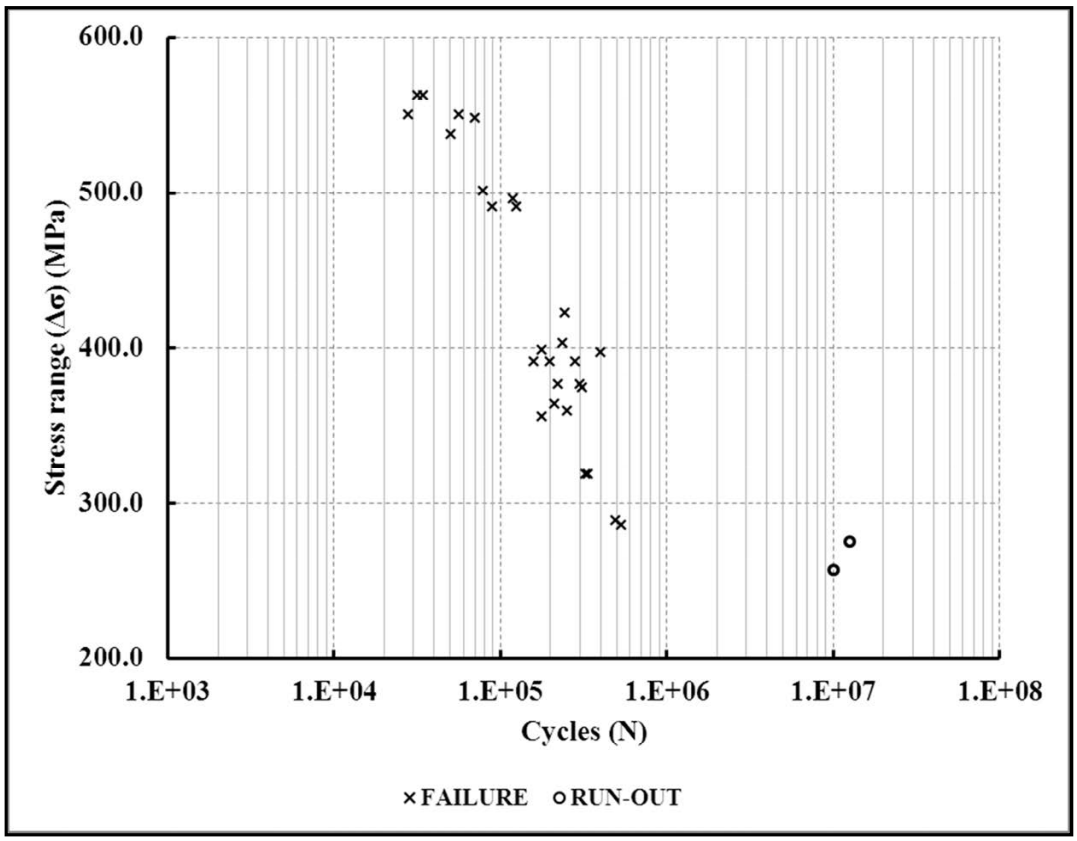

Figure 24. Data from 29 steel reinforced bars with diameter equal to 10 mm and length 590 mm. Run-out tests are included. (Hansen & Heshe, 2001).

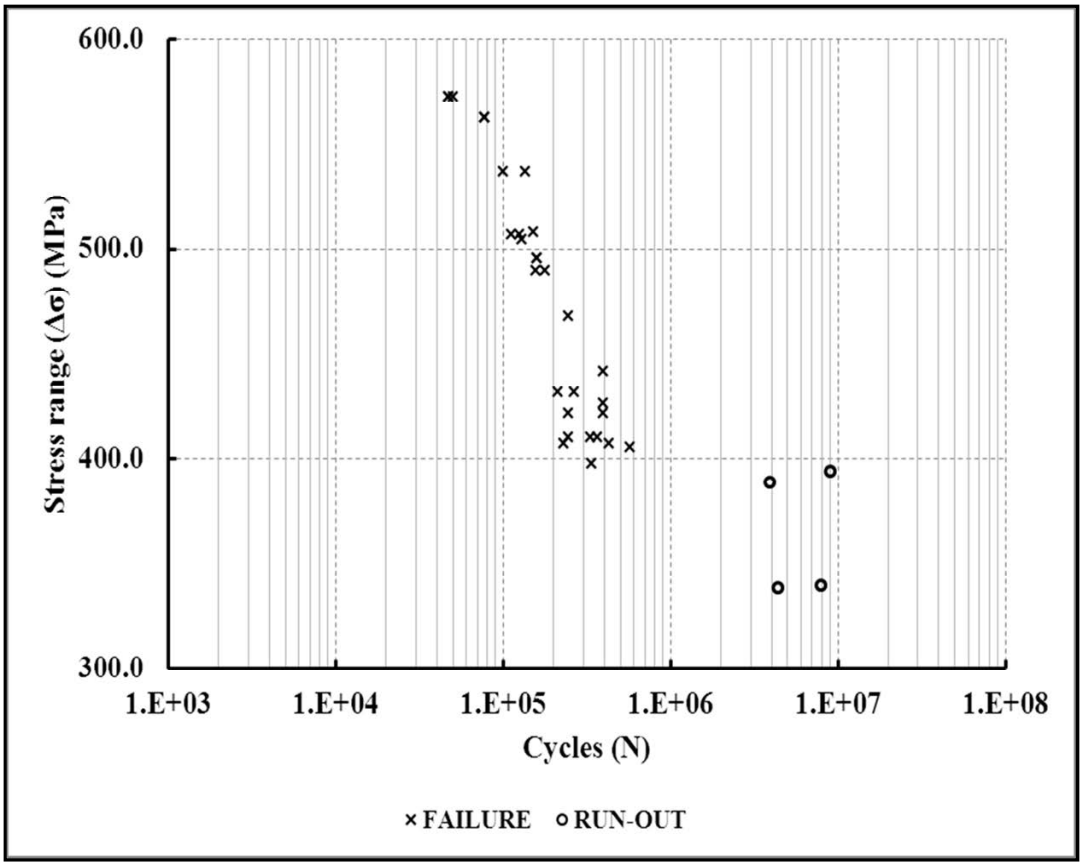

Figure 25. Data from 33 steel reinforcement bars with 16 mm of diameter and length 600 mm tested. Run-out tests are included. (Hansen and Heshe, 2001).

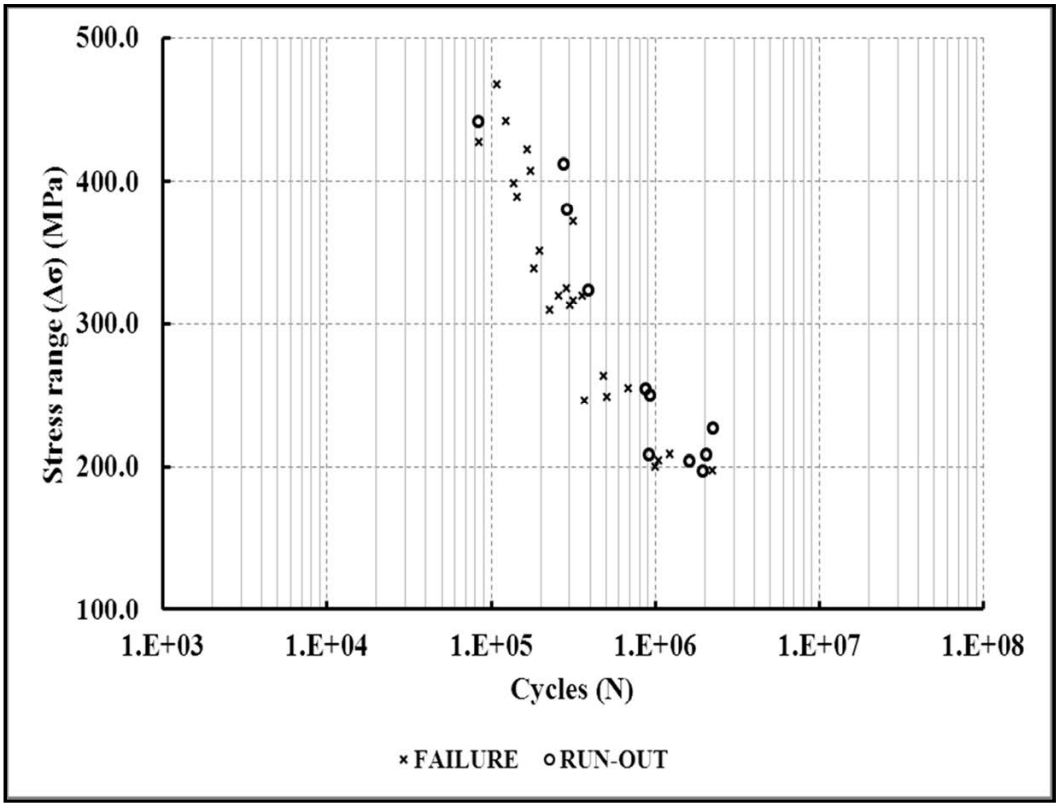

Figure 26. Data from 35 concrete beam specimens (500mm x 300mm x 100mm) with two main embedded steel bars of 16 mm in diameter. Run-out tests are included. (Hansen and Heshe, 2001).

In the following section, a statistical analysis is performed to determine typical fatigue strength uncertainties using the above test data for reinforcement steel bars and for plain concrete. The Maximum-Likelihood Method (MLM) is used following the same general procedure as in e.g. Sørensen et al. (2006) where uncertainty modelling of the fatigue strength capacity of the load-carrying fillet welds is considered. The uncertainty modelling is important in order to determine the characteristic fatigue design curves as well as in order to perform the reliability analyses and eventually to calibrate/assess partial safety factors.

7.2 Statistical analysis for fatigue data of steel reinforcing bars

For steel reinforcing bars used in concrete, a basic linear S-N curve is written:

$$N_i = K \cdot \Delta s_i^{-m} \quad \text{or} \quad \log(N_i) = \log(K) - m\log(\Delta s_i) \tag{42}$$

where 'N_i' is the number of cycles to failure with stress range Δs_i in test number 'i'. K and m are material parameters to be fitted by the Maximum-Likelihood Method using the tests results in Hansen and Heshe (2001).

To account for uncertainties in the fatigue life Equation (42) can be rewritten:

$$\log(N_i) = \log(K) - m\log(\Delta s_i) + \tag{43}$$

where 'ε' represents the uncertainty of the fatigue life modelled by a stochastic variable with mean value equal to zero and standard deviation σ_ε. 'ε' is often assumed normal distributed. The log-likelihood function to be used to estimate the optimal values of the parameters K, m, and σ_ε from test data becomes the following:

$$L(K,m,\quad) = \prod_{i=1}^{n_F} P\left[\log(K) - m\log(\Delta s_i) + \quad = \log(n_i)\right] \times \prod_{i=1}^{n_R} P\left[\log(K) - m\log(\Delta s_i) + \quad > \log(n_i)\right] \qquad (44)$$

n_i is the number of stress cycles to failure or run-out with stress range Δs_i in test number i. n_F is the number of tests where failure occurs, and n_R is the number of tests where failure did not occur after n_i stress cycles (run-outs). The total number of tests is $n = n_F + n_R$. K, m, and σ_ε are obtained from the optimization problem $\max_{K,m,\sigma\varepsilon} L(K,m,\sigma_\varepsilon)$, which can be solved using a standard non-linear optimizer (e.g. NLPQL algorithm, see Schittkowski, 1986).

The two terms in Equation (44) can be obtained from:

$$P\left[\log(K) - m\log(\Delta s_i) + \quad = \log(n_i)\right] = \frac{1}{\sqrt{2}} \exp\left(-\frac{1}{2}\left(\frac{\log(K) - m\log(\Delta s_i) - \log(n_i)}{} \right)^2 \right) \qquad (45a)$$

$$P\left[\log(K) - m\log(\Delta s_i) + \quad > \log(n_i)\right] = \Phi\left(\frac{\log(K) - m\log(\Delta s_i) - \log(n_i)}{} \right) \qquad (45b)$$

K, m, and σ_ε are parameters determined using a limited number of data; consequently, they are subject to statistical uncertainty. Since the parameters are estimated by the Maximum-Likelihood Method, they become asymptotically (number of data should be > 25 – 30) normally distributed stochastic variables with expected values equal to the maximum-likelihood estimator and a covariance matrix equal to (see e.g. Lindley, 1976):

$$C_{K,m,\quad} = \left[-H_{K,m,\quad} \right]^{-1} = \begin{bmatrix} {}^{2}_{K} & {}_{K,m} & {}_{K} & {}_{m} & {}_{K,} & {}_{K} \\ {}_{K,m} & {}_{K} & {}_{m} & {}^{2}_{m} & {}_{m,} & {}_{m} \\ {}_{K,} & {}_{K} & {}_{m,} & {}_{m} & {}^{2} & \end{bmatrix} \qquad (46)$$

$H_{K,m,\sigma\varepsilon}$ is the Hessian matrix with second-order derivatives of the log-likelihood function. σ_K, σ_m, and $\sigma_{\sigma\varepsilon}$ denote the standard deviations of K, m, and σ_ε, respectively, and e.g., $\rho_{K,m}$ is the correlation coefficient between K, m.

In DNV-OS-C502 (2012), the characteristic S-N curve for reinforcing steel is determined as a 2.5 % fractile and used for the fatigue limit state (FLS). This fractile value is used in the following. The characteristic value of logK can be obtained given a number of data and unknown standard deviation according to EN1990 (Eurocode 0, Basis of Structural Design) where Bayesian statistics is used as basis for the estimation of characteristic values. The characteristic S-N curve is therefore estimated by:

$$\log N_i = (\ {}_{\text{LogK}} - k_S \cdot\ ) - m\log\Delta s_i \qquad (47)$$

where ${}_{\text{LogK}}$ is the mean value (best estimate) of logK and k_s is a factor estimated according to EN 1990 for unknown standard deviation (and coefficient of variation).

If statistical uncertainty is included, then K, m, and σ_ε are modelled as stochastic variables. The characteristic S-N curve can be estimated from $P[N_i \le \log(K) - m\cdot\log(\Delta s_i) + \varepsilon] = 0.025$, i.e. for given Δs_i the corresponding characteristic value of N_i is determined. The probability $P[N_i \le \log(K) - m\cdot\log(\Delta s_i) + \varepsilon]$, where ε, K, m, and σ_ε are modelled as stochastic variables, can be

estimated by e.g. the first-order reliability method (FORM), see (Madsen et al. 1986; Ditlevsen and Madsen 1996), and/or by Monte Carlo simulation.

The present thesis includes a statistical analysis of the fatigue tests presented in Hansen and Heshe (2001). This statistical analysis should be considered as an example so that the same procedure can be applied and even updated if more data is available. However, the test data in Hansen and Heshe (2001) is considered to be representative for the scatter in the fatigue life of steel reinforcement. The steel reinforcement fatigue tests were analysed using the Maximum-Likelihood Method (MLM) as described above. The statistical uncertainties were estimated considering both with 'm' free and with 'm' fixed to 5. m=5 corresponds to the slope defined by the low cycle of fatigue level according with the Eurocode 2 where a bi-linear S-N curve is established for reinforcing steel bars with material parameters m_1=5 (low cycle fatigue level) and m_2=9 (high cycle fatigue level). The inflection point is defined at $N^*=10^6$ cycles with a corresponding Δs_c equal to 162.5 (MPa).

The mean and characteristic S-N curves estimated by MLM are shown in Table 11 to 13 using the test data from Hansen and Heshe (2001) shown in Figures 24 to 26.

Table 11. S-N curves estimated assuming that all test data corresponds to failure. (units in [MPa]). Data is from Figures 24 and 25 (Hansen & Heshe, 2001).

	29 tested specimens (Φ=10 mm)		**33 tested specimens (Φ=16 mm)**	
	m (free)	m=5 (fixed)	m (free)	m=5 (fixed)
Mean	$\log N_i=18.73-5.15\log\Delta s_i$	$\log N_i=18.35-5\log\Delta s_i$	$\log N_i=26.03-7.74\log\Delta s_i$	$\log N_i=18.74-5\log\Delta s_i$
Charac.	$\log N_i=18.13-5.15\log\Delta s_i$	$\log N_i=17.75-5\log\Delta s_i$	$\log N_i=25.43-7.74\log\Delta s_i$	$\log N_i=18.04-5\log\Delta s_i$
Eurocode	$\log N_i=17.054-5\log\Delta s_i$ / $\log N_i=25.897-9\log\Delta s_i$ (m_1=5) (m_2=9)			
σ_ε	0.29	0.29	0.29	0.34
σ_{logK}	1.40	0.05	2.08	0.06
σ_m	0.57	------	0.78	------
$\sigma_{\sigma\varepsilon}$	0.04	0.00	0.04	0.04
$\rho_{logK,m}$	1.00	------	1.00	------
$\rho_{logK,\sigma\varepsilon}$	0.01	0.09	-0.03	0.00
$\rho_{m,\sigma\varepsilon}$	0.01	------	-0.03	------
2.5% fractile	k_s=2.08 (DnV-OS-C502)		k_s=2.07 (DnV-OS-C502)	
$\Delta s_{c(mean)}$	296.38 (MPa)($N^*=10^6$)	295.12 (MPa)($N^*=10^6$)	387.13 (MPa)($N^*=10^6$)	353.18 (MPa)($N^*=10^6$)
$\Delta s_{c(Charac.)}$	226.64 (MPa)($N^*=10^6$)	223.87 (MPa)($N^*=10^6$)	323.84 (MPa)($N^*=10^6$)	255.86 (MPa)($N^*=10^6$)
$\Delta s_{c(Eurocode)}$	162.50 (MPa)($N^*=10^6$)	162.50 (MPa)($N^*=10^6$)	162.50 (MPa)($N^*=10^6$)	162.50 (MPa)($N^*=10^6$)

Table 12. S-N curves estimated considering both run-outs and specimens to failure. (units in [MPa]). Data is from Figures 24 and 25 (Hansen & Heshe, 2001).

	29 tested specimens (Φ=10 mm)		**33 tested specimens (Φ=16 mm)**	
	m (free)	m=5 (fixed)	m (free)	m = 5 (fixed)
Mean	$\log N_i=19.08-5.3\cdot\log\Delta s_i$	$\log N_i=18.36-5\cdot\log\Delta s_i$	$\log N_i=27.35-8.2\cdot\log\Delta s_i$	$\log N_i=18.76-5\cdot\log\Delta s_i$
Charac.	$\log N_i=18.44-5.3\cdot\log\Delta s_i$	$\log N_i=17.72-5\cdot\log\Delta s_i$	$\log N_i=26.68-8.2\cdot\log\Delta s_i$	$\log N_i=17.97-5\cdot\log\Delta s_i$
Eurocode	$\log N_i=17.054-5\log\Delta s_i$ / $\log N_i=25.897-9\log\Delta s_i$ (m_1=5) (m_2=9)			
σ_ε	0.31	0.31	0.32	0.38
σ_{logK}	1.53	0.06	2.49	0.07
σ_m	0.59	------	0.94	------
$\sigma_{\sigma\varepsilon}$	0.04	0.04	0.04	0.05
$\rho_{logK,m}$	1.00	------	1.00	------
$\rho_{logK,\sigma\varepsilon}$	0.05	0.03	0.18	0.06
$\rho_{m,\sigma\varepsilon}$	0.05	------	0.18	------
2.5% fractile	k_s=2.08 (DnV-OS-C502)		k_s=2.07 (DnV-OS-C502)	
$\Delta s_{c(mean)}$	300.1 (MPa)($N^*=10^6$)	296.5 (MPa)($N^*=10^6$)	392.8 (MPa)($N^*=10^6$)	356.5 (MPa)($N^*=10^6$)
$\Delta s_{c(Charac.)}$	227.0 (MPa)($N^*=10^6$)	220.8 (MPa)($N^*=10^6$)	325.7 (MPa)($N^*=10^6$)	247.7 (MPa)($N^*=10^6$)
$\Delta s_{c(Eurocode)}$	162.5 (MPa)($N^*=10^6$)	162.5 (MPa)($N^*=10^6$)	162.5 (MPa)($N^*=10^6$)	162.5 (MPa)($N^*=10^6$)

Table 13. S-N curves estimated considering both run-outs and specimens to failure. (units in [MPa]). Data is from Figure 26 (Hansen & Heshe, 2001) where reinforcement bars are embedded in concrete.

	35 tested specimens (Φ=16 mm) (all will fail)		**35 tested specimens (Φ=16 mm) (run-out)**	
	m (free)	m=5 (fixed)	m (free)	m = 5 (fixed)
Mean	$\log N_i=13.57-3.2\cdot\log\Delta s_i$	$\log N_i=17.98-5\cdot\log\Delta s_i$	$\log N_i=13.95-3.4\cdot\log\Delta s_i$	$\log N_i=18.07-5\cdot\log\Delta s_i$
Charac.	$\log N_i=13.27-3.2\cdot\log\Delta s_i$	$\log N_i=17.44-5\cdot\log\Delta s_i$	$\log N_i=13.56-3.4\cdot\log\Delta s_i$	$\log N_i=17.45-5\cdot\log\Delta s_i$
Eurocode	$\log N_i=17.054-5\log\Delta s_i$ / $\log N_i=25.897-9\log\Delta s_i$ ($m_1=5$) ($m_2=9$)			
$\sigma\varepsilon$	0.15	0.26	0.19	0.30
σ_{logK}	0.52	0.04	0.33	0.06
σ_m	0.21	------	0.13	------
$\sigma_{\sigma\varepsilon}$	0.02	0.01	0.03	0.04
$\rho_{logK,m}$	1.00	------	1.00	------
$\rho_{logK,\sigma\varepsilon}$	0.16	0.000	-0.08	0.20
$\rho_{m,\sigma\varepsilon}$	0.16	------	-0.11	------
2.5% fractile	k_s=2.06 (DnV-OS-C502)		k_s=2.06 (DnV-OS-C502)	
$\Delta s_{c(mean)}$	224.4 (MPa)($N^*=10^6$)	248.9 (MPa)($N^*=10^6$)	236.1 (MPa)($N^*=10^6$)	259.4 (MPa)($N^*=10^6$)
$\Delta s_{c(Charac.)}$	181.0 (MPa)($N^*=10^6$)	194.1 (MPa)($N^*=10^6$)	180.6 (MPa)($N^*=10^6$)	195.0 (MPa)($N^*=10^6$)
$\Delta s_{c(Eurocode)}$	162.5 (MPa)($N^*=10^6$)	162.5 (MPa)($N^*=10^6$)	162.5 (MPa)($N^*=10^6$)	162.5 (MPa)($N^*=10^6$)

Results in Table 11 show that if the 29 tests specimens of the first block are considered to fail, the uncertainty of the S-N curves represented by σ_ε (which corresponds to the coefficient of variation of the fatigue life) is estimated to be around 29 %. If run-out tests are taken into account then the uncertainty is increased to 31 %. It is mentioned that there is not an important difference between assuming 'm' free or 'm' fixed to 5.0 in the statistical analysis for this test data.

Table 12 shows the statistical analysis of the second block of test specimens made up of 33 steel bars, and it shows that if all specimens are considered to fail then an uncertainty equal to 29 % is obtained considering 'm' a free parameter and around 34 % if 'm' is fixed to 5.0. If run-out tests are included then the uncertainty is increased to 32 % for 'm' free and to 38 % if 'm' is considered to be fixed to 5.0.

Table 13 with results for steel reinforcement embedded in concrete shows uncertainties estimated to be between 15 % and 19 % if 'm' is considered as a free parameter which is noted to be much smaller than the above uncertainty levels and further the estimated values of logK and 'm' also differ significantly. This indicates a different fatigue strength behaviour if the reinforcement bars are placed in concrete instead of being tested 'in air'. If 'm' is fixed to 5.0, similar results for the first and second block are calculated to approximately 26 % and 30 % respectively, considering all the specimens with failure and run-outs.

In Figures 27 to 38, fitted S-N curves are shown together with the S-N curve proposed by Eurocode 2. Generally, the results from the statistical analyses indicate that the S-N curve proposed by Eurocode 2 can be considered as quite conservative.

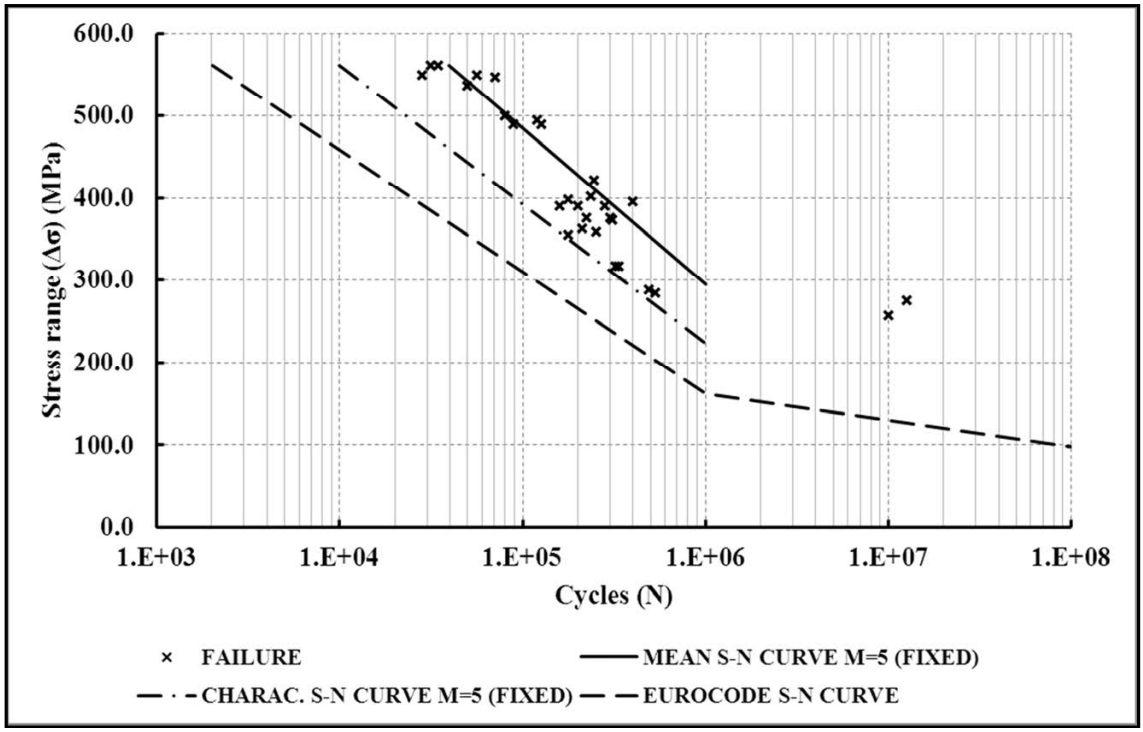

Figure 27. S-N curves assuming that all 29 test data in block 1 corresponds to failure. (units in [MPa]). Data is from Figure 24. 'm' fixed to 5.0.

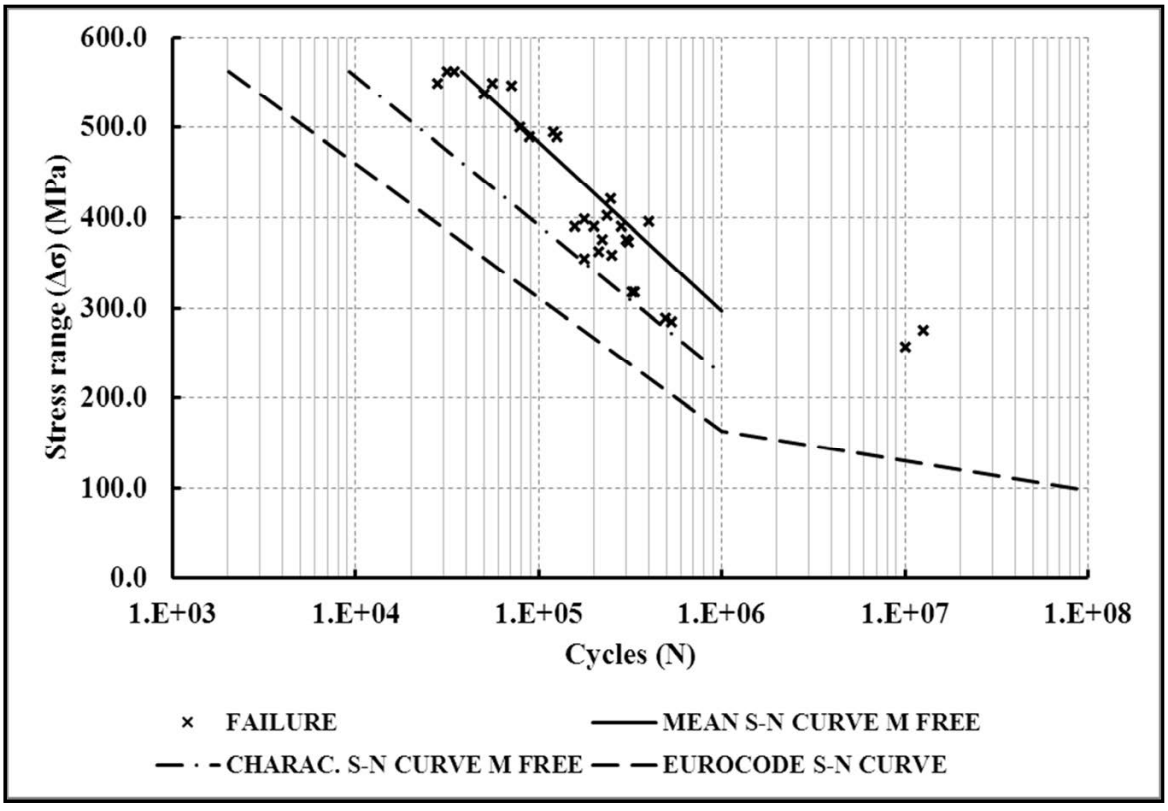

Figure 28. S-N curves assuming that all 29 test data in block 1 corresponds to failure. (units in [MPa]). Data is from Figure 24. 'm' is free.

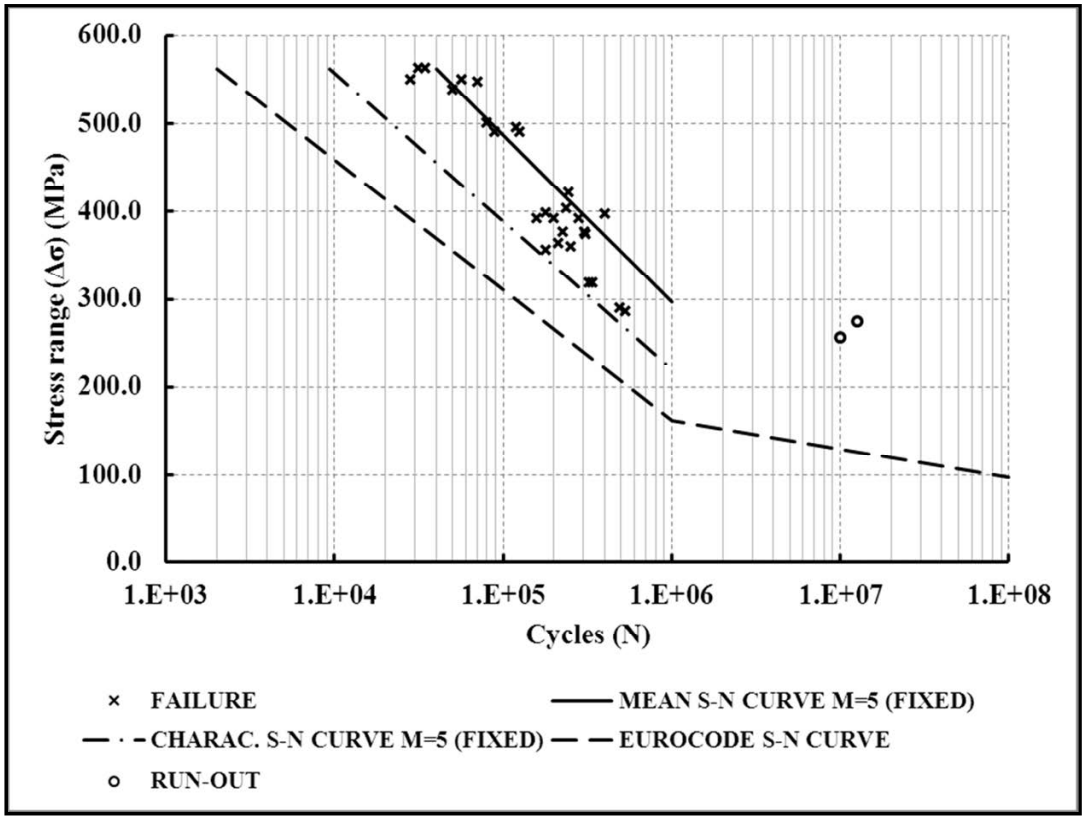

Figure 29. S-N curves for all 29 test data in block 1 considering both run-outs and specimens to failure. (units in [MPa]). Data is from Figure 24. 'm' fixed to 5.0.

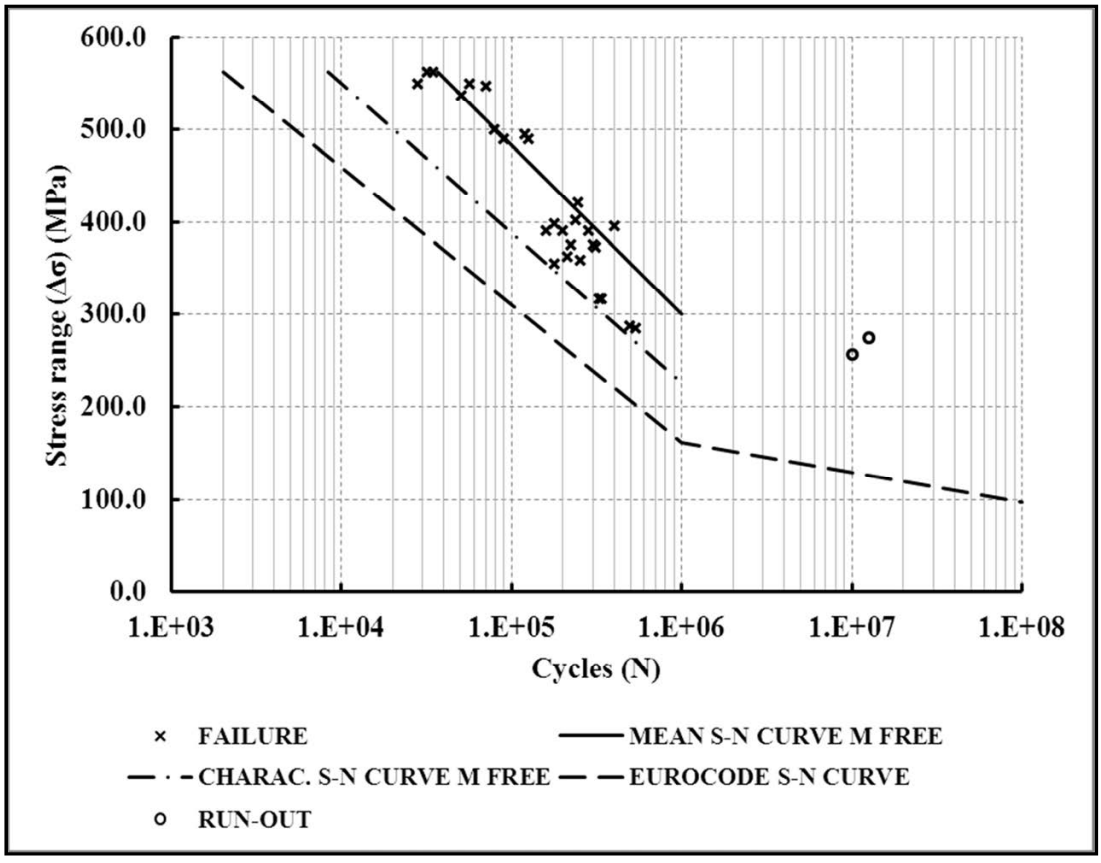

Figure 30. S-N curves for all 29 test data in block 1 considering both run-outs and specimens to failure. (units in [MPa]). Data is from Figure 24. 'm' is free.

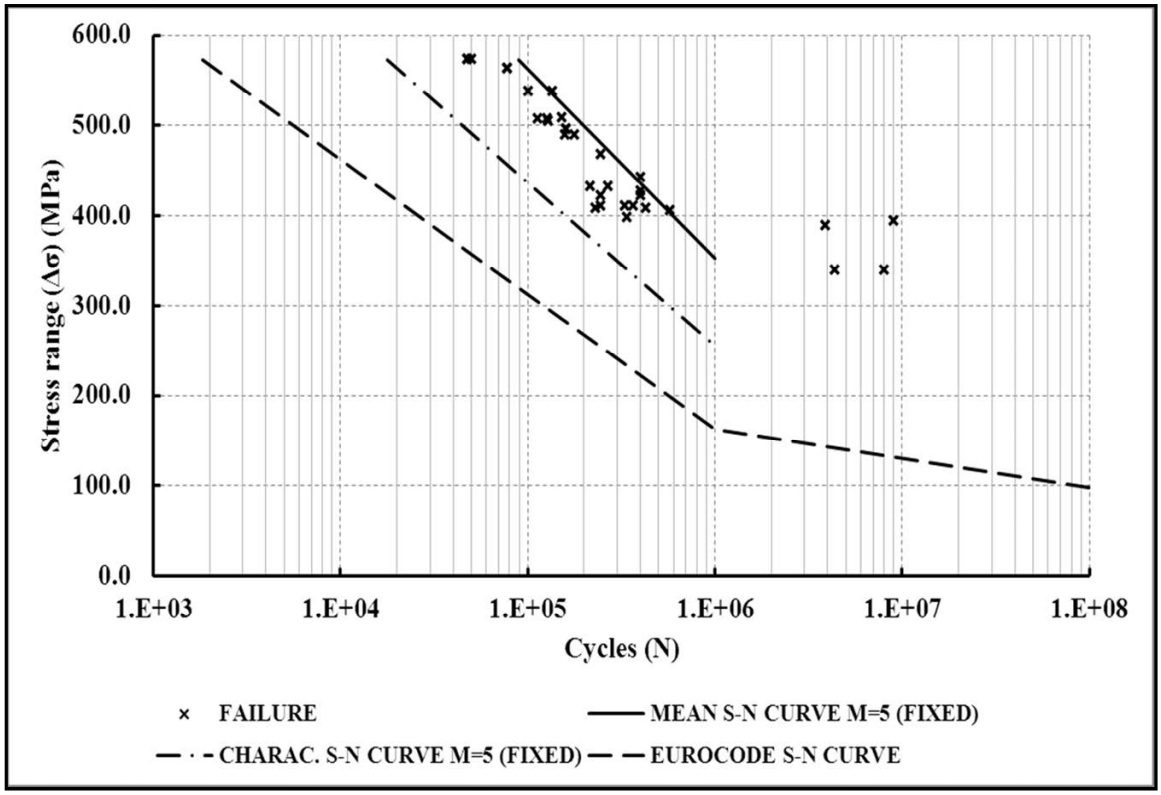

Figure 31. S-N curves assuming that all 33 test data, in block 2, corresponds to failure. (units in [MPa]). Data is from Figure 25. 'm' fixed to 5.0.

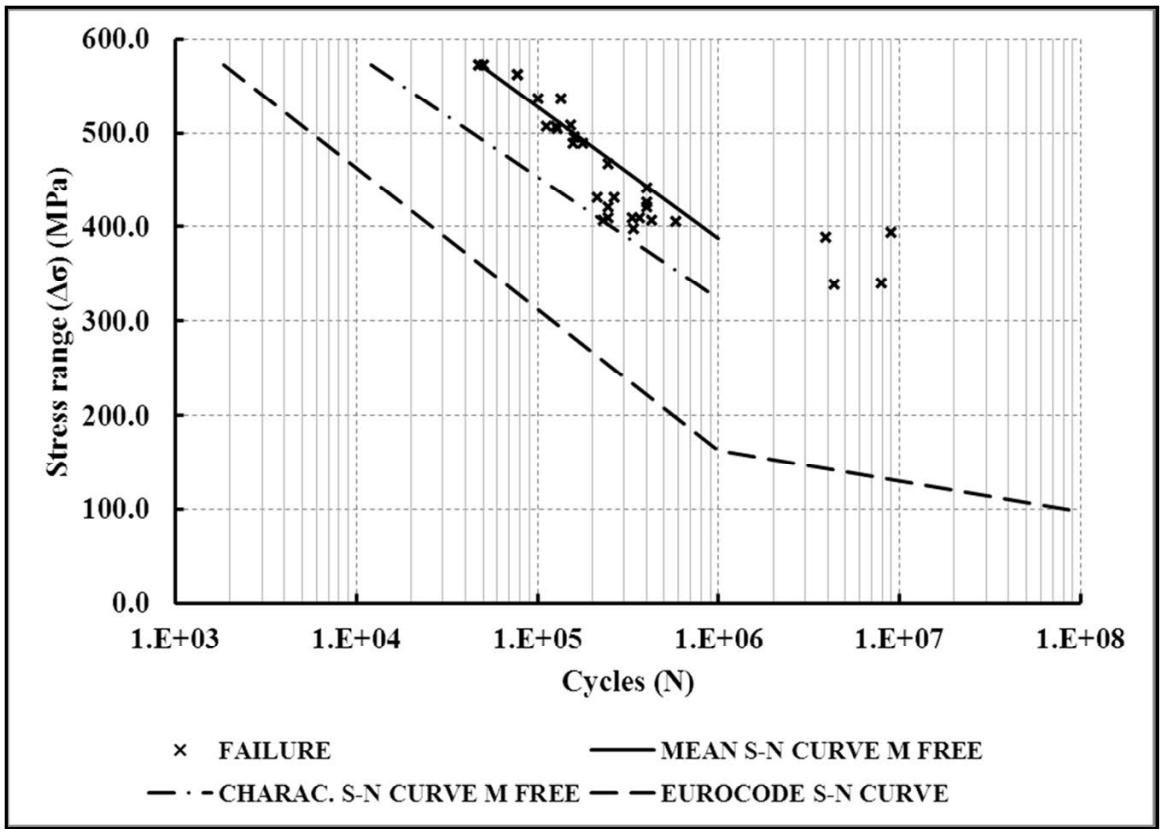

Figure 32. S-N curves assuming that all 33 test data, in block 2, corresponds to failure. (units in [MPa]). Data is from Figure 25. 'm' is free.

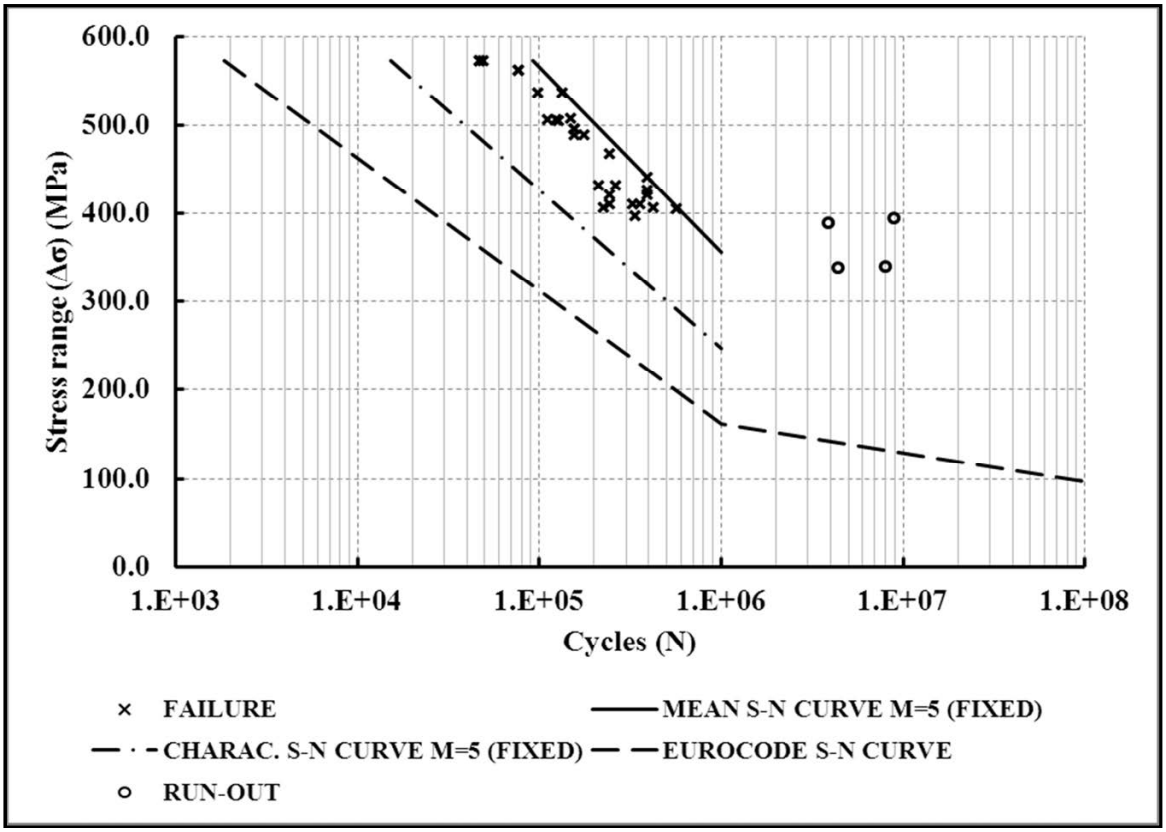

Figure 33. S-N curves for all 33 test data in block 2 considering both run-outs and specimens to failure. (units in [MPa]). Data is from Figure 25. 'm' fixed to 5.0.

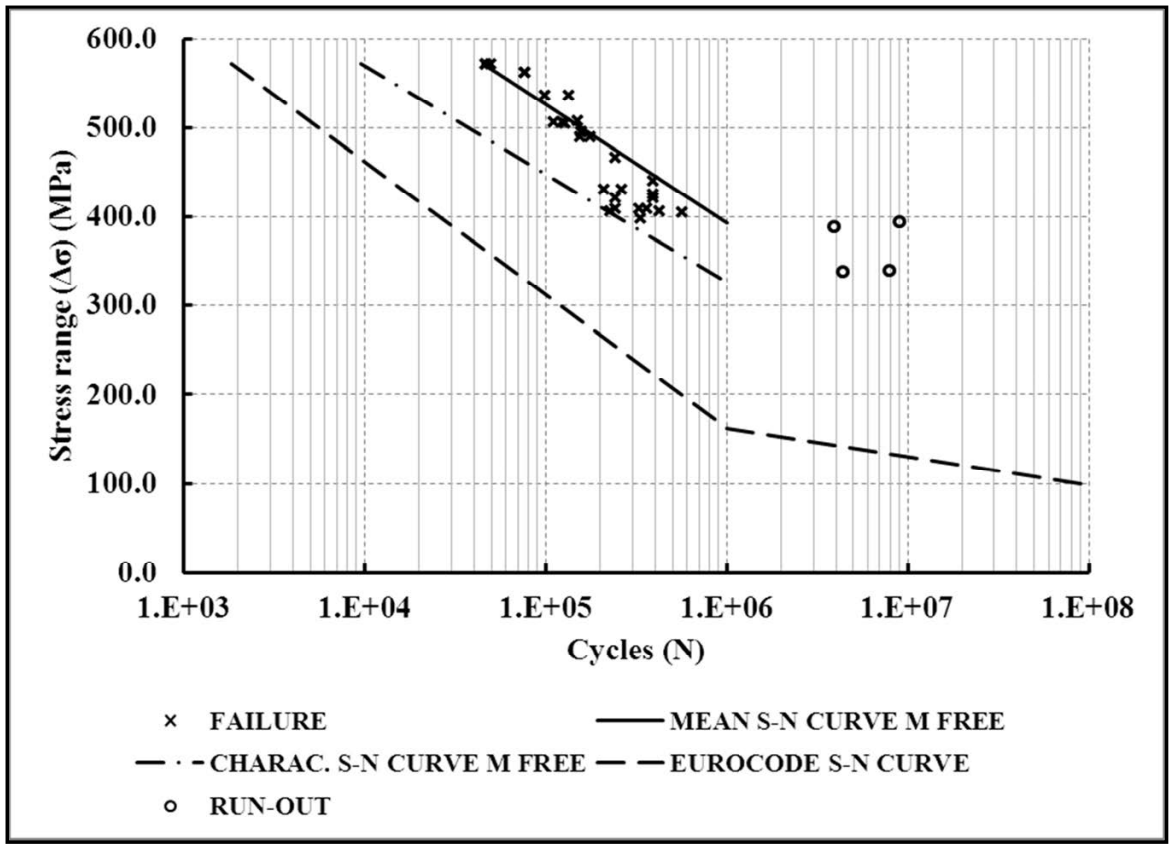

Figure 34. S-N curves for all 33 test data in block 2 considering both run-outs and specimens to failure. (units in [MPa]). Data is from Figure 25. 'm' is free.

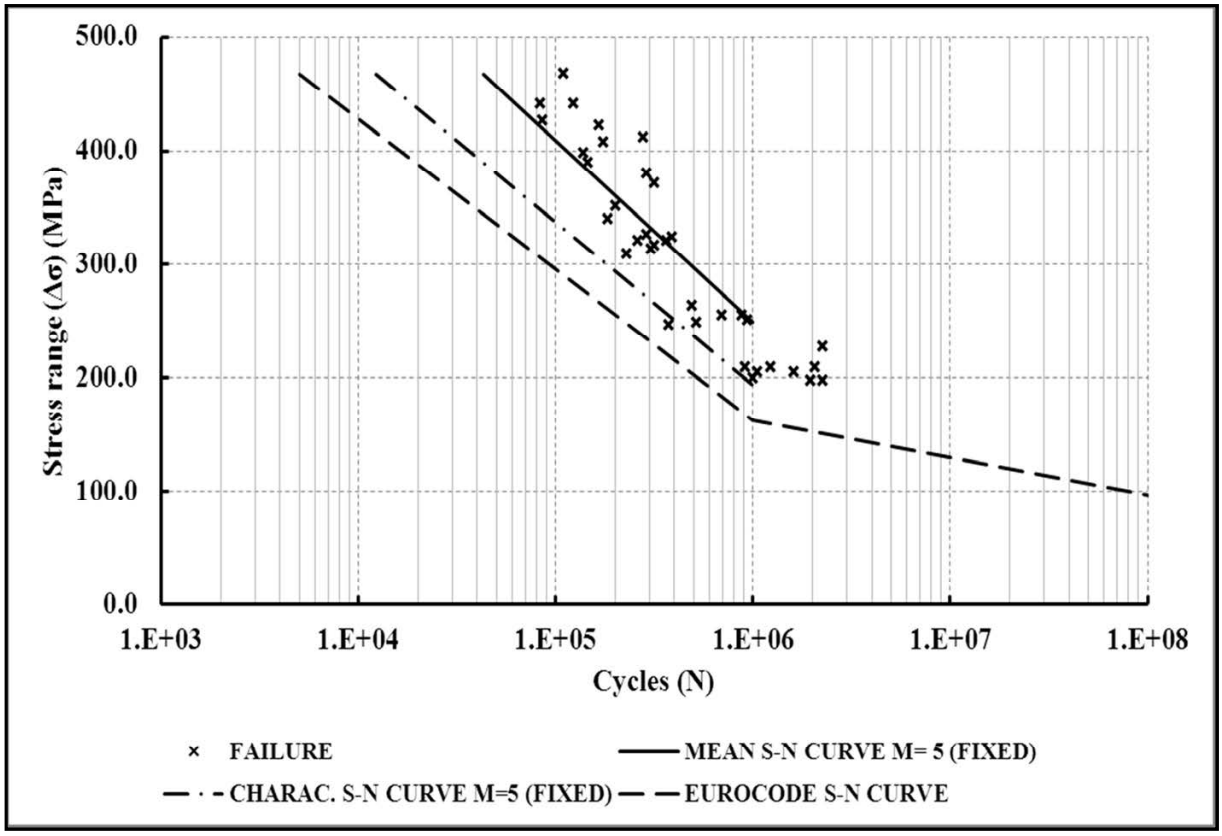

Figure 35. S-N curves assuming that all 35 test data with reinforcement embedded in concrete corresponds to failure. (units in [MPa]). Data is from Figure 26. 'm' fixed to 5.0.

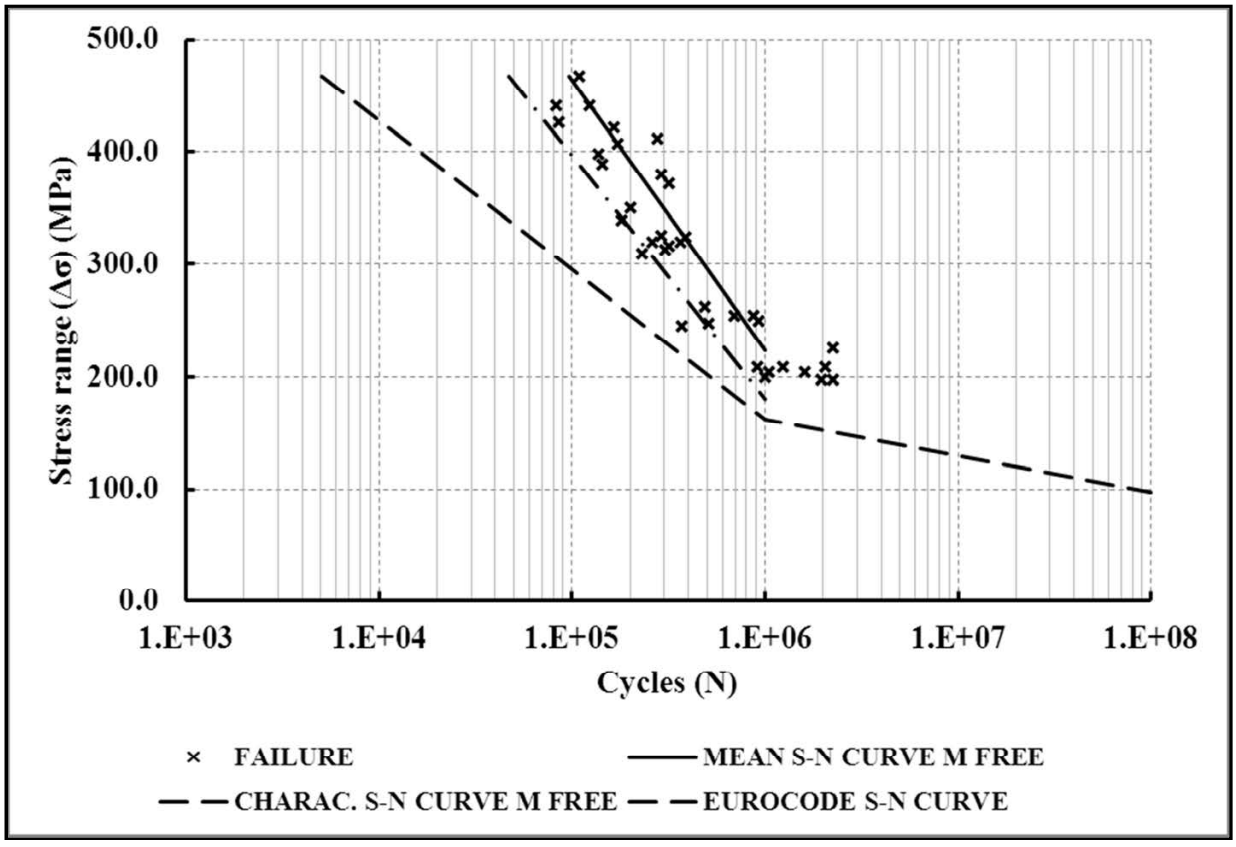

Figure 36. S-N curves assuming that all 35 test data with reinforcement embedded in concrete corresponds to failure. (units in [MPa]). Data is from Figure 26. 'm' is free.

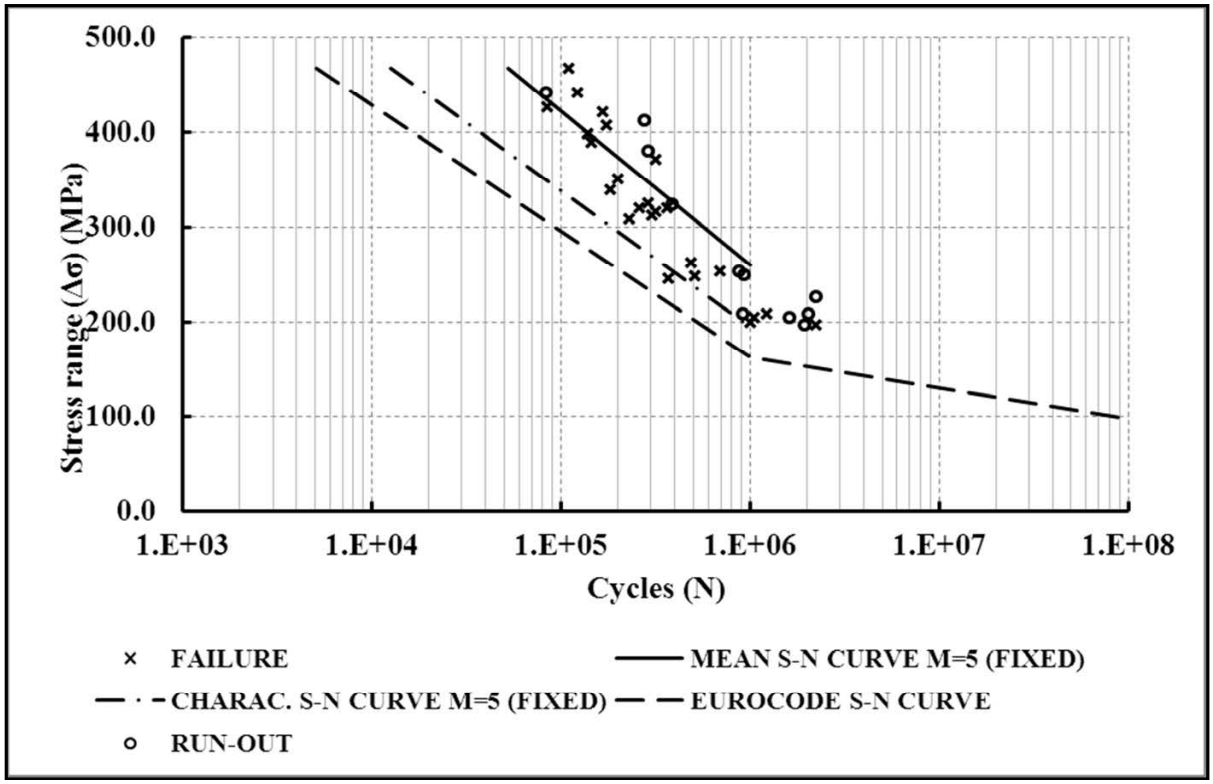

Figure 37. S-N curves assuming that all 35 test data with reinforcement embedded in concrete corresponds to both run-outs and specimens to failure. (units in [MPa]). Data is from Figure 26. 'm' fixed to 5.0.

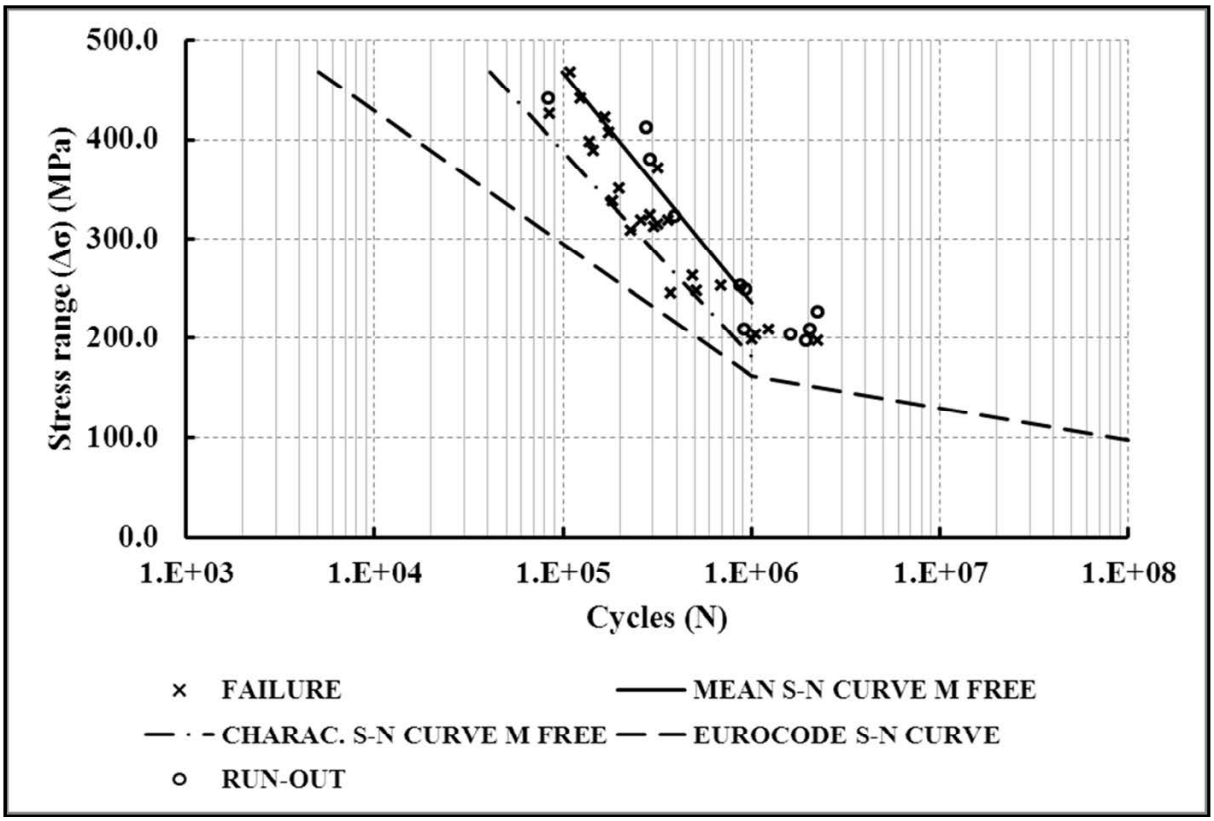

Figure 38. S-N curves assuming that all 35 test data with reinforcement embedded in concrete corresponds to both run-outs and specimens to failure. (units in [MPa]). Data is from Figure 26. 'm' is free.

7.3 Statistical analysis of plain concrete fatigue data

For the statistical modelling of plain concrete fatigue, a basic S-N curve is used which is written according to the New FIB Model Code 2010, see Lohaus et al. (2012) (section 4.2, design concept):

For Log $N_i \leq 8.0$

$$\log N_i = \left(\frac{8}{Y_i - 1} \right) \cdot \left(S_{c,max,i} - 1 \right) \tag{48}$$

For Log $N_i > 8.0$

$$\log N_i = 8 + \frac{8 \cdot \ln(10)}{(Y_i - 1)} \cdot \left(Y_i - S_{c,min,i} \right) \cdot \log \left(\frac{S_{c,max,i} - S_{c,min,i}}{Y_i - S_{c,min,i}} \right) \tag{49}$$

where: $Y_i = \dfrac{0.45 + 1.8 \cdot S_{c,min,i}}{1 + 1.8 \cdot S_{c,min,i} - 0.3 \cdot S_{c,min,i}^2}$

where $S_{c,max,i}$ and $S_{c,min,i}$ are defined in Section 7.1.1 of this thesis.

Only data for Log $N_i \leq 8.0$ is available from Lohaus et al. (2012), see Figure 22. The statistical analysis is, therefore, performed considering only the part of the S-N model below to Log N_i=8.0. Further, the parameter '8' in (48) is considered as a parameter to be fitted using the available tests data. Therefore, Equation (48) can be rewritten as follows:

$$\log N_i = \frac{A}{Y_i - 1} \cdot \left(S_{c,max,i} - 1 \right) \tag{50}$$

By introducing the uncertainty of the fatigue life 'ε' into Equation (50) two difference models can be formulated.

7.3.1 Model (1)

The S-N curve for Log $N_i \leq 8.0$ is written as:

$$\log N_i = \frac{A}{Y_i - 1} \cdot \left(S_{c,max,i} - 1 \right) + \tag{51}$$

where 'A' represents a parameter to be fitted, and 'ε' represents the error term or uncertainty of the fatigue life modelled as a stochastic variable with mean value μ_ε equal to zero and standard deviation σ_ε. 'ε' is assumed normal distributed. This model follows a generalization of the uncertainty modelling used for welded details and also established for the steel reinforcing bars above.

'A' and σ_ε are estimated using the Maximum-Likelihood Method using the data sets available for N, $S_{c,min,i}$ and $S_{c,max,i}$. The log-likelihood function for parameters 'A' and σ_ε is written similarly to the equation used for the reinforcing bars:

$$L(A, \quad) = \prod_{i=1}^{n_F} P\left[\frac{A}{Y_i - 1} \cdot \left(S_{c,max,i} - 1\right) + \quad = \log n_i\right] \times \prod_{i=1}^{n_R} P\left[\frac{A}{Y_i - 1} \cdot \left(S_{c,max,i} - 1\right) + \quad > \log n_i\right] \qquad (52)$$

where n_i is the number of stress cycles to the failure. n_F is the number of tests where failure occurs, and n_R is the number of tests where failure did not occur after n_i stress cycles (run-outs). The total number of tests is $n = n_F + n_R$. 'A' and σ_ε are obtained from the optimization problem $\max_{A,\sigma\varepsilon} L(A, \sigma_\varepsilon)$, which is solved using a standard nonlinear optimizer (NLPQL algorithm, see Schittkowski, 1986).

The terms in Equation (52) can be written for tests no. *i* if the failure occurs:

$$P\left[\frac{A}{Y - 1} \cdot \left(S_{c,max,i} - 1\right) + \quad = \log n_i\right] = \frac{1}{\sqrt{2}} \exp\left(-\frac{1}{2}\left(\frac{\frac{A}{Y_i - 1} \cdot \left(S_{c,max,i} - 1\right) - \log n_i}{}\right)^2\right) \qquad (53a)$$

and if no failure occurs (run-outs):

$$P\left[\frac{A}{Y_i - 1} \cdot \left(S_{c,max,i} - 1\right) + \quad > \log n_i\right] = \Phi\left(\frac{\frac{A}{Y_i - 1} \cdot \left(S_{c,max,i} - 1\right) - \log n_i}{}\right) \qquad (53b)$$

Since the parameters 'A' and σ_ε are determined using a limited amount of data, they are subjected to statistical uncertainty. As described above, the parameters become asymptotically (number of data should be > 25 – 30) normally distributed stochastic variables with expected values equal to the maximum-likelihood estimator and covariance matrix equal to (see, e.g. Lindley, 1976):

$$C_{A, \quad} = \left[- H_{A, \quad}\right]^{-1} = \begin{bmatrix} {}^{2}_{A} & {}_{A, \quad A} \\ {}_{A, \quad A} & {}^{}_{2} \end{bmatrix} \qquad (54)$$

$H_{A,\sigma\varepsilon}$ is the Hessian matrix with second-order derivatives of the log-likelihood function. σ_A, and $\sigma_{\sigma\varepsilon}$ represent the standard deviations of 'A' and σ_ε, respectively. $\rho_{A,\sigma\varepsilon}$ is the correlation coefficient between 'A' and σ_ε.

If statistical uncertainty is not included then a 5 % quantile of the fatigue S-N curve can be obtained from:

$$\log N_{0.05,i} = \frac{A}{Y_i - 1} \cdot \left(S_{c,max,i} - 1\right) - 1.645 \qquad (55)$$

It is noted that in this 'simple' estimate of the characteristic S-N curve, the number of data is assumed 'infinite' (though the factor is 1.645). Note that a k_s factor could have been used to account for the statistical uncertainty as in Equation (47).

In the following two different cases are considered:

Case 1: Data from Figure 22 (Lohaus et al. 2012) is assumed to correspond to tests with failure.
Case 2: Data from Figure 22 (Lohaus et al. 2012) is used considering both failures and run-outs.

Table 14 shows the estimated parameters for the two cases with $\mu_\varepsilon = 0$.

Table 14. Results for Model (1) with $\mu_\varepsilon = 0$.

Considering all specimens to failure (Case 1)			*Considering both run-outs/and failures (Case 2)*		
A	8.94		A	9.22	
ε	μ_ϵ =0	σ_ε = 0.91	ε	μ_ϵ =0	σ_ε = 0.96
σ_A	0.30		σ_A	0.33	
$\sigma_{\sigma\varepsilon}$	0.11		$\sigma_{\sigma\varepsilon}$	0.12	
$\rho_{A,\sigma\varepsilon}$	0.01		$\rho_{A,\varepsilon}$	0.08	

Next, Model (1) is extended by assuming μ_ε to be estimated from the data (and not equal to zero). Therefore, the log-likelihood function is extended and the optimal values of the parameters 'A', μ_ϵ, and σ_ε are obtained together with the estimates on the uncertainty of the parameters σ_A, $\sigma_{\mu\varepsilon}$, and $\sigma_{\sigma\varepsilon}$ as well as the corresponding correlation coefficients.

Table 15 shows the estimated parameters for the two cases where μ_ε is estimated from the test data.

Table 15. Results for Model (1) with μ_ε estimated from the test data.

Considering all specimens to failure (Case 1)		*Considering both run-outs and failures (Case 2)*	
A	6.12	A	6.41
σ_ε	0.62	σ_ε	0.68
μ_ϵ	1.59	μ_ϵ	1.50
σ_A	0.48	σ_A	0.51
$\sigma_{\sigma\varepsilon}$	0.07	$\sigma_{\sigma\varepsilon}$	0.09
$\sigma_{\mu\varepsilon}$	0.24	$\sigma_{\mu\varepsilon}$	0.26
$\rho_{A,\sigma\varepsilon}$	-0.001	$\rho_{A,\sigma\varepsilon}$	0.05
$\rho_{A,\mu\varepsilon}$	-0.90	$\rho_{A,\mu\varepsilon}$	-0.89
$\rho_{\mu\varepsilon,\sigma\varepsilon}$	0.007	$\rho_{\mu\varepsilon,\sigma\varepsilon}$	-0.01

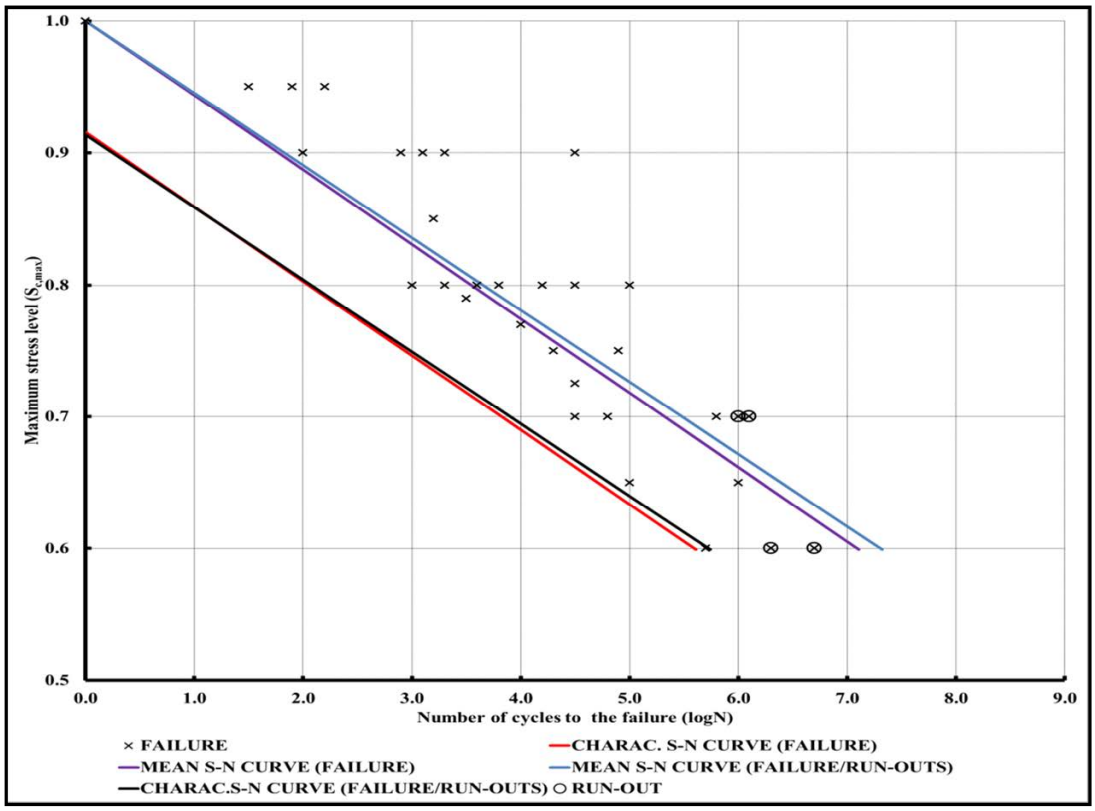

Figure 39. Mean and characteristic S-N curves obtained by Model (1) with μ_ε = 0. Data is from Figure 22 (Lohaus et al. 2012) and $S_{c,min}$ =0.05. (units in [MPa]). Run-out tests are included.

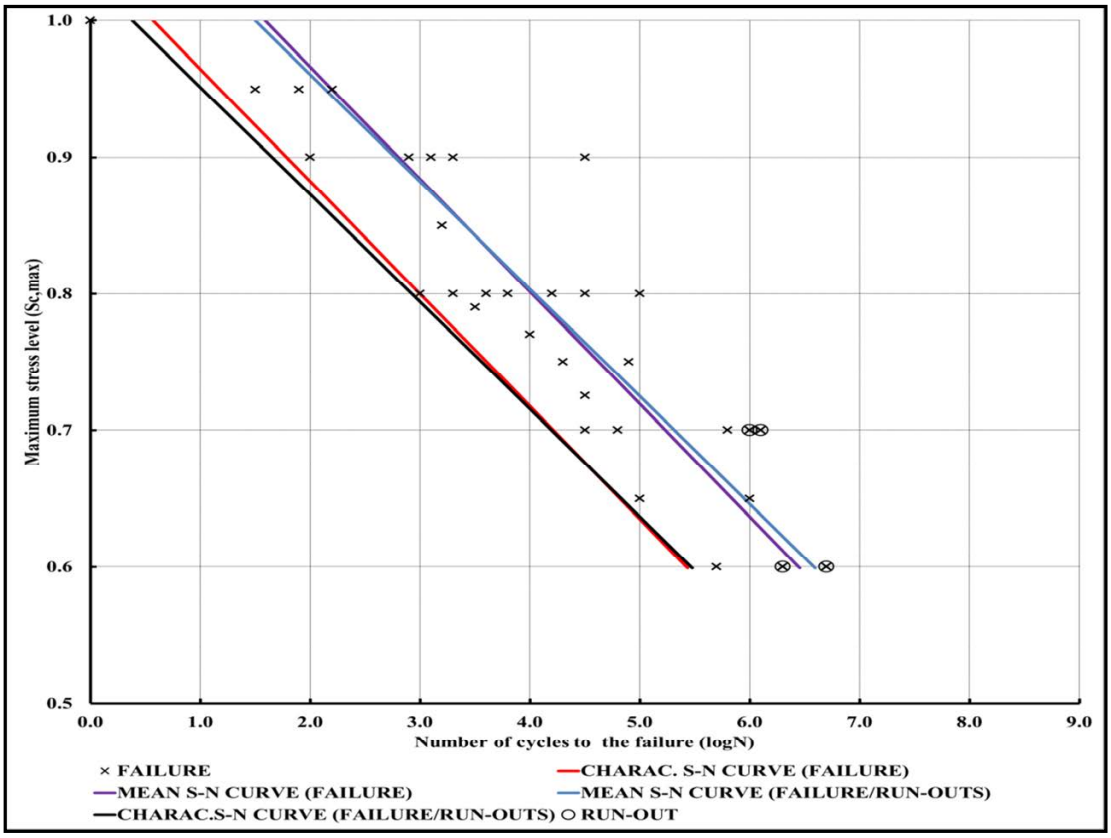

Figure 40. Mean and characteristic S-N curves obtained by Model (1) with μ_ε estimated from the test data. Data is from Figure 22 (Lohaus et al. 2012) and $S_{c,min}$ =0.05. (units in [MPa]). Run-out tests are included.

In Figures 39 and 40, the fitted S-N curves are shown. For the test results available, Tables 14 and 15 show only a minor difference between assuming all tests in failure instead of accounting for run-outs. A significant difference is observed if μ_ε estimated from the test data and not assumed to be equal zero. Visually, from Figures 39 and 40, the mean S-N curve fits the data better, and the uncertainty represented by σ_ε is seen to decrease from approx. 0.96 to about 0.62. Further, the characteristic S-N curve is seen to result in larger fatigue lives.

7.3.2 Model (2)

As an alternative to Model (1), the uncertainty of the fatigue life 'ε' is modelled by:

$$\log N_i = \frac{A+}{Y_i - 1} \cdot \left(S_{c,max,i} - 1\right) \tag{56}$$

where 'ε' is assumed normal distributed with mean value equal to '0' and standard deviation σ_ε. 'A' and σ_ε are estimated using the Maximum-Likelihood Method using a similar procedure as described above.

The fitted results, which are estimated by Method (2) and presented in Table 16, show quite high values of the standard deviation of 'ε'.

Figure 41 shows a plot of the mean and characteristic S-N curves together with the test data. The fits are seen to be quite poor and results in much lower fatigue lives than Model (1) with μ_ε estimated from the data.

Table 16. Results for Model (2)

Considering all specimens to failure (Case 1)		***Considering both run-outs/and failures (Case 2)***	
A	10.91	A	11.40
ε	$\sigma_\varepsilon = 3.99$	ε	$\sigma_\varepsilon = 4.11$
σ_A	0.68	σ_A	0.72
$\sigma_{\sigma\varepsilon}$	0.46	$\sigma_{\sigma\varepsilon}$	0.52
$\rho_{A,\sigma\varepsilon}$	0.05	$\rho_{A,\varepsilon}$	0.08

In Figures 42 to 44, the fitted S-N curves by Model (1) and Model (2) are shown together with the S-N curve proposed by the new FIB Model Code 2010, CEB-FIB Model Code 90 and Eurocode 2 (EN1992-2:2005 fatigue verification of plain concrete in bridges). The characteristic S-N curves obtained by Model (1) with μ_ε estimated from test data do not deviate significantly from the new FIB Model Code 2010, see Figure 43. Larger fatigue lives than the new FIB Model Code 2010 for high values of $S_{c,max,i}$ and smaller fatigue lives for small values of $S_{c,max,i}$. However, more tests data should be included in future statistical analyses to confirm these indicative conclusions, especially data with larger values of $S_{c,min,i.}$

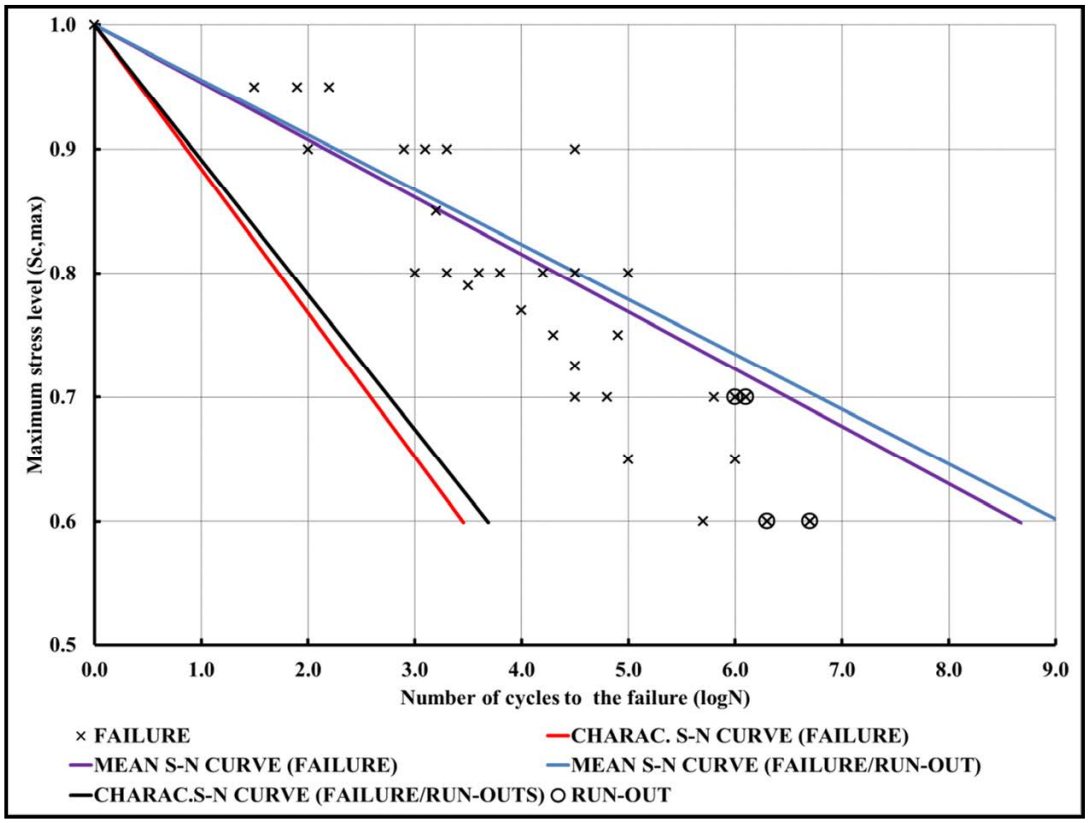

Figure 41. Mean and characteristic S-N curves obtained by Model (2). Data is from Figure 22 (Lohaus et al. 2012) and $S_{c,min}$=0.05. (units in [MPa]). Run-out tests are included.

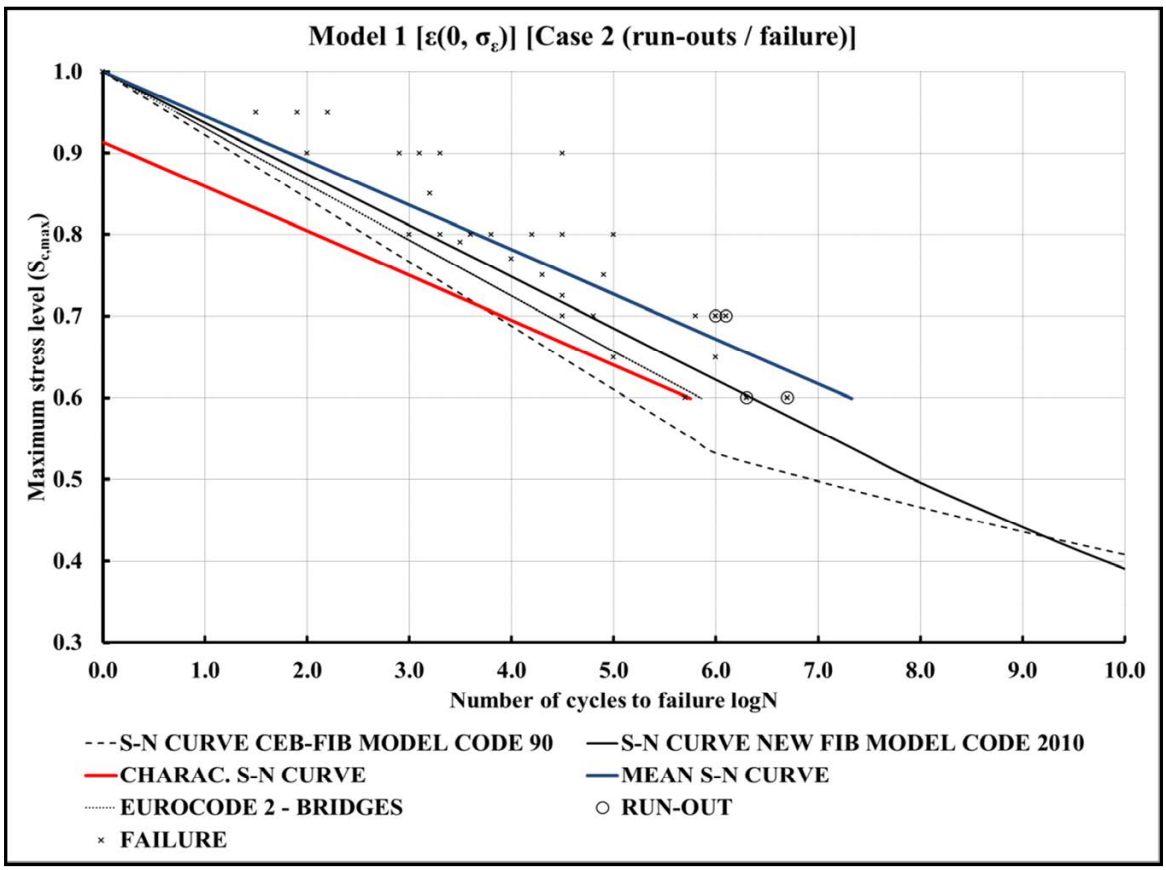

Figure 42. Mean and characteristic S-N curves obtained by Model (1) with $\mu_\varepsilon = 0$ and S-N curves by the new FIB Model Code 2010, CEB-FIB Model Code 90 and Eurocode 2 for concrete bridges (EN1992-2:2005). Data is from Figure 22 (Lohaus et al. 2012) and $S_{c,min}$ =0.05. (units in [MPa]). Run-out tests are included.

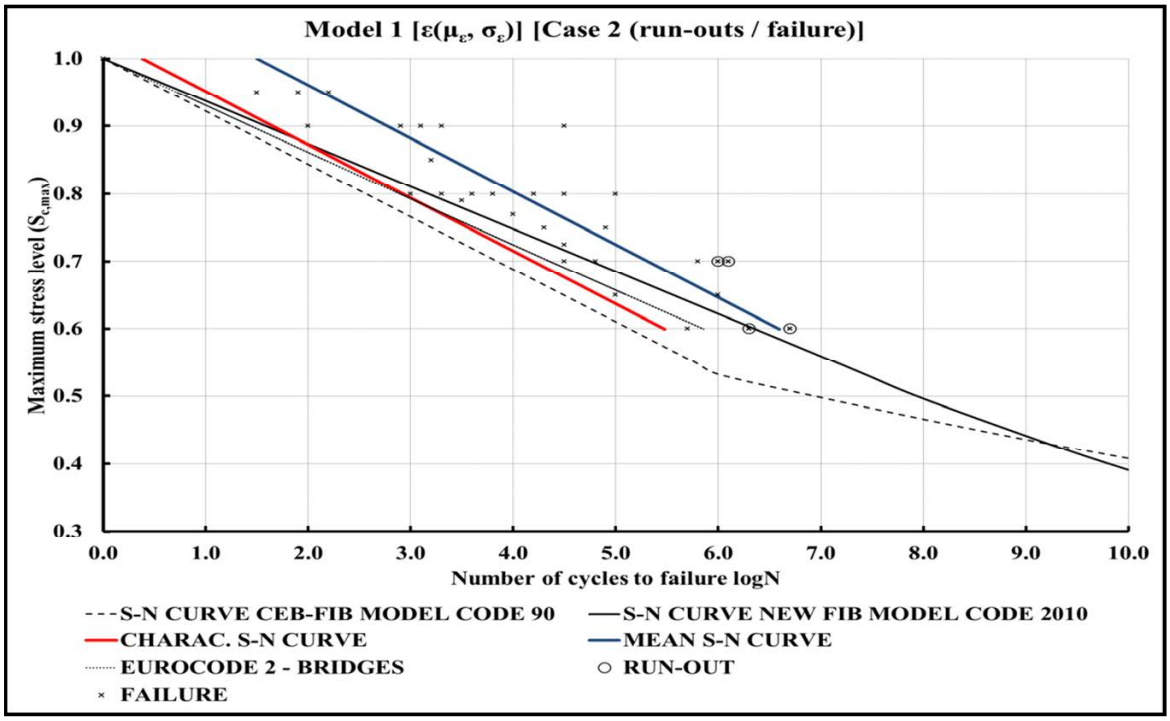

Figure 43. Mean and characteristic S-N curves obtained by Model (1) with μ_ε estimated from test data and S-N curves by the new FIB Model Code 2010, CEB-FIB Model Code 90 and Eurocode 2 for concrete bridges (EN1992-2:2005). Data is from Figure 22 (Lohaus et al. 2012) and $S_{c,min}$ =0.05. (units in [MPa]). Run-out tests are included.

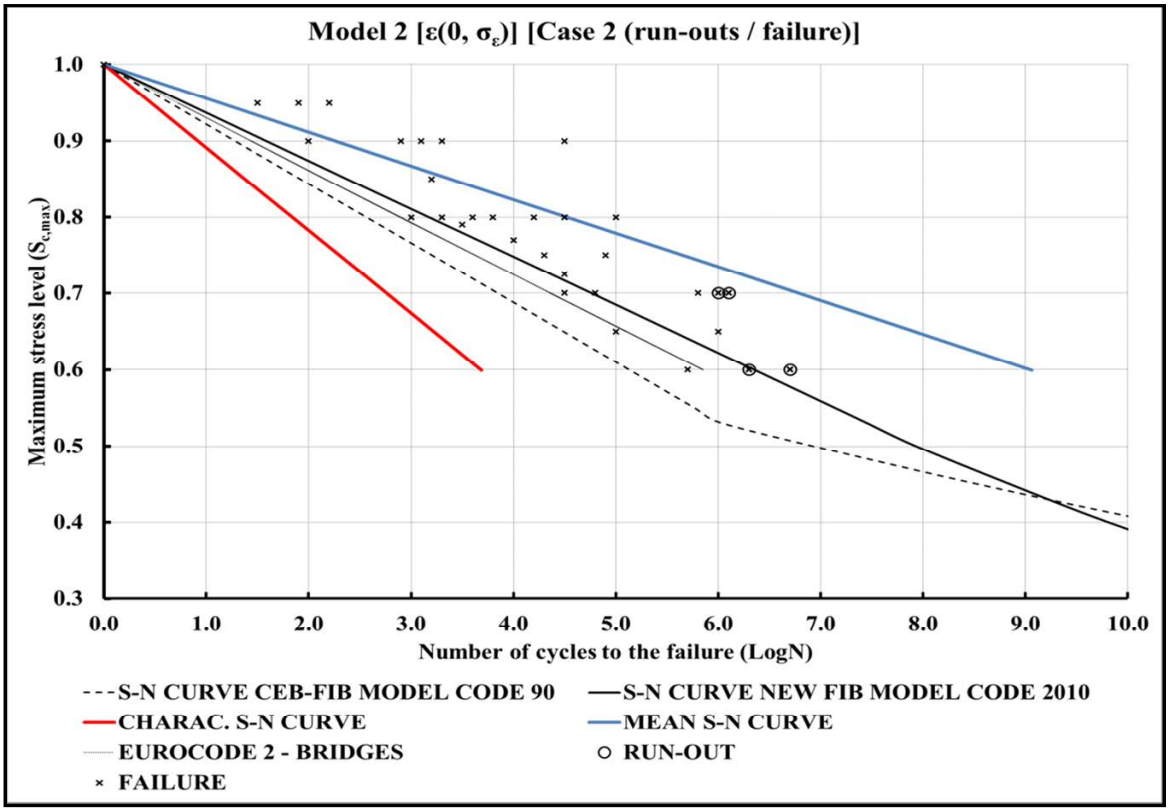

Figure 44. Mean and characteristic S-N curves obtained by Model (2) and S-N curves by the new FIB Model Code 2010, CEB-FIB Model Code 90 and Eurocode 2 for concrete bridges (EN1992-2:2005). Data is from Figure 22 (Lohaus et al. 2012) and $S_{c,min}$ =0.05. (units in [MPa]). Run-out tests are included.

7.4 Stochastic model and reliability assessment

In this section, an illustrative example is shown in order to describe a reliability assessment for fatigue failure on concrete using new FIB Model Code 2010 in combination with Miner's rule. The main structural properties and load fatigue spectrum are described in Appendix A.5. In this section, a probabilistic model for the fatigue strength is formulated based on the new FIB Model Code 2010 and the uncertainty formulation with Model (1) is described in Section 7.3.1 of this thesis.

The following representative limit state equation is used:

$$g = \Delta - \sum_i \frac{t \cdot n_i}{N_i\left(X_w, X_{SCF}, S_{c,max,i}[f_{cd,fat}],\ S_{c,min,i}[f_{cd,fat}], A,\ ,\ z\right)} \qquad (57)$$

where '*t*' is the time ($0 \le t \le T_L$) and T_L is the service life in years (normally until 25 years for wind turbines), 'Δ' is the model uncertainty related to Miner's rule for linear damage accumulation and 'z' is a design parameter determined which in principle is from the corresponding representative design equation. 'Δ' is assumed to be Log-Normal distributed with a mean value=1.0 and coefficient of variation COV_{Δ}. $N_i(X_w, X_{SCF}, S_{c,max,i}[f_{cd,fat}], S_{c,min,i}[f_{cd,fat}], A, \varepsilon, z)$ is the number of cycles to failure in bin *i* estimated by Model (1). X_w and X_{SCF} are Log-normal distributed stochastic variables which model the uncertainty related to the fatigue wind load (X_w) and the fatigue stress ranges given the fatigue load stresses (X_{SCF}). X_w and X_{SCF} are applied as factors on the fatigue load effects. If statistical uncertainty is included, then 'A' and 'ε' are modelled as stochastic variables.

'A' which represents the uncertainty of the parameter to be fitted is modelled by a Normal distribution. 'ε' represents the error term or uncertainty of the fatigue life modelled by a Normal distribution with mean value equal to μ_ε and standard deviation σ_ε. The reliability assessment is performed using the fatigue concrete data obtained by Model (1), see Table 15 (Case 1). f_c is the concrete compression strength which is assumed Log-normal distributed.

The probability of failure and the corresponding reliability indices for two different concrete strengths (80 and 150 MPa) are estimated using the design parameter '**z**' for illustration equal to 3000, 4000 and 5000 which are comparable with the design value z=3467 estimated according with the Model (1) considering the formulation given in new FIB model code 2010. Further, in this example, the design fatigue life, $T_{FAT,}$ is assumed equal to 25 years. The stochastic model is shown in Table 17. (Lohaus et al. 2012).

Table 17. Stochastic model for fatigue of plain concrete. [N: Normal, LN: Log-Normal, D: Deterministic].

Var.	Dist.	Mean	COV	Comments
Δ	LN	1.00	0.30	Damage
X_{SCF}	LN	1.00	0.15	Stresses
X_W	LN	1.00	0.20	Wind/wave loads
f_c	LN	80/150 (MPa)	0.15	Concrete compression strength
A	N	6.12	0.08	Fitted by maximum-likelihood method for data
μ_ε	N	1.59	0.15	from Figure 22 (Lohaus et al. 2012) (Table 15-
σ_ε	N	0.62	0.12	Case 1)
			Design parameters	
z	D	3000/4000/5000	--	Cross-section parameter
f_{ck0}	D	10.0 (MPa)	--	Reference strength
$\beta_{CC}(t_0)$	D	1.0	--	
η_c	D	1.0	--	Estimated according to CEB-FIB Model Code 90
γ_{Sd}	D	1.1	--	
$\gamma_{C,fat}$	D	1.50	--	
T_{fat}	D	25 years	--	Design fatigue life of the onshore wind turbine
T_L	D	25 years	--	Service life of the onshore wind turbine

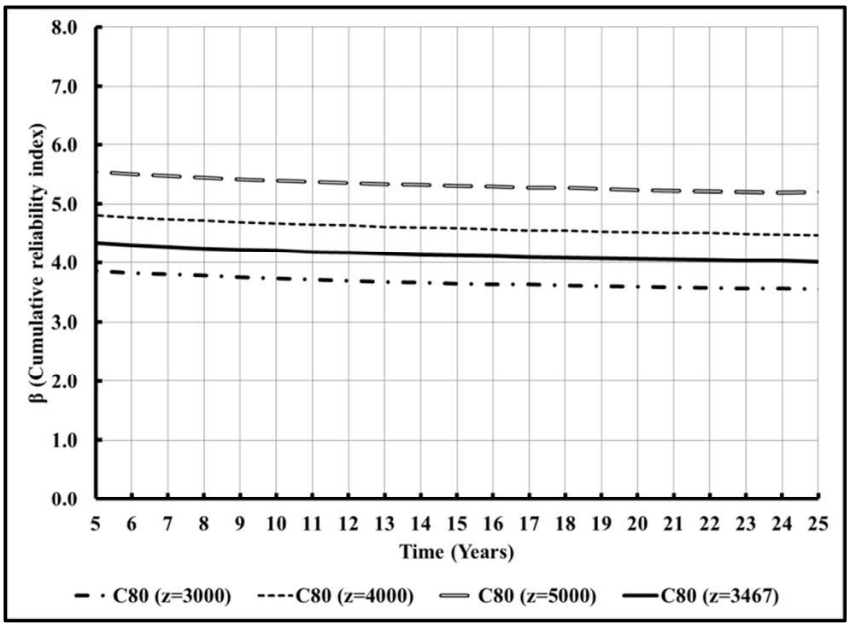

Figure 45. Cumulative reliability indices as function of time for mean concrete strength equal to 80 MPa (C80) and 'z' values equal to 3000, 4000, 5000 and 3467.

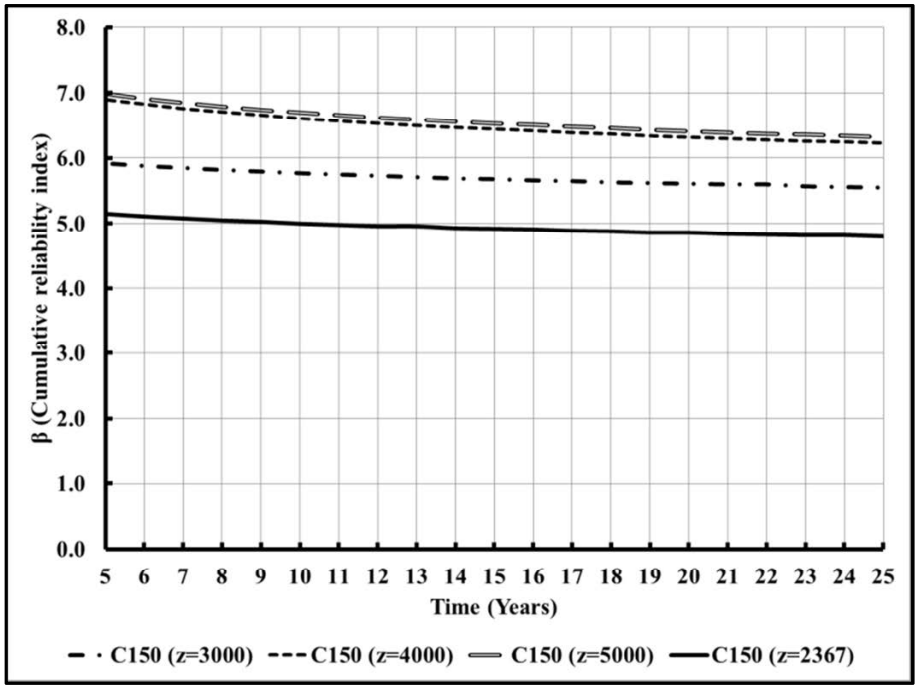

Figure 46. Cumulative reliability indices as function of time for mean concrete strength equal to 150 MPa (C150) and 'z' values equal to 3000, 4000, 5000 and 2367.

The results are shown in Figures 45 and 46. The cumulative reliability indices increase as expected if the design parameter 'z' increases. Further, if the compressive strength of the plain concrete is increased from 80 to 150 MPa, then the cumulative reliability indices are also seen to be increased. Moreover, if the compressive strength capacity is increased, the design parameter 'z' decreases as a consequence of the improvement in the material strength leading to material saving decreasing the costs of the substructure

7.5 Summary

For steel reinforcement bars, the statistical analysis of the considered fatigue data indicates that the coefficient of variation of log N_i is approx. 25-30 %. N_i is the number of cycles to fatigue failure. Further, the results from the statistical analyses indicate that the S-N curve proposed by Eurocode 2 can be considered quite conservative.

For plain concrete, two models are considered in order to introduce the uncertainty in the estimation of the fatigue life. The statistical analysis with Model (1) where the error term is added to the main parameter for determining the fatigue life shows that the uncertainty level is generally larger than for the reinforcement bars (and for welded steel details). It also shows that the characteristic S-N curve is quite close to the S-N curve proposed in FIB Model Code 2010, see Figure 43. However, more data is needed to investigate these findings.

An illustrative example is described where the reliability for fatigue failure of plain concrete is estimated using a stochastic model based on the fatigue model in FIB Model Code 2010 and a stochastic model based on the statistical analysis in Section 7.3. This stochastic model can be further developed and e.g. used as basis for assessment of partial safety factors.

Chapter 8

CONCLUSIONS AND FUTURE WORK

The expected future development within offshore wind energy will require more wind turbines placed at deeper water, implying that more innovations are needed within support structures and also in optimizing the material consumptions including optimal design for the fatigue failure mode. For this reason, maintaining a sustainable wind industry is the main motivation of this PhD thesis, and contributions to new and reliable strategies are proposed in order to decrease the cost of energy (CoE) and, at the same time, maintaining a sufficient reliability level during the life-cycle of both onshore and offshore wind turbines. The strategies are defined in order to reduce structural costs, to increase the lifetime of the substructures and to develop skilled designs. The improved designs should satisfy a structural safety level defined in accordance with the structural risks considered. Therefore, reliability methods such as FORM technique and the Monte Carlo simulation are applied in order to estimate the probability of failure for onshore and offshore wind turbines where fatigue damage is an important failure mode. Probabilistic models for fatigue failure have been established and developed, enabling a rational treatment of the main uncertainties involved in the complex interaction between stochastic loads (wind and waves) and strength of the materials. Both steel and concrete substructures are considered.

Different technical and economic strategies have been presented in appendices A.1 to A.5 where reliability assessments are described. The reliability calculations are performed using special modules added to the PRADSS reliability program (Sørensen 1987).

Appendix A.1 considers fatigue reliability and calibration of fatigue design factors for support structures. A reliability-based calibration to existing code rules, using reliability methods on levels I and III, is performed. The calibration is carried out with a reliability based approach to assess the fatigue design factors required for welded details in support structures for offshore wind turbines. Fatigue design factors (FDF) are calibrated using representative models for uncertainties and fatigue loads. The results show that the FDFs, in general, should be increased compared to the values currently recommended in standards. It is also seen that the FDFs depend highly on the level of uncertainty of the assessment of the loads and the stress concentration factors. As expected for offshore wind turbines, the required fatigue reliability levels can be accepted to be lower than those required for the offshore oil and gas platforms due to the consequences of failure in general being lower. Furthermore, the influence of inspections was considered in order to extend and maintain a given target reliability level. The results show that significant reductions in the required FDF values can be obtained if inspections are performed.

In Appendix A.2, a probabilistic model is formulated for fatigue failure in jacket-type offshore wind turbine substructures, accounting for the operational characteristics of wind turbines and applying the design load case specifications in IEC 61400-1. Furthermore, a comparative analysis between different S-N curves is done. The analysis indicates a considerable effect on the structural reliability depending on the S-N curves used. While the reliability assessment is estimated for one single component or hot spot in Appendix A.2, Appendix A.3 is focused on system effects of fatigue failure modes for welded details in jacket-type OWT substructures. The main results are in accordance with the main concepts of system reliability theory where a series system model with more independence between stochastic variables implies a decrease in the structural system reliability. On the other hand, taking into account load redistribution between the structural components, serie systems of parallel mechanisms show that more independence between stochastic variables can imply an increase in the structural system reliability.

In Appendix A.4, a marginal cost model is presented in order to determine the overall importance of changes in the long-term control strategy. Here, the influence of different operational configurations is represented by the potential income which is the result between the loss of income due to a decrease in produced electricity and saving material due to the decrease of the fatigue damage accumulation. The cost model is addressed in order to find an optimum balance between the costs of the substructures and the annual wind energy production as well as to maximize the benefices coming from adequate operational control configurations which will increase the material saving in the substructures.

Appendix A.5 presents a probabilistic model for fatigue failure of reinforced concrete slab foundations where fatigue cracks are an important issue. The probabilistic fatigue model enables a rational treatment of the uncertainties involved in the complex interaction between fatigue cyclic loads and fatigue failure of the two materials, steel reinforcement bars and concrete. Design and limit state equations relevant for wind turbines are formulated in a novel fatigue damage model based on design principles in the Eurocodes where S-N curves are used in combination with Miner's rule.

In Chapter 7, a statistical analysis is presented considering test data from laboratory fatigue tests which were performed on specimens of (high-strength) concrete (Lohaus et al. 2012) and steel reinforcement bars (Hansen & Heshe, 2001). This statistical analysis is considered as a major contribution of this thesis, and the estimated uncertainties can be used as basis for probabilistic modelling and reliability analysis of wind turbine structures with reinforced concrete components.

For steel reinforcement bars, the statistical analyses of the fatigue data considered indicate that the coefficient of variation of log N_i (where N_i is the number of cycles to fatigue failure) is 25–30 %. Further, the results from the statistical analyses indicate that the S-N curve proposed by Eurocode 2 can be considered to be quite conservative.

For plain concrete, two models for introducing uncertainty in the estimation of the fatigue life are considered. The statistical analyses with Model (1) where the error term is added to the main parameter for determining the fatigue life show that the uncertainty level is generally larger than with reinforcement bars (and with welded steel details) and that the characteristic S-N curve is quite close to the S-N curve proposed in FIB Model Code 2010, see Figure 43. However, more test data should be included in the statistical analyses to confirm these indicative conclusions, especially test data with larger values of $S_{c,min,i.}$

The results obtained using Model (2) result in quite high values of the standard deviation of the uncertainty of the fatigue life and the fits are quite poor. Therefore, Model (2) estimates much lower characteristic fatigue lives than Model (1). Further, an illustrative example is described where a stochastic model is formulated based on the results of the statistical analysis and the reliability for fatigue failure of plain concrete is estimated.

8.1 Future work

For offshore wind turbine support structures, further work is relevant in different aspects to refine stochastic modelling and reliability assessment, especially in relation to fatigue failure. More experimental data should be collected for improvement and validation of the models proposed. For offshore wind turbine substructures, more research and experimental data are needed with respect to calibration of fatigue design factors for inclusion in design standards. This also includes application in decision problems in connection with life time extension/shortening. Also, it is important to include, for system effects, the information from inspections and condition monitoring. Furthermore, wake effects in wind farms should be included in the limit state equations, taking into account the increased turbulence effects and so the increased fatigue loads. Also, the design for fatigue of details made in various types of concrete could be expected to be important for future innovative offshore wind turbine support structures.

The models for system reliability in Appendix A.3 can be further developed for e.g. improved accounting for the influence of wind and wave loads on OWT substructures at different submerged levels and also for operational conditions. Similarly, the influence on the reliability assessment by different operational strategies presented in Appendix A.4 can be extended e.g. for series system effects where optimization of the operational strategy could have an important effect.

Other areas of further work include application of Bayesian approaches for inspections/updating new given information from inspections of one, two or more hot spots, assuming no detection of cracks. This would require fracture mechanics models to be developed for offshore wind turbine steel substructures and calibrated to the S-N approach following a procedure that could be based on the techniques used for oil and gas steel platforms. Also, short-term strategies for control and decision making of offshore wind turbines can be considered for economical optimization, taking into account the fluctuating energy prices and the fatigue accumulation.

For both onshore and offshore wind turbines, further work can be relevant for the fatigue failure mode by further development of the stochastic model established in Appendix A.5 and the statistical analysis presented in Chapter 7. The stochastic model could be applied for reliability assessment in wind farms where substructures made of high-strength concrete could be considered as an alternative to steel substructures. This also requires reliability assessments to be performed considering extreme failure modes. The probabilistic models can next be applied to reliability-based calibration of partial safety factors. The influence of inspection and maintenance strategies plays an important role in the reliability assessment. Therefore, a Bayesian statistical analysis could be done in order to estimate the updated reliability of old reinforced concrete foundations and for optimal planning of inspection, operation and maintenance.

BIBLIOGRAPHY

Ameen, P. & Szymanski, M. (2006). *Fatigue in Plain Concrete: Phenomenon and methods of analysis*. Master's Thesis (2006:5) in the International Master's Programme Structural Engineering. Department of Civil and Environmental Engineering. Division of Structural Engineering. Concrete Structures. Chalmers University of Technology.

Anders, S., & Lohaus, L. (2007). Polymer und fasermodifizierte Hochleistungsbetone für hochdynamisch beanspruchte Verbindungen wie "Grouted Joints" bei Windenergieanlagen. Final report for research scholarship T 4/2002, Stiftung Industrieforschung, Hannover.

Ang, A. H.-S. & Tang, W. H. (1975). *Probability Concepts in Engineering Planning and Design, Vol. 1: Basic Principles*. New York: John Wiley & Sons, Inc.

Ang, A. H.-S. & Tang, W.H. (1984). *Probability Concepts in Engineering Planning and design, Vol. II: Decision, risk and reliability*, New York: John Wiley & Sons, Inc.

Ang A. H.-S. & Tang W.H. (2007). *Probability Concepts in Engineering; Emphasis on Applications to Civil and Environmental Engineering* (2nd Ed. Vol. I: Basic principles). USA: John Wiley and Sons. ISBN: 978-0-471-72064-5. ISBN: 0-471-72064-X

Ayala-Uraga, E. (2009). *Reliability-based assessment of deteriorating ship-shaped offshore structures*. Ph.D. Thesis at Department of Marine Technology. Faculty of Engineering Science and Technology. Norwegian University of Science and Technology (NTNU), Trondheim, Norway.

Benjamin, J. R. & Cornell, C. A. (1970). *Probability, Statistics, and Decision for Civil Engineers*. McGraw-Hill Book Co., New York.

Burton, T., Sharpe, D., Jenkins, N. & Bossanyi, E. (2001). *Wind energy: Handbook.* Chichester, UK: John Wiley & Sons. ISBN: 0471489972

Bossanyi, E.A. (2009). *GH Bladed. User Manual*. Ver. 3.82. Garrad Hassan and Partners Ltd. Doc. no. 282/BR/010.

Brozzetti, J., Hirt, M., Sedlacek, G., Smith, I., & Ryan, I., Eurocode 3: Steel Structures, Fatigue background document to Chap. 9 of EC3.

BS 7910. (2005). *Guide to methods for assessing the acceptability of flaws in metallic structures*.

Choi, S.K., Grandhi, R.V. & Canfield, R.A. (2007). *Reliability-based structural design*. London: Springer-Verlag London Limited. ISBN: 978-1-84628-444-1 (Print) 978-1-84628-445-8 (Online)

Clauss, G., Lehmann, E. & Östergaard, C. (1992). *Offshore structures. Vol. I: Conceptual design and hydromechanics*. Translated by Shield, M.J. FIInfSc, MITI. Springer-Verlag. ISBN 0-387-19709-5. Prined in Germany.

Clauss, G., Lehmann, E. & Östergaard, C. (1994). *Offshore structures. Vol. II: Strength and safety for structural design*. Translated by Shield, M.J. FIInfSc, MITI. Springer-Verlag. ISBN 0-387-19709-5. London limited 1994. Printed in Great Britain.

CEB. Comité Euro-international du Bétun. (1993). *CEB-FIB Model Code 90*. Bulletin d´information, No. 213/214, Thomas Telford Ltd., London.

COMREL & SYSREL: USER MANUAL. (2003). *Componental and System Reliability Analysis Using Built-in Symbolic Processor by RCP GmbH, Reliability Consulting Programs*. Chap. 2.8, Munich, Germany.

Cornelissen, H. A. W. (1984). *Fatigue failure of concrete in tension*. Heron Vol. 29, No 4, pp. 68

Cornelissen, H. A. W. (1986). *State-of-the-art report on fatigue of plain concrete*. Delft, the Netherlands: Delft University of Technology. Report 5-86-3. pp. 62.

Dean, R. G. & Dalrymple, R.A. (1991). *Advanced series on ocean Engineering. Vol. 2: Water, wave mechanics for engineers and scientists*. World scientific publishing Co. Pte. Ltd. Printed in Singapore. ISBN 9810204205.

Ditlevsen, O., & Madsen, H. O. (1996). *Structural Reliability Methods*, Wiley, New York. ISBN: 0471960861

DNV-RP-C203. (2012). *Fatigue design of offshore steel structures*. Recommended Practice DNV-RP-C203; Technical Report; DNV: Høvik, Norway.

DNV-OS-C502, (2012). *Offshore concrete structures*. Det Norske Veritas A.S. (DNV Høvik, Norway).

DNV-OS-J101, (2013). *Design of offshore wind turbine structures*. Det Norske Veritas A.S. (DNV: Høvik, Norway).

DNV No. 95-2018. (1995): *Guideline for Offshore Structural Reliability Analysis.* Technical Report No. 95-2018; DNV: Høvik, Norway.

Dong, W.B., Gao, Z. & Moan, T. (2010). Fatigue reliability analysis of jacket-type offshore wind turbine considering inspection and repair. *In Proceedings of European Wind Energy Conference & Exhibition (EWEC 2010)*, Warsaw, Poland; 20-23 April 2010.

Dyrbye, C. & Hansen, S.O. (1997). *Wind Load on Structures*. Chichester:John Wiley and Sons. ISBN 0-471-95651-1

Elishakoff, I. (1999). *Probabilistic theory of structures* (2nd Ed.). Dover Publications Inc. Mineola, New York.

EN 1990. (2002). Eurocode 0: *Basis of Structural Design*.

EN1992-1-1. (2004). European Committee for Standardization (ECS). Eurocode2–Design of Concrete Structures–Part 1.1: *General rules and rules for buildings*. Brussels.

EN1992-2. (2005). European Committee for Standardization (ECS). Eurocode2: Design of concrete structures-Part 2: *Concrete bridges-Design and detailing rules*. Brussels.

EN 1993-1-9. (2005): Eurocode 3: *Design of Steel Structures, Part 1-9: Fatigue*. Technical Report No. BS EN 1993-1-9:2005; British-Adopted European Standard: London, UK.

European Union. (2009). Directive 2009/28/EC of the European parliament and of the council of 23 April 2009: on the promotion of the use of energy from renewable sources and amending and subsequently repealing Directives 2001/77/EC and 2003/30/EC. *Official Journal of the European Union*.

EWEA. (2011). *EU. Energy Policy to 2050: Achieving 80-95% emissions reductions*. March, 2011. A report by the European Wind Energy Association. http://www.ewea.org/fileadmin/ewea_documents/documents/publications/reports/EWEA_EU_Energy_Policy_to_2050.pdf

Faber M.H., Sørensen J.D., Tychsen J. & Straub D. (2005). Field Implementation of RBI for Jacket Structures. *Journal of Offshore Mechanics and Arctic Engineering*, Trans. ASME, 127(3), pp. 220-226.

Faber M.H., Engelund S., Sørensen J.D. & Bloch A. (2000). Simplified and Generic Risk Based Inspection Planning. *Proceedings of the 19th OMAE*, New Orleans.

Faltinsen, O.M. (1990). *Sea loads on ships and offshore structures*. Published by the Press Syndicate of Cambridge. UK. ISBN 0-521-45870-6

Fib (2012). International Federation for Structural Concrete Model Code 2010, final draft, Volume 1 and 2, March (2012).

Fingersh, L., Hand, M. & Laxson, A. (2006). *Wind turbine design cost and scaling model*. Technical Report. NREL/TP-500-40566. Colorado, USA.

Frandsen, S.T. (2007). *Turbulence and turbulence generated structural loading in wind turbine clusters*. Wind Energy Department. Risø National Laboratory. Roskilde, Denmark. ISBN 87-550-3458-6. ISSN 0106-2840. Risø-R-1188(EN).

Fujita M., Schall G. & Rackwitz R. (1989). Adaptive Reliability-Based Inspection Strategies for Structures Subject to Fatigue. *Proceedings of the 5th ICOSSAR conference*, Vol. 2, San Francisco, pp. 1619-1626

Gao, Z., Saha, N.L.J., Moan, T. & Amdahl, J. (2010). Dynamic Analysis of Offshore Fixed Wind Turbines Under Wind and Wave Loads Using Alternative Computer Codes. *Proceedings of the TORQUE Conference*, FORTH, Heraklion, Crete, Greece.

Ghiocel, D. & Lungu, D. (1975). *Wind, snow and temperatures effects on structures, based on probability*. (translated from the Rumanian by Mihaela Blandu), Tunbridge Wells, Kent, England: Abacus Press

Ghosn M., Moses F. & Frangopol D.M. (2010). Redundancy and Robustness of Highway Bridge Superstructures and Substructures. *Structure and Infrastructure Engineering: Maintenance, Management, Life-Cycle Design and Performance*, 6:1-2, pp. 257-278.

Göransson F. & Nordenmark A. (2011). *Fatigue assessment of concrete foundations for wind power plants*. Master thesis 2011:119. Depart. of Civil and Environmental Engineering. Division of Structural Engineering: Concrete Structures. Chalmers University of Technology. Göteborg, Sweden.

GL. (2005): *Germanischer Lloyd Wind Energie GmbH; Wind Energy Committee. Guideline for the Certification of Offshore Wind Turbines*; Technical Report; Germanischer Lloyd WindEnergie GmbH: Hamburg, Germany.

Grünberg, J., & Oneschkow, N. (2011). *Gründung von Offshore Windenergieanlagen aus filigranen Betonkonstruktionen unter besonderer Beachtung des Ermüdungsverhaltens von hochfestem Beton*. Final report for BMU joint research project. Leibniz University of Hannover.

Hansen, L.P. & Heshe G. (2001). Static, Fire and Fatigue Tests of Ultra High-Strength Fibre Reinforced Concrete and Ribbed Bars. *Nordic Concrete Research*. No. 26, 2001, p. 17-37. ISSN: 0800-6377.

Holmen, J.O. (1984). Fatigue design evaluation of offshore concrete structures. *Matériaux et Construction. Janvier–Février 1984.* Vol. 17, No. 97. Issue 1, pp. 39-42. Kluwer Academic Publishers. DOI 10.1007/BF02474054

Hughes, L., & Rudolph, J. (2011). *Future world oil production: Growth, plateau, or peak?*. Current Opinion in Environmental Sustainability, 3(4), pp. 225-234.

IEC 61400-1. (2005). *International Electrotechnical Committee: Wind Turbines-Part 1: Safety Requirements*. Technical Report No. IEC 61400-1:2005. Geneva, Switzerland. http://www.iec.ch/.

IEC 61400-3. (2009). *International Electrotechnical Committee: Wind Turbines-Part 3: Design Requirements for Offshore Wind Turbines*. Technical Report No. IEC 61400-3:2009. Geneva, Switzerland. http://www.iec.ch/.

ISO 19902. (2007). *Petroleum and natural gas industries—Fixed steel offshore structures*. ISO Standard; ISO: Geneva, Switzerland.

JCSS, (2006). *Probabilistic model code for reliability based design*. Issued by the Joint Committee on Structural Safety. Internet publication: http://www.jcss.byg.dtu.dk/

Jonkman, J. M., Butterfield, S., Musial, W. & Scott. G. (2009). *Definition of a 5MW reference wind turbine for offshore system development.* National Renewable Laboratory. Technical Report NREL/TP-500-38060.

Jonkman J.M. & Buhl, M.L. (2005). *FAST User's Guide*. Technical Report NREL/EL-500-38230.

Kuethe, A. M. & Chow, C.Y. (1998). *Foundation of Aerodynamics: Bases on aerodynamic design* (5th Ed.). New York: John Wiley and Sons. ISBN 0-471-12919-4

Larsen, T.J. (2009). *How 2 HAWC2, the user's manual*, ver. 3-7. Copenhagen (Denmark): Risø. National Laboratory, Technical University of Denmark.

Lassen, T. (1997). *Experimental investigation and stochastic modelling of the fatigue behaviour of welded steel joints*. PhD thesis, Structural reliability theory, paper No. 182, Aalborg University.

Lindley, D. V., (1976). *Introduction to Probability and Statistics from a Bayesian Viewpoint*, Vol. 1+2. Cambridge University Press, Cambridge.

Lohaus, L., Oneschkow, N. & Wefer, M. (2012). Design model for the fatigue behaviour of normal-strength, high-strength and ultra-high-strength. *Structural concrete: journal of the fib*, Vol. 13 (2012), No. 3, p. 180-192. Ernst&Sohn:Berlin. ISSN: 1464-4177. DOI:10.1002/suco.201100054.

Madsen, H.O. & Sørensen, J.D. (1990). Probability-based optimization of fatigue design inspection and maintenance. *In Proceedings of International Symposium on Offshore Structures*, Glasgow, UK, 2-3 July 1990; pp. 421-438.

Madsen H.O. (1987). Model Updating in Reliability Theory. *Proceedings of the ICASP5*, Vancouver, Canada, pp. 565-577.

Madsen, H.O.; Krenk, S. & Lind, N.C., (1986). *Methods of Structural Safety*; Prentice-Hall: Englewood Cliffs, NY, USA. ISBN: 0-13-579475-7

Manwell, J.F., McGowan, J.G. & Rogers, A.L. (2009). *Wind energy explained: theory, design and application* (2nd Ed.). New York. USA: Wiley. ISBN: 9780470015001; ISBN: 0470015004

Martindale, S.G. & Wirsching P.H. (1983), Reliability-Based progressive Fatigue Collaps. *Journal of Structural Engineering*, Vol. 109, pp. 1792-1811, ASCE Paper No. 18181.

Melchers R. E. (1999). *Structural Reliability Analysis and Prediction* (2nd Ed.). Chichester: John Wiley and Sons. ISBN: 0471983241 ; ISBN: 0471987719

Moan, T. (2005) Reliability-based management of inspection, maintenance and repair of offshore structures. *Struct. Infrastruct. Eng*., 1, 33–62.

Moan, T. (2008). *Structural risk and reliability analysis. Lectures notes from Department of Marine Technology*. The Norwegian University of Science and Technology (NTNU). Trondheim, Norway.

Moan, T. (2009). Reliability-Based Life Cycle Assessment of Cracks in Ocean Structures. *Proceedings of the 10th International Conference on Structural Safety and Reliability (ICOSSAR 2009)*. 13-17 September 2009 - Osaka, Japan.

Moan, T., Hovde, G.O. & Blanker, A.M. (1993). Reliability-based fatigue design criteria for offshore structures considering the effect of inspection and repair. *25th annual offshore technology conference*. Houston, Texas, USA. , Paper No. 7189, Proc. OTC. May 3-6, 1993.

Montgomery, D.C. (2009). *Design and analysis of experiments* (7th Ed.). Hoboken, N.J.: John Wiley & Sons. ISBN: 978-0-470-39882-1

Montgomery, D.C. & Runger, G.C. (2011). *Applied statistics and probability for engineers* (5th Ed.). Hoboken, NJ :John Wiley & Sons. ISBN: 978-0-470-50578-6.

Newland, D.E. (1993). *An introduction to random vibration and wevelet analysis* (3rd Ed.). Longman Scientific & Technical, copublished in United States with John Wiley and Sons, inc. New York, NY. ISBN 0582-21584-6.

Newman, J.N. (1999). *Marine Hydrodynamics*. MIT press. Massachusetts Institute of Technology. Cambridge. Massachusetts. USA. ISBN 0-262-14026-8

Nielsen, J.S. (2013). *Risk-Based Operation and Maintenance of Offshore Wind Turbines*. Ph.d. Thesis. DCE thesis: 1901-7294:46. Aalborg University, Department of Civil Engineering, Division of Water and Soil. Aalborg, Denmark.

Nielsen J. J. & Sørensen, J.D. (2011). On Risk-Based Operation and Maintenance of Offshore Wind Turbine Components. *Reliability Engineering and System Safety*. Vol. 96, No. 1, 2011, p. 218-229. DOI: 10.1016/j.ress.2010.07.007.

Nielsen J.J. & Sørensen, J.D. (2010). Planning of O&M for Offshore Wind Turbines Using Bayesian Graphical Models. *ESREL 2010*, Rhodes, Greece. pp.1081-1088. ISBN 978-0-415-60427-7.

NORSOK. (1998). *Design of steel structures*. Rev. 1. Technical Report No. NORSOK N-004; Lysaker, Norway.

OTH (2001). Comparison of fatigue provisions in codes and standards. HSE report OTH 2001/083.

Pearce, F. (2008). *Ten technologies to fix energy and climate* (1st ed.). Great Britain: Chris Goodall. ISBN 978-1-84668-877-5

Raiffa, H., & Schlaifer, R. (1961). *Applied statistical decision theory*. Boston, Mass : Division of Research, Graduate School of Business Administration, Harvard University. ISBN: 0875840175

Rangel-Ramírez, J.G. (2010). *Reliability assessment and reliability-based inspection and maintenance of Offshore Wind Turbines*. Ph.d. Thesis. DCE thesis: 1901-7294:27. Aalborg University, Department of Civil Engineering, Division of Structural Mechanics. Aalborg, Denmark.

Rangel-Ramírez, J.G. & Sørensen J.D. (2010). Framework for probabilistic of calibration of fatigue design factors for offshore wind turbine support structures. *Proc. of reliability and optimization of structural systems.* TUM, München, Germany.

Rouhan, A., Goyet J. & Faber M. H. (2004). Industrial implementation of risk based inspection planning lessons learned from experience (2) the case of steel offshore structures. *Proceedings of OMAE04 23rd International Conference on Offshore Mechanics and Arctic Engineering*. June 20-25, 2004, Vancouver, British Columbia, Canada.

Schittkowski, K., (1986). NLPQL: *A FORTRAN Subroutine Solving Non-Linear Programming Problems.* Ann. Operat. Res., 5, pp. 485–500.

Schwabe, P., Lensink, S. & Hand, M. (2011). *IEA Wind Task 26: Multi-national Case Study of the Financial Cost of Wind Energy*. Work Package 1: Final Report.

Stephens, R.I., Fatemi, A., Stephens, R.R. & Fuchs, H.O. (2001). *Metal fatigue in engineering* (2nd Ed.). New York, NY: John Wiley and Sons, Inc. ISBN 0-471-51059-9.

Skjong R. (1985). Reliability Based Optimization of Inspection Strategies. *Proc. ICOSSAR 85*, Vol. III, Kobe, Japan, pp. 614-618.

Straub, D. (2004). *Generic Approaches to Risk Based Inspection Planning for Steel Structures*. Ph.D. Thesis. Dissertation ETH No. 15529. Swiss Federal Institute of Technology. Zurich, Switzerland.

Straub, D. & Kiureghian, A.D. (2011). Reliability acceptance criteria for deteriorating elements of structural systems. *Journal of Structural Engineering*. Vol. 137, No. 12, ©ASCE, ISSN 0733-9445/2011/12. pp. 1573–1582.

Straub D. & Faber, M.H. (2006). Computational Aspects of Risk-Based Inspection Planning. *Computer-Aided Civil and Infrastructure Engineering*, 21(3), pp. 179-192.

Straub D., Goyet J., Sørensen, J.D. & Faber, M.H. (2006). Benefits of risk based inspection planning for offshore structures, *Proceedings of OMAE'05, 25th International Conference on Offshore Mechanics and Arctic Engineering*, June 4-9, 2006, Hamburg, Germany.

Sørensen, J.D. (1987). *PRADSS: Program for Reliability And Design of Structural Systems. Structural reliability theory*. Paper no. 36 (first draft). Institute of Building Technology and Structural Engineering. Aalborg University. Aalborg, Denmark.

Sørensen, J.D. (2009). Framework of risk-based planning of operation and maintenance for offshore wind turbines. *Wind Energy*, Vol. 12, No. 5, 10.06.2009, p. 493-506. John Wiley & Sons, Inc., Ltd. doi: 10.1002/we.344

Sørensen, J.D. (2011). *Notes in Structural Reliability Theory - and Risk Analysis*. Aalborg University, Aalborg, Denmark.

Sørensen, J.D. (2011). Reliability-based calibration of fatigue safety factors for offshore wind turbines. *Twenty-first International Offshore and Polar Engineering Conference (ISOPE)*. Maui, Hawaii, USA. pp. 463-470. ISSN 1098-6189.

Sørensen, J.D. & Toft H. S. (2010). Probabilistic Design of Wind Turbines. *Energies*, Vol. 3, No. 2, p. 241-257; doi:10.3390/en3020241. ISSN 1996-1073.

Sørensen, J.D., Frandsen, S. & Tarp-Johansen, N.J. (2008). Effective turbulence models and fatigue reliability in wind farms. *Probabilistic Engineering Mechanics*. doi:10.1016/j.probengmech.2008.01.009. Vol. 23, No. 4, 2008, p. 531-538.

Sørensen, J.D., Frandsen, S. & Tarp-Johansen, N.J. (2007). Fatigue reliability and effective turbulence models in wind farms. *ICASP10: Applications of Statistics and Probability in Civil Engineering: Proceedings of the 10th International Conference*, Tokyo, Japan. pp. 443-444. ISBN 978-0-415-45211-3

Sørensen, J.D., Straub, D., & Faber M.H. (2005). Generic Reliability-Based Inspection Planning for Fatigue Sensitive Details: with modifications of fatigue load. Safety and Reliability of Engineering Systems and Structures: *Proceedings of the 9th international conference on structural safety and reliability (ICOSSAR)*. ed./G. Augusti; G.I. Schuëller; M. Ciampoli. Holland: Millpress, p. 1063-1070.

Sørensen, J.D., Tychsen, J., Andersen, J.U. & Brandstrup, R.D. (2006). Fatigue analysis of load-carrying fillet welds. *Journal of Offshore Mechanics and Artic Engieering*, Vol. 128 (2006), p. 65-74. ASME. DOI:10.1115/1.2163876

Sørensen, J.D. & Faber, M.H. (1991). Optimal Inspection and repair strategies for structural systems, *Proc. 4th IFIP Conference on Reliability and Optimization of Structural Systems*, Rackwitz, R. and Thoft-Christensen, P. (Eds), Springer, Berlin, 383-394.

Tarp-Johansen, N.J. (2003). *Examples of fatigue lifetime and reliability evaluation of larger wind turbine components*. Risø-R-1418(EN). Risø national laboratory. Roskilde. ISBN 87-550-3236-2 . ISSN 0106-2840

Tarp-Johansen, N.J., Madsen, P.H. & Frandsen, S. (2003). Calibration of partial safety factors for extreme loads on wind turbines. *European Wind Energy Association*. Brussels, Belgium. Proceedings CD-ROM. CD 2.

Thoft-Christensen P. & Sørensen J.D. (1987). Optimal strategy for inspection and repair of structural systems. *Civil Engineering Systems*, 4, 94-100.

Thoft-Christensen, P. & Murotsu, Y. (1986). *Application of Structural Systems Reliability Theory*. Berlin Heicelberg. NY:Springer-Verlag. ISBN: 0-387-16362-x; ISBN:3-540-16362-x

Thoft-Christensen, P. & Baker, M. J. (1982). *Structural Reliability Theory and Its Applications*. Berlin Heicelberg. NY:Springer-Verlag. ISBN: 0-387-11731-8 ; ISBN: 3-540-11731-8

Thun, H. (2006). *Assessment of fatigue resistance and strength in existing concrete structures*. PhD Thesis. Department of Civil and Environmental Engineering. Luleå University of Technology. Luleå,Sweden.

Toft, H. S. (2010). *Probabilistic design of wind turbines*. Ph.d. Thesis. DCE thesis: 1901-7294:26. Aalborg University, Department of Civil Engineering, Division of Structural Mechanics. Aalborg, Denmark.

Veldkamp, H. F. (2006). *Chances in wind energy: A probabilistic approach to wind turbine fatigue design*. Ph.D. Thesis. DUWIND: Delft University Wind Energy Research Institute. ISBN-10: 90-76468-12-5. ISBN-13: 978-90-76468-12-9.

Waagaard, K. (2003). Design of offshore concrete structures. *28th Conference on our world in concrete & structures*. Singapore. CI-PREMIER PTE LTD. Articule Online Id: 100028064. http://cipremier.com/100028064.

Wallace, J.M. & Hobbs, P.V. (2006). *Atmospheric science: an introductory survey* (2nd Ed.). (Vol. 92 in the International Geophysics Series edited by Dmowska, R., Hartmann, D., and Rossby, H.H). San Diego, CA: Academic Press (Elsevier). ISBN 0-12-732951-X.

Wefer, M. (2010). Materialverhalten und Bemessungswerte von ultrahochfestem Beton unter einaxialer Ermüdungsbean spruchung. Dissertation, Leibniz University of Hannover. Institute of Building Materials Science.

Zittel, W. & Schindle, J. (2007). *Coal: resources and future production*. (No. EWG-Series No 1/2007). Ottobrunn, Germany: Energy Watch Group

APPENDIX ‘A’

Papers

The publications included in appendix ‘A’ are listed below:

• **Paper 1:** Márquez-Domínguez S. & Sørensen J.D., Fatigue Reliability and Calibration of Fatigue Design Factors for Offshore Wind Turbines. *Energies 2012*, 5(6), pp. 1816-1834; doi:10.3390/en5061816 (Published). ISSN 1996-1073 (www.mdpi.com/journal/energies).

• **Paper 2:** Márquez-Domínguez S., Sørensen J.D., Fatigue reliability of offshore wind turbine systems. *Proceedings on the 16th working conference of IFIP Working Group 7.5 on Reliability and Optimization of Structural Systems*, Yerevan, Armenia, June 24-27, 2012. pp. 167-174. ISBN 978-0-9657429-0-0

• **Paper 3:** Márquez-Domínguez S., Sørensen J.D., System reliability for offshore wind turbines: fatigue failure. *Proceedings of the ASME 2013. 32nd International Conference on Ocean, Offshore and Arctic Engineering (OMAE2013)*. Nantes, France. June 9-14, 2013. Paper: OMAE2013-10962 in DVD © 2013 by ASME.

• **Paper 4:** Márquez-Domínguez S., Sørensen J.D. and Rangel-Ramírez, J. G. Reliability-based operation of offshore wind turbines. *Proceedings of the 11th international conference on structural safety and reliability (ICOSSAR2013)*. Columbia University, New York, NY. June 16-20, 2013. pp. 838 (Hbk). ISBN 978-1-138-00086-5 (Hbk + CD-ROM) and ISBN 978-1-315-88488-2 (eBook)

• **Paper 5:** Márquez-Domínguez S., Sørensen J.D. Probabilistic fatigue model for reinforced concrete onshore wind turbine foundations. *Proceedings in press of the ESREL2013 annual conference*. Amsterdam, Netherland. September 29th to October 2nd, 2013.

Appendix A.1

Paper 1

Title: Fatigue reliability and calibration of fatigue design factors for offshore wind turbines.
Authors: Sergio Márquez-Domínguez and John D. Sørensen

Published in: *Energies 2012*, 5(6), pp. 1816-1834; doi:10.3390/en5061816. ISSN 1996-1073 (www.mdpi.com/journal/energies)

Reference: http://www.mdpi.com/1996-1073/5/6/1816

Important note: The titles of Tables 18 and 19 should be interchanged.

http://www.mdpi.com/about/openaccess

MDPI Open Access Information and Policy

All articles published by MDPI are made immediately available worldwide under an open access license. This means:

- everyone has free and unlimited access to the full-text of *all* articles published in MDPI journals, and
- everyone is free to re-use the published material if proper accreditation/citation of the original publication is given.
- open access publication is supported by the authors' institutes or research funding agencies by payment of a comparatively low Article Processing Charge (APC) for accepted articles.

External Open Access Resources

MDPI is a RoMEO green publisher — RoMEO is a database of Publishers' copyright and self-archiving policies hosted by the University of Nottingham

Those who are new to the concept of open access might find the following websites or 'Open Access 101' video informative:

Wikipedia article on 'Open Access'
Peter Suber's 'Open Access Overview'
Information Platform Open Access [in English, in German]
SHERPA's 'Authors and Open Access'

Meaning of Open Access

In accordance with major definitions of open access in scientific literature (namely the Budapest, Berlin, and Bethesda declarations), MDPI defines *open access* by the following conditions:

- peer-reviewed literature is freely available without subscription or price barriers,
- literature is immediately released in open access format (no embargo period), and
- published material can be re-used without obtaining permission as long as a correct citation to the original publication is given.

Until 2008, most articles published by MDPI contained the note: "© *year* by MDPI (http://www.mdpi.org). Reproduction is permitted for noncommercial purposes". During 2008, MDPI journals started to publish articles under the Creative Commons Attribution License. All articles published by MDPI before and during 2008 should now be considered as having been released under the post-2008 Creative Commons Attribution License.

SPARC Open Access 101 Video

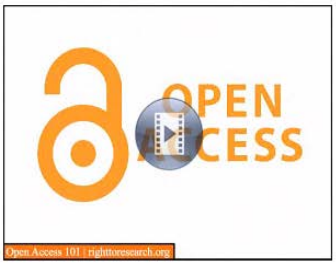

This means that all articles published in MDPI journals, including data, graphics, and supplements, can be linked from external sources, scanned by search engines, re-used by text mining applications or websites, blogs, *etc.* free of charge under the sole condition of proper accreditation of the source and original publisher. MDPI believes that open access publishing fosters the exchange of research results amongst scientists from different disciplines, thus facilitating interdisciplinary research. Open access publishing also provides access to research results to researchers worldwide, including those from developing countries, and to an interested general public. Although MDPI publishes all of its journals under the open access model, we believe that open access is an enriching part of the scholarly communication process that can and should co-exist with other forms of communication and publication, such as society-based publishing and conferencing activities.

Important Note: some articles (especially *Reviews*) may contain figures, tables or text taken from other publications, for which MDPI does not hold the copyright or the right to re-license the published material. Please note that you should inquire with the original copyright holder (usually the original publisher or authors), whether or not this material can be re-used.

Appendix A.2

Paper 2

Title: Fatigue reliability of offshore wind turbine systems

Authors: Sergio Márquez-Domínguez and John D. Sørensen

Published in: Proceedings on the 16th working conference of IFIP Working Group 7.5 on Reliability and Optimization of Structural Systems, Yerevan, Armenia, June 24-27, 2012. pp. 167-174. **ISBN 978-0-9657429-0-0**.

Re: IFIP-request for permission to include paper in thesis

Armen DER KIUREGHIAN [adk@ce.berkeley.edu]
Enviado el: jueves, 04 de julio de 2013 21:04
Para: Sergio Márquez Dominguez
CC: John Dalsgaard Sørensen

Dear Sergio,

I have no objections. I can speak on behalf of AUA as well.

Good luck with your thesis.

Armen

Armen Der Kiureghian
Taisei Professor of Civil Engineering
Department of Civil & Environmental Engineering
723 Davis Hall
University of California
Berkeley, CA 94720-1710
Phone (510) 642-2469; Fax (510) 643-5264
adk@ce.Berkeley.edu
http://www.ce.berkeley.edu/~adk/

On Thu, Jul 4, 2013 at 7:54 AM, Sergio Márquez Dominguez <smd@civil.aau.dk> wrote:

> Dear Armen Der Kiureghian.
> Chairman of the IFIP organaizing committee.
>
> I have contributed with a publication in IFIP 7.5 Working Conference presented in the American University of Armenia, Yerevan from June 24 to 27, 2012. The paper has the title "Fatigue reliability of offshore wind turbine systems". I would like to ask for permission in order to include that paper in the publication of my PhD thesis. The authors of the paper are myself and my PhD supervisor, Professor John Dalsgaard Sørensen.
>
> Best regards,
> Sergio Marquez-Dominguez
> Aalborg University, Aalborg. Denmark.

Fatigue reliability of offshore wind turbine systems

S. Márquez-Domínguez & J.D. Sørensen
Aalborg University, Denmark

ABSTRACT: Optimization of the design of offshore wind turbine substructures with respect to fatigue loads is an important issue in offshore wind energy. A stochastic model is developed for assessing the fatigue failure reliability. This model can be used for direct probabilistic design and for calibration of appropriate partial safety factors / fatigue design factors (FDF) for steel substructures of offshore wind turbines (OWTs). The fatigue life is modeled by the SN approach. Design and limit state equations are established based on the accumulated fatigue damage. The acceptable reliability level for optimal fatigue design of OWTs is discussed and results for reliability assessment of typical fatigue critical design of offshore steel support structures are presented.

1 INTRODUCTION

The wind turbine industry is growing fast. Offshore wind turbines (OWTs) are placed at sites with larger water depths and harsher environment far away from the coast, implying that fatigue and corrosion deterioration processes becomes very important. In order to minimize the cost of energy (CoE), it is important to optimize the design of the substructures with respect to the fatigue limit state. Wind turbines need to be analyzed and designed taking in account complex loads interacting together and highly influenced by the wind turbine control system. The wave and wind loads influence the dynamical behavior of OWTs resulting in increased fatigue damage on the substructure. Different regimens of equivalent turbulence intensity can be analyzed and modeled by aerodynamic codes such as FAST, see Jonkman & Buhl (2005). This code in this paper is used to estimate the wind fatigue load effects, see section 2.

Experience from the oil & gas industry can be used to assess the factors influencing the costs for the design, inspection, repair and failure of OWT substructures. In the oil & gas industry, probabilistic tools have been developed. Design equations and limit state equations are developed using these principles in order to optimize the design of offshore wind turbine substructures with respect to fatigue loads. The fatigue life is modeled by the SN approach, see section 3. Design and limit state equations are established based on the accumulated fatigue damage. The acceptable reliability level for optimal fatigue design of OWTs is discussed and results for reliability assessment of typical fatigue critical design of offshore steel support structures are presented in section 4.

2 WIND TURBINE MODEL

Substructures such as jacket type are difficult to simulate in conventional aeroelastic codes. Therefore, in this paper is assumed that the OWT can be simulated as a fixed-bottom monopile with rigid foundation representing an equivalent jacket OWT substructure in order to obtain rep-

resentative hot spots stresses. The behavior of the representative 5MW NREL OWT model is simulated using the aeroelastic simulation code called FAST (Jonkman et al. 2009). The water depth is assumed to be 30 m and the blades are controlled with pitch active control. The wind field is simulated by different equivalent wind turbulence intensities based on the reference turbulence intensity, 'I_{ref}'. For this study, 'I_{ref}' is equal to 0.12 (low turbulence) corresponding to the 90% quantile of the characteristic value in IEC 61400-1 (2005); see table 1 where equivalent turbulence intensities are shown for different mean wind speeds 'U' and quantile values 'P_{Ieqv}' of the turbulence intensity modeled by a LogNormal distribution (according to IEC 61400-1 (2005)). These equivalent wind turbulence intensities were the main input into Turbsim (Turbulent-wind simulator); see Jonkman (2009), to generate the turbulence field for each equivalent turbulence intensity. The Turbsim output is used as input into AeroDyn which is a set of routines used in connection with FAST to model and predict the aerodynamics of horizontal axis wind turbines (Moriarty & Hansen 2005).

Table 1. Equivalent wind turbulence intensities, I_{eqv}.

U	P_{Ieqv}=0.10	P_{Ieqv}=0.30	P_{Ieqv}=0.50	P_{Ieqv}=0.70	P_{Ieqv}=0.90
m/s	I_{eqv}(%)	I_{eqv}(%)	I_{eqv}(%)	I_{eqv}(%)	I_{eqv}(%)
4	7.0	8.5	9.5	10.5	12.0
6	7.7	9.0	9.9	10.7	12.0
8	8.3	9.4	10.1	10.9	12.0
10	8.7	9.7	10.4	11.0	12.0
12	9.0	9.9	10.5	11.1	12.0
14	9.3	10.1	10.7	11.2	12.0
16	9.5	10.3	10.8	11.3	12.0
18	9.7	10.4	10.9	11.3	12.0
20	9.9	10.5	11.0	11.4	12.0
22	10.0	10.6	11.0	11.4	12.0
24	10.2	10.7	11.1	11.5	12.0

During the simulations an initial blade pitch angle between 0 and 9 degrees is selected suitable for the given simulation in order to keep the power and rotor speed at rated values. A time series of 70 minutes was simulated. However, the first 10 minutes were eliminated in order to obtain a wind turbine behavior similar to operational conditions without any disturbance from initial conditions.

Once the turbine response has been simulated, a point between sea water level and mudline was chosen (around 16 m of height from the mudline). This point will be considered as a representative hot spot where the bending moments and stress concentration are important. The bending moments are calculated considering normal operating conditions with the wind turbine rotor perpendicular to the wind direction. The distribution of wind directions are not taken into account. Therefore, the reliability indices calculated can be considered conservative. After modeling, the stress ranges are grouped in intervals by a rainflow counting analysis in order to calculate the frequency at each wind speed bin. For reliability assessment the OWT can be modeled by a system consisting of hot spots and their interrelations (stochastic and functional interdependencies). This paper only considers a reliability analysis in a critical hot spot.

3 PROBABILISTIC MODEL FOR FATIGUE FAILURE

3.1 *Assessment of reliability*

This section describes how the reliability of the fatigue critical details can be performed using the SN-approach with SN-curves in combination with the Miner's rule as generally recommended in codes and standards, see e.g. EN 1993-1-9 (2005), IEC 61400-1 (2005), DNV (2010), and GL (2005).

If a bilinear SN-curve is applied the SN relation can be written (Faber et al. 2005):

$$N = K_1\left(\Delta s\left(\frac{T}{T_{ref}}\right)^{\alpha}\right)^{-m_1} \quad \text{and} \quad N = K_2\left(\Delta s\left(\frac{T}{T_{ref}}\right)^{\alpha}\right)^{-m_2} \tag{1}$$

where K_1, m_1 = material parameters for $N \le N_C$; K_2, m_2 = material parameters for $N > N_C$; Δs = stress range; N = number of cycles to failure; T = material thickness (50 mm); T_{ref} = reference thickness (25 mm); and α = scale exponent that depends on the detail considered, see DNV-RP-C203. Further, it is assumed that the total number of stress ranges for a given fatigue critical detail can be grouped in n_σ groups/intervals ΔQ_i such that the number of stress ranges in group i is n_i per year. (ΔQ_i, n_i) is obtained by Rainflow counting. Therefore, this procedure is applied for each simulation model with different equivalent wind turbulence intensity.

The code-based, deterministic design equation using the Miner rule is written

$$G = 1 - \sum_i \sum_k \frac{T_{FAT} n_{i,j=5,k}}{K_1^c s_i^{-m_1}} \cdot P(V_i) - \sum_i \sum_k \frac{T_{FAT} n_{i,j=5,k}}{K_2^c s_i^{-m_2}} \cdot P(V_i) = 0 \tag{2}$$

where $s_i = \frac{\Delta Q_{i,j=5,k}}{z}\left(\frac{T}{T_{ref}}\right)^{\alpha}$ = stress range 'k' given mean wind speed V_{i} and turbulence σ_{u_5} (90 % quantile); $n_{\text{i,j=5,k}}$ = number of stress ranges equal to ($\Delta Q_{\text{i,j=5,k}}/z$) given mean wind speed V_{i} and turbulence σ_{u_5}; $P(\text{V}_\text{i})$ = probability of mean wind speed at bin number 'i'; ΔQ_{i} = range of load effect (proportional to stress range s_{i} in group 'i'); z = design parameter, e.g. cross sectional area; T_{FAT} = fatigue design life; K_{i}^{c} = characteristic value of K_{i} ($\log K_{\text{i}}^{\text{C}}$ equal to the mean of $\log K_{\text{i}}$ minus two standard deviations of $\log K_{\text{i}}$).

The probability of failure (and the corresponding reliability index) is calculated using the design value 'z' which is determined from the design equation (2) and used in the following limit state equation to estimate the reliability:

$$g = \Delta - \sum_i \sum_j \sum_k \frac{t \cdot n_{ijk}}{K_1 s_i^{-m_1}} \cdot P\left(\sigma_{u_j} | V_i\right) \cdot P(V_i) - \sum_i \sum_j \sum_k \frac{t \cdot n_{ijk}}{K_2 s_i^{-m_2}} \cdot P\left(\sigma_{u_j} | V_i\right) \cdot P(V_i) = 0 \tag{3}$$

where Δ = model uncertainty related to Miner's rule for linear damage accumulation. Δ is assumed to be Log-Normal distributed with mean value=1 and coefficient of variation COV_{Δ}; $s_i = X_W X_{SCF} \frac{\Delta Q_{ijk}}{z}\left(\frac{T}{T_{ref}}\right)^{\alpha}$ = stress range 'k' given V_{i} and σ_{u_j}; $\text{I} = (\sigma_{u_j} / V_{\text{i}})$ = turbulence intensity; n_{ijk} = number of stress ranges equal to ($\Delta Q_{\text{ijk}} / z$) during 60 minutes given V_{i} and σ_{u_j}; $P(\sigma_{u_j}/\text{V}_\text{i})$ = probability of turbulence in the bin number 'j'. According with the table 1, the discretization is divided in 5 bins such that $P\left(\sigma_{u_j} | V_i\right) = 0.2$ and σ_{u_j} are the quantile values: σ_{u_1} =10%; σ_{u_2} = 30%; σ_{u_3} =50%; σ_{u_4} =70%; σ_{u_5} =90%.

A representative stochastic model is represented in the table 2. The COV values for X_{SCF} and X_{W} should be associated with specific recommendations for how detailed the estimation of stress concentration factors and wind/wave loads should be made; $\text{Log}K_{\text{i}}$ is modeled by a Normal distributed stochastic variable according to a specific SN-curve and follows the recommendations in DnV-C203 (2010). t = time ($0 \le t \le T_{\text{L}}$) where T_{L} indicates the service life. σ_{u_j} is the standard deviation of turbulence at a given mean wind speed U. σ_{u_j} is modeled as Log-Normal distributed with characteristic value $\hat{\sigma}_{u_j}$ defined as the 90% quantile and standard deviation equal to $I_{ref} \cdot 1.4$ m/s. $\hat{\sigma}_{u_j}$ is modeled based on 61400-1(2005):

$$\hat{\sigma}_u(U) = I_{ref} \cdot (0.75 \cdot U + b); \quad b = 5.6 \text{ m/s} \tag{4}$$

The cumulative (accumulated) probability of failure in the time interval [0, t] is obtained by

$$P_F(t) = P(g(t) \le 0) \tag{5}$$

The probability of failure can be estimated by FORM/SORM techniques or simulation, see Madsen et al. (1986), and Sørensen (2011). For OWT components the maximum annual probability of failures between 10^{-3} and 10^{-4} considering that usually no people are in danger in case of failure and the economic losses are limited, see also Sørensen (2012). The upper bound 10^{-4} corresponds to the reliability level often used for unmanned offshore structures for oil and gas. The lower bound 10^{-3} corresponds approximately to the annual probability of failure implicitly used for calibration of partial safety factors for onshore wind turbines. The reliability indices (with reference period one year) corresponding to 10^{-3} and 10^{-4} are 3.1 and 3.7. It is noted that the required reliability level also depends on the consequences for the structural system that fatigue failure occurs in a structural detail.

3.2 *Random fatigue limit model proposed by Lassen et al. (2005).*

As an alternative model for the linear and bilinear SN-curves for welded fatigue critical details normally specified in design codes, Lassen et al. (2005) proposed a non-linear model for estimating the fatigue life, called the random fatigue limit model (RFLM). In this paper it is compared with the above traditional S-N curves considering as basis an 'F'-structural detail from DNV-RP-C203 (2010). RFLM considers both the fatigue life and the fatigue limit as random variables; see Lassen et al. (2005). The advantage of RFLM is that it takes into consideration the variation in the fatigue critical stress range threshold and that run-out results can easily be included. The model gives a nonlinear S-N curve in a log-log scale in the fatigue-limit area; the fatigue life is gradually increasing and is approaching a horizontal line asymptotically instead of the abrupt knee point of the bilinear curve.

The RFLM SN-curve proposed by Lassen et al. (2005) is written:

$$\ln N = \beta_0 - \beta_1 \ln(\Delta\sigma - \gamma) + \varepsilon \tag{6}$$

where β_0, β_1 are constants and γ, ε model the threshold and random variations in fatigue life.

The deterministic parameters, β_0, β_1 and stochastic variables, γ, ε are shown in table 2 corresponding to DNV-RP-C203, class 'F' SN-curve.

The limit state equation considering a RFLM SN-curve is written:

$$g(t) = \Delta - \sum_i \sum_j \sum_k \frac{1}{N(\Delta\sigma_{ijk}, \beta_0, \beta_1, \gamma, \varepsilon)} t \cdot n_{ijk} \cdot P(\sigma_{u_j} | V_i) P(V_i) \tag{7}$$

4 EXAMPLE

A welded detail (hot spot) in an offshore wind turbine steel support structure is considered. The OWT is assumed to have an expected life T_L = 25 years and T_{FAT} = 75 years. Two different kind of fatigue critical details ('F' and 'D') are considered in combination with three different SN-curves (in air, in sea water with cathodic protection and free corrosion according to DnV-C203 (2010)).The annual and accumulated reliability indices were calculated with first order reliability method (FORM) and verified with Monte Carlo Simulation (MCS) using the stochastic model proposed in the Table 2. The alternative fatigue-life model (RFLM) is compared with traditional models based on a linear / bi-linear S-N curve approach, for this case the thickness relationship is considered, see section 3.

5 RESULTS

Tables 3 to 6 show results of different analyses considering 'D' and 'F' fatigue critical details based on DNV-RP-C203 (2010) and Lassen et al. (2005). The following cases are considered:

Table 2. Stochastic model. D: Deterministic, N: Normal, LN: LogNormal.

Variable	Distribution	Exp. value	Standard deviation	Charac. value	Comments
Δ	LN	1	0.30	1	
X_{SCF}	LN	1	0.10	1	Stresses
X_W	LN	1	0.10	1	Wind/Wave loads
'D'-STRUCTURAL DETAIL					
m_1	D	3			
$\log K_1$	N	12.564	0.20	12.164	In air
$\log K_1$	N	12.164	0.20	11.764	Cathodic protection
$\log K_1$	N	12.087	0.20	11.687	Free corrosion
m_2	D	5			
$\log K_2$	N	16.006	0.20	15.606	In air
$\log K_2$	N	16.006	0.20	15.606	Cathodic protection
'F'-STRUCTURAL DETAIL					
m_1	D	3			
$\log K_1$	N	12.255	0.20	11.855	In air
$\log K_1$	N	11.855	0.20	11.455	Cathodic protection
$\log K_1$	N	11.778	0.20	11.378	Free corrosion
m_2	D	5			
$\log K_2$	N	15.491	0.20	15.091	In air
$\log K_2$	N	15.491	0.20	15.091	Cathodic protection
$\log K_1$ and $\log K_2$ are assumed fully correlated					
RANDOM FATIGUE LIMIT MODEL (RFLM) BY T. LASSEN (F-CLASS)					
Variable	Distribution	Exp. value	Standard deviation	Comments	
β_0	D	22.48		Fatigue curve coefficient	
β_1	D	2.100		Fatigue curve coefficient	
$\log\gamma$	N	4.1	0.16	Fatigue Limit	
ε	N	0.0	0.14	Error term	

- Case A: design equation with linear SN-curve (m=3) and limit state equation with linear SN-curve (m=3)
- Case B: design equation with linear SN-curve (m=3) and limit state equation with bilinear SN-curve;
- Case C: design equation with bilinear SN-curve and limit state equation with linear SN-curve (m=3);
- Case D: design equation with bilinear SN-curve and limit state equation with bilinear SN-curve;
- Case E: Design: Bi-linear SN-curve and limit state equation with RFLM model – with and without thickness reduction.

Figures 1 and 2 show the annual and cumulative reliability indices respectively with T_L = 25 years and a T_{FAT} = 75 years with different combinations of the design equation and LSE for structural details from DNV ('F' and 'D') considering the SN-curves 'in sea water with cathodic protection'. The results include the reliability indices corresponding to the accumulated and annual probability of failure at year 25 (=T_L). Further, also the design value 'z' is shown normalized with respect to the design value obtained using the case 'D' combination with cathodic protection for a class 'F'. The results show that the endurance limit is quite important for reliability assessment of fatigue critical details in wind turbine support structures. This is due to the large number of cycles and that the stress ranges are distributed over a wide range. The endurance limit and the slope of the SN-curve for small stress ranges are generally quite uncertain, and more fatigue tests in this range (although costly) would be important for improving the reliability assessment.

For case 'D' which corresponds to the usual design recommendations, the results show that the annual reliability index exceeds the target level 3.1 during the whole lifetime, but the target level 3.7 is reached after 12 years. For case 'A' the reliability level 3.7 is reached after 22 years,

but it is also seen that the design parameter '*z*' (e.g. the cross-sectional area) for case 'A' is increased by 74% compared to case 'D' for a class 'F' detail. If a reliability level with a minimum annual reliability index equal to 3.7 is required then it is necessary for a case 'D' design situation to increase the deterministic design fatigue life or to perform inspections during the lifetime, see below.

In table 7, results are shown using the case 'E' corresponding to a class 'F' structural detail. The results show that with the design parameter '*z*' obtained using a bilinear SN-curve for design that both the annual and the cumulative reliability indices are increased significantly compared to case 'D'. However, it is noted that the RFLM model does not include a thickness reduction effect which could be expected to minimize the difference slightly.

In table 8, results are shown for case 'D' with cathodic protection SN-curves with a wide range of fatigue design lives for T_L = 25 years and class 'F and D' details. The corresponding fatigue design factors (FDFs) are also shown and it is seen that in order to satisfy minimum annual reliability indices larger than 3.1 and 3.7 FDF values equal to 2.5 and 4.9 have to be required. Alternatively, inspections have to be required. Table 8 also shows the design parameter 'z' value need to be increased. For offshore wind turbine substructures the required FDF values and the possibility of performing inspections can be decided based on cost-benefit considerations since typically only monetary consequences will result in case of failures. Further, site-specific conditions can be accounted for.

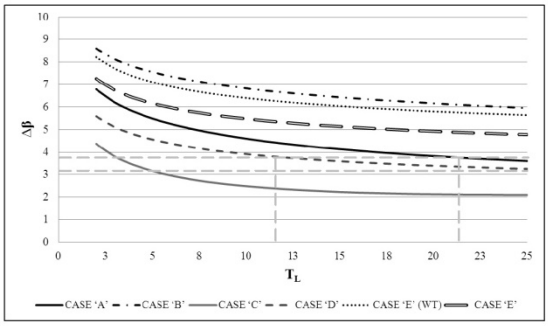

Figure 1: Annual reliability indices for structural details ('D' and 'F').

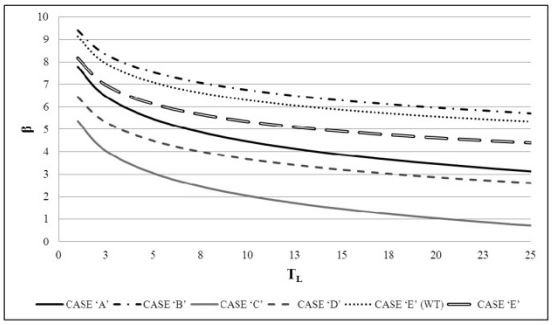

Figure 2: Cumulative reliability indices for structural details ('D' and 'F').

Table 3. Annual and accumulated reliability indices and design values for Case A (T_L = 25 years)

	'D'-DETAIL			'F'-DETAIL		
	In air	Cathodic protection	Free corrosion	In air	Cathodic protection	Free corrosion
β	3.13	3.13	3.13	3.13	3.13	3.13
Δβ	3.60	3.60	3.60	3.60	3.60	3.60
z	1.01	1.37	1.45	1.28	1.74	1.85

Table 4. Annual and accumulated reliability indices and design values for Case B (T_L = 25 years)

	'D'-DETAIL		'F'-DETAIL	
	In air	With cathodic protection	In air	With cathodic protection
β	4.21	5.71	4.21	5.71
Δβ	4.56	5.95	4.56	5.95
Z	1.01	1.37	1.28	1.74

Table 5. Annual and accumulated reliability indices and design values for Case C (T_L = 25 years)

	'D'-DETAIL		'F'-DETAIL	
	In air	With cathodic protection	In air	With cathodic protection
β	1.96	0.72	1.96	0.72
Δβ	2.72	2.10	2.72	2.10
z	0.77	0.78	0.98	1.00

Table 6. Annual and accumulated reliability indices and design values for Case D (T_L = 25 years)

	'D'-DETAIL		'F'-DETAIL	
	In air	With cathodic protection	In air	With cathodic protection
β	2.81	2.61	2.81	2.61
Δβ	3.37	3.25	3.37	3.25
z	0.77	0.78	0.98	**1.00**

Table 7. Annual and accumulated reliability indices and design values for the Case E (F-Detail and T_L = 25 years)

	with thickness relationship	without thickness relationship
β	4.40	5.35
Δβ	4.78	5.64
z	1.00	1.00

Table 8. Influence of 'z' parameter in the annual and cumulative reliability indices, Fatigue Design Factors (FDF) calculated for a wide range of fatigue design live (years) for 'F and D' details with cathodic protection SN-curve considering the case 'D' (T_L = 25 years).

T_{FAT}	25	40	60	75	100	120	140	160	180	200	250
B	1.39	1.92	2.37	2.61	2.93	3.13	3.31	3.45	3.58	3.70	3.95
Δβ	2.46	2.76	3.07	3.25	3.50	3.66	3.80	3.92	4.03	4.13	4.35
z (F)	0.80	0.88	0.95	**1.00**	1.06	1.09	1.13	1.16	1.19	1.22	1.26
z (D)	0.63	0.70	0.76	0.78	0.83	0.87	0.89	0.92	0.93	0.95	1.00
FDF	1.00	1.60	2.40	3.00	4.00	4.80	5.60	6.40	7.20	8.00	10.0

6 CONCLUSIONS

A probabilistic model was formulated for fatigue failure in jacket type offshore wind turbine substructures accounting for the operational characteristics of wind turbines and deterministic design with specifications in IEC 61400. A comparative analysis between different SN-curves shows a large effect on the reliability depending on the SN-curves used. Further, an alternative non-linear SN-curve model, RFLM, was considered. The results with the RFLM model indicates that higher reliabilities can be obtained compared to the traditional bilinear SN-curves. For application within offshore wind turbine substructures more research are needed with respect to calibration of fatigue design factors for inclusion in design standards. Also it is important to account for system effects in case of fatigue failure in different fatigue critical details in one and/or many wind turbine support structures in a wind farm, Also the information from inspections and condition monitoring should be included. Furthermore, wake effects should be included to account for wind farm effects.

7 ACKNOWLEDGEMENT

The authors wish to thank to the financial support from the mexican national council of science and technology (CONACYT) and the norwegian centre for offshore wind energy (NORCOWE) under grant 193821/S60 from the research council of Norway (RCN). NORCOWE is a consortium with partners from industry and science, hosted by the Christian Michelsen research institute.

8 REFERENCES

BS 7910:2005. *Guide to methods for assessing the acceptability of flaws in metallic structures.*

DNV-RP-C203: 2010. *Fatigue design of offshore steel structures.* DnV, April 2010.

EN 1993-1-9:2005. *Eurocode 3: Design of steel structures - Part 1-9: Fatigue.* CEN. 2005.

Faber M.H., Sørensen, J.D., Tychsen J. & Straub D., 2005. Field implementation of RBI for jacket structures. *Journal of Offshore Mechanics and Artic Engineering.* August 2005 Vol. 127.

GL: 2005. Guideline for the certification of offshore wind turbines.

IEC 61400-1:2005. *Wind turbine generator systems – Part 1: Safety requirements.* 2005.

Jonkman, J.M., 2009. *Turbsim User's Guide,* Technical Report NREL/TP-500-46198.

Jonkman J.M., Butterfield S., Musial W. & Scott G., 2009.*Definition of a 5-MW Reference Wind Turbine for Offshore System Development,* Technical Report NREL/TP-500-38060.

Jonkman J.M. & Buhl, M.L., 2005. *FAST User's Guide,* Technical Report NREL/EL-500-38230.

Lassen, T., Darcis Ph., & Recho N., 2005. *Fatigue Behavior of Welded Joints Part 1 — Statistical Methods for Fatigue Life Prediction. Supplement to the welding journal*, December 2005 sponsored by the american welding society and the welding research council.

Madsen, H.O., S. Krenk & N.C. Lind, 1986: *Methods of structural reliability.* Prentice-Hall.

Moriarty, P.J. & Hansen A.C., 2005. *AeroDyn Theory Manual,* Technical Report NREL/TP-500-36881.

Sørensen, J.D., 2012. Reliability-Based Calibration of Fatigue Safety Factors for Offshore Wind Turbines. *International Journal of Offshore and Polar Engineering.* ISSN 1053-5381. Vol. 22, No. 2.

Sørensen, J.D., 2011. Notes in 'Structural Reliability Theory - and Risk Analysis'. Aalborg University.

Appendix A.3

Paper 3

Title: System reliability for offshore wind turbines: fatigue failure

Authors: Sergio Márquez-Domínguez and John D. Sørensen

Published in: Proceedings of the ASME 2013. 32nd International Conference on Ocean, Offshore and Arctic Engineering (OMAE2013). Nantes, France. June 9-14, 2013. Paper: **OMAE2013-10962** in DVD © 2013 by ASME.

RE: OMAE2013: Request for permission to include paper OMAE2013-10962 in thesis

Beth Darchi [DarchiB@asme.org]
Enviado el: miércoles, 07 de agosto de 2013 16:58
Para: Sergio Márquez Dominguez

Dear Mr. Dominguez:
It has been confirmed that your paper was presented at the OMAE2013 Conference, therefore, it is our pleasure to grant you permission to use ASME paper "System Reliability For Offshore Wind Turbines: Fatigue Failure," by Sergio Márquez-Dominguez, John Dalsgaard Sørensen, Paper Number OMAE2013-10962, as cited in your letter for inclusion in a Thesis entitled Reliability-Based Design And Planning Of The Inspections And Monitoring Of Offshore Wind Turbines to be published by Aalborg University, Denmark.

Permission is granted for the specific use as stated herein and does not permit further use of the materials without proper authorization. Proper attribution must be made to the author(s) of the materials. **PLEASE NOTE**: if any or all of the figures and/or Tables are of another source, permission should be granted from that outside source or include the reference of the original source. ASME does not grant permission for outside source material that may be referenced in the ASME works.

As is customary, we request that you ensure full acknowledgment of this material, the author(s), source and ASME as original publisher. Acknowledgment must be retained on all pages printed and distributed.

Many thanks for your interest in ASME publications.

Sincerely,
Beth Darchi
Permissions & Copyrights
ASME, 2 Park Avenue
New York, NY 10016
T: 212-591-7700
F: 212-591-7841
E: permissions@asme.org

From: Sergio Márquez Dominguez [mailto:smd@civil.aau.dk]
Sent: Thursday, July 04, 2013 11:06 AM
To: Copyright
Cc: John Dalsgaard Sørensen
Subject: OMAE2013: Request for permission to include paper OMAE2013-10962 in thesis

Dear OMAE2013,
Copyright.

I have contributed with a publication in the 32nd International Conference on Ocean, Offshore and Arctic Engineering (OMAE2013) in Nantes, France from June 9 to 14, 2013. The paper has the title "SYSTEM RELIABILITY FOR OFFSHORE WIND TURBINES: FATIGUE FAILURE" (OMAE2013-10962). I would like to ask for permission in order to include that paper in the publication of my PhD thesis. The authors of the paper are myself and my PhD supervisor, the Professor John Dalsgaard Sørensen.

Best regards,
Sergio Marquez-Dominguez
Aalborg University, Aalborg. Denmark.

Proceedings of the ASME 2013 32nd International Conference on Ocean, Offshore and Arctic Engineering
OMAE2013
June 9-14, 2013, Nantes, France

OMAE2013-10962

SYSTEM RELIABILITY FOR OFFSHORE WIND TURBINES: FATIGUE FAILURE

S. Márquez-Domínguez
Aalborg University
Sohngaardsholmsvej 57
DK - 9000 Aalborg, Denmark
Email: smd@civil.aau.dk

J.D. Sørensen
Aalborg University
Sohngaardsholmsvej 57
DK - 9000 Aalborg, Denmark
Email: jds@civil.aau.dk

ABSTRACT
Deeper waters and harsher environments are the main factors that make the electricity generated by offshore wind turbines (OWTs) expensive due to high costs of the substructure, operation & maintenance and installation. The key goal of development is to decrease the cost of energy (CoE). In consequence, a rational treatment of uncertainties is done in order to assess the reliability of critical details in OWTs. Limit state equations are formulated for fatigue critical details which are not influenced by wake effects generated in offshore wind farms. Furthermore, typical bi-linear S-N curves are considered for reliability verification according to international design standards of OWTs. System effects become important for each substructure with many potential fatigue hot spots. Therefore, in this paper a framework for system effects is presented. This information can be e.g. no detection of cracks in inspections or measurements from condition monitoring systems. Finally, an example is established to illustrate the practical application of this framework for jacket type wind turbine substructure considering system effects.

Keywords: offshore wind turbines; jacket type substructure; system effects; stochastic model; reliability.

1. INTRODUCTION
Offshore wind capacity has significantly increased in the last years, especially in the North Sea. A key aspect in this development is to decrease the cost of energy (CoE). Energy from offshore wind turbines (OWTs) is expensive, due to several reasons. One of these reasons is the high cost of the substructure, especially when offshore wind farms are placed in deeper waters and harsher environments. In order to minimize CoE, a rational treatment of uncertainties must be considered. This treatment can be done by using modern structural reliability theory, see e.g. [1, 2].

For a single failure mode/element, the reliability assessment can be performed with FORM/SORM as well as with simulation techniques. Offshore structures are considered complex structural systems, which usually consist of a large number of elements with multiple load conditions and more than one failure mode. For these reasons, structural behaviour of the structure on its entire service life is difficult to model and analyse. The idealized goal of modern reliability theory is to determine the probability of failure of the structure, taking into account factors such as the correlation between the strength of single elements, multiple failure modes, etc. Therefore, the design of the substructures with respect to fatigue loads can be optimized as well as an estimation of the structural reliability level can be calculated. For jacket type substructures, a reliability model typically consists of a series system of parallel systems. Elements connected in a parallel system can often take over the load of a collapsed element, but sometimes the whole structure can fail if the weakest element fails (series system), see e.g. [1, 3-4].

This paper considers fatigue failures of welded joints in jacket type OWT substructures where system reliability theory is applied. Experience and expertise from the oil & gas industry are used to assess the factors influencing the costs for the design, inspection, repair and failure of OWTs. Design equations and limit state equations are developed using these principles in order to optimize the design of OWT substructures with respect to fatigue loads.

While offshore wind turbine modelling is presented in Section 2, Section 3 describes how the reliability can be estimated for a single fatigue failure mode in an OWT. The fatigue life is modelled by an S-N approach where design and limit state equations are established based on the accumulated fatigue damage in a hot spot; see Márquez and Sørensen [5]. System reliability models are established in Section 4. An example which considers system reliability theory applied to OWT substructures is presented in Section 5 where an acceptable reliability level is discussed for fatigue design.

Finally, results and conclusions are presented in Sections 6 and 7, respectively.

2. WIND TURBINE MODELLING

A 5MW NREL OWT has been developed by Jonkman et al. [6] where general and structural properties have been defined. In Márquez and Sørensen [5], the 5MW NREL OWT has been used as basis for defining a monopile foundation in order to simulate representative time series of stresses in a particular hot spot. These representative stresses are assumed to represent an equivalent response for an OWT jacket type. It is noted that a complete and detailed structural model of the OWT jacket type foundations must be established in order to determine in detail the static and dynamic structural response incl. the aerodynamic and hydrodynamic loads. In Gao et al., [7] a 'decoupled analysis method' has been proposed to model the dynamic behaviour of jacket OWT substructures. The decoupled analysis method seems to be an efficient procedure used to analyse complex foundations for offshore wind turbines.

In this paper an equivalent fixed-bottom monopile is modelled in FAST [8] in order to predict a similar response to the original jacket, and to be used in development of a system reliability model. In Márquez and Sørensen [5], the aerodynamic behaviour of the representative 5MW NREL OWT is simulated using FAST [8] where the blades are controlled using active pitch control. The wind field is simulated by different equivalent wind turbulence intensities based on a wind turbulence intensity, 'I_{ref}' considered to be equal to 0.12 (low turbulence) corresponding to the 90% quantile as characteristic value, see Table 1 where equivalent turbulence intensities are shown for different mean wind speeds 'U' and quantile values 'P_{leqv}'. The turbulence intensity is modelled by a LogNormal distribution (according to IEC 61400-1[9]). These equivalent turbulence intensities is the main input to Turbsim [10] (Turbulent-wind simulator), to generate the turbulence field for each equivalent turbulence intensity. The Kaimal turbulence spectrum is assumed together with a normal turbulence model (NTM). The Turbsim output is used as input to AeroDyn [11] which is a set of routines used in connection with FAST to model and predict the aerodynamics of horizontal axis wind turbines.

Table 1. Equivalent wind turbulence intensities, I_{eqv}.

P_{leqv}	0.10	0.30	0.50	0.70	0.90
U (m/s)	I_{eqv}(%)	I_{eqv}(%)	I_{eqv}(%)	I_{eqv}(%)	I_{eqv}(%)
4	7.0	8.5	9.5	10.5	12.0
6	7.7	9.0	9.9	10.7	12.0
8	8.3	9.4	10.1	10.9	12.0
10	8.7	9.7	10.4	11.0	12.0
12	9.0	9.9	10.5	11.1	12.0
14	9.3	10.1	10.7	11.2	12.0
16	9.5	10.3	10.8	11.3	12.0
18	9.7	10.4	10.9	11.3	12.0
20	9.9	10.5	11.0	11.4	12.0
22	10.0	10.6	11.0	11.4	12.0
24	10.2	10.7	11.1	11.5	12.0

The hydrodynamic loads are calculated using HydroDyn which is a specialized hydrodynamic module incorporated to FAST. In HydroDyn, an operational sea state is simulated considering a water depth equal to 30 m and linear wave theory applied with Wheeler´s method to generate irregular waves acting on the jacket. Morison's equation is used to calculate the hydrodynamic forces. The linear irregular wave kinematics have been specified through the JONSWAP (Joint North Sea Wave Project) wave spectrum.

A time series of 70 min with a time step of 0.25 sec was simulated. The first 10 minutes were eliminated in order to obtain wind turbine behaviour similar to operational conditions without any disturbance from initial conditions.

Once the turbine response has been simulated, a point between sea water level and mudline was chosen (around 16 m of height from the mudline). This point is considered to define a representative hot spot where bending moments and stress concentration are important. It is worth mentioning that representative bending stresses are generated by wind and wave contributions. The bending moments were calculated considering normal operating conditions with the wind turbine rotor perpendicular to the wind direction. The distribution of wind directions is not taken into account. Therefore, the reliability indices calculated can be considered conservative. After modelling, the stress ranges were grouped in intervals by rainflow counting in order to calculate the frequency at each wind speed bin. For the reliability assessment, the OWT is modelled as a series system model consisting of hot spots and their interrelation (stochastic and functional interdependencies) are taken into account, see below.

3. RELIABILITY ASSESSMENT OF SINGLE FATIGUE FAILURE MODES

This section describes how the reliability of fatigue critical details can be calculated using a S-N approach where S-N curves in combination with Miner's rule are often recommended in codes and standards, such as e.g. IEC 61400-1 [9], EN 1993-1-9 [12], DnV-C203 [13], DNV-OS-J101 [14] and GL:2005 [15]. The structural reliability assessment can be performed considering a single fatigue critical detail (hot spot) located in the substructure.

For fatigue critical details in marine conditions with cathodic protection bi-linear S-N curves should be applied where N_c represents the transition between slopes m_1 and m_2. Bi-linear S-N curves can be written:

$$N = K_1 \left(\Delta s \left(\frac{T}{T_{ref}} \right)^{\nu} \right)^{-m_1} \quad \text{and} \quad N = K_2 \left(\Delta s \left(\frac{T}{T_{ref}} \right)^{\nu} \right)^{-m_2} \qquad (1)$$

where K_1, m_1 are material parameters for $N \le N_C$; K_2, m_2 are material parameters for $N > N_C$; N_C corresponds to the number of cycles at the inflection point ; Δs_c is the stress range at the inflection point (MPa); Δs is the stress range (MPa); T is the material thickness through which a crack will grow (T = 50 mm); T_{ref} is the plate reference thickness (T_{ref} = 25 mm); and ν is a scale exponent, Assuming that the total number of stress

ranges for a given fatigue critical detail can be grouped in n_σ groups/intervals ΔQ_i such that the number of stress ranges in group 'i' is n_i per year. (ΔQ_i, n_i) is obtained by rainflow counting. This procedure is applied for each simulation model with different equivalent wind turbulence intensities.

Equation (2) represents a code-based deterministic design equation based on Miner's rule.

$$G = 1 - \sum_{1} \sum_{s_k \geq \Delta s_C} \frac{T_{FAT} n_{i,j=5,k}}{K_1^c s_k^{-m_1}} P(V_i) - \sum_{1} \sum_{s_k < \Delta s_C} \frac{T_{FAT} n_{i,j=5,k}}{K_2^c s_k^{-m_2}} P(V_i) = 0 \quad (2)$$

where $s_k = \frac{\Delta Q_k}{z} \left(\frac{T}{T_{ref}} \right)^{\nu}$ is the stress range 'k'; $n_{i,j=5,k}$ is the number of stress ranges equal to ($\Delta Q_k/z$) given a mean wind speed V_i and standard deviation of turbulence equal to $\sigma_{u_j=5}$ (90% quantile); $P(V_i)$ is the probability of mean wind speed at bin number 'i'; ΔQ_k is the range of load effect (proportional to stress range s_k in group 'k'); 'z' is a design parameter, e.g. cross sectional area; T_{FAT} is the fatigue design life; K_i^C is the characteristic value of K_i ($\log K_i^C$ equal to the mean of $\log K_i$ minus two standard deviations of $\log K_i$).

The probability of failure (and the corresponding reliability index) is calculated using the design value 'z' which is determined from the design equation (2) and used in the following limit state equation to estimate the reliability:

$$g = \Delta - \sum_i \sum_j \sum_k \frac{t \cdot n_{ijk}}{K_1 s_k^{-m_1}} \cdot P\left(\sigma_{u_j} | V_i\right) \cdot P(V_i) - \sum_i \sum_j \sum_k \frac{t \cdot n_{ijk}}{K_2 s_k^{-m_2}} \cdot P\left(\sigma_{u_j} | V_i\right) \cdot P(V_i) \quad (3)$$

where Δ is the model uncertainty related to Miner's rule for linear damage accumulation. Δ is assumed to be Log-Normal distributed with a mean value = 1 and coefficient of variation COV_Δ; $s_k = X_W X_{SCF} \frac{\Delta Q_k}{z} \left(\frac{T}{T_{ref}} \right)^{\nu}$ is the stress range 'k'; n_{ijk} is the number of stress ranges equal to ($\Delta Q_i/z$) during 60 minutes given V_i and σ_{u_j}; $P\left(\sigma_{u_j} | V_i\right)$ is the probability of standard deviation of turbulence in bin number 'j'. 't' is the time ($0 \leq t \leq T_L$) where T_L is the service life. σ_{u_j} is modelled as Log-Normal distributed with characteristic value $\hat{\sigma}_{u_j}$ defined as the 90% quantile and standard deviation equal to $I_{ref} \cdot 1.4$ m/s with I_{ref} being the reference turbulence intensity. $\hat{\sigma}_{u_j}$ is modelled based on IEC 61400-1 [9]:

$$\hat{\sigma}_u(U) = I_{ref} \cdot (0.75 \cdot U + b); \quad b = 5.6 \text{ m/s} \quad (4)$$

The cumulative (accumulated) probability of failure in the time interval [0, t] is obtained by

$$P_F(t) = P(g(t) \leq 0) \quad (5)$$

The probability of failure can be estimated by FORM/SORM techniques or simulation, see [1, 3-4]. The reliability index, β(t) corresponding to the cumulative probability of failure, $P_F(t)$ is defined by

$$\beta(t) = -\Phi^{-1}(P_F(t)) \quad (6)$$

where $\Phi(\,)$ is the standardized normal distribution function.

The annual probability of failure is obtained from

$$\Delta P_F(t) = P_F(t) - P_F(t - \Delta t); \; t > 1 \text{ year and } \Delta t = 1 \text{ year} \quad (7)$$

The acceptable maximum annual probability level of failure (ΔP_F) is considered to be in the range between 10^{-3} and 10^{-4} corresponding to (β) values between 3.1 and 3.7, see [16]. It is noted that the required reliability level also depends on the damage consequences for the structural system, instead of fatigue failure that occurs in a structural detail (hot spot).

A representative stochastic model based on DnV-C203 (2012) [13] is shown in Table 2. The stochastic model considers three different S-N curves representing typical fatigue behaviour of welded details. The S-N curves are for 'in air', 'marine with cathodic protection' and 'marine with free corrosion' environments.

Table 2. Stochastic model. D: Deterministic, N: Normal, LN: LogNormal and γ: Characteristic value.

Var.	Distr.	Mean	Std. Dev.	γ	Comments	
Δ	LN	1	0.30	1		
X_{SCF}	LN	1	0.10	1	Stresses	
X_W	LN	1	0.10	1	Wind/Wave loads	
STRUCTURAL DETAIL: S-N CURVE 'D'						
m_1	D	3				Δs_c
$\log K_1$	N	12.564	0.20	12.164	In air	52.6
$\log K_1$	N	12.164	0.20	11.764	C. protection	83.4
$\log K_1$	N	12.087	0.20	11.687	F. corrosion	
m_2	D	5				
$\log K_2$	N	16.006	0.20	15.606	In air	
$\log K_2$	N	16.006	0.20	15.606	C. protection	
STRUCTURAL DETAIL: S-N CURVE 'F'						
m_1	D	3				Δs_c
$\log K_1$	N	12.255	0.20	11.855	In air	41.5
$\log K_1$	N	11.855	0.20	11.455	C. protection	65.8
$\log K_1$	N	11.778	0.20	11.378	F. corrosion	
m_2	D	5				
$\log K_2$	N	15.491	0.20	15.091	In air	
$\log K_2$	N	15.491	0.20	15.091	C. protection	
$\log K_1$ and $\log K_2$ are assumed fully correlated.						

4. RELIABILITY ASSESSMENT CONSIDERING STRUCTURAL SYSTEMS

Jacket-type OWT foundations can be considered as built up in modules where each tubular element or brace is connected to the main frame (jackets legs) by welded tubular joints where hot spot are generally located. Welded tubular joints can be

classified i.e. in T, Y, X, K and KT. According to oil and gas expertise, the welded toes in tubular connections are potential areas of high fatigue stress concentration. Generally, hot spots are located in the brace toe and the brace saddle of each brace-chord intersection; see Fig. 1. For each hot-spot a limit state equation is established and the correlation/dependency is defined by the correlation between the stochastic variables involved. In this paper generalized series system failure models are established, joining different parallel mechanisms in a sequence of failure where every parallel mechanism involves a different number of failure elements represented by hot spots. Thus, el number of hot-spots in every parallel mechanism will define the mechanism level (L1… Ln). In consequence, a failure sequence for a steel substructure can be represented by a series system of parallel systems or a generalized series system model, where the failure sequence can be now modelled as single elements in a series system. A realistic OWT substructure can be represented by a generalized series system model where correlation between stochastic variables is considered in the system reliability assessment by a linearized system of limit state equations (LSEs). In this paper, only fatigue failure modes are considered where wind loads are assumed to dominate the fatigue damage in the fatigue critical details considered. Further work can be done considering a separate effect of wind and wave establishing a generalized series system model. The main contribution of this paper is the reliability analysis considering linearized limit state equations for different hot spots located in the same substructure where different correlation models for fatigue critical details can be analysed. Finally, Reliability assessment of series systems of parallel systems is described e.g. in [1, 3-4]. Software packages such as SYSREL [17] can be used to perform the numerical calculations. One can note that structural robustness considerations based on risk and reliability measures are closely related to systems reliability, see [18], and therefore the models presented in this paper can be used in robustness assessments of offshore wind turbine substructures, see discussion below.

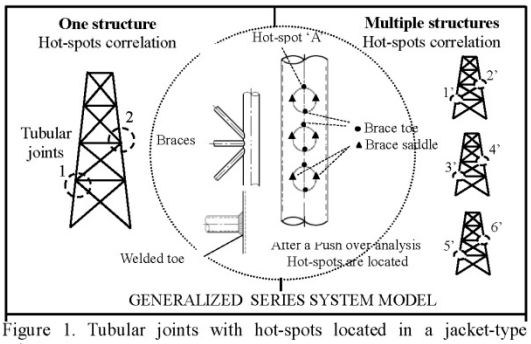

Figure 1. Tubular joints with hot-spots located in a jacket-type substructure.

5. EXAMPLE: SYSTEM RELIABILITY OF OFFSHORE STEEL WIND TURBINE SUBSTRUCTURES

Two structural concepts, system redundancy and robustness, are considered in this example, in combination with reliability analyses of the systems models. *System redundancy* is the ability of a structural system to redistribute the applied load after ductile failure of one or several of its remaining elements. Thereby, *redundancy* means capability of a structure to continue to carry loads after the ductile failure of the most critical members. Thus, the load supported by the failed element will be distributed to neighbouring elements. On the other hand, '*robustness'* is, among other things; related to the capability of the system to still carry some load after the brittle fracture of one or more critical elements, see [19].

In this example, the importance of system redundancy in a jacket type wind turbine substructure is determined by considering generic system effects in potential fatigue hot spots which can be combined taking into account interactions between limit state equations (LSEs). The interaction between LSEs will define the generalized series system model to be assessed. Therefore, the fatigue failure is configured in a general system for one OWT substructure.

In Márquez and Sørensen [5], a stochastic model, which has been explained in Section 3, considers two different kinds of fatigue critical details ('F' and 'D'). These details were analysed in combination with three different S-N curves (c.f. Table 2), where the annual and accumulated reliability indices were calculated by FORM and verified with Monte Carlo simulations (MCS). Similarly, an alternative fatigue-life model (RFLM) [20] was compared with traditional models considering linear and bi-linear S-N curves. In this example, a linearized FORM-type general system model is applied for different fundamental failure mechanisms. The mechanisms can be established with a non-linear finite element analysis such as a pushover analysis which calculates the progressive damage of the substructure due to failure fatigue in different welded joints. The pushover analysis can also be used to determine the time to total structural collapse. However, the pushover analysis is quite complicated since the wind and wave loads in combination with the wind turbine control system have to be accounted for a specific OWT location, Additionally, the hydrodynamic loads on the substructures as well as the structural behaviour of the steel substructures in different configurations such as with elements failed and stress distribution in every welded joint will increase the difficulty of the analysis, see [21]. The combination of hot spots will define different mechanisms of failure and these mechanisms will be correlated in general system models or sequences of failure. A real substructure has a high number of mechanisms. Therefore, some dominant sequences of fatigue failures for an OWT substructure are considered, see in Fig. 2 where the OWT is assumed to have an expected life of T_L = 25 years and T_{FAT} = 75 years. Figure 3 shows a general series system of parallel systems for the different fatigue failure mechanisms considered in the Fig. 2. For simplicity in Fig. 3, parallel mechanisms with same number of hot-spots have been joined in failure

sequences. However, in a real jacket-type substructure different failure mechanisms with different mechanism levels need to be considered. These mechanisms are configured in fatigue failure sequences which define a sequence of progressive damage resulting in the collapse of the whole structure. The predetermined fatigue failure sequence will determine the system reliability. Thus, if one element inside a parallel system fails, the surrounding elements are expected to redistribute the load between them. It is noted that extreme loads occurring in between fatigue failures are not accounted for in this example.

In order to explain the procedure of analysis, an OWT substructure is considered without wake effects and with a bi-linear S-N curve corresponding to 'sea water with cathodic protection'. The analysis is performed considering a bi-linear design with a bi-linear limit state equation (LSE) for a single OWT in a single hot spot (i.e. hot spot 'A' in Fig. 2). This reliability analysis can result in linearized LSEs for different hot spots located in the same substructure where different correlation models for fatigue critical details can be analysed. The procedure can be extended to correlate different hot spots in more than one substructure. For instance, when the substructure or substructures get the expected design life (T_L = 25 years), the accumulated beta and alpha vector in every individual design point are used as input parameters to conform the linearized FORM type general system model. The referenced accumulated reliability index (β_o) is for this example determined to be equal to 2.61 for a single fatigue failure (hot spot), and the corresponding alpha vector at that design point is represented by α_Δ=-0.3364, α_{SCF}=0.5515, α_W=0.5515 and α_{LogK}=-0.5278, see [5].

With the linearized system models (where the limit state equations are linearized in their individual beta points, see Eq. (8)), the system reliability indices are calculated using SYSREL for different sequence of failure or series system models.

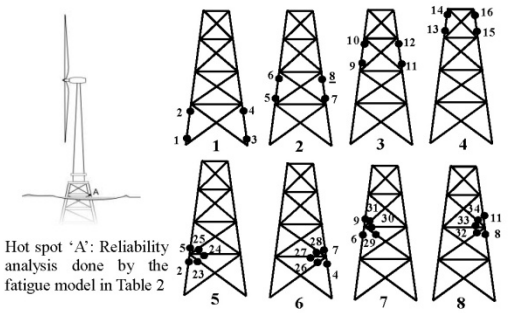

Figure 2. Examples of fundamental mechanisms after a pushover analysis, considering progressive damage until structural collapse.

The correlation/dependency between the stochastic variables is an important key to be analysed in a general system configuration. In this example, the correlation/dependency between stochastic variables is represented by different cases of combination to analyse the series system reliability behaviour of a single OWT support as well as steel substructures correlated within a wind farm.

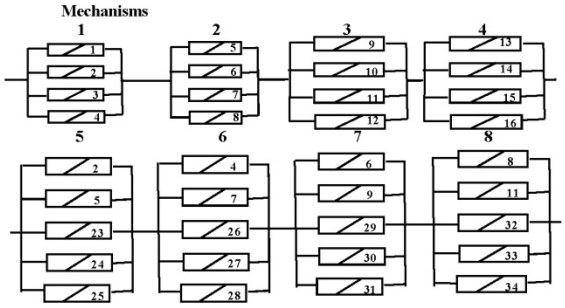

Figure 3. Generalized series system models considered in Fig. 2.

For a single OWT substructure, 8 cases of correlation/ dependencies between the stochastic variables are established in Table 3, where the correlation between the stochastic variables considers the influence between hot spots located in welded joints. The interaction between the stochastic variables in the 8 cases of analysis is described briefly in the following. For instance, in Case 1 the load history (X_W), fatigue stresses (X_{SCF}), fatigue damage (X_Δ) and also X_{LOGK}'s are considered to have full correlation between them in different fatigue critical details. In Case 2, it is considered that the X_{LOGK}'s can be assumed statistically independent. Next Cases 3, 4 and 5 show the sequence of correlation between the stochastic variables in the model which can continue until the whole system is considered completely independent. Cases 6 and 7 will determine the influence of the wind and wave load as well as the stress ranges when they are considered totally independent of each other in the stochastic model, adding a full correlation of X_{LOGK} in the system. Finally, Case 8 establishes the fatigue progressive damage uncertainty (X_Δ) being completely independent of the general stochastic model as well as X_{LOGK} is considered completely correlated in the model. In all cases, the group of stochastic variables (X_Δ), (X_{SCF}), (X_W) and (X_{LOGK}) are assumed statistically independent. These cases and relationships should be considered as cases covering the possible correlation combinations that could be relevant for a substructure.

Table 3. Cases of combination established for a single OWT substructure considering the influence of the correlation or independence between stochastic variables in different hot spots. 'C' and 'I' represent 'correlation' or 'independency' between the stochastic variables considered in the system.

Cases	X_Δ	X_{SCF}	X_W	X_{LOGK}
1	C	C	C	C
2	C	C	C	I
3	C	C	I	I
4	C	I	I	I

5	I	I	I	I
6	C	C	I	C
7	C	I	C	C
8	I	C	C	C

In order to develop the linearized FORM-type in a general system model, the 8 cases of analysis are represented by a linearized system of limit state equations $\beta_{oi} - \alpha_i^T \cdot u = 0$ where 'u' vector is considered to be standard normal distributed, α_i is the alpha vector at the design points considered as well as β_{oi} represents the accumulated reliability index for the hot spots considered. For instance, for Case 2 the linearized system equations are shown in (8).

$$\begin{aligned}
&\beta_1 - \alpha_{\Delta_1} \cdot u_\Delta - \alpha_{SCF_1} \cdot u_{SCF} - \alpha_{W_1} \cdot u_W - \alpha_{LogK_1} \cdot u_{LogK1} = 0 \\
&\beta_2 - \alpha_{\Delta 2} \cdot u_\Delta - \alpha_{SCF2} \cdot u_{SCF} - \alpha_{W2} \cdot u_W - \alpha_{LogK_2} \cdot u_{LogK2} = 0 \\
&\vdots \\
&\beta_i - \alpha_{\Delta_i} \cdot u_\Delta - \alpha_{SCF_i} \cdot u_{SCF} - \alpha_{W_i} \cdot u_W - \alpha_{LogK_i} \cdot u_{LogKi} = 0
\end{aligned} \tag{8}$$

OWT substructures are designed to resist wind and wave loads which influence all structural elements. These loads will define the stresses as well as the progressive fatigue damage in an OWT substructure. Each element in one substructure for illustration is assumed to have two welded joint where the stresses are concentrated (hot spots) in this paper. Until now in this example, correlation between hot spots in one OWT has been considered. For two substructures located at different places in a wind farm, wind and wave effects will be different between hot spots located in two different substructures. Therefore, correlation between substructures has to be modelled. For instance, for two substructures, each structure could experience the same long-term load history, but the sequence of the loads intensities could vary, see [21]. For this reason, the above example can be extended to analyse hot spots located in two different substructures, considering how they influence each other. The influence between them can be established by a correlation between stochastic variables especially X_W and X_{SCF}. The correlation is modelled by 5 increments which are configured in 5 new cases of analysis, see Table 4 where, as a starting point, X_W and X_{SCF} are considered completely independent, and the X_{LOGK}'s are considered to be completely independent.

Table 4. Cases of combination established between two OWT substructures considering correlation or independence between stochastic variables in different hot spots.

Cases	X_Δ	X_{SCF}	X_W	X_{LOGK}
1	C	I	I	I
2	C	C (0.25)	C (0.25)	I
3	C	C (0.50)	C (0.50)	I
4	C	C (0.75)	C (0.75)	I
5	C	C	C	I

The number of sequential mechanisms could have an important influence on the system reliability index. In consequence, the generalized series system models are analysed considering different failure sequences with 3 sequences linked in a series system, each with 1, 2 or 5 failure modes in the sequence modelled as a parallel system. Thus, an increased number of hot spots are assigned to the general system model which will influence the accumulated system reliability indices, see Fig. 4.

6. RESULTS

System redundancy in a jacket type wind turbine substructure is considered using a linearized series system model without wake effects. System reliability indices for each failure sequence are calculated with SYSREL [17] using the appropriate series system model which is explained in Section 5. Failure sequences in Fig. 4 are considered and analysed until the mechanism level 5 (L5). Two failure sequences are established with 3 and 5 parallel mechanisms concatenated (S3 and S5). The mean accumulated system reliability indices (β^S) were calculated by Ditlevsen bounds. The mean accumulated system reliability indices (β^S) are normalized (β^{SNi}) with respect to the accumulated reliability index (β_o) for one critical detail (β_o = 2.61). Note that for β^{SNi}, 'i' represents the mechanism level. Therefore, for a single OWT substructure, the mean system reliability indices (β^{SNi}) are presented in the Tables 5 and 6 for 3 and 5 mechanisms concatenated, respectively.

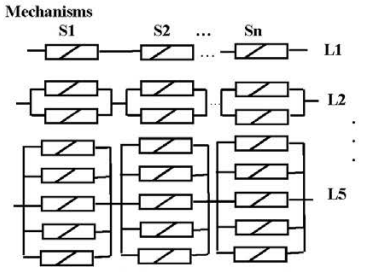

Figure 4. Sequences of failure (S_n) where 'n' is the number of mechanisms concatenated and 'L' represents the mechanism level.

Table 5. Normalized mean accumulated system reliability indices (β^{SN}) for hot spots located in a substructure. The general series system model is configured by 3 mechanisms concatenated.

Cases	β^{SN_1}	β^{SN_2}	β^{SN_3}	β^{SN_4}	β^{SN_5}	$\rho_{i,j}$
1	1.000	1.000	1.000	1.000	1.000	1.000
2	0.881	1.069	1.164	1.228	1.274	0.721
3	0.855	1.202	1.387	1.510	1.601	0.417
4	0.848	1.386	1.730	1.985	2.186	0.113
5	0.847	1.471	1.917	2.283	2.600	0.000
6	0.877	1.078	1.180	1.248	1.297	0.696
7	0.877	1.078	1.180	1.248	1.297	0.696
8	0.923	1.022	1.076	1.111	1.136	0.887

Tables 7 and 8 show results for two substructures with hot spots correlated between them, considering sequences of failure of 3 and 5 mechanisms. The mean accumulated system reliability indices (β^{SNi}) are obtained for increased correlation between loads and stress intensities. The correlation between linearized equations is represented by ρ_{ij} which is calculated by $\rho_{ij} = \overline{\alpha}_i^T \overline{\alpha}_j$. In a series system model (level 1), a high correlation coefficient implies larger reliability. On the other hand, for a parallel system the independency between elements implies higher system reliability. For independent stochastic variables, α_i^2 gives the percentage of the total uncertainty associated with u_i, see [4]. If i.e. X_{SCF1}, X_{SCF2} and X_{SCF3} are correlated then $\alpha_{SCF1}^2 + \alpha_{SCF2}^2 + \alpha_{SCF3}^2$ gives the percentage of the total uncertainty considered by X_{SCF}, see Tables 7 and 8.

Table 6. Normalized mean accumulated system reliability indices (β^{SN}) for hot spots located in a substructure. The general series system model is modelled by 5 mechanisms linked.

Cases	β^{SN_1}	β^{SN_2}	β^{SN_3}	β^{SN_4}	β^{SN_5}	$\rho_{i,j}$
1	1.000	1.000	1.000	1.000	1.000	1.000
2	0.838	1.033	1.131	1.197	1.245	0.721
3	0.783	1.147	1.338	1.465	1.558	0.417
4	0.770	1.335	1.688	1.948	2.153	0.113
5	0.769	1.423	1.880	2.251	2.572	0.000
6	0.829	1.039	1.144	1.216	1.267	0.696
7	0.829	1.039	1.144	1.216	1.267	0.696
8	0.894	0.994	1.051	1.086	1.112	0.887

Table 7. Normalized mean accumulated system reliability indices (β^{SN}) for hot spots located in two OWT substructures in-wind farm with 3 mechanisms concatenated.

Cases	β^{SN_1}	β^{SN_2}	β^{SN_3}	β^{SN_4}	β^{SN_5}	$\rho_{i,j}$
1	0.848	1.386	1.73	1.985	2.186	0.113
2	0.851	1.287	1.537	1.710	1.839	0.265
3	0.855	1.202	1.387	1.510	1.601	0.417
4	0.864	1.129	1.265	1.354	1.420	0.569
5	0.881	1.069	1.164	1.228	1.274	0.721

Table 8. Normalized mean accumulated system reliability indices (β^{SN}) for hot spots located in different OWT substructures in-wind farm (without wake effects) with 5 mechanisms linked.

Cases	β^{SN_1}	β^{SN_2}	β^{SN_3}	β^{SN_4}	β^{SN_5}	$\rho_{i,j}$
1	0.770	1.335	1.688	1.948	2.153	0.113
2	0.774	1.232	1.491	1.668	1.800	0.265
3	0.783	1.146	1.338	1.465	1.558	0.417
4	0.801	1.078	1.218	1.310	1.378	0.569
5	0.838	1.033	1.131	1.197	1.245	0.721

A graphical representation of the normalized accumulated mean system reliability indices is shown in Figs. 5-8 in order to get a better illustration of the different cases. The mean (of upper and lower Ditlevsen bounds) system reliability indices (β^S) for a single substructure are shown in Fig. 5. Similarly, system reliability indices considering the correlation between hot spots in two substructures are presented in Fig. 6.

In Figs. 5 and 6, two different sequences of failure are illustrated for each mechanism level L1 to L5, namely S3 and S5 which represent failure sequences with 3 and 5 fatigue failure mechanisms. L1 represents a series system with only 1 element (hot spot) considered in each failure sequence. Levels L2 to L5 are parallel mechanisms each with 2 to 5 elements (hot spots) joined in a general series system model. In Fig. 5, the aligned points in columns represent the 8 cases explained in Tables 3 while in Fig. 6; these points show the 5 cases in Table 4. In addition, the dashed line shows the accumulated reliability index (β_o) for the design life after 25 years. Case 1 represents full correlation between stochastic variables for the different levels of the sequences of failure. Case 5 means full independence between the stochastic variables, see Table 3. Thus, the sequential order between the cases defines the correlation between the stochastic variables starting from Case 1 represented by the dashed line. For instance, for a failure sequence with level L1, full correlation between stochastic variables means higher system reliability. On the other hand, if parallel systems are connected into a general series system (L2 to L5) the accumulated system reliability indices will increase with decreasing correlation between the stochastic variables. Figure 5 also shows that if the number of mechanisms is increased in the sequences of failure from 3 to 5, a decrease in the accumulated system reliability indices (β^S) is observed.

All cases considered in Tables 3 and 4 are shown in Annex A where, as in Fig. 5, only 7 points appear for one substructure with correlated hot spots because Cases 6 and 7 (Table 3) are for full correlation between X_W and X_{SCF}. In consequence, Cases 6 and 7 represented by the sign (+) have equal system reliability indices (β^S).

Figure 5. Accumulated system reliability indices (β^S) calculated by Ditlevsen bounds for Cases 1 to 8 (see Table 3) in an OWT substructure with hot spots correlated and considering sequences of failure with 3 and 5 mechanisms concatenated.

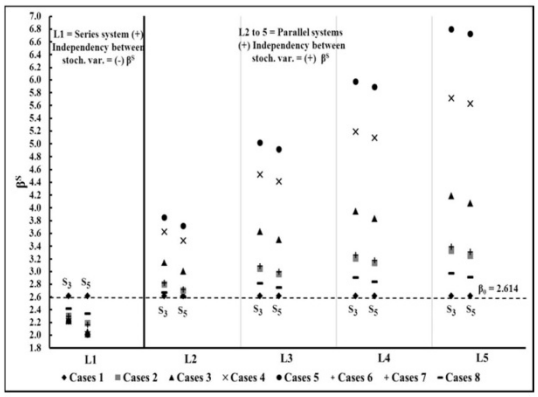

The example is extended with analyse of multiple substructures with correlated hot spots, see Fig. 6 where results are shown for the 5 cases given in Table 4. Figure 6 represents the correlation effect between loads and stresses for two different OWT substructures. In a similar way as Fig. 5, the sequential order between the cases will define the correlation effect between X_W and X_{SCF}. Case 5 means full correlation between X_W and X_{SCF}, see Table 4. Figure 6 also shows a decrement in the mean accumulated system reliability indices (β^S) if the number of mechanisms is increased from 3 to 5, S3 to S5 respectively. In the Annex 'A', this analysis is shown.

Figure 6. Accumulated system reliability indices (β^S) calculated by Ditlevsen bounds for Cases 1 to 5 (see Table 4) in two substructures within a wind farm considering sequences of failure of 3 and 5 mechanisms concatenated.

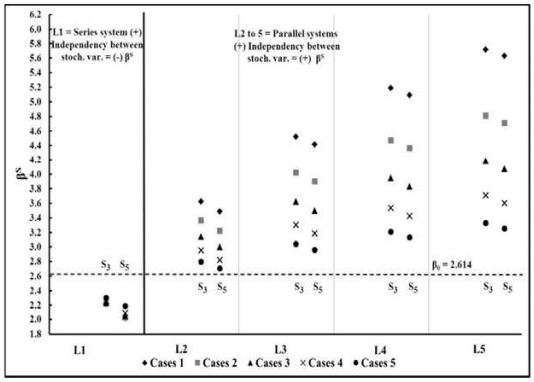

A comparative analysis between the different cases is shown in Figs. 7 and 8, where S1 to S5 represent the number of mechanisms joined to a failure sequence. It is seen that if the number of mechanisms is increased, the system accumulated reliability indices (β^S) will be reduced, as expected. For instance, in Fig. 7, Cases 2 and 8 (Table 3) are compared in order to analyse the correlation effect mainly between X_A and X_{LOGK}. Similarly, in Fig. 8, Cases 3 and 7 (Table 3) are shown considering the effect of correlation between X_{LOGK} and X_W. It is seen that the accumulated system reliability indices will significantly decrease if X_{LOGK}'s are considered full correlated in a failure sequence with parallel mechanisms concatenated (L3 and L5). On the other hand, in a sequence of failure with level L1, the accumulated system reliability indices show a slight increase. Therefore, it is crucial to model these correlations carefully.

Figure 7. Accumulated system reliability indices (β^S) for Cases 2 and 8 (Table 3) considering X_{LOGK} correlated in the stochastic model.

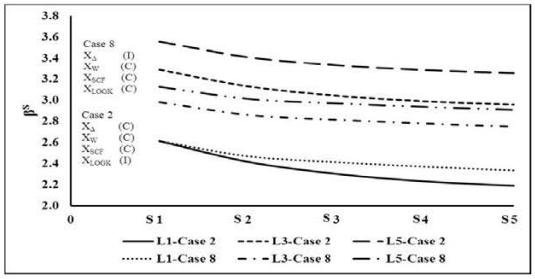

Figure 8. Accumulated system reliability indices (β^S) for Cases 3 and 7 (Table 3) considering X_{LOGK} correlated in the stochastic model.

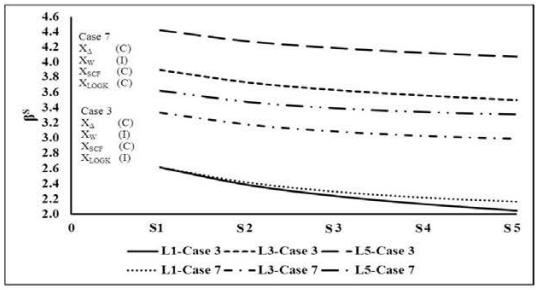

7. CONCLUSIONS

This paper focuses on system effects of fatigue failure modes for welded details in jacket type OWT substructures. Steel OWT substructures typically experience load redistribution if one of them fails, see comments in Martindale [21]. But, it is important to remark that a weakened substructure could reach a collapse during a storm - which is not considered in this paper. Further, the influence of inspection and maintenance strategies (I&M) play an important role in the reliability assessment.

Further work can be relevant in different aspects incl.:

- Influence of wind and wave loads in OWT substructures at different submerged levels.
- OWTs in a wind farm taking into account wake effects.
- A Bayesian approach can be applied to account for inspections/updating new given information from inspections of one, two or more hot spots, assuming no detection of cracks. In this case, a fracture mechanics model needs to be calibrated to the S-N approach.

8. ACKNOWLEDGMENTS

The authors wish to thank the financial support from the Mexican National Council of Science and Technology (CONACYT) and the project "Reliability-Based Analysis Applied for Reduction of Cost of Energy for Offshore Wind Turbines".

9. REFERENCES

[1] Madsen, H. O., Krenk, S., and Lind, N. C., 1986, "Methods of Structural Reliability," Prentice-Hall.

[2] Thoft-Christensen, P., and Murotsu, Y., 1986, "Application of Structural Systems Reliability Theory," Springer Verlag.

[3] Thoft-Christensen, P. and Baker, M. J., 1982, "Structural Reliability Theory and Its Applications," Springer Verlag.

[4] Sørensen, J. D., 2011, "Notes in Structural Reliability Theory - and Risk Analysis," Aalborg University, Aalborg, Denmark.

[5] Márquez-Domínguez, S., and Sørensen, J. D., 2012, "Fatigue Reliability of Offshore Wind Turbine Systems," Accepted for Publication in Proc. 16th IFIP International Conference on System Modeling and Optimization, Yerevan, Armenia.

[6] Jonkman, J.M., Butterfield, S., Musial, W., and Scott, G., 2009, "Definition of a 5-MW Reference Wind Turbine for Offshore System Development," Technical Report NREL/TP-500-38060.

[7] Gao, Z., Saha, N.L.J., Moan, T., and Amdahl, J., 2010, "Dynamic Analysis of Offshore Fixed Wind Turbines Under Wind and Wave Loads Using Alternative Computer Codes," Proc. TORQUE Conference, FORTH, Heraklion, Crete, Greece.

[8] Jonkman, J.M., and Buhl, M.L., 2005, "FAST User's Guide," Technical Report NREL/EL-500-38230.

[9] IEC 61400-1, 2005, "Wind Turbine Generator Systems – Part 1: Safety Requirements".

[10] Jonkman, J.M., 2009, "Turbsim User's Guide," Technical Report NREL/TP-500-46198.

[11] Moriarty, P.J., and Hansen A.C., 2005, "AeroDyn Theory Manual," Technical Report NREL/TP-500-36881.

[12] EN 1993-1-9, 2005, "Eurocode 3: Design of Steel Structures - Part 1-9: Fatigue".

[13] DNV-RP-C203, 2012, "Fatigue Design of Offshore Steel Structures," DnV.

[14] DNV-OS-J101, 2011, "Design of Offshore Wind Turbine Structures," DnV.

[15] GL: 2005, "Guideline for the Certification of Offshore Wind Turbines".

[16] Sørensen, J.D., 2012, "Reliability-Based Calibration of Fatigue Safety Factors for Offshore Wind Turbines," International Journal of Offshore and Polar Engineering, ISSN 1053-5381, Vol. 22, No. 2.

[17] COMREL & SYSREL: USER MANUAL, 2003, "Componental and System Reliability Analysis Using Built-in Symbolic Processor by RCP GmbH, Reliability Consulting Programs," Chap. 2.8, Munich, Germany.

[18] Sørensen, J.D., Rizzuto, E., Narasimhan, H., and Faber, M.H., 2012, "Robustness – Theoretical Framework," Structural Engineering International, Vol. 1, pp. 66-72.

[19] Ghosn M., Moses F. and Frangopol D.M., 2010, "Redundancy and Robustness of Highway Bridge Superstructures and Substructures," Structure and Infrastructure Engineering: Maintenance, Management, Life-Cycle Design and Performance, 6:1-2, pp. 257-278.

[20] Lassen, T., Darcis Ph., and Recho N., 2005, "Fatigue Behavior of Welded Joints Part 1 — Statistical Methods for Fatigue Life Prediction, Supplement to the Welding Journal," Sponsored by the American Welding Society and the Welding Research Council.

[21] Martindale, S.G., and Wirsching P.H., 1983, "Reliability-Based progressive Fatigue Collapse," Journal of Structural Engineering, Vol. 109, pp. 1792-1811, ASCE Paper No. 18181.

ANNEX A

REPRESENTATIVE SCHEME OF GENERAL SYSTEM RELIABILITY CASES ANALYZED

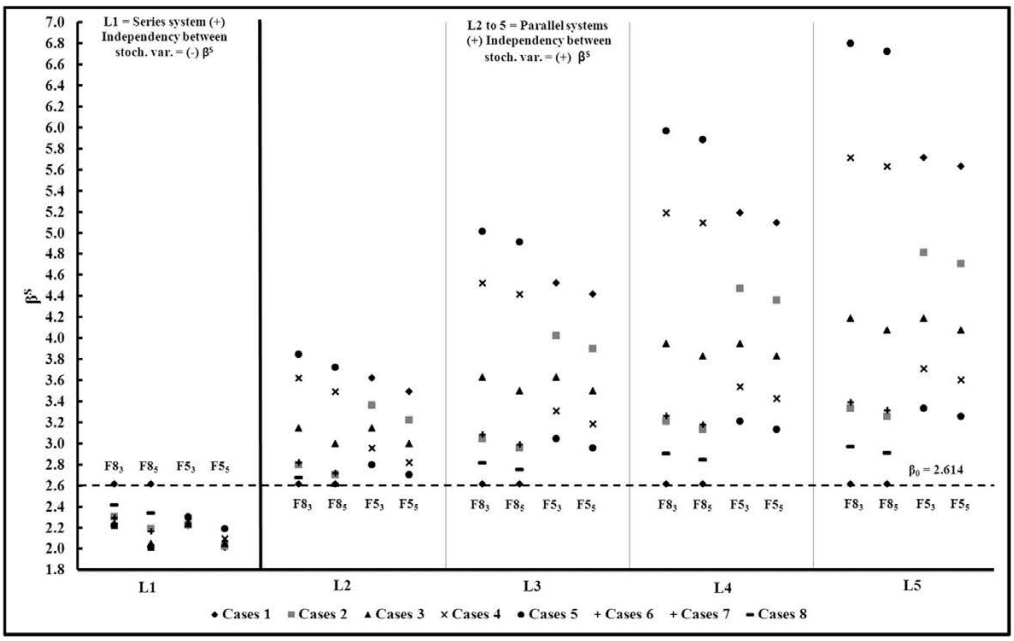

In the example above mentioned, the following models were described by fatigue failure sequences configured with different mechanism levels, see Figs. 5 and 6:

$F8_3$ = Cases 1 to 8 (Table 3) for 1 substructure with hot spots correlated in a sequence of failure with 3 joined mechanisms (S3).

$F8_5$ = Cases 1 to 8 (Table 3) for 1 substructure with hot spots correlated in a sequence of failure with 5 correlated mechanisms (S5).

$F5_3$ = Cases 1 to 5 (Table 4) for 2 substructures with hot spots correlated in a sequence of failure with 3 linked mechanisms (S3).

$F5_5$=Cases 1 to 5 (Table 4) for 2 substructures with hot spots correlated in a sequence of failure with 5 concatenated mechanisms (S5).

where:

L1 = Single series system (L1) where more (+) independence between stochastic variables means a decrement in (-) the structural system reliability (β^S).

L2 to 5 = Series systems of parallel systems with mechanism levels L2 to L5 where more (+) Independence between stochastic variables means an increment in (+) the structural system reliability (β^S).

Appendix A.4

Paper 4

Title: Reliability-based operation of offshore wind turbines

Authors: Sergio Márquez-Domínguez, John D. Sørensen and José G. Rangel-Ramírez

Published in: Proceedings of the 11th international conference on structural safety and reliability (ICOSSAR2013). Columbia University, New York, NY. June 16-20, 2013. Pp. 838 (Hbk). **ISBN 978-1-138-00086-5 (Hbk + CD-ROM) and ISBN 978-1-315-88488-2 (eBook)**

FW: ICOSSAR2013: Request for permission to include paper in thesis

Bijnsdorp, Leon [Leon.Bijnsdorp@taylorandfrancis.com]
Enviado el: lunes, 08 de julio de 2013 11:15
Para: Sergio Márquez Dominguez

Dear Sergio Marquez-Dominguez,

You e-mail below was forwarded to me for further handling. This is fine with us, providing that you make proper credit to the source file, including a copyright notice ((c) 2013 Taylor & Francis Group, London, UK. Used with permission). If you have any questions, please feel free to contact me.

Kind regards,

Léon Bijnsdorp
Léon Bijnsdorp
Editor Conference Proceedings

CRC Press / Balkema
Taylor & Francis Group - an informa business
Schipholweg 107c, 2316 XC Leiden, The Netherlands
P.O. Box 11320, 2301 EH Leiden, The Netherlands
T: +31 71 524 3089
www.crcpress.com & www.taylorandfrancis.com

From: Sergio Márquez Dominguez [mailto:smd@civil.aau.dk]
Sent: vrijdag 5 juli 2013 23:09
To: Goosen, Lukas
Cc: John Dalsgaard Sørensen; jr@cessarer.com
Subject: ICOSSAR2013: Request for permission to include paper in thesis

Dear Mr. Lukas Goosen,
Production Manager CRC Press / Balkema

I have contributed with a publication in the 11th International Conference on Structural Safety & Reliability (ICOSSAR 2013) in Columbia University. New York, NY from June 16 to 20, 2013. The paper has the title "Reliability-based operation of offshore wind turbines". I would like to ask for permission in order to include that paper in the publication of my PhD thesis. The authors of the paper are myself, my PhD supervisor, Professor John Dalsgaard Sørensen and J. G. Rangel-Ramírez a colleague of Veracruz University in Mexico.

Best regards,
Sergio Marquez-Dominguez

Reliability-based operation of offshore wind turbines

S. Márquez-Domínguez & J. D. Sørensen
Aalborg University, Aalborg, Denmark

J. G. Rangel-Ramírez
Universidad Veracruzana, Córdoba-Orizaba, México

ABSTRACT: Offshore wind turbines (OWTs) are operated with defined power production specifications which are inherently linked to reliability levels. OWTs within a wind farm will face heavier turbulence from wakes generated by surrounding wind turbines. Therefore, changes in the control configuration of operational states will influence the fatigue loads of the structural components. So, varying production periods, operational wind speed and desired energy production may have a significant effect on the reliability of the structural components. This paper addresses the influence of different operational configurations on the structural reliability assessing life cycle during operational periods. In consequence, a stochastic model is established which considers how the influence of the operational conditions will determine the fatigue reliability, setting up different load-stress ranges, wind intensities and wind turbulence for single OWTs in-wind farm locations. An illustrative example is presented.

1. INTRODUCTION

Offshore wind industry is moving further away from the coasts which lead to more severe environmental conditions as well as subjecting the OWTs to larger uncertainties. The major sources of uncertainties are associated with strong wind and wave loads on the OWTs. These locations potentially make the offshore wind energy production larger but also expensive due to high costs of the OWT substructures, which must resist higher fatigue loads, corrosion and wear caused by the harsh environmental conditions. In order to maintain a sustainable industry, the key goal is to decrease the cost of energy (CoE). Therefore, a detailed treatment of the uncertainties must be done in order to improve the design and optimize the plans of installation, operation and maintenance of the offshore wind infrastructure. The treatment of the uncertainties must consider that OWTs are operated with specific and detailed power production configurations, which are inherently linked to fatigue reliability levels in the components to be analysed.

If OWTs are operated below their design power rate, the structural elements will be imposed to lower fatigue loads. Besides, OWT locations in a wind farm can play an important role for fatigue performance of the OWTs since they face heavier turbulence from wakes generated by surrounding wind turbines.

Operational conditions are characterized by the wind speeds at the site, the wind turbine power curve, the operational modes, and the wind farm layout respectively. Changes in the control configuration of operational states imply a direct influence on the fatigue loads of the structural components. Consequently, varying the production periods, operational wind speed and desired energy production may, therefore, have a significant effect on the reliability of the wind turbine components, and this influence can be reflected in the initial design by potential savings.

This paper addresses the influence of the long-term operational strategy on the structural reliability of OWTs, by assessing its life cycle cost-benefits using different operational configurations. This implies different stress ranges at different wind speeds with different wind turbulence intensities. The influence of the overall operational control on the fatigue load may be important when OWTs are intended to be fully exploited in their fatigue life. In the same manner, the wind farm location can vary the operational conditions and add or reduce the fatigue load. The in-wind farm location and associated wind effects are taken into account by an operational matrix where the operational control strategy considers the wind action coming from different directions. In this paper, a stochastic model is described, taking into account the influence of the operational conditions which determine the fatigue reliability accounting for different load-stress ranges, wind intensities and wind turbulence for the case of a single OWT located in-wind farm. S-N curves and Miner's rule are

used to model the fatigue life. Design and limit state equations are established for the accumulated fatigue damage in a single wind turbine without wake effects. An example is established which considers the impact of the operational configurations in the service life of the OWT substructure where welded steel joints in the support structure are considered.

2. INFLUENCE OF OPERATIONAL ASPECTS

The wind speed changes randomly in time and space requiring the use of complex control systems integrated in the wind turbine such as active pitch control, yaw control, etc. which determine the potential power output of the OWT and can help keep reasonable levels of structural integrity. Anyway, important extreme and fatigue stresses are produced in different structural components by the wind action during different operational states of the OWT; for instance, in Figure 1, a hot spot 'A' is located in a jacket type wind turbine substructure where the stresses coming from external forces (i.e. wind, turbulence, wave, etc.) are reflected.

In general, different wind turbine components are affected by stresses produced by a variation of external forces that are concentrated in hot spots. Control systems establish a pretty narrow relationship between stresses, wind speed and turbulence intensity in a single wind turbine and also for OWTs located in a wind farm. Control systems are considered to be mediators between the structural response and external loads. Therefore, in order to determine the impact of the control system, a reliability analysis can be done which considers stochastic models based on fatigue probabilistic approaches; see (Tarp-Johansen, 2003) and (Veldkamp, 2006). In (Sørensen et al. 2007) and (Sørensen et al. 2008), turbulence models have been applied in wind farms in order to perform a fatigue reliability analysis where the efficiency of the complex system controls has been proved, considering OWTs under wake effects. The turbulence model is based on the structural behaviour of the OWTs exposed to wind farms flows, e.g. the models developed by (Frandsen, 2007). In consequence, service and fatigue life are highly influenced by the response of the control systems and the efficiency of operational configuration initially established.

3. WIND TURBINE MODELLING

A 5MW NREL OWT has been developed by (Jonkman et al. 2009) where general and structural properties are defined. In Márquez & Sørensen (2012) and also Márquez & Sørensen (2013), the 5MW NREL OWT has been modelled defining the basis for a monopile foundation in order to simulate representative time series of stresses in a particular hot spot. These representative stresses are assumed to represent an equivalent response for an OWT jacket type.

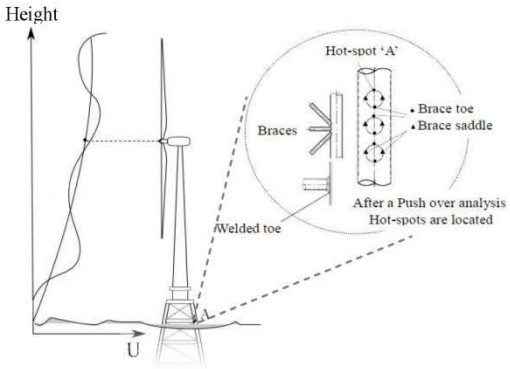

Figure 1. Wind influence and turbulence intensity in an OWT substructure.

It is noted that a complete and detailed structural model of the OWT jacket type foundation must be established in order to determine, in detail, the static and dynamic structural response incl. the aerodynamic and hydrodynamic loads. In Gao et al., (2010), a 'decoupled analysis method' has been proposed to model the dynamic behaviour of jacket OWT substructures. The decoupled analysis method seems to be an efficient procedure used to analyse complex foundations for offshore wind turbines.

The wind turbine model is established by taking into account the influence of the operational conditions which determine the fatigue reliability setting up different mean wind speeds and turbulence intensities. Once the turbine response has been simulated, a point between sea water level and mudline is chosen, namely hot spot 'A' in Figure 1, where representative stresses are generated by wind and wave contributions. Bending moments used in the stochastic model for the fatigue analysis are calculated considering normal operating conditions with the wind turbine rotor perpendicular to the wind direction. The distribution of wind directions is not taken into account. Therefore, the reliability indices calculated can be considered conservative. After modelling, the stress ranges are grouped in intervals by rainflow counting in order to calculate the frequency at each mean wind speed bin.

4. FATIGUE PROBABILISTIC MODELS AND RELIABILITY ASSESSMENT

Operational changes could have an important influence on fatigue damage for offshore wind turbines. This section describes how the reliability of fatigue critical details can be estimated using a S-N approach with S-N curves in combination with Miner's

rule which is often recommended in codes and standards, such as e.g. EN 1993-1-9 (2005), IEC 61400-1 (2005), DnV-C203 (2012), DnV-OS-J101 (2011) and GL:2005. The structural reliability assessment can be performed by considering a single fatigue critical detail (hot spot) located in the substructure.

For fatigue critical details in marine conditions with cathodic protection, bi-linear S-N curves should be applied where N_c represents the transition between slopes m_1 and m_2. Bi-linear S-N curves can be written as:

$$N = K_1\left(\Delta s\left(\frac{T}{T_{ref}}\right)^{\nu}\right)^{-m_1} \quad \text{and} \quad N = K_2\left(\Delta s\left(\frac{T}{T_{ref}}\right)^{\nu}\right)^{-m_2} \tag{1}$$

where K_1, m_1 are material parameters for $N \le N_C$; K_2, m_2 are material parameters for $N > N_C$; N_C corresponds to the number of cycles at the inflection point; Δs_c is the stress range at the inflection point (MPa); Δs is the stress range (MPa); T is the material thickness through which a crack will grow (T = 50 mm); T_{ref} is the plate reference thickness (T_{ref} = 25 mm); and 'ν' is a scale exponent, assuming that the total number of stress ranges for a given fatigue critical detail can be grouped in n_σ groups/intervals ΔQ_i so that the number of stress ranges in group 'i' is n_i per year. (ΔQ_i, n_i) is obtained by rainflow counting. This procedure is applied for each simulation model with different equivalent wind turbulence intensities.

Equation (2) represents a code-based deterministic design equation based on Miner's rule.

$$G = 1 - \sum_i \sum_{s_k \ge \Delta s_C} \frac{T_{FAT} n_{i,j=5,k}}{K_1^C s_k^{-m_1}} P(V_i) - \sum_i \sum_{s_k < \Delta s_C} \frac{T_{FAT} n_{i,j=5,k}}{K_2^C s_k^{-m_2}} P(V_i) = 0 \tag{2}$$

where $s_k = \frac{\Delta Q_k}{z}\left(\frac{T}{T_{ref}}\right)^{\nu}$ is the stress range 'k'; $n_{i,j=5,k}$ is the number of stress ranges equal to ($\Delta Q_k/z$) given a mean wind speed V_i and standard deviation of turbulence equal to $\sigma_{u_{j=5}}$ (90% quantile); $P(V_i)$ is the probability of mean wind speed at bin number 'i'; ΔQ_k is the range of load effect (proportional to stress range s_k in group 'k'); 'z' is a design parameter, e.g. cross sectional area; T_{FAT} is the fatigue design life; K_i^C is the characteristic value of K_i ($\log K_i^C$ equal to the mean of $\log K_i$ minus two standard deviations of $\log K_i$).

The probability of failure (and the corresponding reliability index) is calculated using the design value 'z' which is determined from the design Equation (2) and used in the following limit state equation to estimate the reliability:

$$g = \Delta - \sum_i \sum_j \sum_k \frac{t \cdot n_{ijk}}{K_1 s_k^{-m_1}} \cdot P\left(\sigma_{u_j} | V_i\right) \cdot P(V_i) - \sum_i \sum_j \sum_k \frac{t \cdot n_{ijk}}{K_2 s_k^{-m_2}} \cdot P\left(\sigma_{u_j} | V_i\right) \cdot P(V_i) \tag{3}$$

where 'Δ' is the model uncertainty related to Miner's rule for linear damage accumulation. 'Δ' is assumed to be LogNormal distributed with a mean value = 1 and coefficient of variation COV_Δ; $s_k = X_W X_{SCF} \frac{\Delta Q_k}{z}\left(\frac{T}{T_{ref}}\right)^{\nu}$ is the stress range 'k'; n_{ijk} is the number of stress ranges equal to ($\Delta Q_i/z$) during 60 minutes given V_i and σ_{u_j}; $P\left(\sigma_{u_j} | V_i\right)$ is the probability of standard deviation of turbulence in bin number 'j'. 't' is the time ($0 \le t \le T_L$) where T_L is the service life. σ_{u_j} is modelled as LogNormal distributed with characteristic value $\hat{\sigma}_{u_j}$ defined as the 90% quantile and standard deviation equal to $I_{ref} \cdot 1.4$ m/s with I_{ref} being the reference turbulence intensity. $\hat{\sigma}_{u_j}$ is modelled based on IEC 61400-1(2005):

$$\hat{\sigma}_u(U) = I_{ref} \cdot (0.75 \cdot U + b); \quad b = 5.6 \text{ m/s} \tag{4}$$

Table 1. Stochastic model. D: Deterministic, N: Normal, LN: LogNormal and γ: Characteristic value.

Var.	Dis	Mean	Std. dev.	γ	Comments	
Δ	LN	1	0.30	1		
X_{SCF}	LN	1	0.10	1	Stresses	
X_W	LN	1	0.10	1	Wind/Wave loads	
STRUCTURAL DETAIL: S-N CURVE 'D'						
m_1	D	3				Δs_c
$\log K_1$	N	12.564	0.20	12.164	In air	52.6
$\log K_1$	N	12.164	0.20	11.764	C. protection	83.4
$\log K_1$	N	12.087	0.20	11.687	F. corrosion	
m_2	D	5				
$\log K_2$	N	16.006	0.20	15.606	In air	
$\log K_2$	N	16.006	0.20	15.606	C. protection	
STRUCTURAL DETAIL: S-N CURVE 'F'						
m_1	D	3				Δs_c
$\log K_1$	N	12.255	0.20	11.855	In air	41.5
$\log K_1$	N	11.855	0.20	11.455	C. protection	65.8
$\log K_1$	N	11.778	0.20	11.378	F. corrosion	
m_2	D	5				
$\log K_2$	N	15.491	0.20	15.091	In air	
$\log K_2$	N	15.491	0.20	15.091	C. protection	
$\log K_1$ and $\log K_2$ are assumed fully correlated.						

The cumulative (accumulated) probability of failure in the time interval [0, t] is obtained by:

$$P_F(t) = P(g(t) \le 0) \tag{5}$$

The probability of failure can be estimated by FORM/SORM techniques or simulation, see e.g. (Madsen et al. 1986, Melchers, 1999 and Sørensen, 2011). The reliability index, $\beta(t)$, corresponding to the cumulative probability of failure, $P_F(t)$, is defined by:

$$\beta(t) = -\Phi^{-1}(P_F(t)) \quad (6)$$

where $\Phi(\ )$ is the standardized normal distribution function.

The annual probability of failure is obtained from:

$$\Delta P_F(t) = P_F(t) - P_F(t-\Delta t);\ t > 1\,\text{year and}\ \Delta t = 1\,\text{year} \quad (7)$$

The acceptable maximum annual probability level of failure (ΔP_F) is considered to be in the range between 10^{-3} and 10^{-4} corresponding to (β) values between 3.1 and 3.7, see (Sørensen, 2012).

A representative stochastic model based on DnV-C203 (2012) is shown in Table 1. The stochastic model considers three different S-N curves representing typical fatigue behaviour of welded details. The S-N curves are for 'in air', 'marine with cathodic protection' and 'marine with free corrosion' environments.

5. EXAMPLE OF THE OPERATIONAL CONTROL INFLUENCE IN THE STRUCTURAL DESIGN: COSTS VS BENEFITS.

For a specific OWT project, a socio-economic, life-cycle cost-benefit based study can be conducted considering investment cost, operational cost, finance cost, and annual energy production, in order to assess the cost of the wind energy (CoE) taking into account the operational control influence in the structural design where the optimal 'equilibrium' between costs and benefits maximizing the CoE is the main goal for decision making.

In this paper, an example is established based on the influence of operational control changes that can be applied during the service life of an OWT substructure. The operational control determines the annual energy production which is obtained considering different operational strategies applied to the representative 5MW NREL OWT. These strategies are defined in Table 2 which can be established at different time intervals and also in different seasons.

Table 2. Operational strategies. 'U' is the operational mean wind speed in (m/s) and 'T' represents the service life (T_L) equal to 25 years.

Cases	Strategy
1	(4-6)U(1-25)T
2	(4-6)U(1-25)T+(6-8)U(1-25)T
3	(4-6)U(1-25)T+(6-8)U(1-25)T+(8-10)U(1-25)T
4	(4-6)U(1-25)T+(6-8)U(1-25)T+(8-10)U(1-25)T+(10-12)U(1-25)T
5	(22-24)U(1-25)T
6	(20-22)U(1-25)T+(22-24)U(1-25)T
7	(18-20)U(1-25)T+(20-22)U(1-25)T+(22-24)U(1-25)T
8	(16-18)U(1-25)T+(18-20)U(1-25)T+(20-22)U(1-25)T +(22-24)U(1-25)T
9	(14-16)U(1-25)T+(16-18)U(1-25)T+(18-20)U(1-25)T +(20-22)U(1-25)T+(22-24)U(1-25)T
10	(4-6)U(6-25)T+(6-8)U(21-25)T+(18-20)U(18-25)T +(20-22)U(12-25)T+(22-24)U(11-25)T
11	(4-6)U(1-25)T+(22-24)U(1-25)T
12	(4-6)U(6-25)T+(6-8)U(16-25)T
13	(4-6)U(5-25)T+(6-8)U(18-25)T
14	(4-6)U(5-25)T+(6-8)U(20-25)T
15	(4-6)U(5-25)T+(6-8)U(21-25)T
16	(4-6)U(1-25)T+(20-22)U(25-25)T+(22-24)U(1-25)T
17	(4-6)U(7-25)T+(20-22)U(1-25)T+(22-24)U(1-25)T
18	Year 11 eliminated
19	(4-6)U(15-25)T+T(20-22)U(1-25)T+(22-24)U(1-25)T
20	(4-6)U(15-25)T+(18-20)U(1-25)T+(20-22)U(1-25)T +(22-24)V(1-25)T
21	(4-6)U(15-25)T+(16-18)U(1-25)T+(18-20)U(1-25)T+ (20-22)U(1-25)T+(22-24)U(1-25)T
22	(4-6)U(15-25)T+(6-8)U(21-25)T+(20-22)U(1-25)T +(22-24)U(1-25)T
23	(4-6)U(1-25)T+(20-22)U(1-25)T+(22-24)U(1-25)T
24	(4-6)U(1-25)T+(18-20)U(1-25)T+(20-22)U(1-25)T +(22-24)U(1-25)T

In Table 2, 24 cases are established which consider operational wind speed bins where the wind turbine is considered to be parked, i.e. not producing power, but at the same time it does not contribute to fatigue accumulation. Case 1 defined by '(4-6)U(1-25)T' where 'U' is the mean wind speed in (m/s) and 'T' is time in years. So it means that the wind turbine is assumed to be parked for the mean wind speed bin 4-6 m/s from year 1 to 25, considering that, in this example, the whole design lifetime (T_L) is equal to 25 years. The annual energy production for every case is determined by the power curve established for the 5MW NREL OWT, see Figure 2a. Once the power curve has been established, the next step is to estimate the wind turbine production during the service life (T_L) using statistical techniques, see (Manwell et al. 2002) where for a given wind regimen probability distribution, p(U), and a known 5MW NREL OWT power curve, $P_w(U)$, the average wind machine power, $\overline{P}_W$, is calculated by:

$$\overline{P}_W = \int_1^{T_L} \int_{U_{Cut-in}}^{U_{Cut-out}} P_W(U) \cdot p(U) \cdot dU \quad (8)$$

where p(U) is assumed to be given by a Weibull distribution, see Figures 2b and 2c. Equation (8) can be written by considering the cumulative distribution function defined by dP(U):

$$\overline{P}_W = \int_{1}^{T_L} \int_{U_{Cut-in}}^{U_{Cut-out}} P_W(U) \cdot dP(U) \cdot dU \qquad (9)$$

Thus, the cumulative Weibull distribution is given by:

$$P(U) = 1 - \exp\left[-\left(\frac{U}{A}\right)^B\right] \qquad (10)$$

where: 'A' is a scale factor considered to be equal to 10 m/s and 'B' is a shape factor equal to 2.30. Replacing the integrals in Equation 9 by summations over N_B bins and T_L, the following expression can be used to calculate the average wind machine power after the service life of the OWT:

$$\overline{P}_W = \sum_{i=1}^{T_L} \sum_{j=1}^{N_B} \left\{ \exp\left[-\left(\frac{U_{j-1}}{A}\right)^B\right] - \exp\left[-\left(\frac{U_j}{A}\right)^B\right] \right\} P_W\left(\frac{U_{j-1} + U_j}{2}\right) \qquad (11)$$

Figure 2d shows the contribution at different bins of the power production considering the procedure defined by Equation 11.

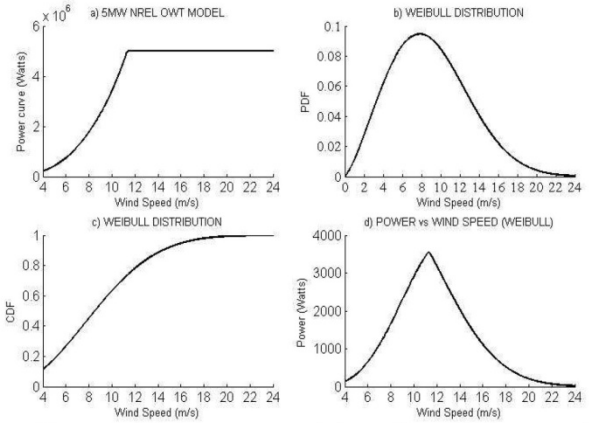

Figure 2. Wind power vs. wind speed considering normal operational rates

In order to establish an optimal operational control, the influence of the Weibull 'tails' on the annual energy production needs to be considered. The optimal control configuration has the important task to produce maximum annual wind energy with acceptable quality reducing the fatigue loads. The main key to find the optimal operational strategy is to take into account the minimum losses of annual energy production. Consequently, operational changes during small period rates can reduce the number and size of fatigue cycles during the service life of the OWT. Thereby, an optimal energy control configuration can improve the original design without decreasing the annual reliability level of the substructure which implies an important influence on the cost-benefit relationship.

The reduction in the fatigue loads means an impact on the structural reliability which can be estimated using the stochastic model described in Table 1 together with the different operational configuration rates given in Table 2, which will affect the fatigue life of the OWT substructure. The stochastic model defined in Table 1 is established for a fatigue critical detail in an OWT substructure which is assumed to have an expected service life (T_L) of 25 years and a design fatigue life (T_{FAT}) equal to 75 years. 'D and F' S-N curves are considered with cathodic protection where bi-linear design and bi-linear limit state equation are used.

The probability of failure for a given limit state equation can be obtained using FORM technique and compared with simulation methods. Then, the accumulated and annual reliability index can be calculated as well as the design parameter (z) in the design point i.e. hot spot 'A' located in Figure 1.

The costs of the optimal 'reduced' operational strategy are determined by considering the small reduction in the annual energy production during the service life of the OWT. On the other hand, the benefit is estimated from the initial design due to material savings of the substructure. Therefore, the decision problem considered in this paper is formulated as an optimization problem considering the cost-benefit relationship as follow:

$$\begin{aligned} &\max_{p(z,op)} \ \Delta W(z,op) = B_T(z,op) - C_T(z,op) \\ &\text{s.t. } \Delta P_t(t,z,op) \le \Delta P_F^{maz} \quad , \quad t = 1,2,\ldots,T_L \end{aligned} \qquad (12)$$

The optimization model maximizes the cost-benefit where 'B_T' is the total expected benefits during the service life 'T_L' considering the influence of the operational strategies (op) and material design (z). 'C_T' is the total costs due to energy losses. It is assumed that marginal changes in expected benefits and total costs can be written as $\Delta B_T(z,op) = C_z \cdot \Delta z$ where 'C_z' represents the cost of the steel in the market and 'Δz' is the marginal change in saved material area in the substructure. Further, $\Delta C_T(z,op) = C_E \cdot \Delta E$ where 'C_0' is the cost of the energy in the supplier marked and 'ΔE' is the change in loss of energy due to changes in the operational configuration (op). Therefore, the change in income (ΔW) will depend of the operational strategy (op) and the ratio of the unit costs $R = \left(\frac{C_E}{C_Z}\right)$.

6. RESULTS

In Table 3, the results for a structural reliability assessment are presented for a single fatigue critical detail, i.e. hot-spot 'A' located in the substructure

(see Figure 1) considering 'normal wind turbine operational conditions' and without reductions in operation rates. For the fatigue critical details in marine conditions, 'D and F' bi-linear S-N curves with cathodic protection are applied considering a bi-linear design equation and a bi-linear limit state equation (LSE), see Section 4. The FORM technique is applied in order to calculate the accumulated (β) and annual ($\Delta\beta$) reliability indices which, for this example, are estimated to be the same for both S-N curves. The design parameter 'z' is seen to be different representing the difference between the two SN-curves, see also Márquez & Sørensen (2012).

Table 3. Annual and cumulated reliability indices for a fatigue critical detail (Hot-spot 'A' in Figure 1) considering 'normal operational conditions'.

S-N curve	β_o	$\Delta\beta_o$	z
D	2.61	3.25	0.96
F	2.61	3.25	1.21

To fulfil the constraint in Equation (12), the results in the following are obtained so that for a given case where the wind turbine is not operating for some wind speed bins, the design is modified so the reliability level is obtained as in Table 3. This is represented by the change in design, 'Δz', as well as the decrement in produced energy, 'ΔE', and the change in income, 'ΔW'.

Table 4 shows the influence of parking the wind turbine at different wind speed bins. 'AEC' is the energy produced in each wind speed range by the 5MW NREL OWT where the total sum represents the total annual energy production generated by the OWT after 25 years. Table 4 also shows the marginal change in saved material area in the substructure, 'Δz', and the change in energy production, 'ΔE', using the stochastic model described in Section 4. It is seen, as expected, that the largest changes occur for mean wind speeds in the interval between 10-18 m/s. Therefore, it is not realistic to stop the energy production between these wind speeds, and, in consequence, the marginal cost model defined by Equation (12) should not be applied.

Table 4. Bins' contribution to the energy production and marginal change in saved material area in the substructure for an OWT energy production after 25 years of production.

Bins	Δz (%)	ΔE (%)	AEC (MWhr)
(4-6)U(1-25)T	0.80	2.79	15274.02
(6-8)U(1-25)T	1.10	8.93	48928.28
(8-10)U(1-25)T	1.50	18.32	100316.2
(10-12)U(1-25)T	2.70	26.38	144485.4
(12-14)U(1-25)T	8.80	20.82	114007.7
(14-16)U(1-25)T	4.70	12.38	67805.96
(16-18)U(1-25)T	2.00	6.30	34487.74
(18-20)U(1-25)T	1.00	2.74	15002.99
(20-22)U(1-25)T	0.50	1.02	5576.438
(22-24)U(1-25)T	0.20	0.32	1767.927
		Total:	547652.7

Table 5. Cost-Benefit influence of different operational strategies shown in Table 2 for 'D and F' S-N curves considering a steel unit cost in the market (C_Z=1.00) and the ratio of the unit costs equal to C_E/C_Z = 0.30.

Case (op)	Δz (%)	ΔE (%)	ΔW(p)
1	0.80	2.79	-0.04
2	2.00	11.72	-1.52
3	3.50	30.04	-5.51
4	6.60	56.42	-10.33
5	**0.20**	**0.32**	**0.10**
6	0.30	1.34	-0.10
7	0.80	4.08	-0.42
8	1.80	10.38	-1.31
9	3.80	22.76	-3.03
10	1.00	5.66	-0.70
11	0.90	3.11	-0.03
12	1.10	5.80	-0.64
13	1.10	5.20	-0.46
14	1.00	4.49	-0.35
15	1.00	4.13	-0.24
16	**1.00**	**3.15**	**0.06**
17	1.00	3.46	-0.04
18	0.00	4.00	-1.20
19	0.70	2.46	-0.04
20	1.10	5.20	-0.46
21	2.10	11.49	-1.35
22	0.90	4.24	-0.37
23	1.10	4.13	-0.14
24	1.60	6.87	-0.46

Table 5 shows the results for the cases defined in Table 2. For some operational strategies, it is possible to obtain a favourable cost-benefit relationship, assuming a steel unit cost in the marked (C_Z=1.00) and the ratio of the unit costs equal to C_E/C_Z = 0.30. After that, it is clear that Cases 5 and 16 can be considered as optimal 'reduced' operational strategies corresponding to an optimum 'equilibrium' between costs and benefits maximizing the CoE. Both cases are related to reduced operation for mean wind speeds just below the cut-out wind speed, 25 m/s. It is noted that Case 18 represents an extraordinary major failure (i.e. blade crash, wind turbine fire, tower cracks, etc.) where the wind turbine has to suddenly stop to produce energy for a long time (i.e. 1 year) so that 'Δz' should not be changed (Δz = 0), and, consequently, the owners can have a loss around 4% in the energy production.

The annual energy losses are shown in Figure 3 for the cases given in Table 2. The reduction of the steel material is shown in Figure 4 together with possible incomes and benefits obtained after 25 years, assuming C_z=1.0 and R=C_E/C_z=0.30. Figure 4 shows a strong relationship between saved material and losses of energy, considering the operational configuration strategies defined in Table 2.

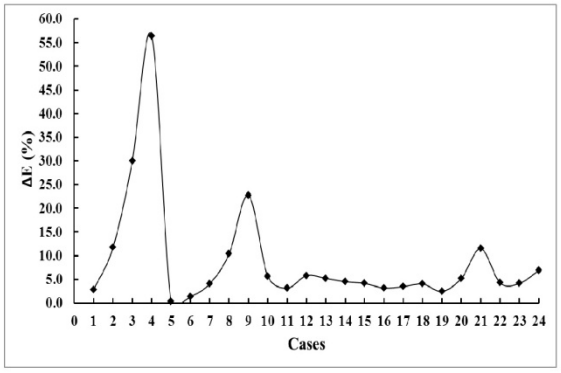

Figure 3. Annual energy losses for cases defined in Table 2.

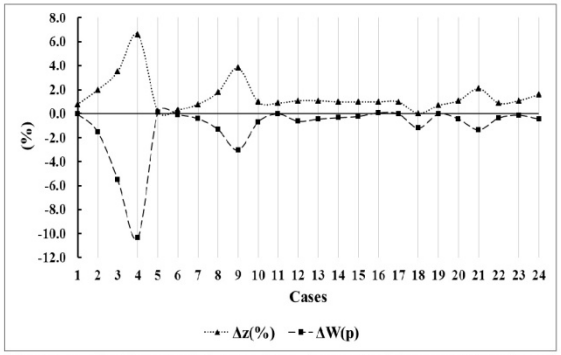

Figure 4. Steel material saved vs. increased incomes produced in the OWT substructure considering the operational configuration strategies defined in Table 2. C_z=1.0 and C_E/C_z=0.30.

The optimal decision on operational strategy depends on the potential positive incomes ΔW(p) for the different operational strategies. It is worth mentioning that special care should be considered when the operational strategy needs to be defined, especially with bins wind speed where the wind turbine is considered to be parked and C_E/C_z, in order to obtain positive incomes.

7. CONCLUSION AND DISCUSSION

This paper addresses the influence of different operational configurations represented by the potential income taking into account the loss of income due to a decrement in produced electricity and saving material due to the decrease of the fatigue damage accumulation. Offshore wind turbines within a wind farm will have different wind conditions partly influenced by surrounding wind turbines. One possibility is to increase/decrease the power on short-term time scales depending on the fluctuating prices. This is not considered in this paper. Instead a marginal cost model is presented to determine the overall importance of changes in the long-term control strategy. This is done by considering cases where it is assumed that the wind turbine is parked at some mean wind speeds. This will result in loss of energy produced, but, at the same time, the contribution to accumulated fatigue is reduced. A probabilistic model is presented to estimate the influence on the reliability. The marginal influences are investigated in particular, showing the changes in energy produced and the material saved, but maintaining the same reliability level as in the case with full operation during the whole lifetime.

An illustrative example is presented showing the influence of different operational strategies applied to the operational OWT control configuration by varying the production periods. The operational strategies were established during the service life of an OWT substructure where the operational conditions are characterized by the wind speeds at the site and the wind turbine power curve. The annual energy production is obtained considering different operational strategies applied to the representative 5MW NREL OWT. The example shows that, especially for high mean wind speeds, it is possible to obtain a higher total income if operation is limited for these wind speeds. It is noted that this conclusion is highly dependent, among others, on the relative costs of electricity and the marginal costs of materials saved due to decreased fatigue loads.

Further work can be relevant in different aspects including:

- Influence of wind and wave loads in OWT substructures at different submerged levels considering different operational strategies.
- OWTs in a wind farm taking into account operational control strategies dealing with wake effects.
- A Bayesian approach can be applied to account for inspections/updating new given information from inspections of one, two or more hot spots, assuming no detection of cracks. In this case, a fracture mechanics model needs to be calibrated to the S-N approach.
- Short-term strategies where the control of the wind turbine is optimized depending on fluctuating energy prices.

8. ACKNOWLEDGMENTS

The author wishes to thank to the financial support from the Mexican National Council of Science and Technology (CONACYT) and from the project "Reliability-based analysis applied for reduction of cost of energy for offshore wind turbines" supported by the Danish Council for Strategic Research, grant no. 2104-08-0014.

9. REFERENCES

DNV-RP-C203. 2012. Fatigue design of offshore steel structures. DnV.

DNV-OS-J101. 2011. Design of offshore wind turbine structures. DnV.

EN 1993-1-9. 2005. Eurocode 3: Design of Steel Structures - Part 1-9: Fatigue.

Frandsen, S.T. 2007. Turbulence and turbulence generated structural loading in wind turbine clusters. Risø National Laboratory. Roskilde, Denmark. January 2007. Risø-R-1188(EN).

Gao, Z., Saha, N.L.J., Moan, T. & Amdahl, J. 2010. Dynamic analysis of offshore fixed wind turbines under wind and wave loads using alternative computer codes. Proc. of the TORQUE2010 conference, FORTH, Heraklion, Crete, Greece.

GL:2005. Guideline for the certification of offshore wind turbines.

IEC 61400-1. 2005. Wind turbine generator systems – part 1: safety requirements.

Jonkman, J.M., Butterfield, S., Musial, W. & Scott G. 2009. Definition of a 5-MW reference wind turbine for offshore system development. Technical Report NREL/TP-500-38060.

Madsen, H. O., Krenk, S., & Lind, N. C. 1986. Methods of structural reliability. Prentice-Hall.

Manwell, J. F., McGowan, J. G. & Rogers A. L. 2002. Wind energy explained theory, design and application. First edition. John Wiley & Sons Ltd. Section 2.5. pp. 60-62.

Márquez-Domínguez, S. & Sørensen, J.D. 2012. Fatigue reliability of offshore wind turbine systems. Accepted for publication in proc. 16th IFIP International conference on system modeling and optimization, Yerevan, Armenia.

Márquez-Domínguez, S. & Sørensen, J.D. 2013. System reliability for offshore wind turbines: fatigue failure. Accepted for publication in proc. of the 32nd International Conference on Ocean, Offshore and Arctic Engineering, OMAE2013, Nantes, France.

Melchers, R.E. 1999. Structural reliability analysis and prediction. Second edition. John Wiley & Sons.

Sørensen, J.D., Frandsen, S. & Tarp-Johansen, N.J. 2007. Fatigue reliability and effective turbulence models in wind farms. Applications of statistics and probability in Civil Engineering – Kanda, Takada & Furuta (Eds).

Sørensen, J.D., Frandsen, S. & Tarp-Johansen, N.J. 2008. Effective turbulence models and fatigue reliability in wind farms. Probabilistic Engineering Mechanics, Elsevier.

Sørensen, J. D. 2011. Notes in structural reliability theory - and risk analysis. Aalborg university, Aalborg, Denmark.

Sørensen, J.D. 2012. Reliability-based calibration of fatigue safety factors for offshore wind turbines. International journal of offshore and polar engineering. ISSN 1053-5381. Vol. 22, No. 2.

Tarp-Johansen, N.J. 2003. Examples of fatigue lifetime and reliability evaluation of larger wind turbine components. Risø national laboratory. Roskilde. March 2003.

Veldkamp, H. F. 2006. Chances in wind energy – A probabilistic approach to wind turbine fatigue design. Doctoral thesis at Technical University of Delft.

Appendix A.5

Paper 5

Title: Probabilistic fatigue model for reinforced concrete onshore wind turbine foundations

Authors: Sergio Márquez-Domínguez and John D. Sørensen

Published in: Proceedings in press of the ESREL 2013 annual conference. Amsterdam, Netherland. September 29th to October 2nd, 2013.

RE: ESREL 2013: Request for permission to include paper in thesis

Steenbergen, R.D.J.M. (Raphaël) [raphael.steenbergen@tno.nl]
Enviado el: lunes, 08 de julio de 2013 13:14
Para: Sergio Márquez Dominguez
CC: esrel2013 (conference@esrel2013.org)

Dear Sergio,

This is OK.

All the best with your thesis.

Raphaël Steenbergen

From: Sergio Márquez Dominguez [mailto:smd@civil.aau.dk]
Sent: 04 July 2013 17:20
To: esrel2013
Cc: John Dalsgaard Sørensen
Subject: ESREL 2013: Request for permission to include paper in thesis

Dear ESREL 2013,

I have contributed with a publication in the international conference ESREL 2013 which will be presented in Amsterdan, Netherland from September 29 to October 2nd, 2013. The paper has the title "Probabilistic fatigue model for reinforced concrete onshore wind turbine foundations". I would like to ask for permission in order to include that paper in the publication of my PhD thesis. The authors of the paper are myself and my PhD supervisor, Professor John Dalsgaard Sørensen.

Best regards,
Sergio Marquez-Dominguez
Aalborg University, Aalborg. Denmark.

Probabilistic fatigue model for reinforced concrete onshore wind turbine foundations

S. Márquez-Domínguez & J. D. Sørensen
Aalborg University, Aalborg, Denmark

ABSTRACT: Reinforced concrete slab foundation (RCSF) is the most common onshore wind turbine foundation type installed by the wind industry around the world. Fatigue cracks in a RCSF are an important issue to be considered by the designers. Causes and consequences of the cracks due to fatigue damage in RCSFs are discussed in this paper. A probabilistic fatigue model for a RCSF is established which makes a rational treatment of the uncertainties involved in the complex interaction between fatigue cyclic loads and reinforced concrete. Design and limit state equations are established considering concrete shear capacity in combination with fatigue damage based on design principles in the Eurocodes. The stochastic model is developed to cover the 'concrete shear-fatigue capacity' illustrated by an example considering the reliability assessment on a RCSF.

Keywords: wind turbine; fatigue concrete; shear capacity; reliability; stochastic model; reinforced concrete slab foundation.

1. INTRODUCTION

Reinforced concrete slab foundation (RCSF) is the most common onshore wind turbine foundation type. Björck (2012) pointed out that cracks on onshore wind turbine foundations seem an important and increasing problem to be considered when designing wind turbines foundations. For this reason, causes and consequences of the cracks due to fatigue damage on RCSFs need to be studied in detail not only for new facilities but also for existing foundations taking into account the remaining lifetime. Cracks on RCSFs could be considered a physical response caused by the accumulation of cyclic loads due to the random interaction between wind loads, wakes and the wind turbine rotor. This stochastic interaction is considered the main source of fatigue damage which seriously affects the integrity of the RCSFs. Further, fatigue damage observed on onshore wind turbine foundations proves this as an important issue for investigation. Furthermore, structural damage and economic consequences need to be analysed with respect to structural reliability criteria in order to improve the structural design and in consequence to lower the cost of energy (CoE).

In this paper, an overall probabilistic fatigue model applied to RCSFs is established which can be used as basis for reliability assessments. The fatigue stochastic model makes it possible to have a rational treatment of the main uncertainties involved in the complex behaviour between fatigue cyclic loads and reinforced concrete. In this paper, a reliability assessment is considered for the shear capacity of a RCSF.

Design of RCSFs requires both geotechnical and structural design. The geotechnical design focuses on the soil-structure interaction and considers deformation and strength of the soil. The structural design focuses on the structural elements exposed to axial forces, shear forces and overturning moments. Furthermore, with help from the probabilistic theories and stochastic models, the reliability of the RCSFs can be estimated by considering the main parameter uncertainties enveloped in the onshore wind turbine design, such as geometry uncertainties, material quality, loads uncertainties, etc.

Design and limit state equations (LSE) are established considering the shear capacity in combination with fatigue damage based on design principles established in the Eurocodes; EN1992-1-1:2004 and EN1992-2:2005, respectively. In EN1992-2:2005, a method for fatigue verification of concrete under shear for bridges is presented. This paper is aimed to apply that fatigue verification on RCSFs establishing a shear-fatigue stochastic model for wind turbines in order to estimate the structural reliability during its service life. Svensson (2010) and Göransson & Nordenmark (2011) present a deterministic fatigue de-

sign considering the fatigue behaviour of RCSFs. Moreover, Thun (2006) presented a probabilistic model for ultimate shear fatigue capacity in a plain concrete railway bridge slab. Even though the cyclic loads are similar, the fatigue loads of a wind turbine in a wind farm are more complex, and, therefore, this model has to be modified for wind turbine applications.

The probability of failure can be estimated by FORM/SORM techniques or simulation, see e.g. Madsen et al. (1986), Melchers (1999) and Sørensen (2011). The probability of structural damage for RCSFs is calculated by the 'shear-fatigue stochastic model' based on theoretical basis established in the S-N curve given in EN1992-2:2005. The reliability assessment can be used to plan and update the maintenance and repair programs applied to onshore wind farms preserving a reliability level during the whole service life.

Cracks in RCSFs do not have immediate consequences on shear or bearing structural capacity, but together with accumulated fatigue damage the cracks could compromise the service life, stability and long-term structural behaviour. Furthermore, damaged slabs could imply a time dependent reliability problem where corrosion in the steel reinforcement will decrease the fatigue life of RCSFs.

In section 2, causes and consequences of cracks in onshore wind turbines are addressed. In Section 3, the main static design characteristics of a RCSF are established based on Göransson & Nordenmark (2011). Section 4 describes the fatigue loads used in the stochastic model developed in Section 5 where it is described how a reliability assessment for 'shear-fatigue capacity' can be performed. Finally, an illustrative example and conclusions are presented in Sections 6 and 7, respectively.

2. ORIGIN, CAUSES AND CONSEQUENCES OF CRACKS IN WIND TURBINE FOUNDATIONS

The presence and development of cracks in reinforced concrete elements are subjected to significant uncertainties. Moreover, cracks in reinforced concrete elements are difficult to avoid since they are considered partly cracked from the beginning due to many factors, e.g. effects of shrinkage, moisture and temperature. These factors also affect the fatigue life of the reinforced concrete elements; see e.g. Nilson (2001) and Park & Paulay (1988) where general theories on reinforced concrete behaviour are presented. On the other hand, tensile cyclic stresses are considered as a main source of cracks in concrete elements. Cornelissen (1984) mentions that "*the tensile strength governs the cracking behaviour and therefore also, among other characteristics, the stiffness, the damping action, the bond to embedded steel, and the durability of concrete. The tensile strength is also of importance with regard to the behaviour of concrete in shear*".

However, wind turbines are exposed to random wind loads developing irregular fluctuating stresses which could cause cyclic strain deformations and fatigue damage during the service life. Thereby, these irregular fluctuating stresses are represented by tensile and compressive cyclic stresses. Adequate tension strength controls the apparition and opening/widening of cracks which decrease the stiffness and durability of concrete elements. Therefore, tension strength is important to the shear-fatigue capacity design for the reinforced concrete foundations which are exposed to extremely high shear forces concentrated in the connection between the foundation and the tower by an embedded steel ring in the concrete. The steel ring transfers the overturning moments and shear forces caused by the external loads to the concrete foundation. This shear forces and overturning moments are the most critical sources of tensile stresses affecting the fatigue life.

Information about origin, causes and consequences of cracks in reinforced concrete foundations based on visits to onshore wind turbine farms is presented in Björck (2012) where a classification of the causes of cracks is explained considering different phases during the service life of the RCSFs.

3. MAIN DESIGN CHARACTERISTIC

Reinforced concrete slab foundations are generally a large flat slab of reinforced concrete with or without small slope. Typically the bottom and top reinforcement for squared and octagonal foundations are placed in two directions, perpendicular to each other, while the top reinforcement through the anchor ring is placed in a radial way. For circular slabs, the top and bottom reinforcement can be structured radially. The foundations should be designed to have an enough bearing capacity to transfer the gravitational and dynamic loads to the ground. In this paper, a reinforced concrete foundation described in Göransson & Nordenmark (2011) is considered such as an illustrative example of a typical reinforced slab foundation design, see Table 1.

Table 1. Main design characteristic for a typical reinforced foundation, Göransson & Nordenmark (2011)

Main design characteristics	
Hub-height	99.5 m
Design wind speed at the hub-height	8.5 m/s
Shape	Square
Slope at the top	Not considered
Concrete class	C30/37
Width	16.0 m
Height	2.00 m

Concrete cover	0.05 m
Weight	12.8 MN
Reinforcement type B500B	
Bottom: two layers, steel bars 25 [mm] of diameter, separated 150 [mm]	s =0.15 m
Top: two layers, steel bars 25 [mm] of diameter, separated 150 [mm]	s =0.15 m
Average depth of the bottom reinforcement.	d_b = 1.913 m
Average depth of the top reinforcement.	d_t = 0.087 m
Ring: geometrical properties	
Anchor / Height	1.70 m / 2.45 m
Outer / Inner diameter	4.20 m / 3.56 m
Diameter average	3.88 m
Preliminary design data	
Soil pressure	237.0 KPa
Rotational stiffness	17,877MNm/deg
Bottom reinforcement A_s	76,812 mm^2
Top reinforcement A_s	18,621mm^2
Shear reinforcement A_{sv}	54,329 mm^2

4. FATIGUE LOADS CONSIDERED FOR THE RCSF PROPOSED

Table 2 shows a fatigue overturning moment spectrum taken from Göransson & Nordenmark (2011). The fatigue load spectrum is given by the number of cycles n_i for each combination of mean moments and peak-to-peak moments (moment ranges). Maximum and minimum overturning moments can then be estimated and the stress ratio, R, can be obtained for every bin. In general, a reinforced slab foundation should be designed taking into account compression and shear stresses as well as tensile fatigue loads carried by the steel reinforcement. Normally, the tensile fatigue loads affect the lower part of the reinforced concrete cross section. A probabilistic fatigue model for steel reinforcement is not considered in this paper. In the example below, the tensile spectrum in Table 2 from columns 4 to 10 is used as a compressive spectrum.

Table 2. Fatigue overturning moment spectrum based on Göransson & Nordenmark (2011).

	Peak-to-peak fatigue load bins [kNm]									
	Overturning moments [kNm]									
(n_i)	-26200 to -16400	-16400 to -6500	-6500 to 3300	3300 to 13200	13200 to 23000	23000 to 32900	32900 to 42700	42700 to 52600	52600 to 62400	62400 to 72200
1.0E+9	0	0	0	0	0	0	0	0	0	0
5.0E+8	0	0	0	0	0	0	0	0	0	0
2.0E+8	0	0	0	10	10	10	0	0	0	0
1.0E+8	0	0	0	10	2000	2000	10	0	0	0
5.0E+7	0	0	10	2000	2000	4000	10	0	0	0
2.0E+7	0	0	10	2000	6000	6000	2000	0	0	0
1.0E+7	0	0	10	2000	9900	9900	4000	0	0	0
5.0E+6	0	0	2000	4000	13900	13900	6000	0	0	0
2.0E+6	0	0	2000	4000	15900	17800	8000	0	0	0
1.0E+6	0	0	2000	6000	19800	21800	9900	0	0	0
5.0E+5	0	0	4000	9900	21800	25800	11900	0	0	0
2.0E+5	0	0	6000	13900	25800	27700	11900	0	0	0
1.0E+5	0	0	8000	15900	27700	29700	13900	0	0	0
5.0E+4	0	0	9900	17800	13700	31700	13900	10	0	0
2.0E+4	0	0	13900	19800	35600	35600	15900	10	0	0
1.0E+4	0	0	13900	19800	39600	35600	17800	10	0	0
5.0E+3	0	0	19800	21800	47500	39600	25800	10	0	0
2.0E+3	0	10	23800	31700	57400	39600	25800	2000	0	0
1.0E+3	2000	41600	59400	87100	89000	98900	79200	8000	2000	2000

5. PROBABILISTIC MODEL AND RELIABILITY ASSESSMENT

Onshore wind turbines are exposed to dynamic cyclic loads, typically 10^7 cycles per year. This section describes how the reliability of shear-fatigue capacity can be estimated using a S-N approach in combination with Palmgren-Miner rule as recommended in various codes and standards, e.g. Eurocodes EN1992-1-1:2004 and EN1992-2:2005 for fatigue verification for reinforced concrete building and bridges. In DNV-OS-J101 and DNV-OS-C502, fatigue verification is considered for offshore concrete structures. In this paper, the fatigue verification model in EN1992-2:2005 will be used as basis. The reinforced concrete is built by two materials, plain concrete and steel reinforcement bars. The probabilistic model developed in this paper is considering only the concrete behaviour under a fatigue load spectrum. The steel reinforcement contribution to the tensile strength and shear capacity is not considered in this study. Accumulated fatigue damage for

plain concrete is assumed to be modelled by the Miner's rule:

$$\sum_{i}^{k}\frac{n_i}{N_i}\le\Delta \qquad (1)$$

where Δ is equal to 1.0 for a deterministic design and a stochastic variable in a probabilistic modelling, k is the number of bins or intervals with constant amplitude fatigue loading, n_i is the actual number per year of constant amplitude cycles in bin i and N_i is the number of constant amplitude cycles to failure with fatigue load corresponding to bin i. N_i can be estimated by S-N curves. For fatigue in reinforced concrete elements, linear S-N curve should be applied considering that the reinforced concrete does not seem to have the tendency to develop a fatigue limit or endurance limit.

In Oh (1986), a mathematical relation for fatigue analysis of plain concrete in flexure has been established based on the Basquin equation which considers irregular amplitude stresses taking into account the stress ratio R which is defined in Equation (3). Therefore, following the relation based on S-N curves given in EN1992-2:2005, N_i can be estimated by:

$$N_i = 10^{14\frac{1-E_{cd,max}}{\sqrt{1-R}}} \qquad (2)$$

Where

$$R_i = \frac{E_{cd,min}}{E_{cd,max}} \qquad (3)$$

and

$$E_{cd,min} = \frac{\sigma_{cd,min}}{z\cdot f_{cd,fat}} \quad ; \quad E_{cd,max} = \frac{\sigma_{cd,max}}{z\cdot f_{cd,fat}} \qquad (4)$$

$\sigma_{cd,max}$ and $\sigma_{cd,min}$ are the maximum and minimum cyclic fatigue stress in bin number i obtained by rainflow counting, respectively. R_i is the shear stress ratio. $f_{cd,fat}$ is the reduced fatigue strength of the concrete calculated according to EN 1992-1-1:2004. For fatigue verification of the reinforced concrete under compressive and shear fatigue cyclic loads, $f_{cd,fat}$, can be estimated by Equations (5) and (6), respectively.

$$f_{cd,fat} = 0.85\cdot\beta_{CC}(t_0)\cdot f_{cd}\left(1-\frac{f_{ck}}{250}\right) \qquad (5)$$

$$f_{cd,fat} = 0.60\cdot\beta_{CC}(t_0)\cdot f_{cd}\left(1-\frac{f_{ck}}{250}\right) \qquad (6)$$

Here, $\beta_{CC}(t_0)$ is a coefficient for the concrete strength at initial load application, t_0 i.e., the time of the start of the cyclic loading on concrete in days. In this paper, $\beta_{CC}(t_0)$ is considered equal to 1.00. f_{cd} is the design compressive strength of the concrete estimated by the ratio ($f_{ck}/\gamma_{S,fat}$) where f_{ck} is the characteristic compressive strength of concrete (defined as a 5% quantile) and $\gamma_{C,fat}$ is the partial factor considered for concrete in fatigue verification (equal to 1.50 in EN 1992-1-1:2004, see Table 3).

Based on the above models, a code-based deterministic design equation can be developed based on the Palmgren-Miner rule and the S-N approach:

$$G = 1-\sum_{i}\frac{T_{FAT}\cdot n_i}{N_i(\sigma_{cd,max},\sigma_{cd,min},z)} = 0 \qquad (7)$$

where T_{FAT} is the design life typically equal to 25 years.

A probabilistic model for the fatigue strength is formulated based on Tepfers (1979). EN1992-2:2005, N_i can be estimated by:

$$\frac{\sigma_{cd,max}}{z\cdot f_c} = 1-X_B(1-R)\log N \qquad (8)$$

where f_c can be the concrete compression strength or the shear capacity strength. Therefore, f_c will depend of the application considered. X_B models the uncertainty in the S-N curve based on the data obtained from laboratory tests to the concrete specimens under controlled condition procedures, which are done in order to estimate the fatigue life of the concrete under different load conditions: tension, compression and flexion. Through the years, various values of X_B have been obtained in different studies, e.g. a COV for X_B has been observed as large as 34.5% by Thun (2006). Quite different S-N curves are obtained by different researchers. Aas-Jakobsen (1970) did compression tests and estimated X_B to be equal to 0.064, In Tepfers and Kutti (1979), X_B is estimated as equal to 0.0685 from tension test, In Cornelissen (1984 and 1986), an S-N curve valid for tensile strength capacity is proposed, which, according to Thun (2006), is used as basis for the Eurocode fatigue verification with X_B equal to 1/14 (0.071) for bridges and building; this is used in this paper for onshore wind turbines foundations. In Oh (1986), plain concrete in beams is considered for flexure strength. The fatigue testing for flexure in beams results in estimating X_B approximately equal to 0.069. Johansson (2004) proposes X_B to be between 0.064 and 0.080 estimated from fatigue tests and analyses on reinforced concrete bridge deck models.

The probability of failure (and the corresponding reliability index) is calculated using the design parameter z determined from the design equation (7) and used in the following limit state equation:

$$g = \Delta-\sum_{i}\frac{t\cdot n_i}{N_i(X_W,X_{SCF},\sigma_{cd,max},\sigma_{cd,min},z)} \qquad (9)$$

where t is time and Δ is the model uncertainty related to Miner's rule for linear damage accumulation. Δ is assumed to be Log-Normal distributed with a mean value = 1.0 and coefficient of variation COV_Δ.

$Ni(X_w, X_{SCF}, \sigma_{cd,max}, \sigma_{cd,min}, z)$ is the number of cycles to failure in bin i obtained from (8) where X_w and X_{SCF} are stochastic variables modelling the uncertainty in assessing the fatigue wind load (X_w) and the fatigue stress ranges given the fatigue load (X_{SCF}). X_w and X_{SCF} are applied as factors on the fatigue load effects.

The above stochastic model can be generalised to take into account a more detailed model for the mean wind speed V_i and the turbulence σ_{uj}. The limit state equation can be written as:

$$g = \Delta - \sum_i \sum_j \frac{t \cdot n_{ij}}{N_i\left(X_w, X_{SCF}, \sigma_{cd,max,ij}, \sigma_{cd,min,ij}, z\right)} \cdot P\left(\sigma_{u_j} | V_i\right) \cdot P(V_i) \qquad (10)$$

where $P(V_i)$ is the probability of mean wind speed bin i. $P(\sigma_{uj}|V_i)$ is the probability of standard deviation of turbulence in bin number j given mean wind speed bin i. n_{ij} is the number of fatigue stress cycles in bin i,j and $\sigma_{cd,max}$, $\sigma_{cd,min}$ are the corresponding stresses. σ_{uj} can be modelled as Log-Normal distributed with characteristic value $\hat{\sigma}_{u_j}$ defined as the 90% quantile and standard deviation equal to (I_{ref}·1.4 m/s) with I_{ref} being the reference turbulence intensity. $\hat{\sigma}_{u_j}$ is modelled based on IEC 61400-1:

$$\hat{\sigma}_u(U) = I_{ref} \cdot (0.75 \cdot U + b); \quad b = 5.6 \text{ m/s} \qquad (11)$$

The characteristic value $\hat{\sigma}_{u_j}$ is used in a corresponding deterministic design equation.

Table 3 shows the representative stochastic model.

Table 3. Stochastic model

Var.	Dist.	Mean	COV	Comments
Δ	LN	1.00	0.30/0.10	Miner's rule
X_{SCF}	LN	1.00	0.30/0.10	Stresses
X_W	LN	1.00	0.30/0.10	Wind loads
f_c	LN	30 MPa	0.30/0.13	Compressive strength, *JCSS (2006)*
X_B	LN	0.0685	0.20/0.15	Shear concrete model, *Tepfers (1979)*
$\gamma_{c,FAT}$		1.5	--	Partial coefficient, *EN1992-1-1:2004*

The cumulative (accumulated) probability of failure in the time interval [0, t] is obtained by:

$$P_F(t) = P(g(t) \le 0) \qquad (12)$$

The probability of failure can be estimated by FORM/SORM techniques or simulation, see e.g. Madsen et al. (1986), Melchers (1999) and Sørensen (2011). The reliability index, $\beta(t)$ corresponding to the cumulative probability of failure, $P_F(t)$ is defined by:

$$\beta(t) = -\Phi^{-1}(P_F(t)) \qquad (13)$$

where $\Phi(\ )$ is the standardized normal distribution function. The annual probability of failure conditioned on survival up to time t is obtained from:

$$\Delta P_F(t) = (P_F(t + \Delta t) - P_F(t)) / \Delta t / P_F(t) \qquad (14)$$

where Δt is a time increment, typically 1 year. The corresponding annual reliability index is denoted $\Delta\beta$.

The reliability index needs to be compared to a tentative target reliability index which is specified for the entire structural system based on socio-economic principles, including life safety aspects. For wind turbines, the acceptable maximum annual probability level of failure (ΔP_F) is considered to be in the range between 10^{-3} and 10^{-4} corresponding to (β) values between 3.1 and 3.7, see Sørensen, (2012).

6. EXAMPLE

An illustrative example is presented in the following where the stochastic model described above is applied for assessing the concrete fatigue reliability for a reinforced concrete slab foundation with design life T_L equal to 25 years and the representative fatigue loads shown in Table 2. A sensitivity analysis is performed based on different values of the coefficient of variations, COVs in Table 3, see cases in Tables 4 to 6 where cumulative (β) and annual reliability indices ($\Delta\beta$) are shown considering compressive and shear strength capacities estimated by Equations(5) and (6).

The reliability level obtained by the stochastic model and the deterministic design equation from the Eurocodes is seen as satisfactory when compared to the reliability level generally required for wind turbines.

Table 4. Cumulative (β) and annual reliability indices ($\Delta\beta$) at year 25 estimated by COV (X_W) = 0.3, COV (X_{SCF}) = 0.3 and varying COVs for Δ, f_c and X_B.

Cases	Uncertainty			Compressive strength		Shear strength	
	Δ	f_c	X_B	β	$\Delta\beta$	β	$\Delta\beta$
1	0.30	0.30	0.20	2.50	3.80	3.16	4.24
2	0.30	0.30	0.15	2.51	3.83	3.19	4.28
3	0.30	0.13	0.20	2.29	3.66	3.07	4.13
4	0.30	0.13	0.15	2.31	3.70	3.10	4.18
5	**0.10**	**0.30**	**0.20**	**2.50**	**3.82**	**3.16**	**4.24**
6	**0.10**	**0.30**	**0.15**	**2.51**	**3.82**	**3.19**	**4.28**
7	**0.10**	**0.13**	**0.20**	**2.30**	**3.60**	**3.07**	**4.14**
8	**0.10**	**0.13**	**0.15**	**2.30**	**3.64**	**3.11**	**4.22**

Table 5. Cumulative (β) and annual reliability indices (Δβ) at year 25 estimated by COV (X_W) = 0.3, COV (X_{SCF}) = 0.1 and varying COVs for Δ, f_c and X_B.

Cases	Uncertainty			Compressive strength		Shear strength	
	Δ	f_c	X_B	β	Δβ	β	Δβ
9	0.30	0.30	0.20	2.85	3.99	3.67	4.39
10	0.30	0.30	0.15	2.88	4.02	3.69	4.6
11	0.30	0.13	0.20	2.79	3.88	3.58	4.31
12	0.30	0.13	0.15	2.85	3.94	3.85	4.66
13	**0.10**	**0.30**	**0.20**	**2.86**	**3.96**	**3.69**	**4.4**
14	**0.10**	**0.30**	**0.15**	**2.90**	**4.02**	**3.69**	**4.6**
15	**0.10**	**0.13**	**0.20**	**2.80**	**3.82**	**3.61**	**4.33**
16	**0.10**	**0.13**	**0.15**	**2.84**	**3.92**	**3.88**	**4.65**

Table 6. Cumulative (β) and annual reliability indices (Δβ) at year 25 estimated by COV (X_W) = 0.1, COV (X_{SCF}) = 0.1 and varying COVs for Δ, f_c and X_B.

Cases	Uncertainty			Compressive strength		Shear strength	
	Δ	f_c	X_B	B	Δβ	β	Δβ
17	0.30	0.30	0.20	3.50	4.27	3.67	4.38
18	0.30	0.30	0.15	3.61	4.47	4.78	5.27
19	0.30	0.13	0.20	3.39	4.15	3.59	4.32
20	0.30	0.13	0.15	4.37	4.88	4.69	5.18
21	**0.10**	**0.30**	**0.20**	**3.55**	**4.28**	**3.70**	**4.40**
22	**0.10**	**0.30**	**0.15**	**3.63**	**4.69**	**4.83**	**5.31**
23	**0.10**	**0.13**	**0.345**	**2.14**	**3.42**	**2.25**	**3.48**
24	**0.10**	**0.13**	**0.20**	**3.38**	**4.18**	**3.62**	**4.34**
25	**0.10**	**0.13**	**0.15**	**4.41**	**4.98**	**4.73**	**5.13**

The results show that the uncertainty on Miner's rule, Δ, is not important when compared to the other uncertainties whereas the uncertainty of the S-N curve (represented by X_B) is quite important, see Cases 21 to 25 in Table 6. Further, the uncertainty of assessing the fatigue load (fatigue wind load (X_w) and fatigue stress ranges given the fatigue load (X_{SCF})), as expected, are also important for the reliability. Finally, the uncertainty of f_c has some importance; it is noted by decreasing the COV (with fixed expected value) the characteristic value increase implying that the reliability decrease.

Figures 1 and 2 show the cumulative reliability indices for the compressive strength as function of time for some of the results given in Tables 4 to 6. The reliability is seen to decrease slightly with time.

In Figures 3 and 4, the cumulative reliability indices are shown for the shear strength capacity model which seems to have higher reliability indices than those estimated by the compressive strength capacity model.

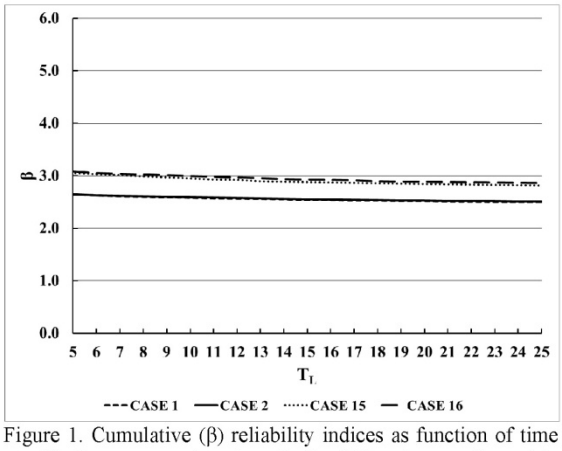

Figure 1. Cumulative (β) reliability indices as function of time considering compressive strength for different cases showed in Tables 4 to 6.

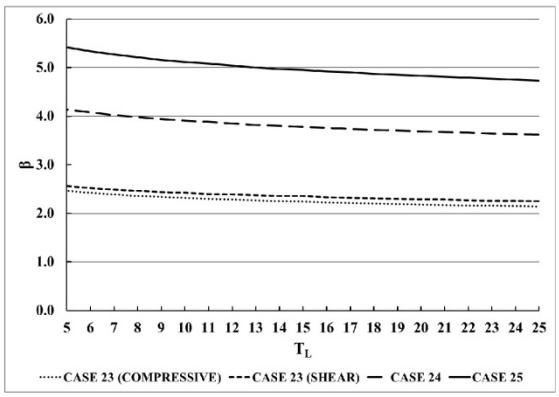

Figure 2. Cumulative (β) reliability indices as function of time considering compressive strength capacity for different cases showed in Tables 4 to 6.

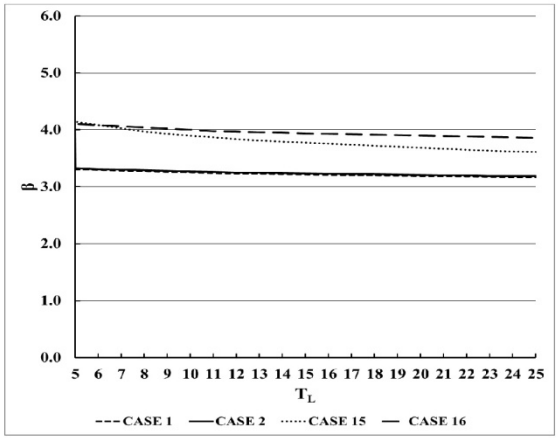

Figure 3. Cumulative (β) reliability indices as function of time considering shear strength capacity for different cases showed in Tables 4 to 6.

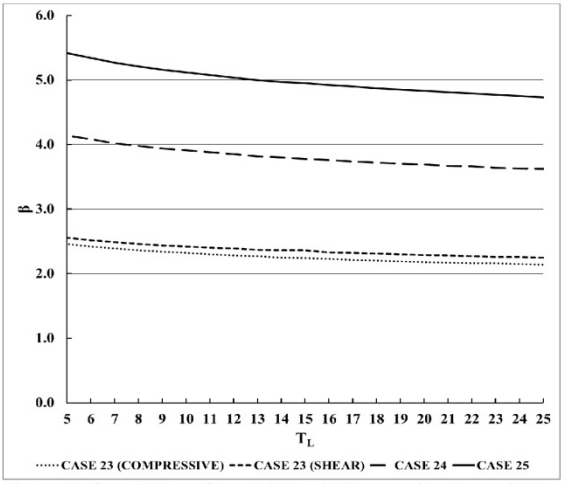

Figure 4. Cumulative (β) reliability indices as function of time considering shear strength capacity for different cases showed in Tables 4 to 6.

7. CONCLUSIONS

Reinforced concrete slab foundations are widely used for onshore wind turbine foundations. Fatigue cracks are an important issue to be considered. Causes and consequences of the cracks due to fatigue damage on RCSFs are discussed, and the paper focuses on assessing the reliability of fatigue failure of the concrete.

A probabilistic fatigue model is established making possible a rational treatment of the uncertainties involved in the complex interaction between fatigue cyclic loads and concrete. Design and limit state equations relevant for wind turbines are formulated, considering concrete shear capacity in combination with fatigue damage model based on design principles in the Eurocodes which are using S-N curves in combination with Miner's rule.

An illustrative example is presented, which indicates that the reliability level obtained using the Eurocode design rule results in reliability levels that are higher than those generally required for wind turbines. Further, the results show that the uncertainty related to the S-N curve is very important for the reliability. Therefore, more data should be analysed for different types of concrete in order to expand and improve the stochastic modelling of the S-N curves.

Further work can be relevant in different aspects including:

- The model could be extended to offshore wind turbine gravity based foundations.
- The stochastic model could be applied in a wind farm taking into account wake effects in onshore and even offshore wind turbine facilities.
- The stochastic model could be extended to allow for reliability assessment considering extreme failure modes related to e.g. shear and bending failures.
- The stochastic model can be extended in order to consider also fatigue of reinforcement in different concrete elements.
- The influence of inspection and maintenance strategies (I&M) play an important role in the reliability assessment. Therefore, a Bayesian statistical analysis could be done in order to estimate the updated reliability of old reinforced concrete foundations.
- A fracture mechanic model could be developed in order to estimate the development of the cracks.

8. ACKNOWLEDGMENTS

The author wishes to thank to the financial support from the Mexican National Council of Science and Technology (CONACYT) and the project "Reliability-Based Analysis Applied for Reduction of Cost of Energy for Offshore Wind Turbines".

9. REFERENCES

Aas-Jakobsen K. 1970. Fatigue of concrete beams and columns. Bulletin No.70-1, Institutt for betonkonstruksjoner, NTH Trondheim. September 1970, p. 148.

Björck, A. 2012. Cracks in onshore wind power foundations; causes and consequences. Elforsk rapport 11:56. Stockholm; Sweden. www.elforsk.se/

Cornelissen, H. A. W. 1984. Fatigue failure of concrete in tension. Heron Vol. 29, No 4, pp. 68

Cornelissen, H. A. W. 1986. State-of-the-art report on fatigue of plain concrete. Delft, The Netherlands: Delft University of Technology. Report 5-86-3. pp. 62.

DNV-OS-C502. 2012. Offshore concrete structures Det Norske Veritas A.S. (DNV).

DNV-OS-J101. 2013. Design of offshore wind turbine structures. Det Norske Veritas A.S. (DNV).

EN1992-1-1. European Committee for Standardization (ECS). 2004. Eurocode2–Design of Concrete Structures–Part 1.1: General rules and rules for buildings. Brussels.

EN 1992-2. European Committee for Standardization (ECS). 2005. Eurocode2: Design of concrete structures-Part 2: Concrete bridges-Design and detailing rules. Brussels.

Göransson F. & Nordenmark A. 2011. Fatigue assessment of concrete foundations for wind power plants. Master thesis 2011:119. Depart. of Civil and Environmental Engineering. Division of Structural Engineering: Concrete Structures. Chalmers University of Technology. Göteborg, Sweden.

IEC 61400-1. 2005. Wind turbine–Part 1: Design requirements. (3rd edition).

JCSS:2006. Probabilistic model code for reliability based design. Issued by the Joint Committee on Structural Safety. Internet publication: www.jcss.ethz.ch.

Johansson, U. 2004. Fatigue tests and analysis of reinforced concrete bridge deck models. Institutionen för byggvetenskap, Kungl. Tekniska högskolan, Stockholm, 198 pp.

Madsen, H. O., Krenk, S., & Lind, N. C. 1986. *Methods of structural reliability*. Prentice-Hall.

Melchers, R.E. 1999. *Structural reliability analysis and prediction*. (2nd edition). John Wiley & Sons.

Miner M. A. 1945. Cumulative damage in fatigue. *Journal of Applied Mechanics, Trans. ASME*, Vol. 12, No.1. March 1945. A159-A164.

Nilson, A.H. 2001. *Design of concrete structures*. Edit. McGraw-Hill. (Inc. 12th edition). New York. USA. ISBN: 0-07-046586-X.

Oh, B.H. 1986. Fatigue analysis of plain concrete in flexure. *J. Struct. Eng*. 1986.112:273-288.

Palmgren A. 1924. Die lebensdauer von Kugellagern (The fatigue life of ball bearings). *Zeitschrift Verein Deutscher Ingenieure*, Vol 68, No. 1924, p. 339-341.

Park, R. & Paulay, T. 1988. *Reinforced concrete strcutures*. Edit. Limusa. 4th reprinted. Mexico. ISBN: 968-18-0100-8.

Svensson, H. 2010. Design of foundations for wind turbines. Master thesis ISSN 0281-6679. Div. of Structural Mechanics, Lund University. Lund, Sweden.

Sørensen, J. D. 2011. Notes in structural reliability theory and risk analysis. Aalborg University. Aalborg, Denmark.

Sørensen, J.D. 2012. Reliability-based calibration of fatigue safety factors for offshore wind turbines. *International Journal of Offshore and Polar Engineering*. ISSN 1053-5381. Vol. 22, No. 2.

Tepfers, R. 1979. Tensile fatigue strength of plain concrete. *Journal of the ACI*, Aug., 1979, Vol. 76, pp. 919-933.

Tepfers, R. & Kutti, T. 1979. Fatigue strength of plain, ordinary and lightweight concrete. *ACI Journal*, Proceedings Vol 76, No. 5, p. 635-652.

Thun, H. 2006. Assessment of fatigue resistance and strength in existing concrete structures. PhD Thesis. Department of Civil and Environmental Engineering. Luleå University of Technology. Luleå,Sweden.

To my family with love

The main objective of the thesis is to develop probabilistic fatigue models for use in optimal planning of operation and maintenance for onshore and offshore wind turbine substructures so as to reduce the expected lifetime costs.

The thesis is focused on fatigue damage of steel and reinforced concrete substructures. Additionally, statistical analyses are performed based on test data from plain concrete specimens and steel reinforcement bars. Application of the estimated uncertainties in probabilistic models for reliability assessment of reinforced concrete substructures is presented and application for reliability-based calibration of partial safety factors for wind turbine standards is illustrated and discussed.

ISSN 1901-7294
DCE Thesis No. 49